NONDESTRUCTIVE EVALUATION OF LAYERED MATERIALS USING THE E-PULSE TECHNIQUE

By

Garrett J. Stenholm

A THESIS

Submitted to
Michigan State University
in partial fulfillment of the requirements
for the degree of

MASTER OF SCIENCE

Department of Electrical and Computer Engineering

2002

ABSTRACT

NONDESTRUCTIVE EVALUATION OF LAYERED MATERIALS USING THE E-PULSE TECHNIQUE

By

Garrett J. Stenholm

Certain materials can be layered in configurations such that they absorb radiated energy at selected frequencies. The selection of frequencies is dependent on the electrical and conductive properties and thickness of the material layers. During routine use, these properties can be unintentionally changed and the ability to detect these changes is necessary to ensure the material absorbs the energy at the intended frequency. Using the extinction pulse (E-pulse) to evaluate layered materials is an extension of its original use as a method to discriminate radar targets.

Application of the E-pulse method to the diagnosis of layered materials is examined for four layered material configurations. These configurations include a single conductor backed layer of lossless material, a single conductor backed layer of lossy material, a single conductor backed layer of magnetic radar absorbing material (MagRAM), and a single conductor backed layer of lossless material covered by an impedance sheet.

To my wife Michelle and
to my children Joseph and Zoë
for their patience and continued support

ACKNOWLEDGEMENTS

I would like to acknowledge and extend my gratitude to Dr. Edward J. Rothwell for his guidance. I would also like to thank Dr. Dennis P. Nyquist and Dr. Leo C. Kempel for their outstanding instruction.

TABLE OF CONTENTS

LIST OF TABLES

LIST OF FIGURES

ABBREVIATIONS

E-Pulse – Extinction Pulse

EDN – E-Pulse Discrimination Number

EDNa – E-Pulse Discrimination Number (version a)

EDR – E-Pulse Discrimination Ratio

EDRa – E-Pulse Discrimination Ratio (version a)

INTRODUCTION

The basis of the E-pulse technique lies in the fact that the late-time scattered response of a conducting target to a transient, wide-band pulse is a sum of damped sinusoids. These damped sinusoids are composed of an infinite number of complex natural frequencies. Given knowledge of these natural frequencies, an E-pulse can be generated that when convolved with the response yields zero late-time energy. The natural frequencies of a conducting target are unique and, therefore, so are the E-pulses for each target. The E-pulse can be looked at as a filter which is target specific and can be used to discriminate that target.

The response of a layered material to a transient, wide-band pulse is also a sum of damped sinusoids. Therefore, the E-pulse technique can be extended to layered materials. The complex natural frequencies which compose the damped sinusoids depend on the material properties, such as the thickness, permittivity, permeability, and conductivity of the layers.

Application of the E-pulse method to the diagnosis of layered materials is examined for four layered material configurations. These configurations include a single conductor backed layer of lossless material, a single conductor backed layer of lossy material, a single conductor backed layer of magnetic radar absorbing material (MagRAM), and a single conductor backed layer of lossless and lossy material covered by an impedance sheet.

Chapter 1 opens with an overview of the E-pulse method. Included in this overview is a brief description of the application of the E-pulse technique as a method of

discriminating radar targets. This is followed by an analysis of the mathematics behind the E-pulse, as well as a discussion of different types of E-pulses. The late-time natural frequencies of a target are the basis of the E-pulse technique so a discussion on the determination of the natural frequencies is presented. Chapter 1 then discusses the application of the E-pulse to layered material. It is shown that the response of lossless layered materials to transient excitations is a sum of damped sinusoids. The chapter closes with an example as a proof of principle.

Beginning with chapter 2, each material configuration is explored beginning with a discussion of the determination of the natural frequencies for each specific configuration. For each material configuration, results are generated for noise free measurements followed by an exploration into the effects of noise on the measurements.

Chapter 2 investigates the effects of changing thickness and permittivity of the layers of lossless materials, as well as the effects of aspect angle and the number of modes used to generate the E-pulses. A method to quantify the results is then discussed and is followed by the presentation of the results. Chapter 3 considers the effects of changing thickness, permittivity, permeability, and conductivity of the layers of lossy materials. Chapter 4 opens with a discussion of the method used to extract the natural frequencies from a scattered response waveform. Following is an investigation into the applicability of the E-pulse technique for analyzing changes in the material properties of MagRAM. Chapter 5 investigates layered materials covered by an impedance sheet. This includes using the E-pulse to detect changes in the surface resistance which depends on the conductivity and thickness of the impedance sheet. Chapter 6 closes the thesis with conclusions that include a summary and discussion of future works.

Chapter 1

Overview of the E-Pulse Technique

Initial applications of the E-pulse technique were in the area of radar target discrimination. As a general technique, its methods can be applied to layered material evaluation to determine changes in material parameters. A brief description of the original use for the E-pulse will be discussed followed by its application to layered material evaluation.

1.1 E-Pulse Technique for Radar Discrimination

It has been shown [1] that the late-time response of a conducting radar target to a band-limited transient excitation can be decomposed into a sum of damped sinusoids as follows,

$$r(t) = \sum_{n=1}^{N} a_n e^{\sigma_n t} \cos(\omega_n t + \phi_n), \quad t > T_l, \tag{1.1}$$

where $s_n = \sigma_n + j\omega_n$ is the aspect independent natural frequency of the nth target mode, a_n and ϕ_n are the aspect dependent amplitude and phase of the nth mode, $T_l = 2T$ (T is the one-way transit time to the target) is the beginning of late time, and N modes are assumed to be excited by the incident electric field.

A waveform, $e(t)$, can be generated using the natural frequencies of the target, $s_n = \sigma_n + j\omega_n$, which when convolved with the target response, results in a null solution,

$$c(t) = e(t) * r(t) = 0, \quad t > T_L = T_l + T_e \tag{1.2}$$

where T_e is the duration of $e(t)$. This waveform is called an extinction pulse or E-pulse.

Two scenarios exist when determining the E-pulse for a target. For the first scenario, the natural frequencies are known, either through prior knowledge of the target characteristics or through theoretical determination. Theoretical determination of the natural frequencies is practical only when considering targets with simple geometry as the natural frequencies are based solely on the geometry of the radar target [1]-[4]. Given the natural frequencies of a target, the response can be modeled by substitution into equation (1.1). Consequently, the E-pulse is determined by substituting the modeled response, $r(t)$, into equation (1.2) and finding the roots of the equation. Theoretical determination of the natural frequencies for non-conductive and conductive materials will be shown in the later chapters.

The second scenario supposes that the natural frequencies are not known, but that the actual response waveform of a target is known, as would be the case when attempting to identify an unknown target. The natural frequencies of the target can be extracted numerically by substituting this target response waveform directly into equation (1.2) as $r(t)$, and again solving for the roots of the equation.

Since the natural frequencies are dependent on the geometry of the targets, the E-pulses generated from these unique natural frequencies are also unique and thus target specific. A database of E-pulses can be built for all known targets and can be referenced against all incoming radar responses to identify radar targets.

Determining the E-pulse can be done in the time domain or through the use of the Laplace transform equations,

$$F(s) = \mathfrak{L}\{f(t)\} = \int_0^\infty f(t) e^{-st} dt, \tag{1.3}$$

and

$$f(t) = \mathfrak{L}^{-1}\{F(s)\} = \frac{1}{2\pi j} \int_{Br} F(s) e^{st} ds. \tag{1.4}$$

Both cases are considered in the following sections.

1.1.1 Time Domain Analysis

Given the first scenario, that the natural frequencies are known, an E-pulse can be generated using equation (1.2). Writing the convolution equation (1.2) in integral form, substituting (1.1) and simplifying yields the following [1], [2],

$$\begin{aligned} c(t) &= \int_0^{T_e} e(\tau) r(t-\tau) d\tau \\ &= \int_0^{T_e} e(\tau) \sum_{n=1}^{N} a_n e^{\sigma_n (t-\tau)} \cos\left[\omega_n (t-\tau) + \phi_n\right] d\tau \\ &= \sum_{n=1}^{N} a_n e^{\sigma_n t} \left[A_n \cos(\omega_n t + \phi_n) + B_n \sin(\omega_n t + \phi_n)\right], \quad t > T_L \end{aligned} \tag{1.5}$$

where

$$\begin{Bmatrix} A_n \\ B_n \end{Bmatrix} = \int_0^{T_e} e(\tau) e^{-\sigma_n \tau} \begin{Bmatrix} \cos \omega_n \tau \\ \sin \omega_n \tau \end{Bmatrix} d\tau. \tag{1.6}$$

Satisfying the null solution of (1.2) for $t > T_L$ requires

$$A_n = B_n = 0, \quad 1 \le n \le N, \tag{1.7}$$

where N is the number of modes composing the E-pulse. Therefore, solving the integral equation,

$$\int_0^{T_e} e(\tau) e^{-\sigma_n \tau} \begin{Bmatrix} \cos \omega_n \tau \\ \sin \omega_n \tau \end{Bmatrix} d\tau = 0, \quad 1 \le n \le N \tag{1.8}$$

for $e(\tau)$ gives the E-pulse that will force the convolution with the target response, $r(t)$, to zero for $t > T_L$.

1.1.2 Transform Domain Analysis

Again, this analysis assumes the complex natural frequencies, $\{s_n\}$, are known. Transforming the convolution equation (1.2) using the Laplace transform yields,

$$\mathfrak{L}\{c(t)\} = \mathfrak{L}\{e(t) * r(t)\}, \tag{1.9}$$

$$\mathfrak{L}\{c(t)\} = \mathfrak{L}\{e(t)\}\mathfrak{L}\left\{\sum_{n=1}^{N} a_n e^{\sigma_n t} \cos(\omega_n t + \phi_n)\right\}, \tag{1.10}$$

$$= E(s) \sum_{n=1}^{N} \frac{a_n}{2} \mathfrak{L}\left\{e^{j\phi_n} e^{(\sigma_n + j\omega_n)t} + e^{-j\phi_n} e^{(\sigma_n - j\omega_n)t}\right\}, \tag{1.11}$$

$$= E(s) \sum_{n=1}^{N} \frac{a_n}{2} \left[\mathfrak{L}\left\{e^{j\phi_n} e^{s_n t}\right\} + \mathfrak{L}\left\{e^{-j\phi_n} e^{s_n^* t}\right\}\right], \tag{1.12}$$

$$= E(s) \sum_{n=1}^{N} \frac{a_n}{2} \left(\frac{e^{j\phi_n}}{s - s_n} + \frac{e^{-j\phi_n}}{s - s_n^*}\right), \tag{1.13}$$

where $E(s)$ the Laplace transform domain representation of $e(t)$. Equation (1.13) is the Laplace transform domain equivalent of equation (1.2).

To find $c(t) = 0$, equation (1.13) is transformed back to the time domain. Using the inverse Laplace transform equation (1.4) and invoking Cauchy's residue theorem to solve the resulting integral gives [1],

$$c(t) = \sum_{n=1}^{N} \frac{a_n}{2} \left(E(s_n) e^{s_n t + j\phi_n} + E\left(s_n^*\right) e^{s_n^* t - j\phi_n} \right). \tag{1.14}$$

Therefore, $c(t)$ in (1.14) is equal to zero when $E(s_n) = E\left(s_n^*\right) = 0$, so

$$E(s_n) = \mathfrak{L}\{e(t)\} = \int_0^{T_e} e^{-s_n t} e(t)\, dt = 0, \quad 1 \le n \le N, \tag{1.15}$$

$$E\left(s_n^*\right) = \mathfrak{L}\{e(t)\} = \int_0^{T_e} e^{-s_n^* t} e(t)\, dt = 0, \quad 1 \le n \le N. \tag{1.16}$$

Substituting $s_n = \sigma_n + j\omega_n$ gives,

$$E(s_n) = \int_0^{T_e} e(t) e^{-\sigma_n t} e^{-j\omega_n t}\, dt = 0, \quad 1 \le n \le N, \tag{1.17}$$

$$E\left(s_n^*\right) = \int_0^{T_e} e(t) e^{-\sigma_n t} e^{j\omega_n t}\, dt = 0, \quad 1 \le n \le N. \tag{1.18}$$

Using Euler's formula, which states $e^{j\psi} = \cos\psi + j\sin\psi$,

$$E(s_n) = \int_0^{T_e} e(t) e^{-\sigma_n t} \left[\cos(\omega_n t) - j\sin(\omega_n t)\right] dt = 0, \quad 1 \le n \le N, \tag{1.19}$$

$$E\left(s_n^*\right) = \int_0^{T_e} e(t) e^{-\sigma_n t} \left[\cos(\omega_n t) + j\sin(\omega_n t)\right] dt = 0, \quad 1 \le n \le N. \tag{1.20}$$

Equations (1.19) and (1.20) hold true only if the integral over both the cosine and sine functions are zero,

$$\int_0^{T_e} e(t) e^{-\sigma_n t} \begin{Bmatrix} \cos\omega_n t \\ \sin\omega_n t \end{Bmatrix} dt = 0, \quad 1 < n < N. \tag{1.21}$$

Equation (1.21) is identical to equation (1.8), thus verifying that the transform domain analysis is equivalent to the time domain analysis for finding the necessary integral equation to solve for the E-pulse. The frequency analysis is more complicated than the time domain analysis. However, some aspects of its analysis, specifically the condition $E(s_n) = 0$, will be used later to help in the extraction of the natural frequencies.

1.1.3 Solution to the Integral Equation

When the natural frequencies are known, the solution to the integral equation,

$$\int_0^{T_e} e(t) e^{-\sigma_n t} \begin{Bmatrix} \cos \omega_n t \\ \sin \omega_n t \end{Bmatrix} dt = 0, \quad 1 < n < N, \tag{1.22}$$

as shown in [1], [2], [3], and [4], begins by assuming a decomposition of the E-pulse into a "forcing" component, $e^f(t)$, which is a known function and present during $0 \le t < T_f$, and an "extinction" component, $e^e(t)$, which is present during $T_f \le t < T_e$;

$$e(t) = e^f(t) + e^e(t). \tag{1.23}$$

Substituting (1.23) into (1.22) gives,

$$\int_{T_f}^{T_e} e^e(t) e^{-\sigma_n t} \begin{Bmatrix} \cos \omega_n t \\ \sin \omega_n t \end{Bmatrix} dt = -\int_0^{T_f} e^f(t) e^{-\sigma_n t} \begin{Bmatrix} \cos \omega_n t \\ \sin \omega_n t \end{Bmatrix} dt. \tag{1.24}$$

The extinction component of the E-pulse, $e^e(t)$, can be represented as an expansion over a chosen set of basis functions, $\{f_m(t)\}$ as follows,

$$e^e(t) = \sum_{m=1}^{2N} A_m f_m(t), \tag{1.25}$$

where $f_m(t)$ represents the m'th basis function and A_m represents the amplitude of the m'th basis function. (The choice of appropriate basis functions will be discussed later in this chapter). Substituting (1.25) into the integral equation (1.24) leads to

$$\sum_{m=1}^{2N} A_m M_{m,n}^{c,s} = -F_n^{c,s}, \quad 1 \le n < N, \tag{1.26}$$

where

$$M_{m,n}^{c,s} = \int_{T_f}^{T_e} f_m(t) e^{-\sigma_n t} \begin{Bmatrix} \cos \omega_n t \\ \sin \omega_n t \end{Bmatrix} dt, \tag{1.27}$$

$$F_n^{c,s} = \int_{0}^{T_f} e^f(t) e^{-\sigma_n t} \begin{Bmatrix} \cos \omega_n t \\ \sin \omega_n t \end{Bmatrix} dt, \tag{1.28}$$

and A_m are the only unknowns in this set of $2N$ simultaneous linear equations. The linear equations in (1.26) can be expressed using matrix notation,

$$\begin{bmatrix} M_{m,n}^{c} \\ \hline M_{m,n}^{s} \end{bmatrix} \begin{bmatrix} A_1 \\ \vdots \\ A_{2N} \end{bmatrix} = - \begin{bmatrix} F_1 \\ \vdots \\ F_{2N} \end{bmatrix}. \tag{1.29}$$

Solving equation (1.29) numerically for A_m gives the amplitudes of the basis functions. These can then be substituted into equation (1.25), which, along with (1.23), give the E-pulse.

1.1.4 Forced and Natural E-pulses

As previously explained, the E-pulse is decomposed into a forcing component and an extinction component to facilitate its computation. This leads to two distinct cases of E-pulses, the natural E-pulse and the forced E-pulse.

As stated, the forcing component exists during the time period $0 \le t < T_f$. If T_f is zero, then only the extinction component of the E-pulse in equation (1.23) exists. Equation (1.29) thus becomes a homogeneous matrix equation whose non-trivial solutions for A_m exist only when the determinant of the coefficient matrix is zero,

$$\det\left[\frac{M^{c}_{m,n}}{M^{s}_{m,n}}\right] = 0. \tag{1.30}$$

Solutions for $e^{e}(t)$ exist only for specific durations of T_e and can be found by solving the zeros of equation (1.30). This is a natural E-pulse, so called because the E-pulse depends not on the excitation of the target but merely on its natural resonant frequencies.

When T_f is nonzero, there exists a forcing component in equation (1.23) as well as the extinction component. This forcing component then determines the solution to equation (1.29) and the extinction component is created to extinguish the response due to the forcing component. This E-pulse exists for all values of T_e except those associated with the natural E-pulse, and is called a forced E-pulse.

1.2 E-Pulse Technique for Layered Material Evaluation

In addition to using the E-pulse technique for radar target discrimination, it can also be used to identify the material parameters of layered material. Just as the late-time response of a conducting target to transient excitations can be decomposed into a sum of damped sinusoids with frequencies based on their geometry, it will be shown that the late-time response of layered material to transient excitations can be decomposed into a sum of damped sinusoids with frequencies dependent on their material properties, e.g., the layer thickness, permittivity, permeability, and conductivity. Given the ability to

determine the complex natural frequencies of a layered material, either by theoretical calculation or extraction from known responses, an E-pulse can be generated to assess the properties of a material.

1.2.1 Late-time Response as a Sum of Damped Sinusoids

In order to validate the E-pulse technique for use in evaluating layered materials it must first be shown that the late-time response of a layered material to transient excitations is a sum of damped sinusoids. An analysis using the singularity expansion method (SEM) [4] is considered for the geometry shown for a lossless, conductor backed slab as seen in Figure 1-1. The incident wave, which propagates along the wave vector

$$\mathbf{k}_0^i = \hat{\mathbf{x}} k_{x,0} + \hat{\mathbf{z}} k_{z,0}, \tag{1.31}$$

strikes the material interface at an angle, θ_i where some of the wave is reflected and some of the wave, described by the wave vector,

$$\mathbf{k}_1^t = \hat{\mathbf{x}} k_{x,1} + \hat{\mathbf{z}} k_{z,1}, \tag{1.32}$$

enters the material and is reflected by the conductor backing.

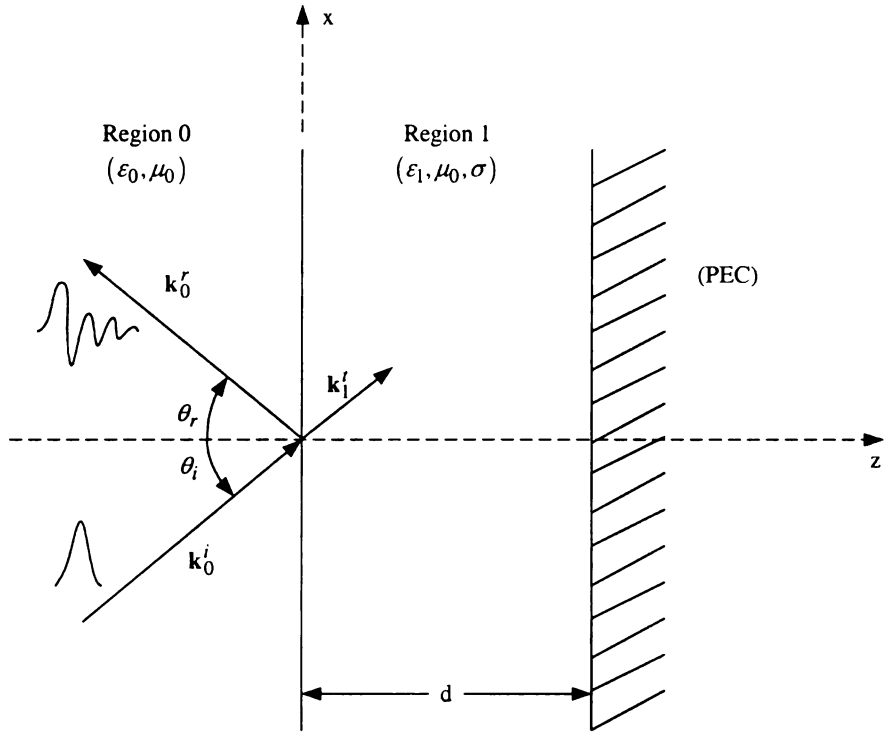

Figure 1-1 Interrogation of simple layered material by transient excitation.

The reflected wave then travels back through the material layer and strikes the interface and again some of the wave is reflected and some of the wave is transmitted through the interface. This process repeats until all of the energy of the wave escapes the layer through the interface. In a lossy material some of the energy is lost within the layer due to dissipation.

The total reflected wave is described in Figure 1-1 by the wave vector,

$$\mathbf{k}_0^r = \hat{\mathbf{x}} k_{x,0} - \hat{\mathbf{z}} k_{z,0}. \tag{1.33}$$

The scattered reflections are determined from the interfacial reflection coefficient,

$$\Gamma = \frac{Z_1 - Z_0}{Z_1 + Z_0}, \tag{1.34}$$

where,

$$Z_0 = \begin{cases} \dfrac{k_0 \eta_0}{k_{z,0}}, & \textit{perpendicular polarization} \\ \dfrac{k_{z,0} \eta_0}{k_0}, & \textit{parallel polarization} \end{cases}, \tag{1.35}$$

$$Z_1 = \begin{cases} \dfrac{k_1 \eta_1}{k_{z,1}}, & \textit{perpendicular polarization} \\ \dfrac{k_{z,1} \eta_1}{k_1}, & \textit{parallel polarization} \end{cases}. \tag{1.36}$$

For the lossless case (σ=0) with perpendicular polarization,

$$Z_0 = \frac{\eta_0 \omega \sqrt{\mu_0 \varepsilon_0}}{\omega \sqrt{\mu_0 \varepsilon_0} \sqrt{1 - \sin^2 \theta_i}}, \tag{1.37}$$

$$= \frac{\eta_0}{\sqrt{1 - \sin^2 \theta_i}}, \tag{1.38}$$

and

$$Z_1 = \frac{\omega\sqrt{\mu_0\varepsilon_1}\sqrt{\frac{\mu_0}{\varepsilon_1}}}{\omega\sqrt{\mu_0\varepsilon_0}\sqrt{\varepsilon_{1r} - \sin^2\theta_i}} \tag{1.39}$$

$$= \frac{\eta_0}{\sqrt{\varepsilon_{1r} - \sin^2\theta_i}} \tag{1.40}$$

Since $\varepsilon_{1r} > 1$, then $Z_1 < Z_0$ and thus $\Gamma < 0$. For the lossless case (σ=0) with parallel polarization,

$$Z_0 = \frac{\eta_0\omega\sqrt{\mu_0\varepsilon_0}\sqrt{1-\sin^2\theta_i}}{\omega\sqrt{\mu_0\varepsilon_0}} \tag{1.41}$$

$$= \eta_0\sqrt{1-\sin^2\theta_i} \tag{1.42}$$

and

$$Z_1 = \frac{\omega\sqrt{\mu_0\varepsilon_0}\sqrt{\frac{\mu_0}{\varepsilon_1}}\sqrt{\varepsilon_{1r} - \sin^2\theta_i}}{\omega\sqrt{\mu_0\varepsilon_1}} \tag{1.43}$$

$$= \frac{\eta_0\sqrt{\varepsilon_{1r} - \sin^2\theta_i}}{\varepsilon_{1r}}. \tag{1.44}$$

And again, it can easily be shown that since $\varepsilon_{1r} > 0$ then $Z_1 < Z_0$ and thus $\Gamma < 0$.

Therefore, for both polarizations, $\Gamma < 0$ a fact that will be referenced later. These interfacial reflection coefficients are used to find the total reflected wave as shown in [5]. The total reflection coefficient is,

$$R(\omega) = \frac{\Gamma - P^2(\omega)}{1 - \Gamma P^2(\omega)}, \tag{1.45}$$

in which

$$P(\omega) = e^{-jk_{z,1}d} \tag{1.46}$$

is called the propagation factor, d is the thickness of the material, and the wave vector is

$$k_{z,1} = \sqrt{k_1^2 - k_0^2 \sin^2\theta_i} \tag{1.47}$$

$$= \frac{\omega}{c}\sqrt{\varepsilon_{1r} - \sin^2\theta_i}\,. \tag{1.48}$$

To further analyze the reflected wave, it is recognized that $s = j\omega$ and thus $\omega = -js$.

Through substitution the total reflected wave can be described in s-plane notation,

$$R(s) = \frac{\Gamma - e^{-j2d\left(\frac{-js}{c}\right)\sqrt{\varepsilon_{1r} - \sin^2\theta_i}}}{1 - \Gamma e^{-j2d\left(\frac{-js}{c}\right)\sqrt{\varepsilon_{1r} - \sin^2\theta_i}}}, \tag{1.49}$$

$$= \frac{\Gamma - e^{-s\tau}}{1 - \Gamma e^{-s\tau}}, \tag{1.50}$$

where

$$\tau = \frac{2d\sqrt{\varepsilon_{1r} - \sin^2\theta_i}}{c}, \tag{1.51}$$

and c is the speed of light,

$$c = \frac{1}{\sqrt{\mu_0\varepsilon_0}}. \tag{1.52}$$

As described in [4], the singularity expansion method (SEM) is a way to represent the solution to electromagnetic scattering problems in terms of the singularities in the complex frequency domain. The pole terms associated with a scattered response determine the natural frequencies of the scatterer. Therefore, the pole terms of (1.50) determine the natural frequencies of the layered material. In the time domain this leads to

a representation of the scattered response as a sum of damped sinusoids. Expanding the denominator of (1.50) using the binomial series,

$$(1-Z)^{-1} = \sum_{n=0}^{\infty} Z^n = 1 + Z + Z^2 + Z^3 + \cdots, \tag{1.53}$$

gives,

$$R(s) = \left(\Gamma - e^{-s\tau}\right) \sum_{n=0}^{\infty} \left(\Gamma e^{-s\tau}\right)^n \tag{1.54}$$

$$= \Gamma \sum_{n=0}^{\infty} \Gamma^n e^{-sn\tau} - \sum_{n=0}^{\infty} \Gamma^n e^{-(n+1)s\tau} \tag{1.55}$$

$$= \Gamma + \sum_{n=1}^{\infty} \Gamma^{n+1} e^{-sn\tau} - \sum_{m=1}^{\infty} \Gamma^{m-1} e^{-ms\tau} \tag{1.56}$$

$$= \Gamma + \left(\Gamma^2 - 1\right) \sum_{n=1}^{\infty} \Gamma^{n-1} e^{-sn\tau} \tag{1.57}$$

Transforming to the time domain using the inverse Laplace transform (1.4) and the time-shifting theorem gives,

$$R(t) = \Gamma \delta(t) + \left(\Gamma^2 - 1\right) \sum_{n=1}^{\infty} \Gamma^{n-1} \delta(t - n\tau)$$

(1.58)

$$= \Gamma \delta(t) + u(t-\tau)\left(\Gamma^2 - 1\right) \sum_{n=-\infty}^{\infty} \Gamma^{n-1} \delta(t - n\tau) \tag{1.59}$$

$$= \Gamma \delta(t) + u(t-\tau) \frac{1-\Gamma^2}{\Gamma} \sum_{n=-\infty}^{\infty} -\Gamma^n \delta(t - n\tau). \tag{1.60}$$

Using

$$-\Gamma^n = \frac{|\Gamma|^{n+1}}{\Gamma}(-1)^n, \tag{1.61}$$

gives

$$R(t) = \Gamma\delta(t) + u(t-\tau)\frac{\left(1-\Gamma^2\right)}{\Gamma}\sum_{n=-\infty}^{\infty}\frac{|\Gamma|^{n+1}}{\Gamma}(-1)^n\,\delta(t-n\tau). \tag{1.62}$$

Since $e^{-jn\pi} = (-1)^n$, this becomes

$$R(t) = \Gamma\delta(t) + u(t-\tau)\frac{\left(1-\Gamma^2\right)}{\Gamma}\sum_{n=-\infty}^{\infty}\frac{|\Gamma|^{n+1}}{\Gamma}e^{-jn\pi}\delta(t-n\tau) \tag{1.63}$$

$$= \Gamma\delta(t) + u(t-\tau)\frac{\left(1-\Gamma^2\right)}{\Gamma^2}|\Gamma|^{\left(\frac{t}{\tau}+1\right)}e^{-j\frac{t}{\tau}\pi}\sum_{n=-\infty}^{\infty}\delta(t-n\tau). \tag{1.64}$$

Using the Poisson-Sum formula [6],

$$\sum_{n=-\infty}^{\infty}\delta(t+n\tau) = \frac{1}{\tau}\sum_{n=-\infty}^{\infty}e^{jn\omega_0 t}, \tag{1.65}$$

where $\omega_0 = \frac{2\pi}{\tau}$ leads to,

$$R(t) = \Gamma\delta(t) + u(t-\tau)\frac{\left(1-\Gamma^2\right)}{\Gamma^2\tau}|\Gamma|^{\left(\frac{t}{\tau}+1\right)}e^{-j\frac{t}{\tau}\pi}\sum_{n=-\infty}^{\infty}e^{j\frac{2\pi}{\tau}nt} \tag{1.66}$$

$$= \Gamma\delta(t) + u(t-\tau)\frac{\left(1-\Gamma^2\right)}{\Gamma^2\tau}|\Gamma|^{\left(\frac{t}{\tau}+1\right)}\sum_{n=-\infty}^{\infty}e^{j(2n-1)\pi\frac{t}{\tau}}. \tag{1.67}$$

Separating the summation into two components gives

$$R(t) = \Gamma\delta(t) + u(t-\tau)\frac{1-\Gamma^2}{\Gamma^2\tau}|\Gamma|^{\left(\frac{t}{\tau}+1\right)}\left[\sum_{n=1}^{\infty}e^{j(2n-1)\pi\frac{t}{\tau}} + \sum_{m=-\infty}^{0}e^{j(2m-1)\pi\frac{t}{\tau}}\right]. \tag{1.68}$$

By making the power of the exponent negative in the second summation, it's range is then the same as the first summation and the two can be combined giving

$$R(t)=\Gamma\delta(t)+u(t-\tau)\frac{1-\Gamma^2}{\Gamma^2\tau}|\Gamma|^{\left(\frac{t}{\tau}+1\right)}\sum_{n=1}^{\infty}\left[e^{j(2n-1)\pi\frac{t}{\tau}}+e^{-j(2n-1)\pi\frac{t}{\tau}}\right] \quad (1.69)$$

Using

$$e^{(t+\tau)\frac{1}{\tau}\ln|\Gamma|}=|\Gamma|^{\left(\frac{t}{\tau}+1\right)} \quad (1.70)$$

gives

$$R(t)=\Gamma\delta(t)+u(t-\tau)\frac{1-\Gamma^2}{\Gamma^2\tau}e^{(t+\tau)\frac{1}{\tau}\ln|\Gamma|}\sum_{n=1}^{\infty}\left[e^{j(2n-1)\pi\frac{t}{\tau}}+e^{-j(2n-1)\pi\frac{t}{\tau}}\right] \quad (1.71)$$

and recognizing that

$$e^{\frac{1}{\tau}\ln|\Gamma|\tau}=|\Gamma| \quad (1.72)$$

leads to

$$R(t)=\Gamma\delta(t)+u(t-\tau)\frac{1-\Gamma^2}{\Gamma\tau}e^{\frac{1}{\tau}\ln|\Gamma|t}\sum_{n=1}^{\infty}\left[e^{j(2n-1)\pi\frac{t}{\tau}}+e^{-j(2n-1)\pi\frac{t}{\tau}}\right]. \quad (1.73)$$

Finally, recognizing that the quantity within the summation notation can be expressed as a cosine leads to the final form of the scattered response,

$$R(t)=\Gamma\delta(t)+u(t-\tau)\frac{1-\Gamma^2}{\Gamma\tau}e^{\frac{1}{\tau}\ln|\Gamma|t}\sum_{n=1}^{\infty}\cos(2n-1)\frac{\pi}{\tau}t\,. \quad (1.74)$$

It can be seen from (1.74) that the scattered response is thus made up of a sum of damped sinusoids.

1.2.2 E-pulse Diagnostics for Layered Materials

Having shown that the scattered response of a lossless layered material is equal to a sum of damped sinusoids the E-pulse technique can be used as a diagnostic tool. This is also true for a conducting material ($\sigma \neq 0$), but this is considerably more difficult to show. The goal of applying the E-pulse technique to layered materials is to give the ability to determine changes in material parameters, (e.g., thickness, permittivity, permeability, and conductivity). As with radar target identification, the E-pulse technique begins with identifying the natural frequencies of the intended targets and using this history as a baseline to sense changes.

Periodic testing of layered materials using the E-pulse can determine any changes in the material parameters. Since the convolution of an E-pulse with the response waveform used to generate it gives a zero result in the late time, any result other than zero shows that there has been some change in the properties of the material from the baseline measurement.

1.2.3 Demonstration of Principle – E-pulse Construction and Convolution

As a demonstration of how the E-pulse technique works, Figure 1-2 is the response of a layered material with $\mu = \mu_0$, $\varepsilon = 9\varepsilon_0$, $\sigma = 0$, and d = 10mm to a transient excitation. The natural frequencies of this material, as shown in Table 1-1, are calculated from the material properties using the software program NAT_FREQ.cpp, which is included in appendix A, and a natural E-pulse, shown in Figure 1-3, is generated using the Fortran program KPNAT.for, which is included in appendix B. When the response is convolved with this E-pulse, using the Fortran program PCONV2.for, included in

appendix C, the resulting late time convolution will be zero as required by (1.2). The resulting convolution waveform is shown in where the late time is indicated by the arrow.

It can be seen that the convolution is zero in the late time. To contrast this, the relative permittivity of the material is changed from 9 to 10 and the resulting response waveform, shown in Figure 1-5, is convolved with the E-pulse generated from the original waveform. The late time response, as indicated by the arrow in the convolution waveform, Figure 1-6, is by inspection, not equal to zero. This would indicate a change in the material properties.

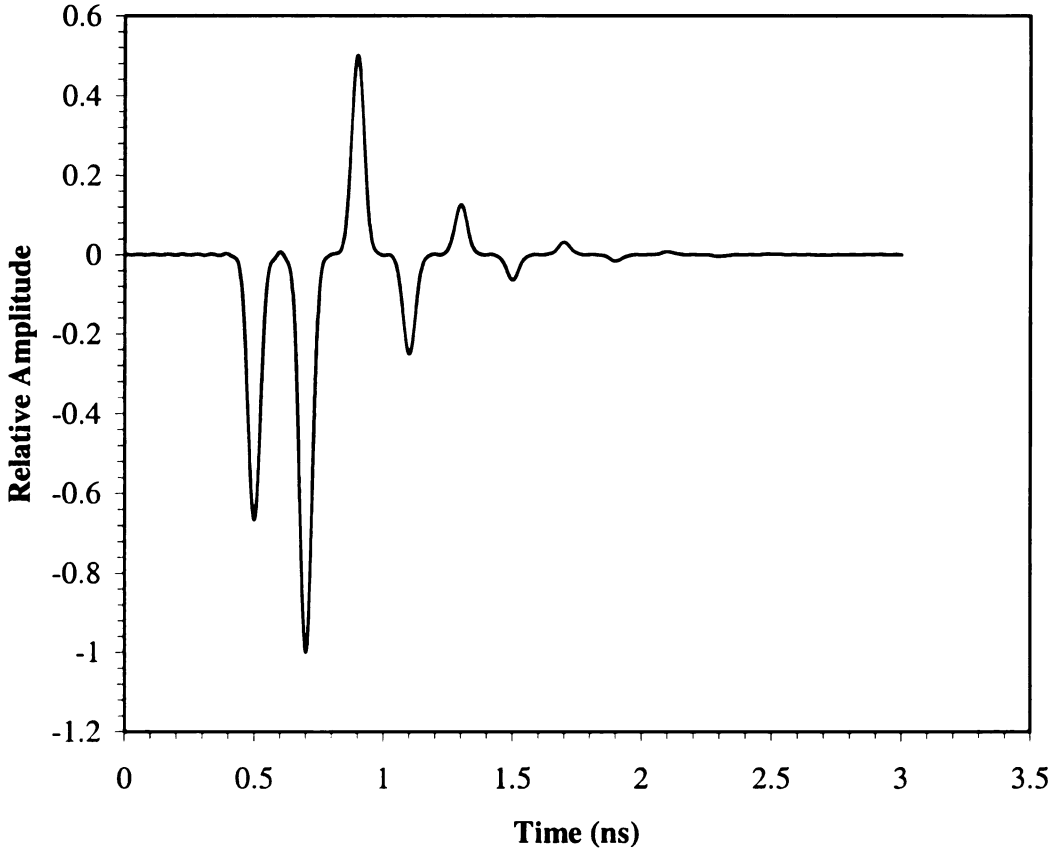

Figure 1-2 Typical response waveform of a layered material,

$\mu = \mu_0$, $\varepsilon = 9\varepsilon_0$, $\sigma = 0$, and d = 10mm .

N	σ_n x 10^9	ω_n (Gr/sec)
1	-3.463	15.697
2	-3.463	47.092
3	-3.463	78.487
4	-3.463	109.882
5	-3.463	141.227

Table 1-1 Natural frequencies of layered material, $\varepsilon_r = 9\varepsilon_0, \mu_0, \sigma = 0, \mathrm{d} = 10\mathrm{mm}$.

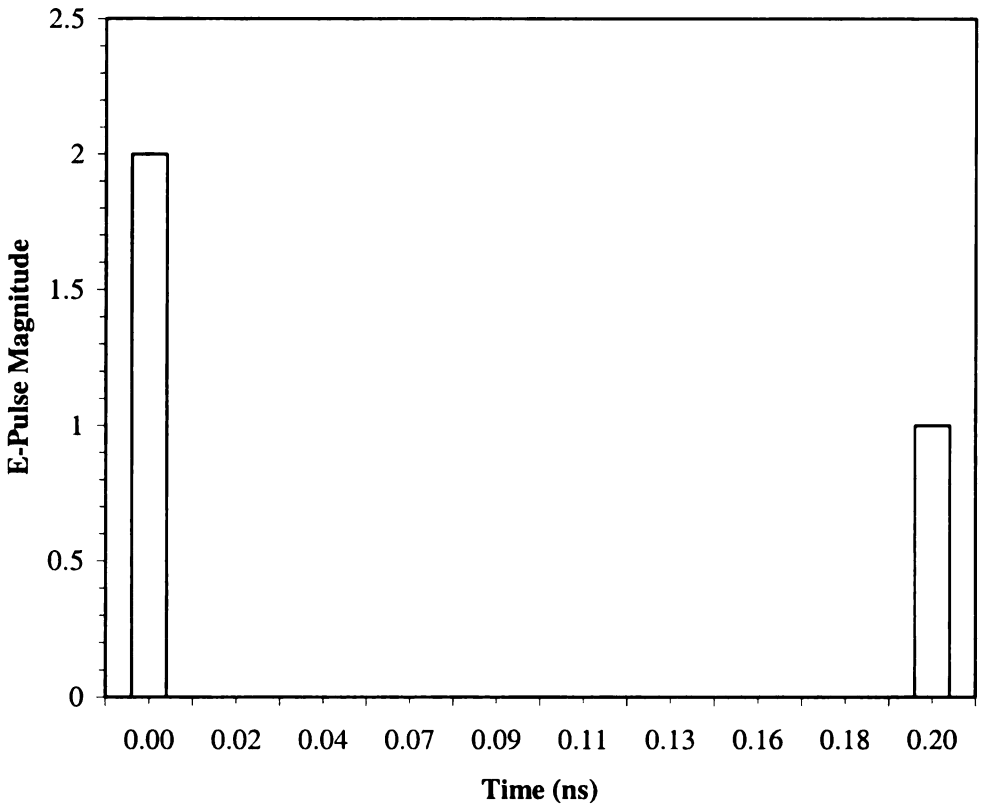

Figure 1-3 E-pulse generated from natural frequencies of layered material.

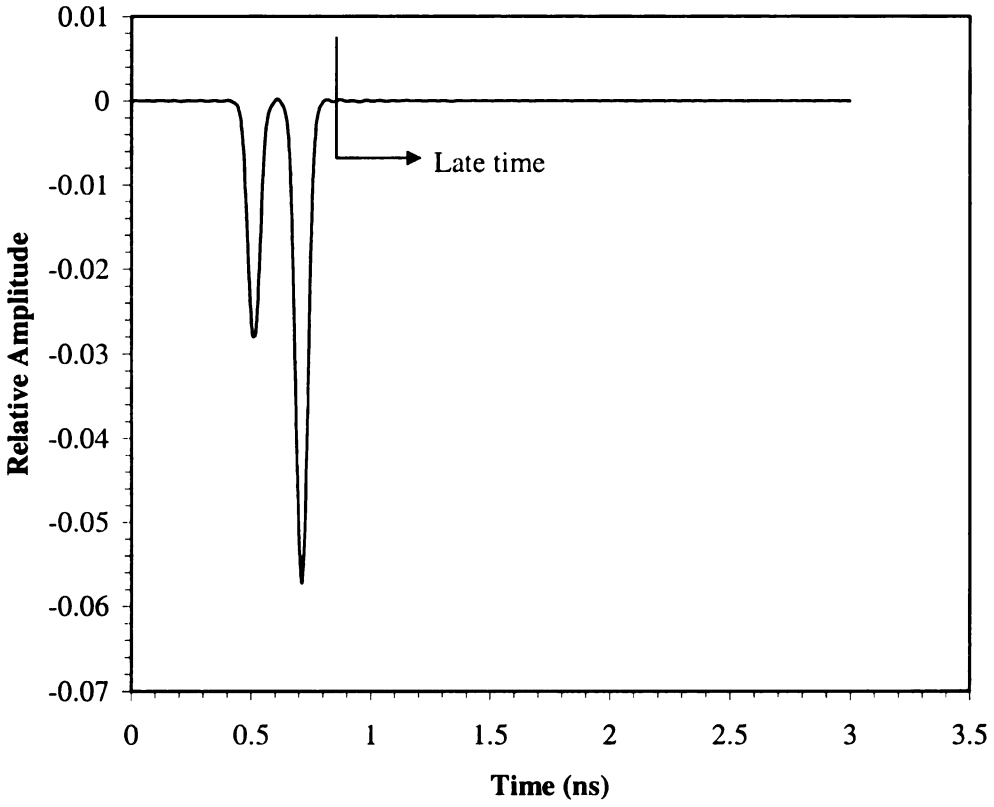

Figure 1-4 Convolution of E-pulse with correct response waveform.

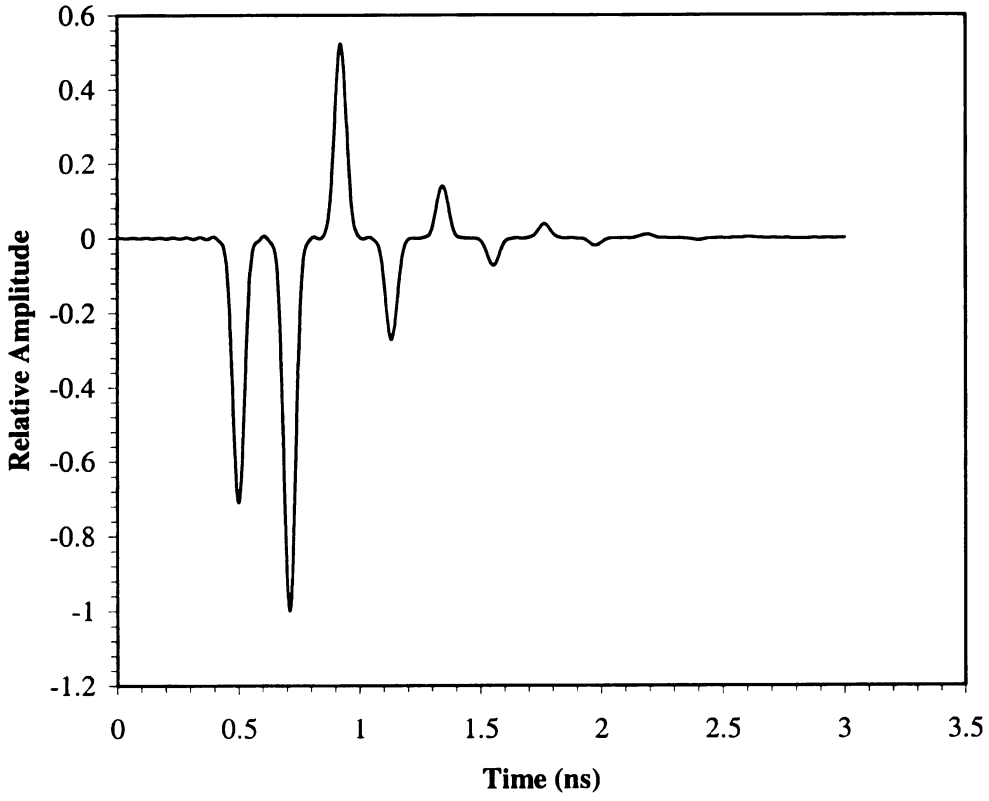

Figure 1-5 Response waveform for layered material,

$\mu = \mu_0$, $\varepsilon = 10\varepsilon_0$, $\sigma = 0$, and d = 10mm .

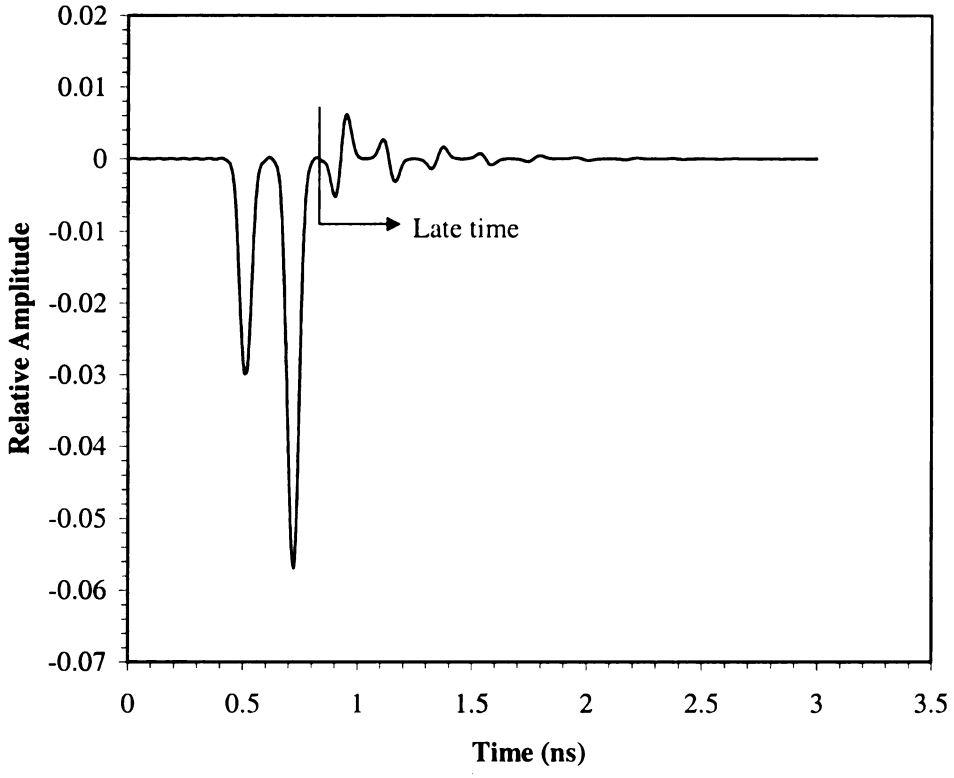

Figure 1-6 Convolution of E-pulse with incorrect response waveform.

Chapter 2

Single Lossless Layer

2.1 Determination of Natural Frequencies for Non-Conductive Materials

The success of the E-pulse technique lies with the ability to determine the natural frequencies of the target under investigation. As has been previously mentioned, the natural frequencies for simple layered materials can be determined theoretically. For a more complex structure, the natural frequencies can be extracted from its scattered response. A simple structure will be defined as a single layer, conductor backed material with real permeability and either real or complex permittivity. A complex structure will be defined as either a single layered material with both complex permittivity and permeability or a multiple layered material. This chapter will discuss the most simple case of a single layer, conductor backed material with real permittivity and permeability (σ=0).

Determining the natural frequencies of simple layered material with no conductivity is done by finding the poles of (1.50). Thus,

$$D(s) = 1 - \Gamma e^{-s\tau} = 0, \tag{2.1}$$

or

$$\Gamma e^{-(\sigma + j\omega)\tau} = 1, \tag{2.2}$$

or

$$\left(\Gamma e^{-\sigma\tau}\right)\left(e^{-j\omega\tau}\right) = 1. \tag{2.3}$$

Since $\Gamma e^{-\sigma\tau}$ is real, then $e^{-j\omega\tau}$ is real and thus equals 1 or -1. Therefore $\Gamma e^{-\sigma\tau}$ also has to equal 1 or -1 to satisfy (2.3). It was shown previously that $\Gamma < 0$, so both quantities must be equal to -1, and

$$e^{-\sigma\tau} = -\frac{1}{\Gamma}. \tag{2.4}$$

Since $-1 \le \Gamma < 0$, the right hand side of (2.4) is positive and greater than zero and so

$$\sigma\tau = -\ln\frac{1}{|\Gamma|}, \tag{2.5}$$

or

$$\sigma = \frac{1}{\tau}\ln|\Gamma| < 0. \tag{2.6}$$

Also,

$$e^{-j\omega\tau} = -1, \tag{2.7}$$

and so

$$\omega\tau = \pm(2n+1)\pi, \quad n = 0,1,2,\cdots, \tag{2.8}$$

or

$$\omega_n = \pm(2n+1)\frac{\pi}{\tau}. \tag{2.9}$$

Therefore, the natural frequencies are

$$\boxed{s_n = \frac{1}{\tau}\ln|\Gamma| \pm j(2n+1)\frac{\pi}{\tau}, \quad n = 0,1,2,\cdots}. \tag{2.10}$$

Note that these frequencies match those in (1.74) and can be calculated given that the relative permittivity, ε_r, thickness of the material layer, d, angle of incidence, θ_i, and the

polarization of the excitation are known. These natural frequencies can then be used to generate E-pulses for the layered material.

2.2 Computation of the EDNa and EDRa

Detecting changes in the properties of materials is done by evaluating the energy in the late-time portion of the convolved waveform. Evaluation of the energy in the late-time convolution can be done by inspection when large changes in material properties occur. However, to determine minor changes in the material properties it is necessary to implement a scheme to quantify the changes. Thus, a threshold level can be determined and a quantitative comparison can be performed for those changes that are not evident by inspection. The determination of changes in the measurements can then be automated and human subjectivity can be eliminated.

This quantitative analysis of the convolution late-time energy was first demonstrated by P. Ilavarasan, et.al. in [7]. Ilavarasan defined the E-Pulse discrimination number (EDN) as,

$$EDN = \left[\int_{T_L}^{T_L+W} c_e^2(t)\,dt \right] \left[\int_0^{T_e} e^2(t)\,dt \right]^{-1}, \tag{2.11}$$

where $\int c_e^2(t)\,dt$ is the energy in the convolution waveform, $\int e^2(t)\,dt$ is the energy in the E-pulse waveform, T_L is the start of late-time, W is some time later than T_L determined such that most of the energy of the late-time is considered, and T_e is the duration of the E-pulse. Essentially, the EDN is the late-time energy of the convolution waveform normalized by the E-pulse energy.

This definition of the EDN is appropriate for applications in target discrimination where one target response is convolved with a database of many E-pulses for known targets. However, in the case of layered material diagnostics, Ilavarasan's definition of the EDN is not appropriate. This leads to the definition of version 'a' of the E-Pulse discrimination number (EDNa),

$$EDNa = \left[\int_{T_L}^{T_L+W} c_e^2(t)\,dt \right] \left[\int_0^{T_e} e^2(t)\,dt \int_{T_L}^{T_L+W} r^2(t)\,dt \right]^{-1}, \tag{2.12}$$

where $\int r^2(t)\,dt$ is the energy in the response waveform. When analyzing layered materials there is only one E-pulse generated from a baseline response measurement of the material and from this an EDNa is calculated. The E-pulse is then convolved with the scattered response of the material at a later time and a new EDNa is calculated and compared to the baseline EDNa. In order to account for any possible changes in the amplitude measurement of the response, the EDN must be normalized by the response waveform energy as well as by the E-pulse energy.

Through the use of the EDNa, minor changes in the material properties can be detected. An initial baseline response measurement can be used to generate an E-Pulse for a specified layered material. Using these two waveforms, the EDNa is calculated and should be zero. However, practical measurements will contain some level of noise and inaccuracies in determining the exact natural frequencies will prevent the EDNa from completely vanishing. To allow consistent comparisons of changes in the EDNa, a variant of the E-Pulse discrimination ratio (EDR) described by Ilavarasan in [7] is defined as

$$EDRa(dB) = 10\log_{10}\left\{\frac{EDNa}{baseline\ EDNa}\right\}. \tag{2.13}$$

If the material does not undergo any changes from its baseline, the calculated EDNa should not change from its baseline measurement and the EDRa should yield a 0dB reading. On the other hand, if the material undergoes a change in one of its properties, the EDNa measurement will increase and consequently so will the EDRa. Depending on the how much change is tolerated in the layered material properties, a threshold can be established and the EDRa measurement can be used to determine whether the threshold has been exceeded.

The EDRa will not be utilized for the noise-free data cases. Theoretically, since the data is noise free, the EDNa for the baseline case will be zero. Therefore, calculating the EDRa for all cases except the baseline will be indeterminate since the denominator in (2.13) will be zero. The EDRa will be used only when analyzing the noise corrupted data. In those cases, the baseline EDNa will never be zero, due to the noise, so an appropriate EDRa value can be calculated.

2.2.1 Change in Layer Thickness

The first material property to be examined will be the thickness of the material layer. The following examples involve noise free responses constructed using the baseline material properties shown in Table 2-1.

Several scattered responses of layered materials were simulated using the Fortran program MLPREF.for, which is included in appendix D. The properties of the layered materials used to create the responses are shown in Table 2-2. Input for the MLPREF.for program is the material properties (e.g., number of layers, thickness of layers,

permittivity, permeability, etc.). Output from MLPREF.for is the scattered response data presented in the frequency domain. Analysis of the response data requires it to be in the time domain so another software program, UTIL2B.exe, was used to process the frequency domain data. The magnitude data for the frequency response generated using MLPREF.for for a typical layered material is shown in Figure 2-1. The frequency content is a user defined input in MLPREF.for and the frequency range 0-18GHz was chosen for this case. Since the layer is backed by a conductive plate the magnitude of the frequency response is one, as expected.

Since there is a discontinuity in the data at 18 GHz, the inverse Fourier transform (IFFT) data will include many high frequencies, as shown in Figure 2-2. This makes it difficult to analyze the time domain data. In order to remove the effects of the discontinuity, the frequency domain data was processed with a Gaussian modulated cosine windowing function with a width, $\tau = 0.06\ ns$, and a center frequency of 0 GHz, as seen in Figure 2-3, before running the IFFT program. The result, shown in Figure 2-4, is a cleaner time domain response waveform containing the same pertinent information as Figure 2-2, but without the unnecessary high frequency content.

Thickness of layer	d=10mm
Permittivity of layer	$\varepsilon=9\varepsilon_0$
Permeability of layer	$\mu=\mu_0$
Conductivity of layer	$\sigma=0$
Angle of incidence of excitation	$\theta=0^\circ$
Polarization of excitation	Parallel polarization
Number of modes used to calculate E-pulse	5 modes

Table 2-1 Material properties of the baseline layered material.

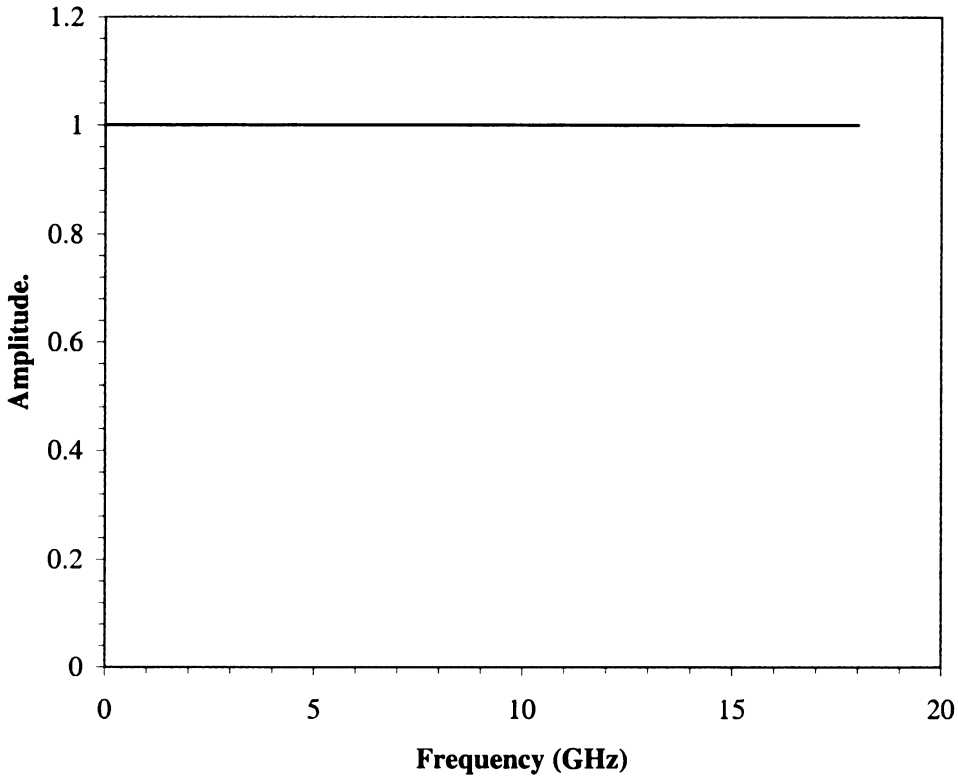

Figure 2-1 Magnitude data for response generated using MLPREF.for.

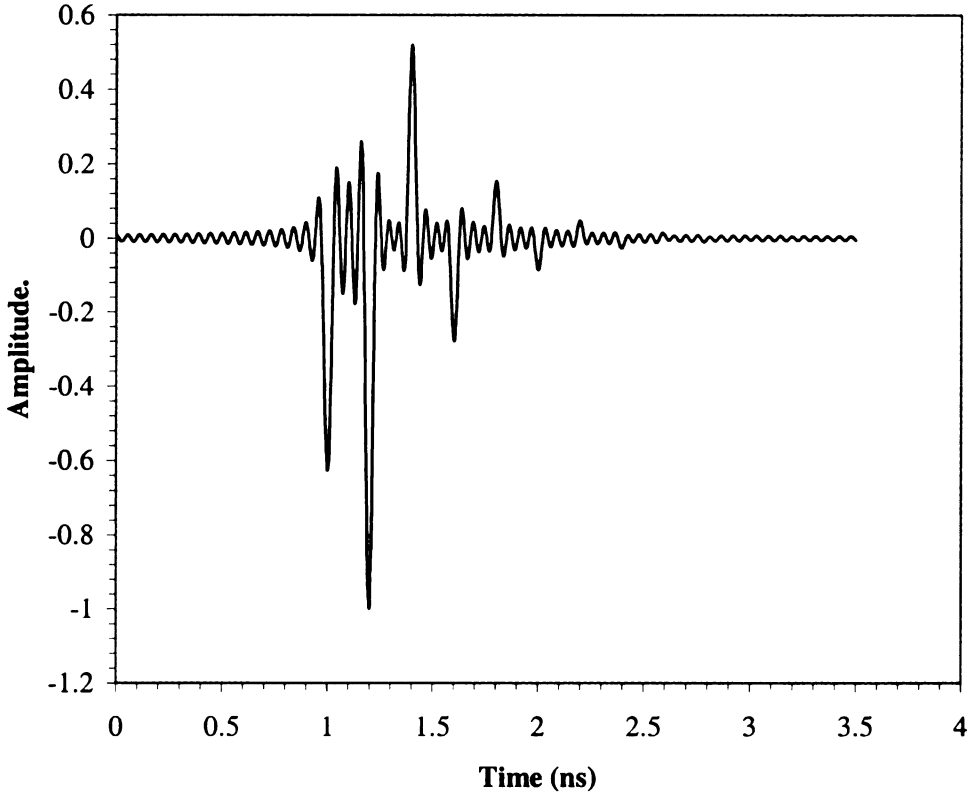

Figure 2-2 IFFT of response data without windowing function.

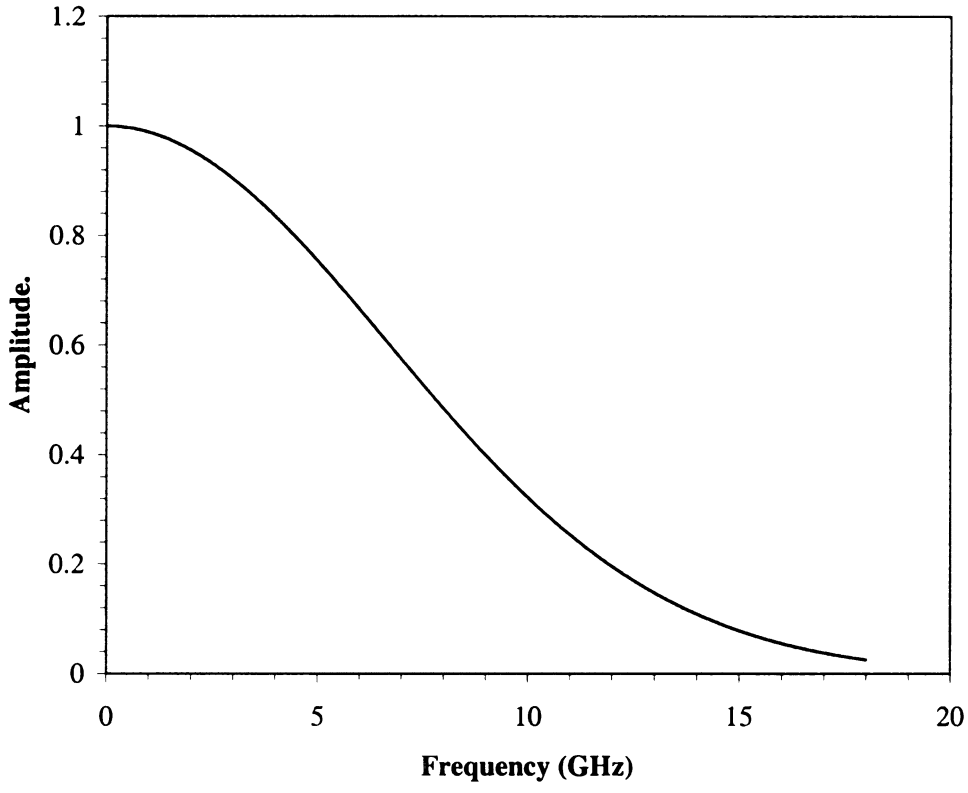

Figure 2-3 Frequency domain data with window function applied.

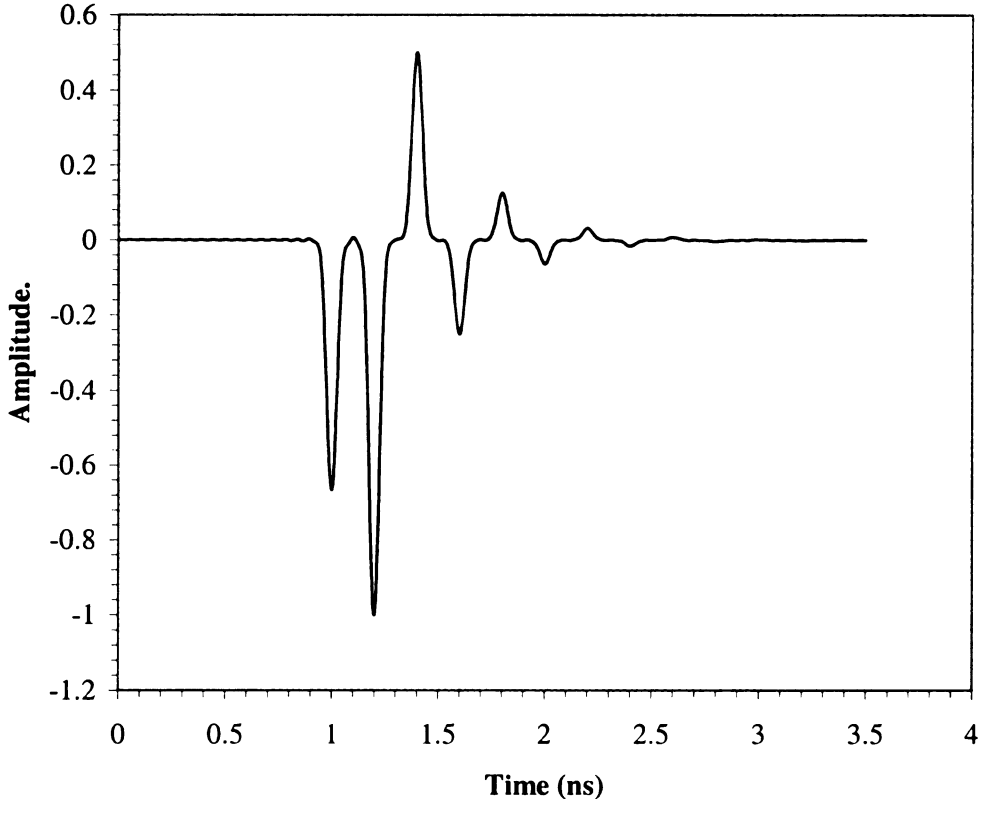

Figure 2-4 IFFT of response data with windowing function.

It would not be practical to present every waveform simulated, so a few are shown as examples. Referring to Table 2-2 for the material reference for each response, the extremes of the measurements, material 'A' and material 'P', are shown in Figure 2-5 and Figure 2-6. Each spike in the plots is a reflection of the incident wave. It can easily be seen that the thicker the material, the farther apart each reflection is separated. It is very difficult to see any difference in the responses between the materials that have relatively minor changes in their thickness. This is shown by plotting the response waveforms for materials 'G', 'H', and 'I' on the same plot, Figure 2-7.

To evaluate these response waveforms for changes in the thickness of the layer, each response is convolved with an E-pulse, shown in Figure 2-8. This E-pulse is generated using the Fortran program KPNAT.for. The program generates the E-pulse from the natural frequencies of the baseline material, shown in Table 1-1, using (2.10). This E-pulse will be known as the baseline E-pulse. Figure 2-9 shows the convolution of the material H response with the baseline E-pulse. It can be seen that the energy in the late time,

$$T_L = 2T_{tr} + T_p + T_d \,, \tag{2.14}$$

where T_{tr} is the one-way transit time through the layer (which varies depending on properties of the layer and the aspect angle), T_p is the incident excitation pulse width (0.1ns), and T_d is the time before the excitation pulse strikes the face of the layer (0.5ns), is zero as expected. In comparison, the convolutions of the other responses are shown in Figure 2-10, Figure 2-11, Figure 2-12, and Figure 2-13. It is evident in all of these plots, even when the thickness is only changed by 2.5%, as is the case for both material 'G' and material 'I', that the late-time energy is greater than zero. This signifies a change in the

thickness.

Material	ε	μ	σ	Thickness (mm)	Polarization	Angle of incidence, θ_i
A	$9\varepsilon_0$	μ_0	0	5	Parallel	0
B	$9\varepsilon_0$	μ_0	0	6	Parallel	0
C	$9\varepsilon_0$	μ_0	0	7	Parallel	0
D	$9\varepsilon_0$	μ_0	0	8	Parallel	0
E	$9\varepsilon_0$	μ_0	0	9	Parallel	0
F	$9\varepsilon_0$	μ_0	0	9.5	Parallel	0
G	$9\varepsilon_0$	μ_0	0	9.75	Parallel	0
H (baseline)	$9\varepsilon_0$	μ_0	0	10	Parallel	0
I	$9\varepsilon_0$	μ_0	0	10.25	Parallel	0
J	$9\varepsilon_0$	μ_0	0	10.5	Parallel	0
K	$9\varepsilon_0$	μ_0	0	11	Parallel	0
L	$9\varepsilon_0$	μ_0	0	12	Parallel	0
M	$9\varepsilon_0$	μ_0	0	13	Parallel	0
N	$9\varepsilon_0$	μ_0	0	14	Parallel	0
P	$9\varepsilon_0$	μ_0	0	15	Parallel	0

Table 2-2 Material properties for changing thickness.

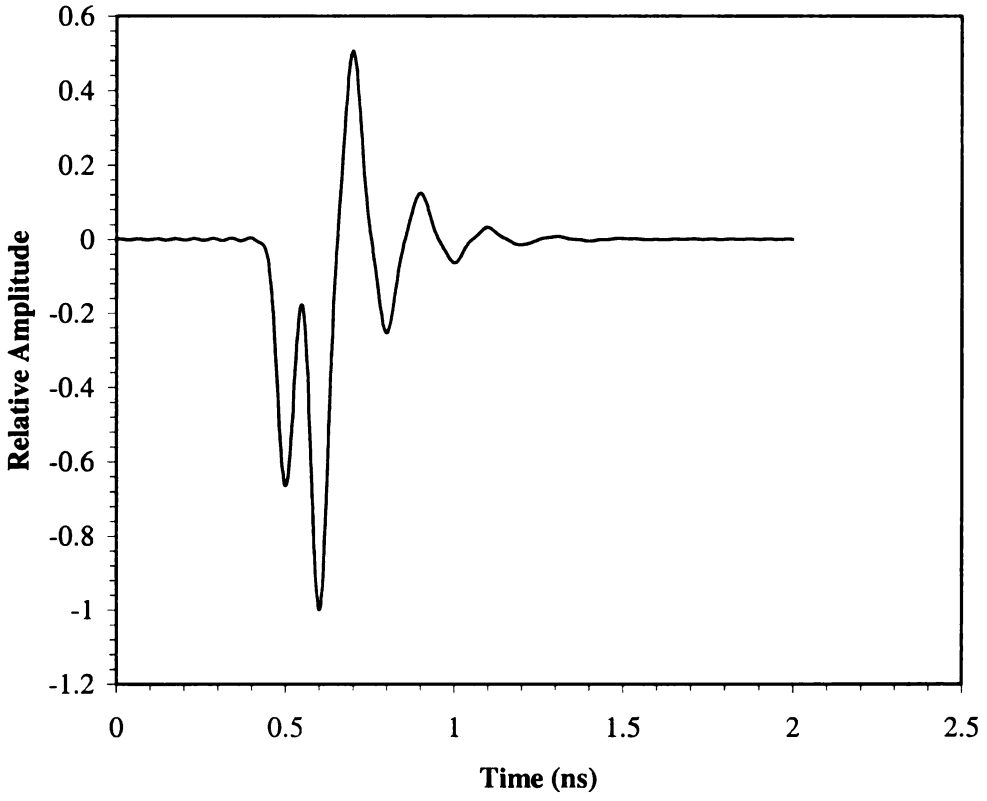

Figure 2-5 Response waveform for material 'A'.

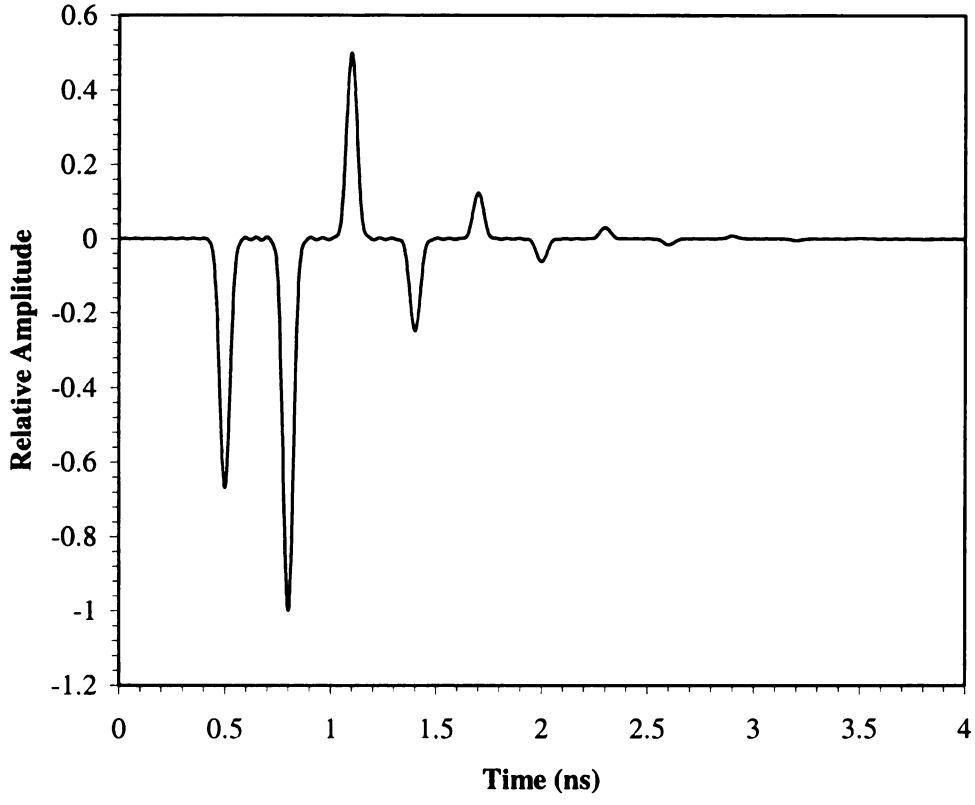

Figure 2-6 Response waveform for material 'P'.

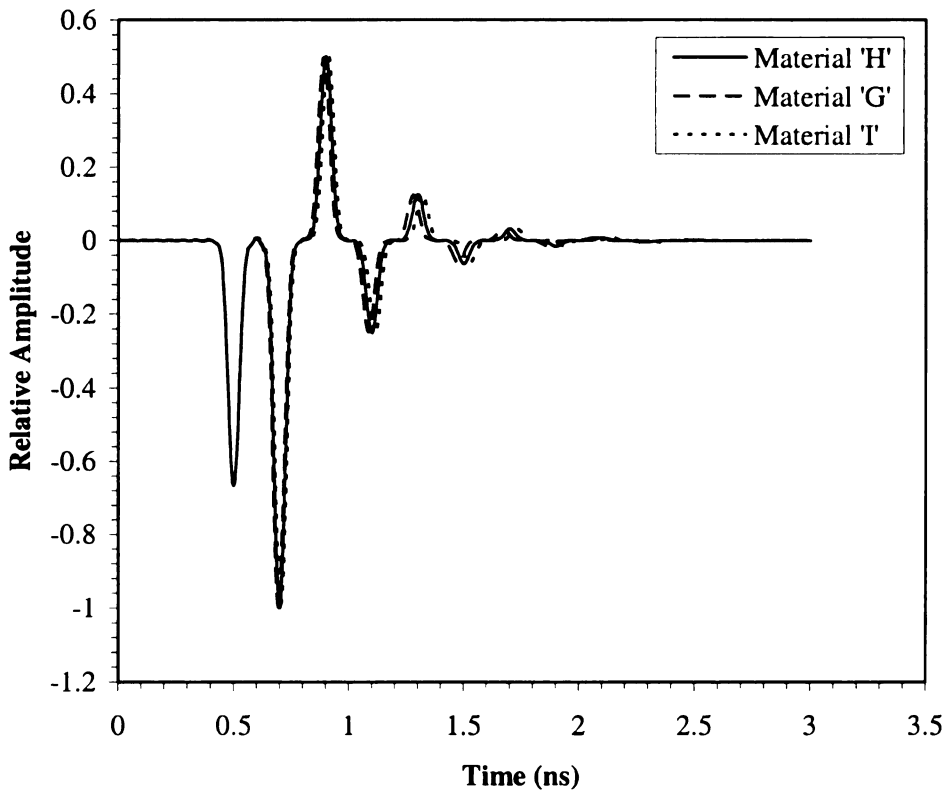

Figure 2-7 Comparison of response waveforms for materials 'G', 'H', and 'I'.

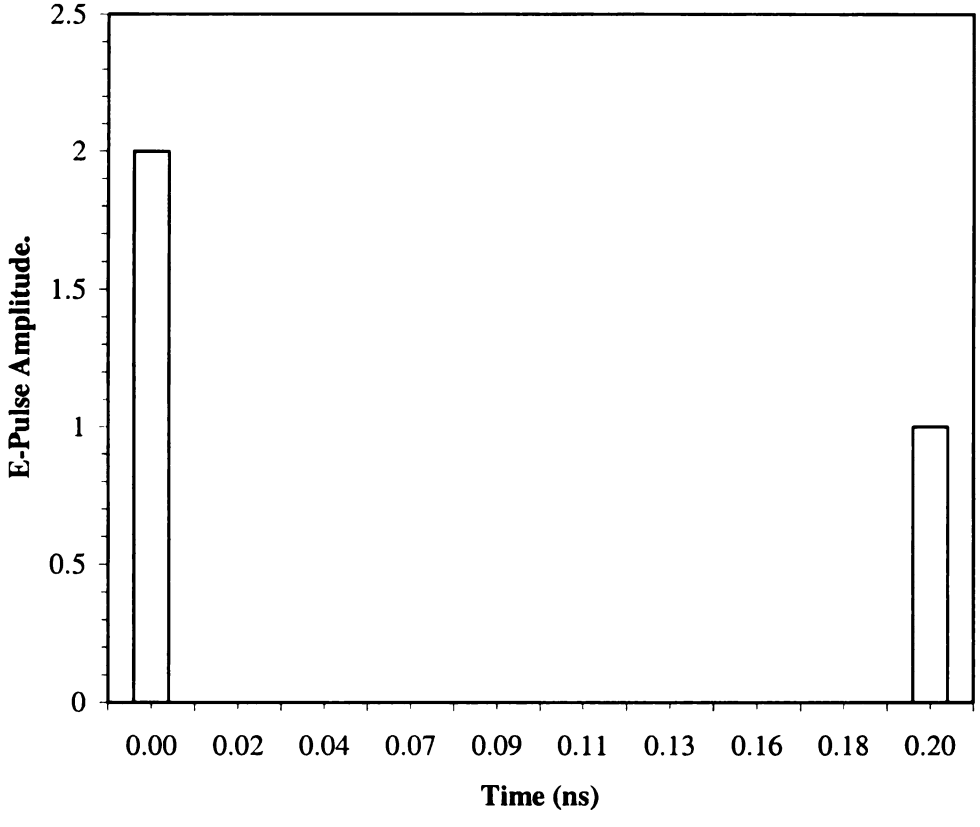

Figure 2-8 E-pulse generated from the baseline material properties.

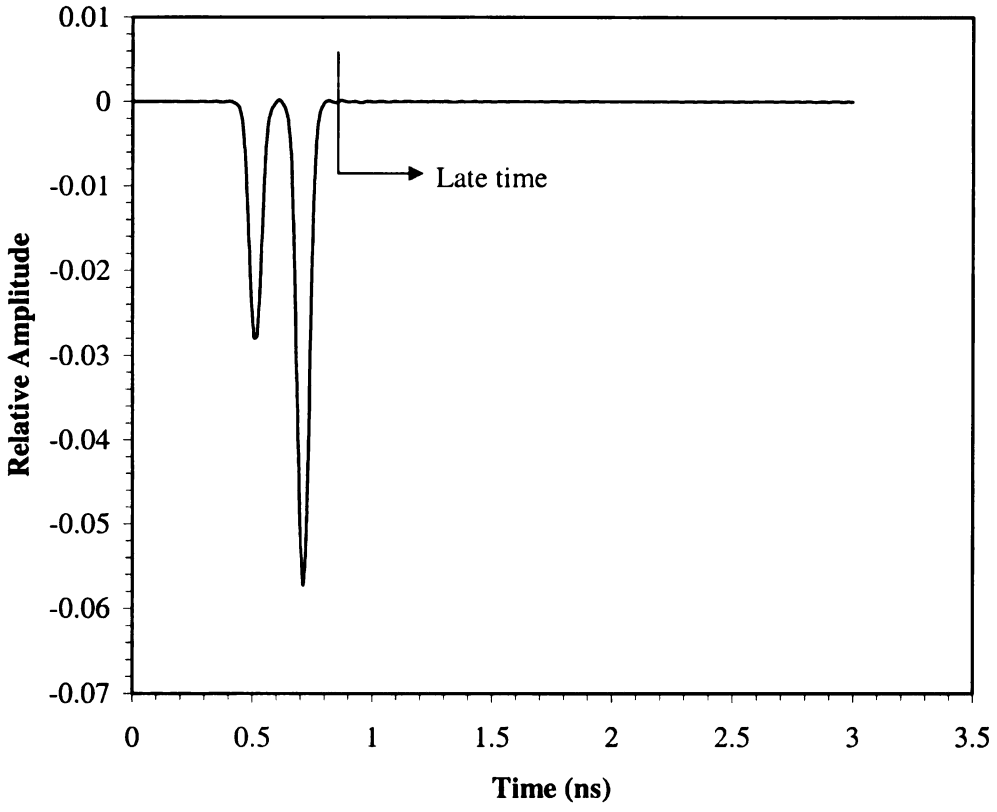

Figure 2-9 Convolution of baseline response with baseline E-pulse.

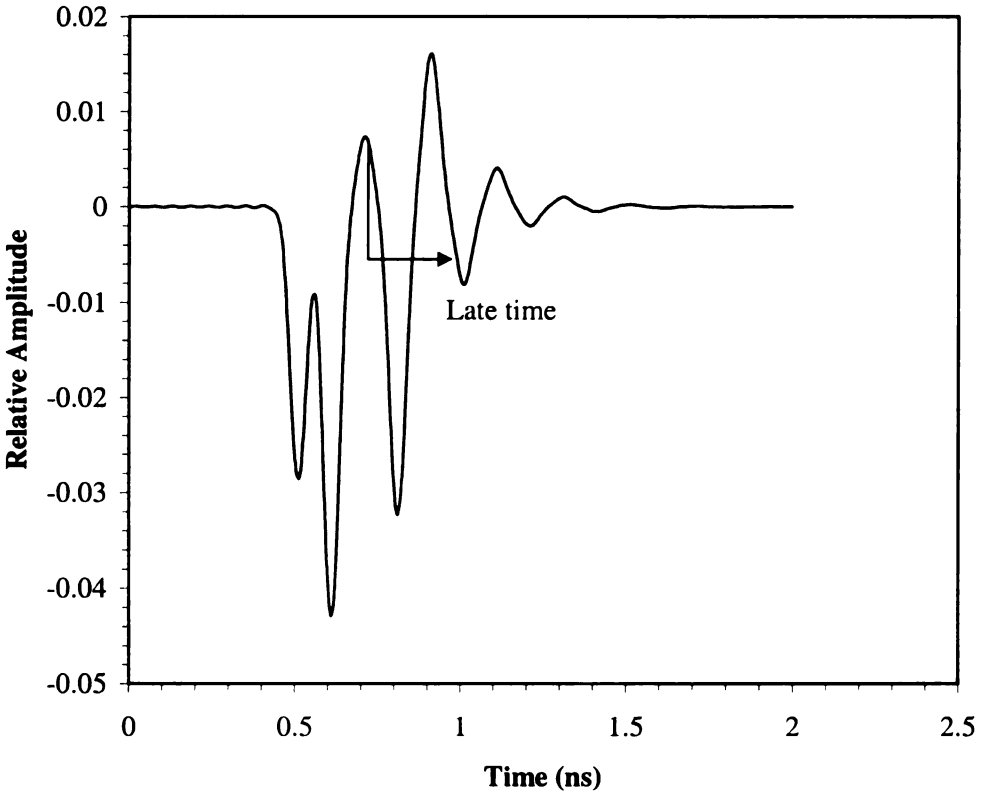

Figure 2-10 Convolution of material 'A' response with baseline E-pulse.

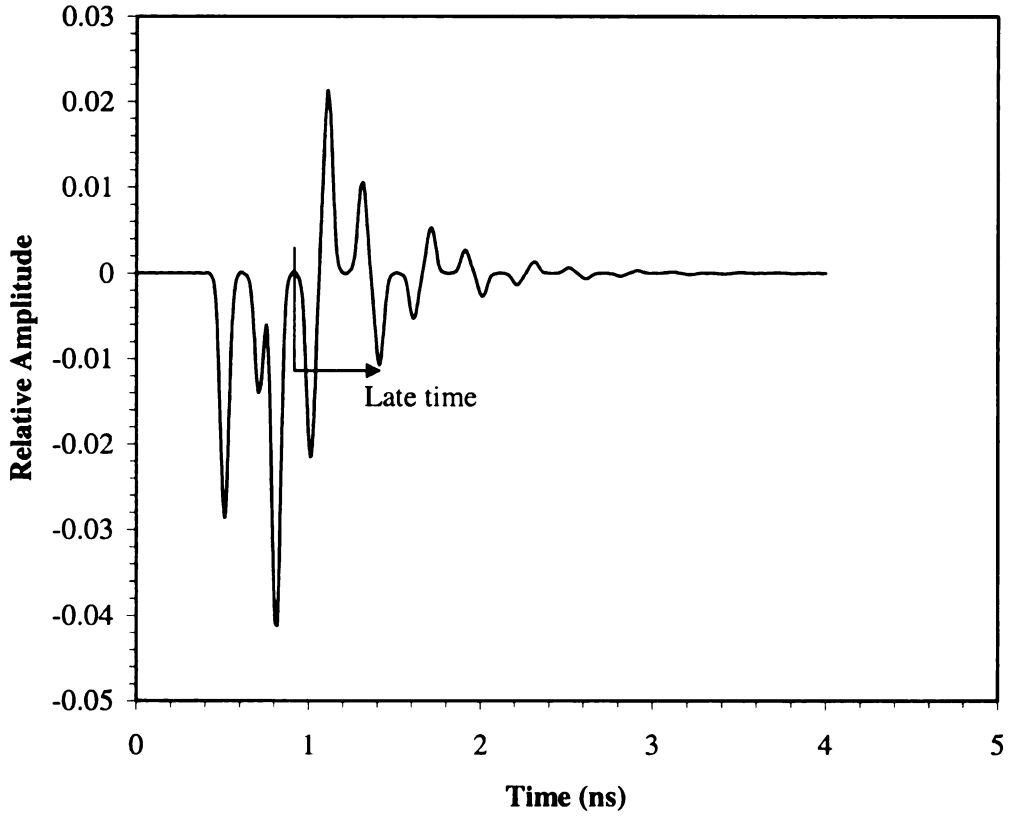

Figure 2-11 Convolution of material 'P' response with baseline E-pulse.

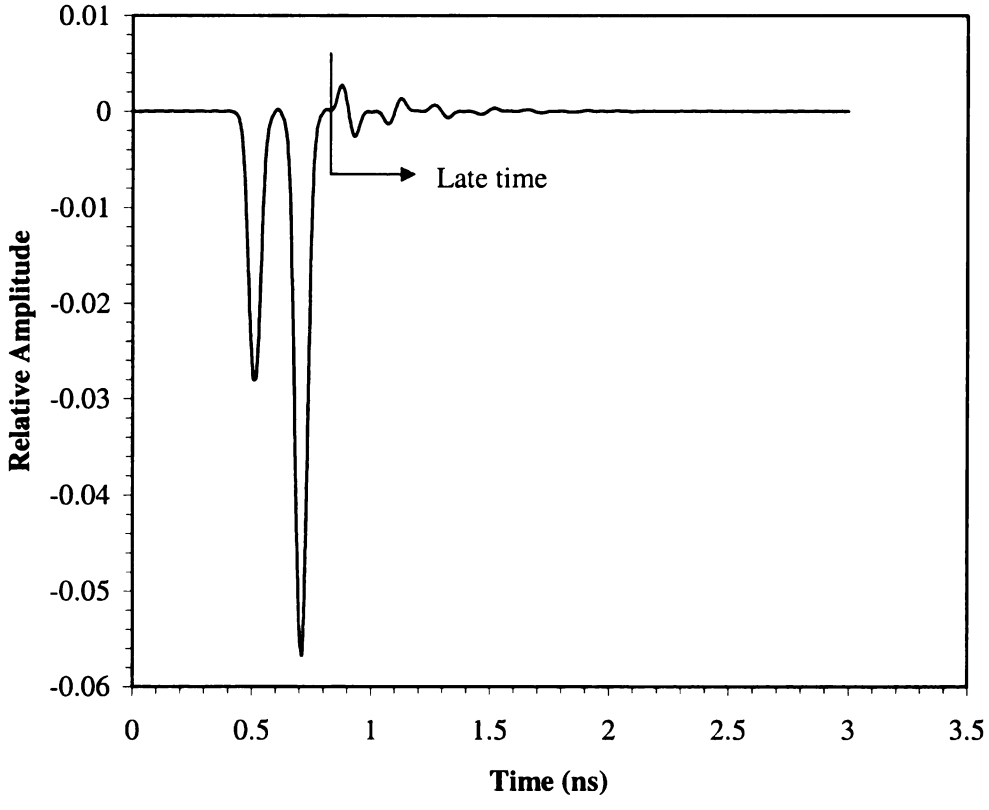

Figure 2-12 Convolution of material 'G' response with baseline E-pulse.

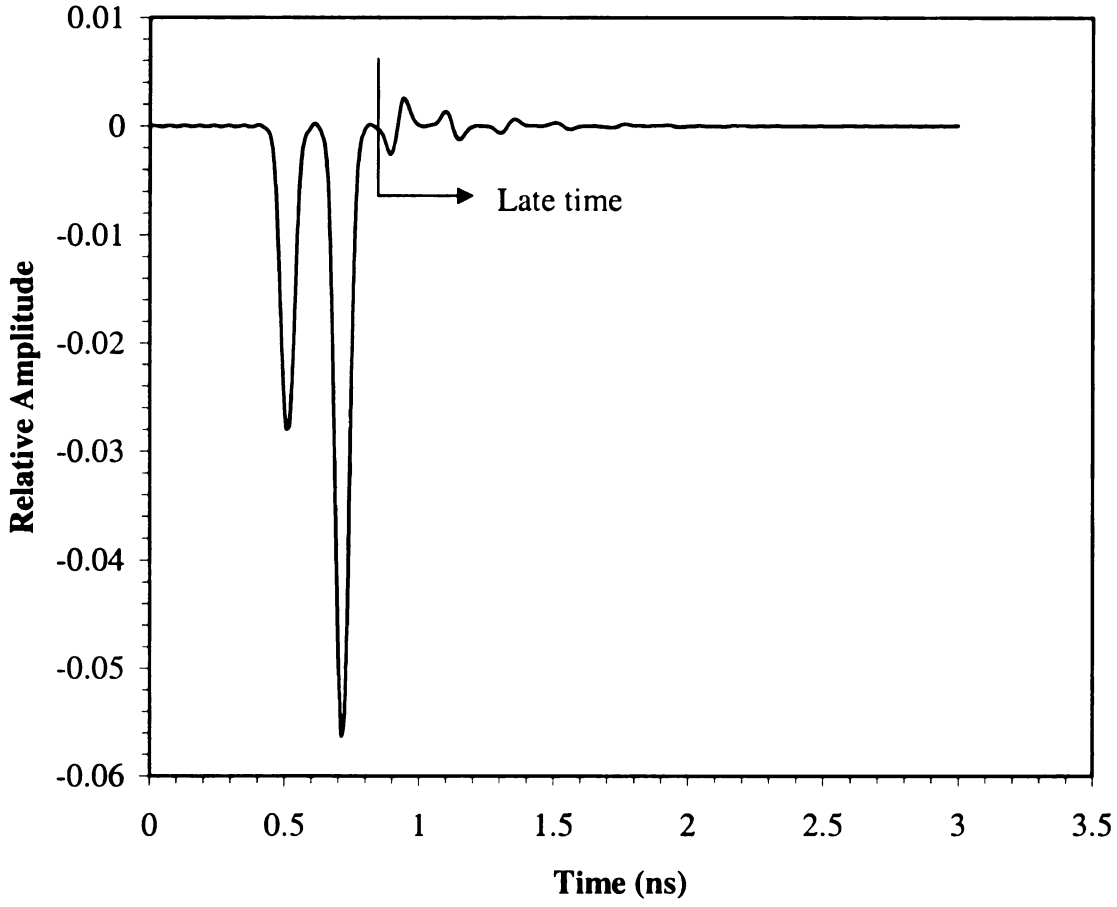

Figure 2-13 Convolution of material 'I' response with baseline E-pulse.

To quantify the results, the EDNa is calculated. These values for each of the materials examined are shown in Table 2-3. Since this data is noise free, theoretically the EDNa should be zero for the baseline material. This is not the case due to numerical error in generating the response waveforms and in calculating the convolutions. Using only 5 modes to generate the E-pulse also contributes to the error. Figure 2-14 shows a plot of the tabulated EDNa calculations. It can be seen that as the change in thickness from the baseline increases the EDNa increases as well. Determining how much change in thickness can be detected using the EDNa plots depends on the noise level. This will be discussed later in this chapter.

Material	Thickness	EDNa
A	5	7.30E-03
B	6	6.63E-03
C	7	5.15E-03
D	8	3.10E-03
E	9	9.73E-04
F	9.5	2.61E-04
G	9.75	6.78E-05
H	10	3.70E-07
I	10.25	6.24E-05
J	10.5	2.51E-04
K	11	9.54E-04
L	12	3.06E-03
M	13	4.94E-03
N	14	5.95E-03
P	15	6.33E-03

Table 2-3 EDNa calculations for change in thickness.

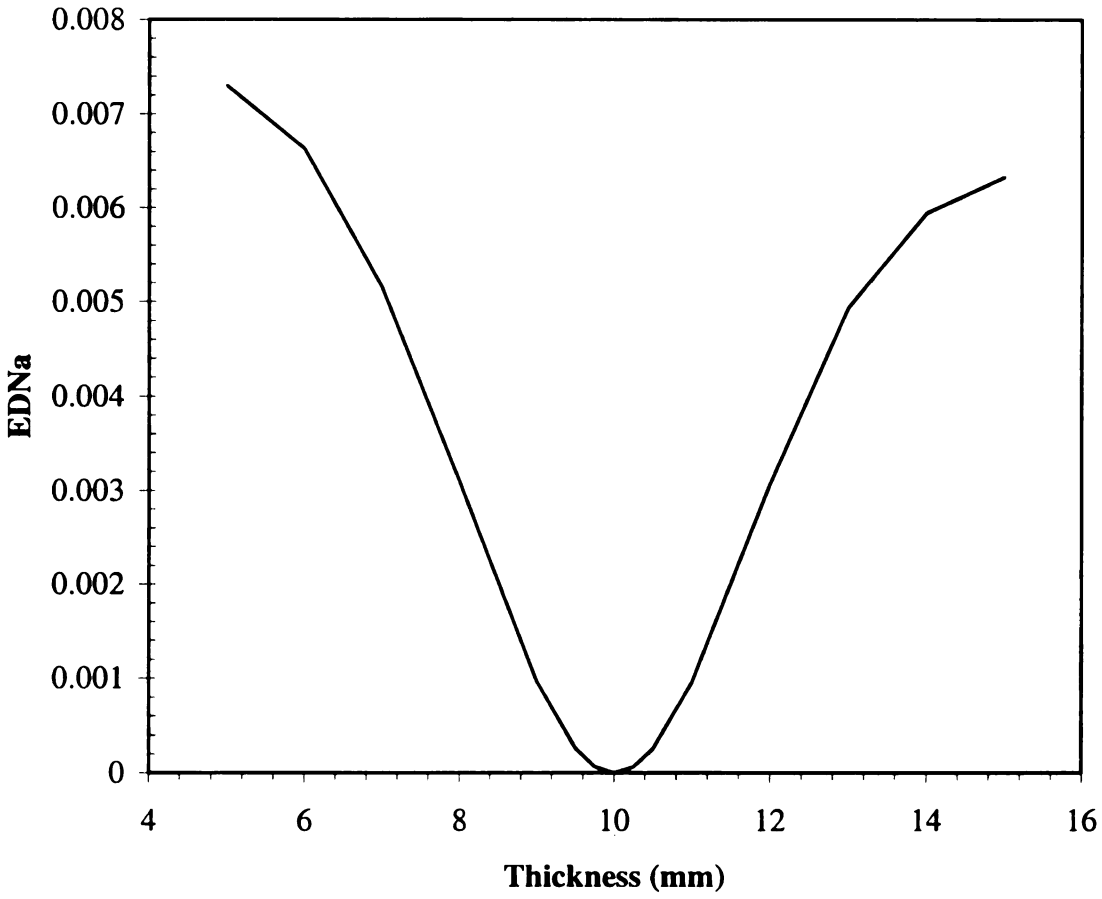

Figure 2-14 EDNa vs. change in thickness for single lossless layer.

2.2.2 Change in Layer Relative Permittivity

The ability to diagnose changes in the relative permittivity of the material layer is now examined. The following examples involve noise free responses and the baseline material properties are the same as for changes in thickness and are shown in Table 2-1.

Several scattered responses of layered materials were again simulated using MLPREF.for. The properties of the layered materials used to create the responses are shown in Table 2-4.

Again only a limited selection of examples was chosen. Citing Table 2-4 for the material reference for each response, the extremes of the measurements, material 'A' and material 'P', are shown in Figure 2-15 and Figure 2-16, respectively. It can be seen that the permittivity affects the separation of the reflections just as the thickness of the layer does. It is very difficult to see any difference in the responses between the materials that have relatively minor changes in their permittivity. This is shown by plotting the response waveforms for materials 'G', 'H', and 'I' on the same plot, Figure 2-17.

Evaluation of these response waveforms for changes in the permittivity of the layer is done exactly as before with changes in thickness. Each response is convolved with an E-pulse, shown in Figure 2-8, which is generated from the natural frequencies of the baseline material, shown in Table 1-1. This will again be known as the baseline E-pulse. The same convolution, as seen previously in Figure 2-9, of the material 'H' response with the baseline E-pulse shows the energy in the late time as zero. In comparison, the convolutions of the other responses are shown in Figure 2-18, Figure 2-19, Figure 2-20, and Figure 2-21. It is evident in all of these plots, even when there is relatively minimal change in the permittivity, as is the case for both material 'G' and

material 'I', that the late-time energy is greater than zero. This signifies a change in the permittivity of the material layer.

Material	ε	μ	σ	Thickness (mm)	Polarization	Angle of incidence, θ_i
A	$4\varepsilon_0$	μ_0	0	10	Parallel	0
B	$5\varepsilon_0$	μ_0	0	10	Parallel	0
C	$6\varepsilon_0$	μ_0	0	10	Parallel	0
D	$7\varepsilon_0$	μ_0	0	10	Parallel	0
E	$8\varepsilon_0$	μ_0	0	10	Parallel	0
F	$8.5\varepsilon_0$	μ_0	0	10	Parallel	0
G	$8.75\varepsilon_0$	μ_0	0	10	Parallel	0
H (baseline)	$9\varepsilon_0$	μ_0	0	10	Parallel	0
I	$9.25\varepsilon_0$	μ_0	0	10	Parallel	0
J	$9.5\varepsilon_0$	μ_0	0	10	Parallel	0
K	$10\varepsilon_0$	μ_0	0	10	Parallel	0
L	$11\varepsilon_0$	μ_0	0	10	Parallel	0
M	$12\varepsilon_0$	μ_0	0	10	Parallel	0
N	$13\varepsilon_0$	μ_0	0	10	Parallel	0
P	$14\varepsilon_0$	μ_0	0	10	Parallel	0

Table 2-4 Material properties for changing permittivity.

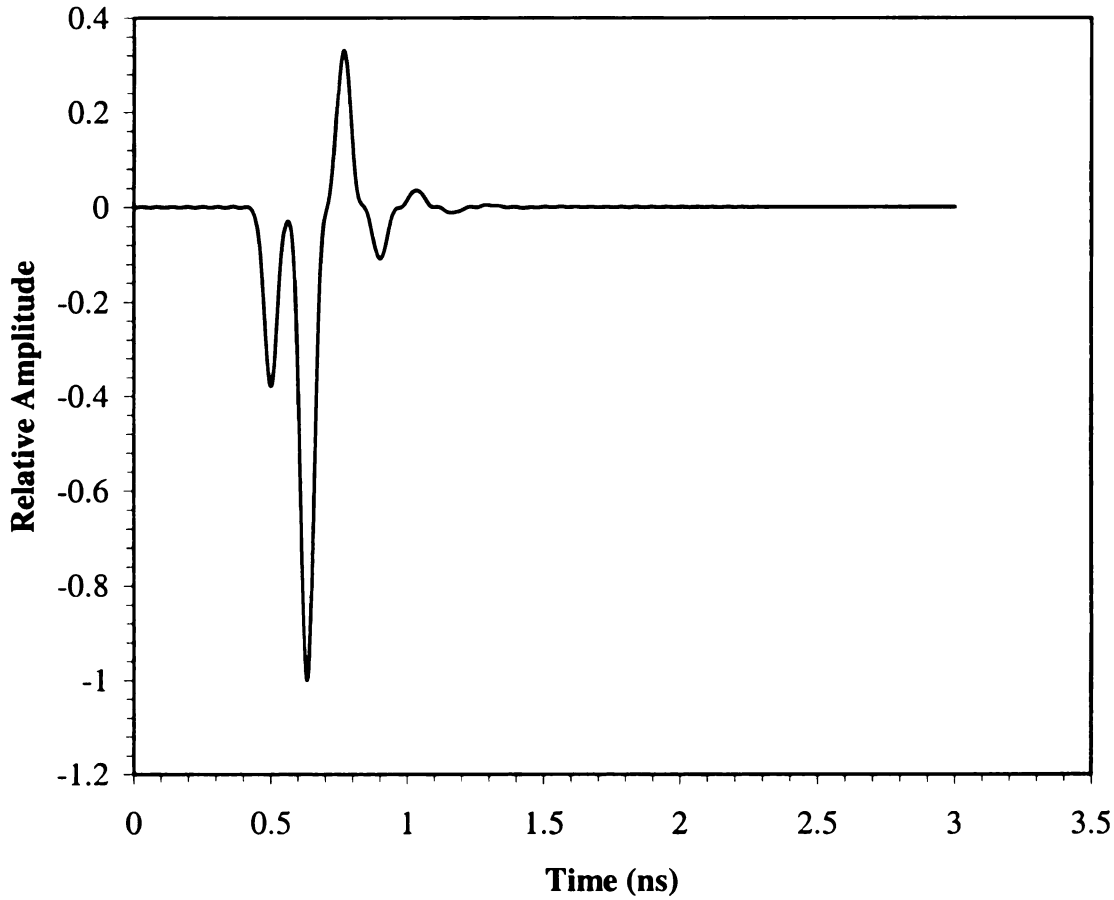

Figure 2-15 Response waveform for material 'A'.

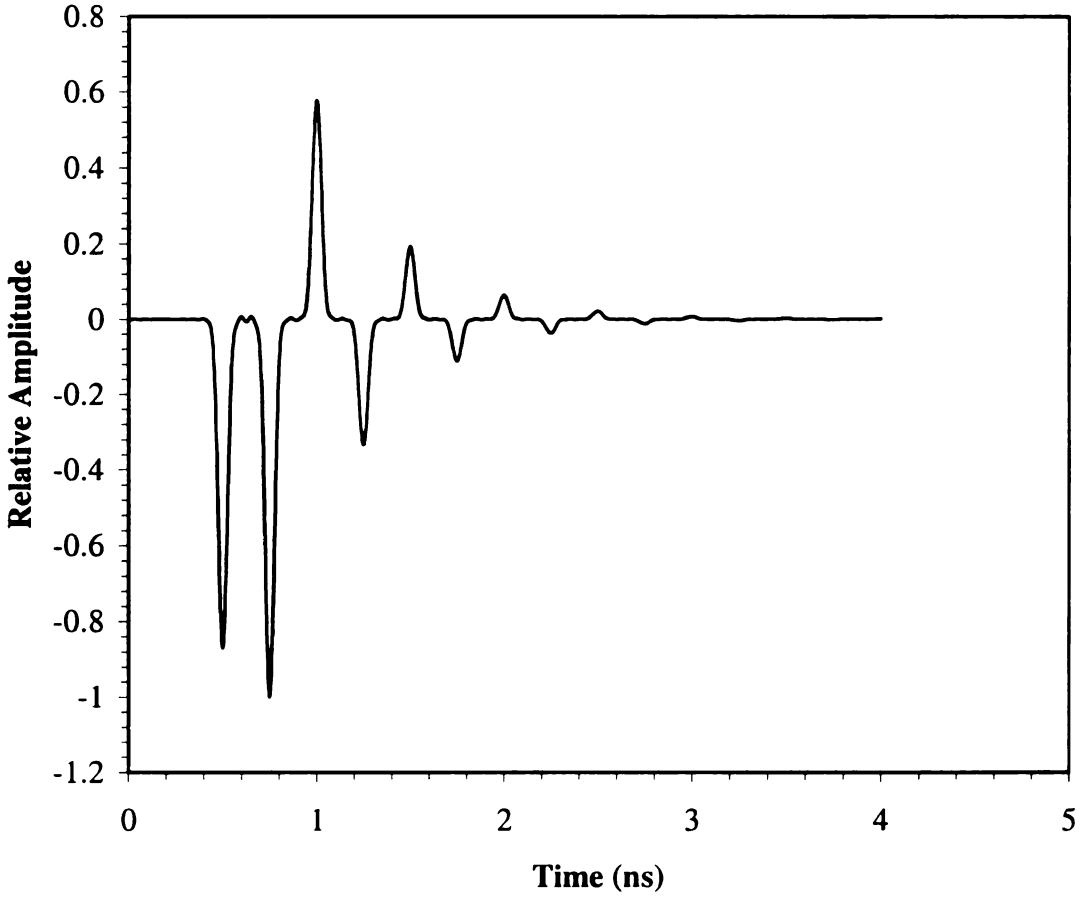

Figure 2-16 Response waveform for material 'P'.

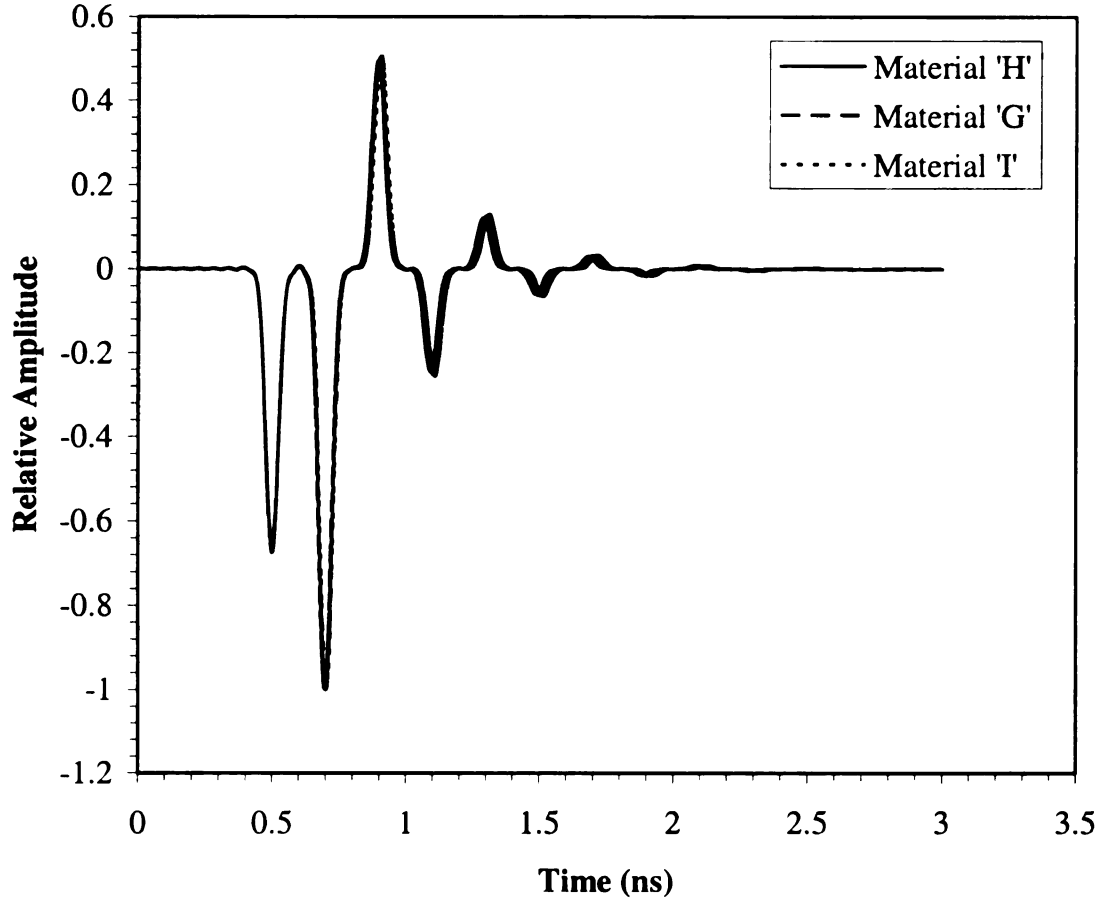

Figure 2-17 Comparison of response waveforms for materials 'G', 'H', and 'I'.

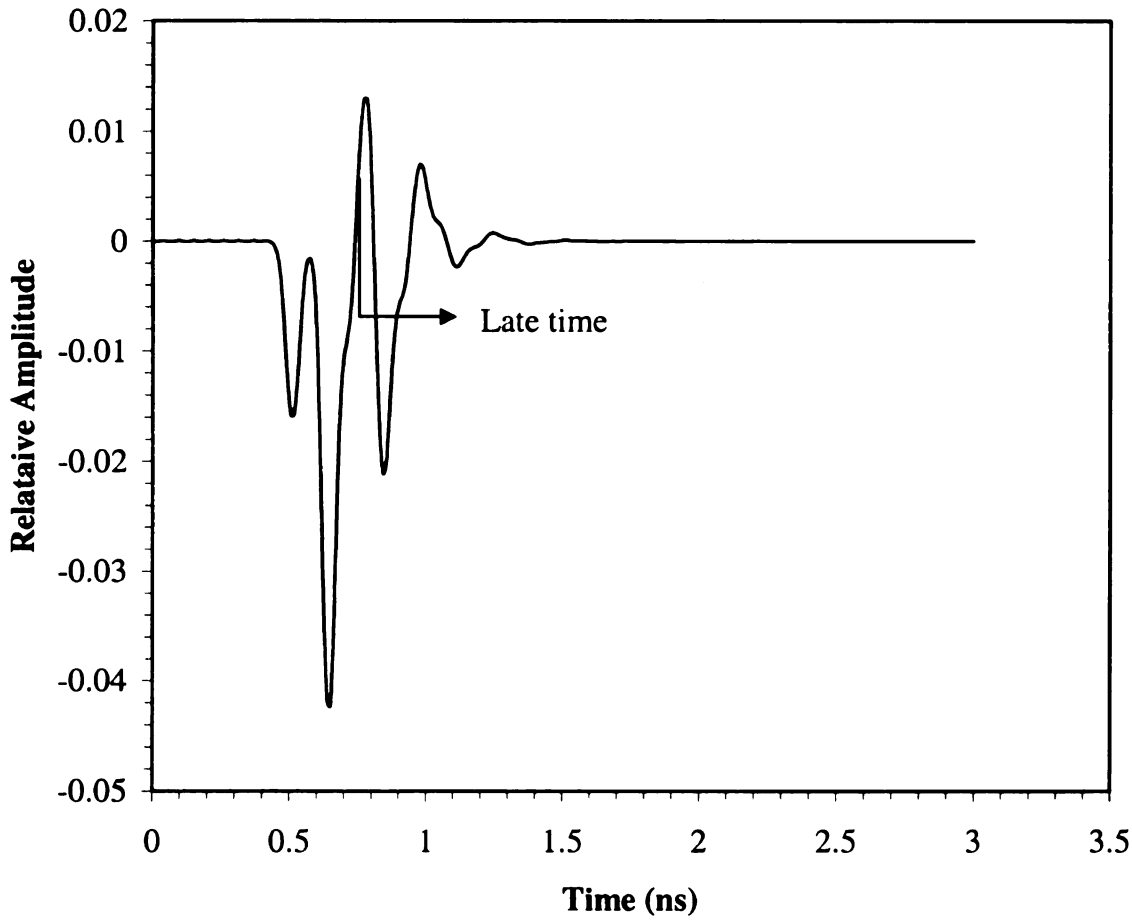

Figure 2-18 Convolution of material 'A' response with baseline E-pulse.

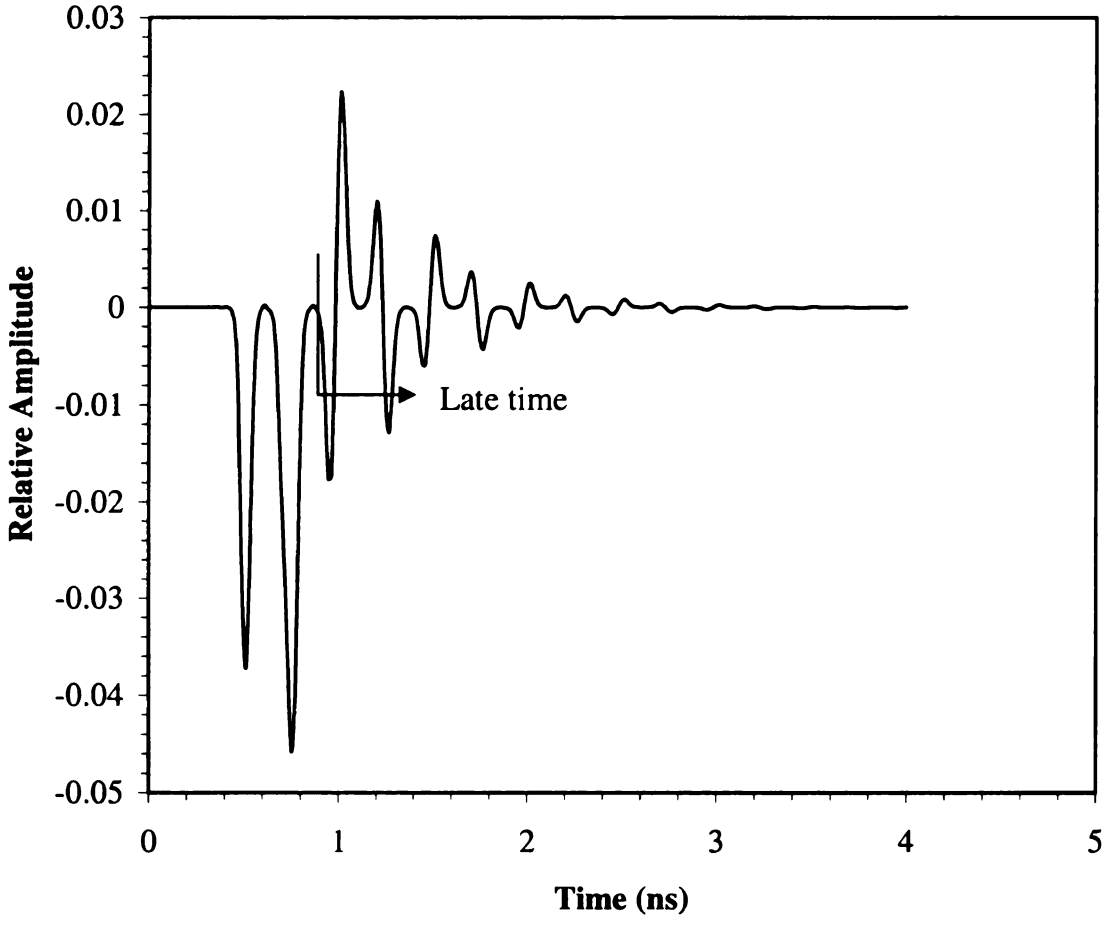

Figure 2-19 Convolution of material 'P' response with baseline E-pulse.

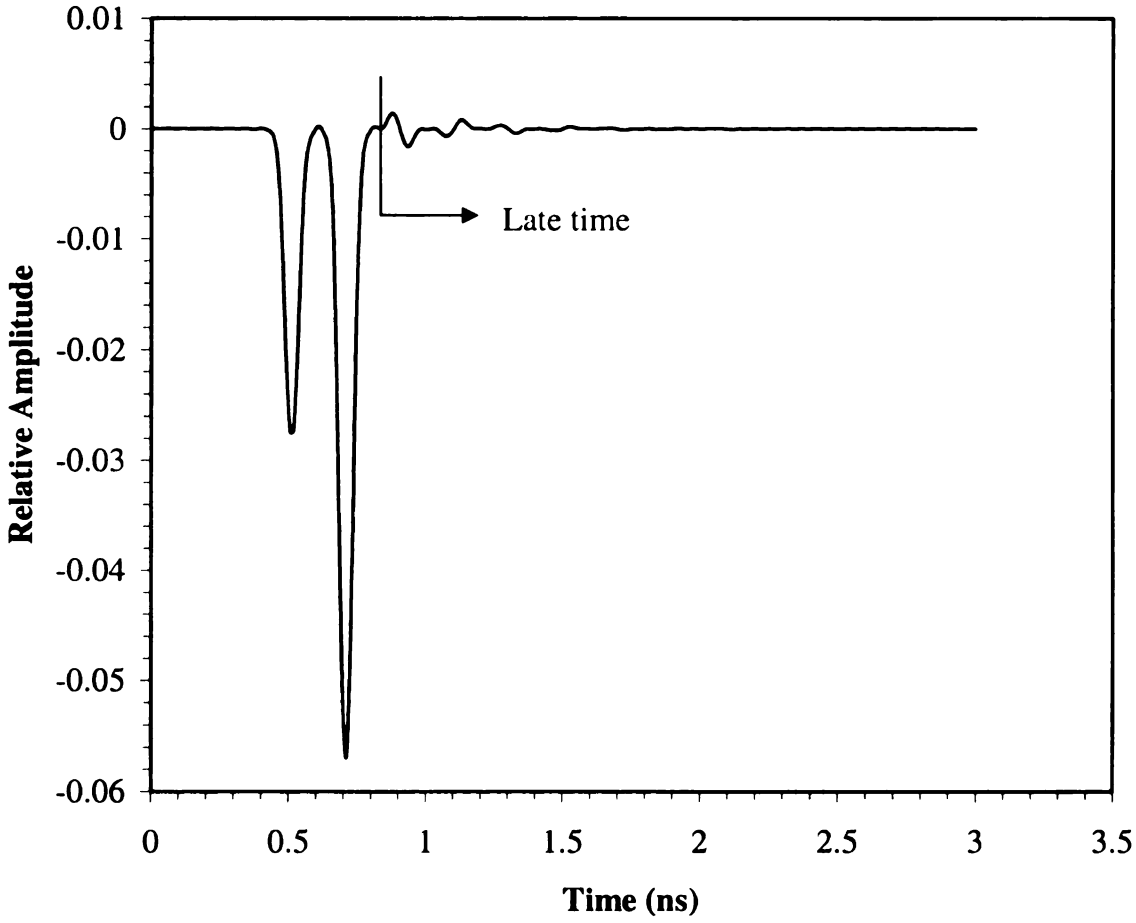

Figure 2-20 Convolution of material 'G' response with baseline E-pulse.

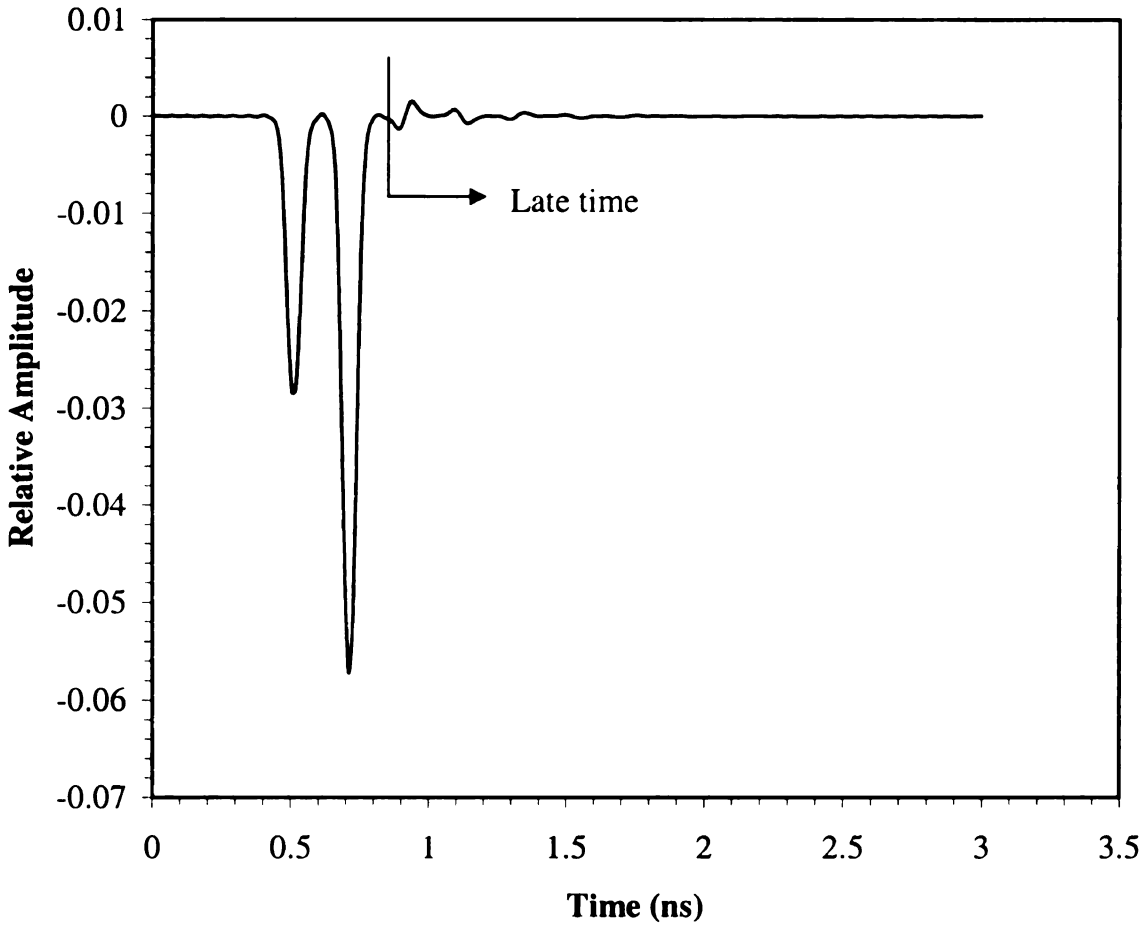

Figure 2-21 Convolution of material 'I' response with baseline E-pulse.

To quantify the results, the EDNa values are calculated. The values of EDNa for each of the materials examined are shown in Table 2-5. Figure 2-22 shows a plot of the tabulated EDNa calculations. It can be seen that as the change in thickness from the baseline increases the EDNa calculations increase as well. Determining how much change in permittivity can be detected using the EDNa plots depends, again, on the noise level.

Material	ε_r	EDNa
A	4	4.80E-03
B	5	3.89E-03
C	6	2.61E-03
D	7	1.29E-03
E	8	3.40E-04
F	8.5	8.65E-05
G	8.75	2.25E-05
H	9	3.70E-07
I	9.25	1.90E-05
J	9.5	7.69E-05
K	10	3.01E-04
L	11	1.09E-03
M	12	2.14E-03
N	13	3.23E-03
P	14	4.22E-03

Table 2-5 EDNa calculations for change in permittivity.

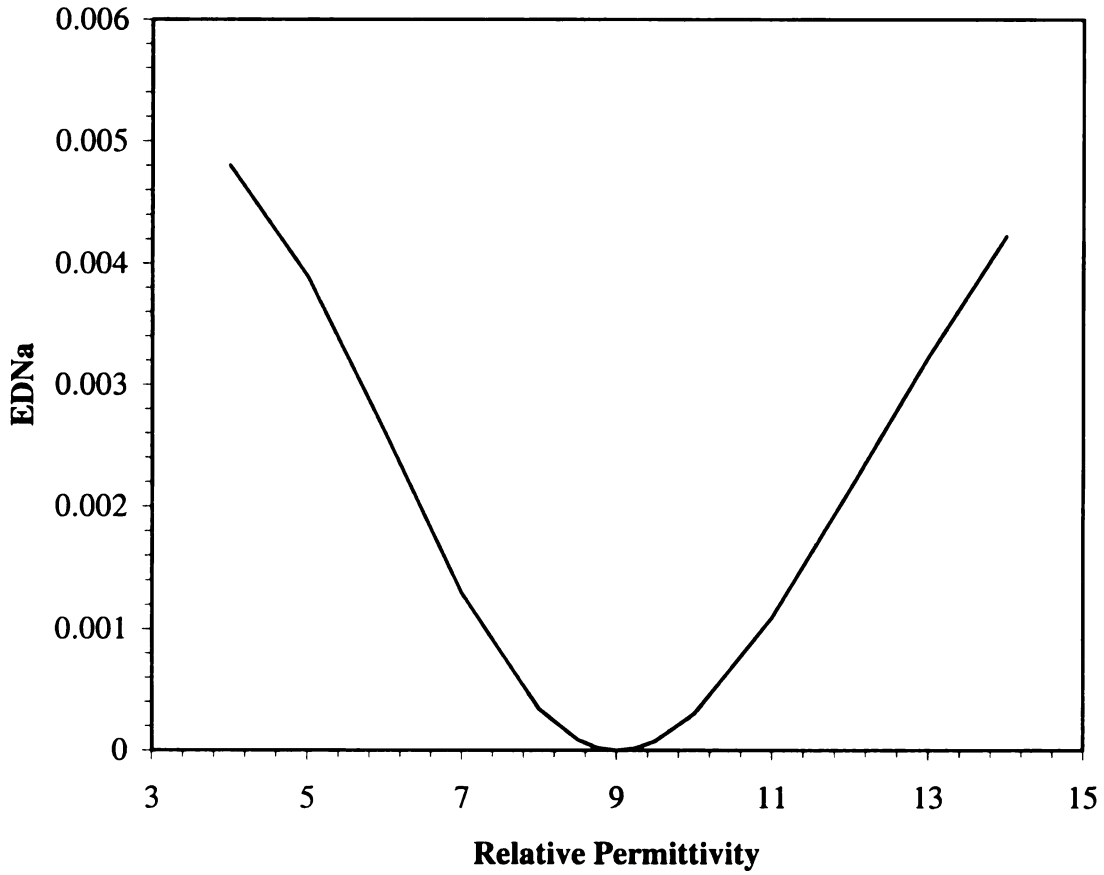

Figure 2-22 EDNa vs. change in relative permittivity for single lossless layer.

2.2.3 Change in Aspect Angle

The next property to be investigated is the angle of incidence of the transient excitation. One of the advantages of the E-pulse in discriminating radar targets is that it is independent of the aspect angle of the incident field. In applications to layered material it is expected that the aspect angle should have some effect on the EDNa, although it is hoped that the effect is small if the change in angle is small.

Table 2-6 and Table 2-7 list the material properties used to create the response waveforms with changing aspect angle. The following examples involve noise free responses. The baseline material is again the same as for the two previous cases of changing thickness and permittivity. These properties are shown in Table 2-1.

Several scattered responses of layered materials were again simulated using MLPREF.for. Since the polarization of the incident wave affects the response from the material both perpendicular and parallel polarizations are considered. The properties of the layered materials for parallel polarization are shown in Table 2-6. The properties of the layered materials for perpendicular polarization are shown in Table 2-7. For each polarization, several angles were simulated beginning from 0° to 10° in increments of 1° and then from 10° to 45° in 5° increments.

For both parallel and perpendicular polarizations, the angles 0°, 5° and 45° are shown as examples. The baseline material response for parallel polarization, material 'A', is shown in Figure 2-23. The baseline material response for perpendicular polarization, material 'AA', is shown in Figure 2-24. The material responses for an aspect angle of 5°, material 'F' and material 'FF' are shown in Figure 2-25 and Figure

2-26, respectively. The material responses for an aspect angle of 45°, material 'S' and material 'SS' are shown in Figure 2-27 and Figure 2-28, respectively.

Each response is convolved with the baseline E-pulse shown in Figure 2-8. Figure 2-29 and Figure 2-30 show the convolution of the baseline material, material 'A' response and material 'AA' response, respectively, with the baseline E-pulse. It can be seen that the energy in the late-time is again zero as expected. In comparison, the convolutions of the other responses are shown in Figure 2-31, Figure 2-32, Figure 2-33, and Figure 2-34. It can bee seen in Figure 2-31 and Figure 2-32 that for a small change in the aspect angle the late-time energy stays relatively low. However, as the angle gets very large the late-time energy increases. Since the natural frequencies of a layered material depends on θ_i, the E-pulse method is not independent of the aspect angle for layered materials. This is because a layered material is not a finite-sized body and does not allow the excitation to completely pass beyond the material, as in the case of a radar target.

Material	ε	μ	σ	Thickness (mm)	Polarization	Angle of incidence, θ_i
A(baseline)	$9\varepsilon_0$	μ_0	0	10	Parallel	0
B	$9\varepsilon_0$	μ_0	0	10	Parallel	1
C	$9\varepsilon_0$	μ_0	0	10	Parallel	2
D	$9\varepsilon_0$	μ_0	0	10	Parallel	3
E	$9\varepsilon_0$	μ_0	0	10	Parallel	4
F	$9\varepsilon_0$	μ_0	0	10	Parallel	5
G	$9\varepsilon_0$	μ_0	0	10	Parallel	6
H	$9\varepsilon_0$	μ_0	0	10	Parallel	7
I	$9\varepsilon_0$	μ_0	0	10	Parallel	8
J	$9\varepsilon_0$	μ_0	0	10	Parallel	9
K	$9\varepsilon_0$	μ_0	0	10	Parallel	10
L	$9\varepsilon_0$	μ_0	0	10	Parallel	15
M	$9\varepsilon_0$	μ_0	0	10	Parallel	20
N	$9\varepsilon_0$	μ_0	0	10	Parallel	25
P	$9\varepsilon_0$	μ_0	0	10	Parallel	30
Q	$9\varepsilon_0$	μ_0	0	10	Parallel	35
R	$9\varepsilon_0$	μ_0	0	10	Parallel	40
S	$9\varepsilon_0$	μ_0	0	10	Parallel	45

Table 2-6 Material properties for changing angle, parallel polarization.

Material	ε	μ	σ	Thickness (mm)	Polarization	Angle of incidence, θ_i
AA(baseline)	$9\varepsilon_0$	μ_0	0	10	Perpendicular	0
BB	$9\varepsilon_0$	μ_0	0	10	Perpendicular	1
CC	$9\varepsilon_0$	μ_0	0	10	Perpendicular	2
DD	$9\varepsilon_0$	μ_0	0	10	Perpendicular	3
EE	$9\varepsilon_0$	μ_0	0	10	Perpendicular	4
FF	$9\varepsilon_0$	μ_0	0	10	Perpendicular	5
GG	$9\varepsilon_0$	μ_0	0	10	Perpendicular	6
HH	$9\varepsilon_0$	μ_0	0	10	Perpendicular	7
II	$9\varepsilon_0$	μ_0	0	10	Perpendicular	8
JJ	$9\varepsilon_0$	μ_0	0	10	Perpendicular	9
KK	$9\varepsilon_0$	μ_0	0	10	Perpendicular	10
LL	$9\varepsilon_0$	μ_0	0	10	Perpendicular	15
MM	$9\varepsilon_0$	μ_0	0	10	Perpendicular	20
NN	$9\varepsilon_0$	μ_0	0	10	Perpendicular	25
PP	$9\varepsilon_0$	μ_0	0	10	Perpendicular	30
QQ	$9\varepsilon_0$	μ_0	0	10	Perpendicular	35
RR	$9\varepsilon_0$	μ_0	0	10	Perpendicular	40
SS	$9\varepsilon_0$	μ_0	0	10	Perpendicular	45

Table 2-7 Material properties for changing angle, perpendicular polarization.

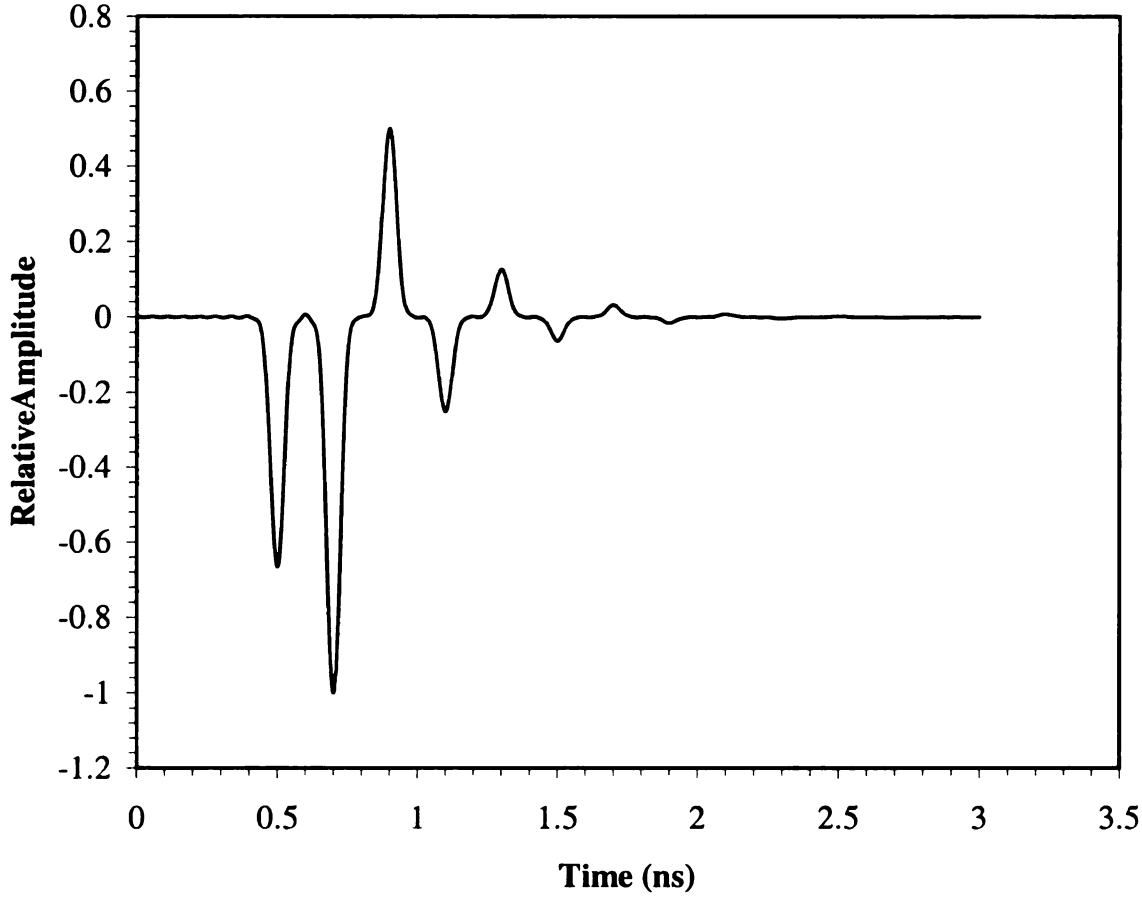

Figure 2-23 Response waveform for material 'A'.

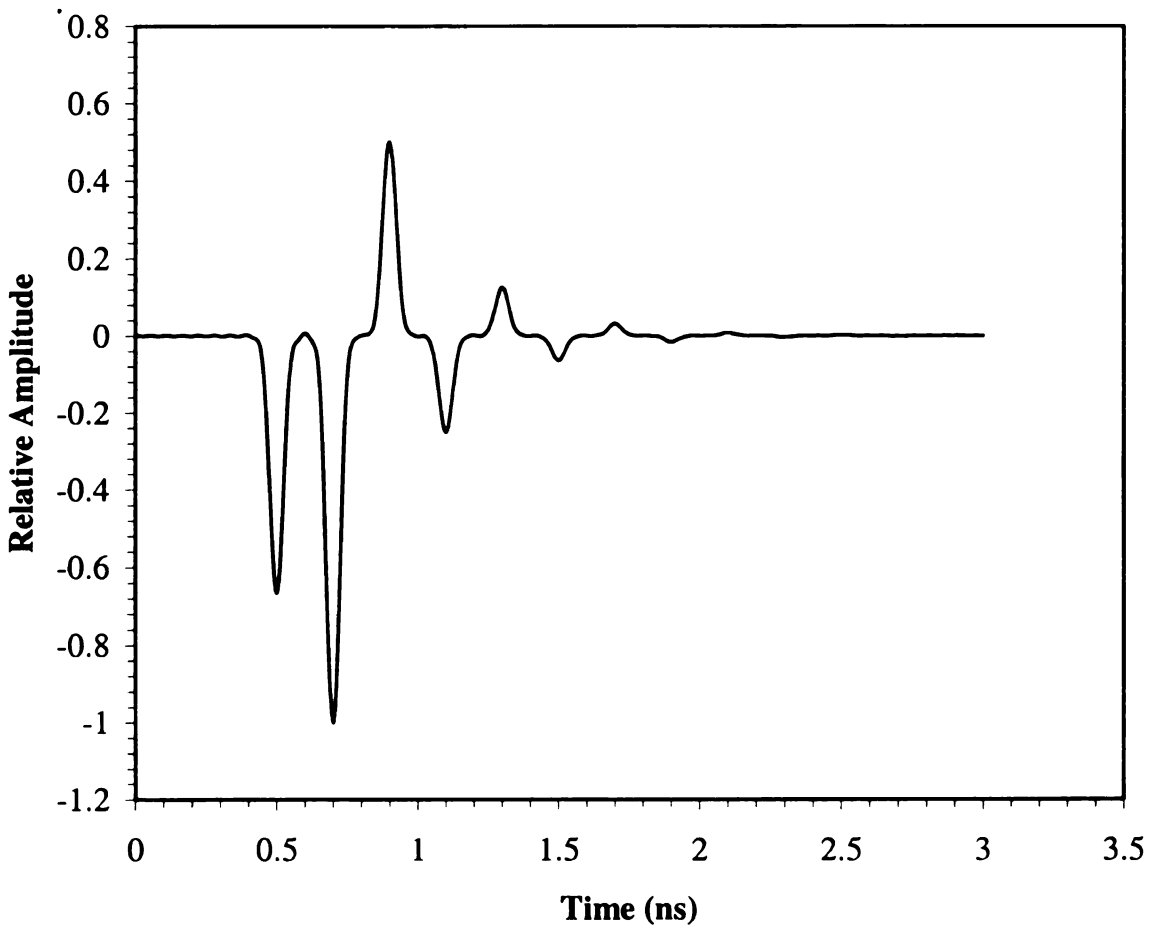

Figure 2-24 Response waveform for material 'AA'.

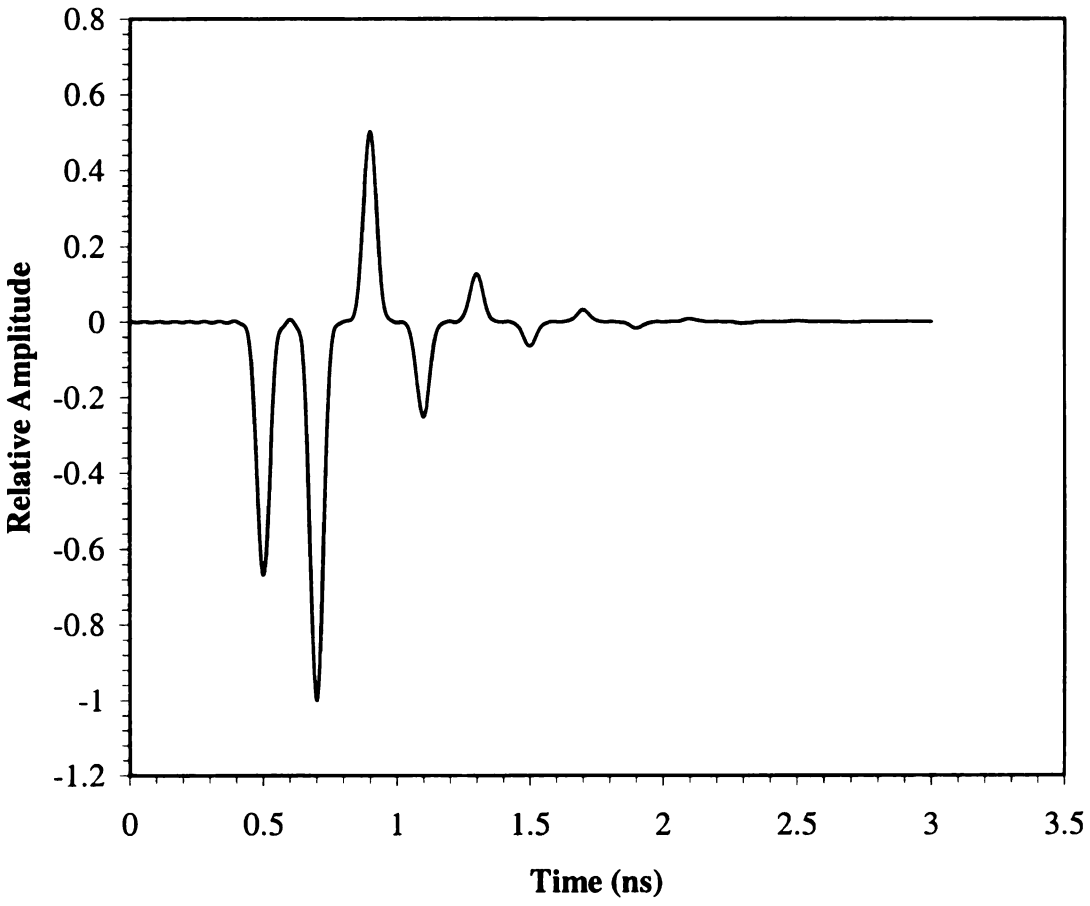

Figure 2-25 Response waveform for material 'F'.

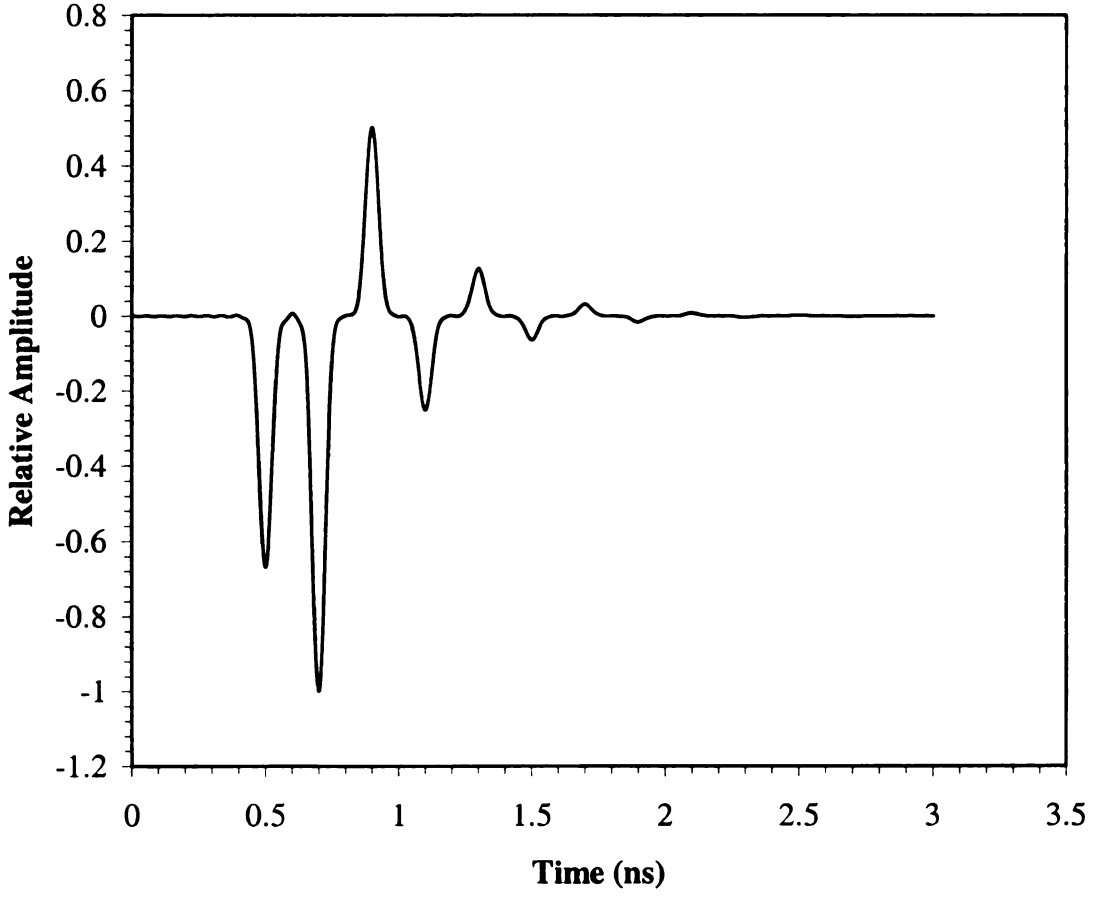

Figure 2-26 Response waveform for material 'FF'.

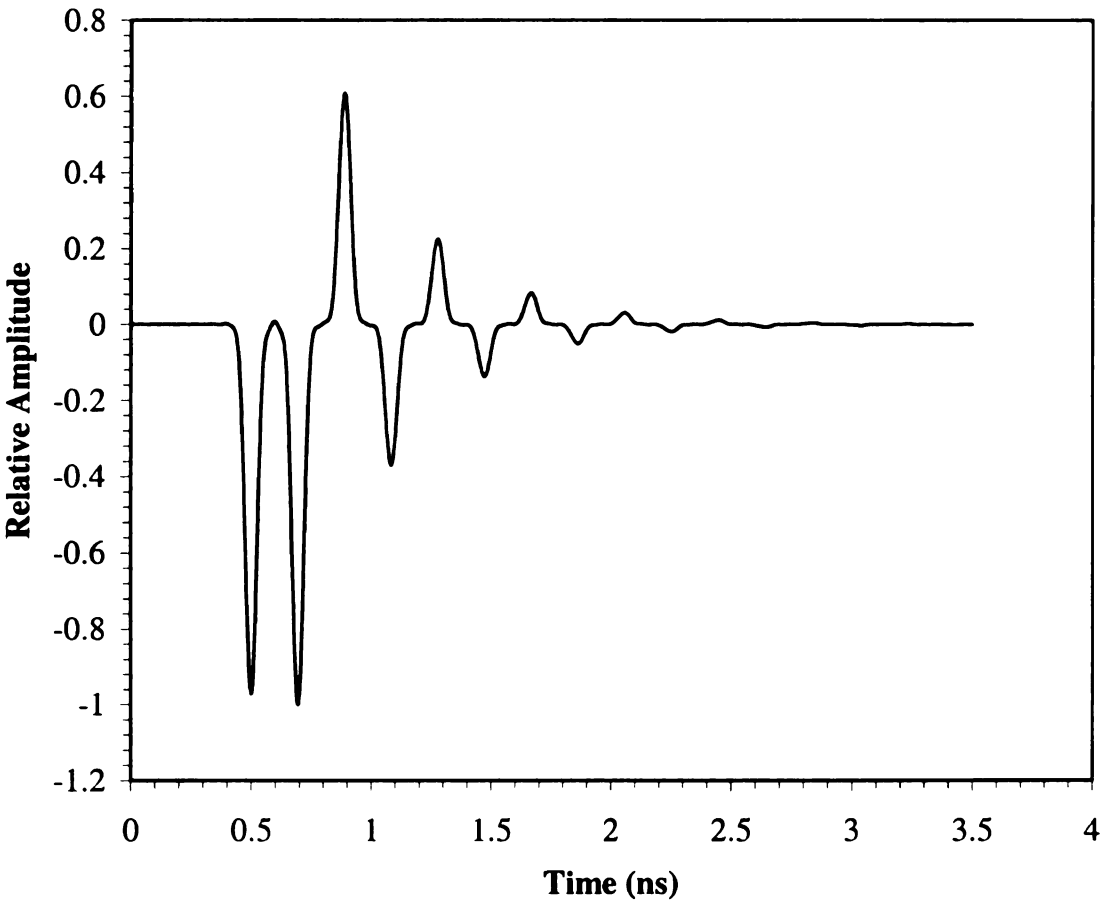

Figure 2-27 Response waveform for material 'S'.

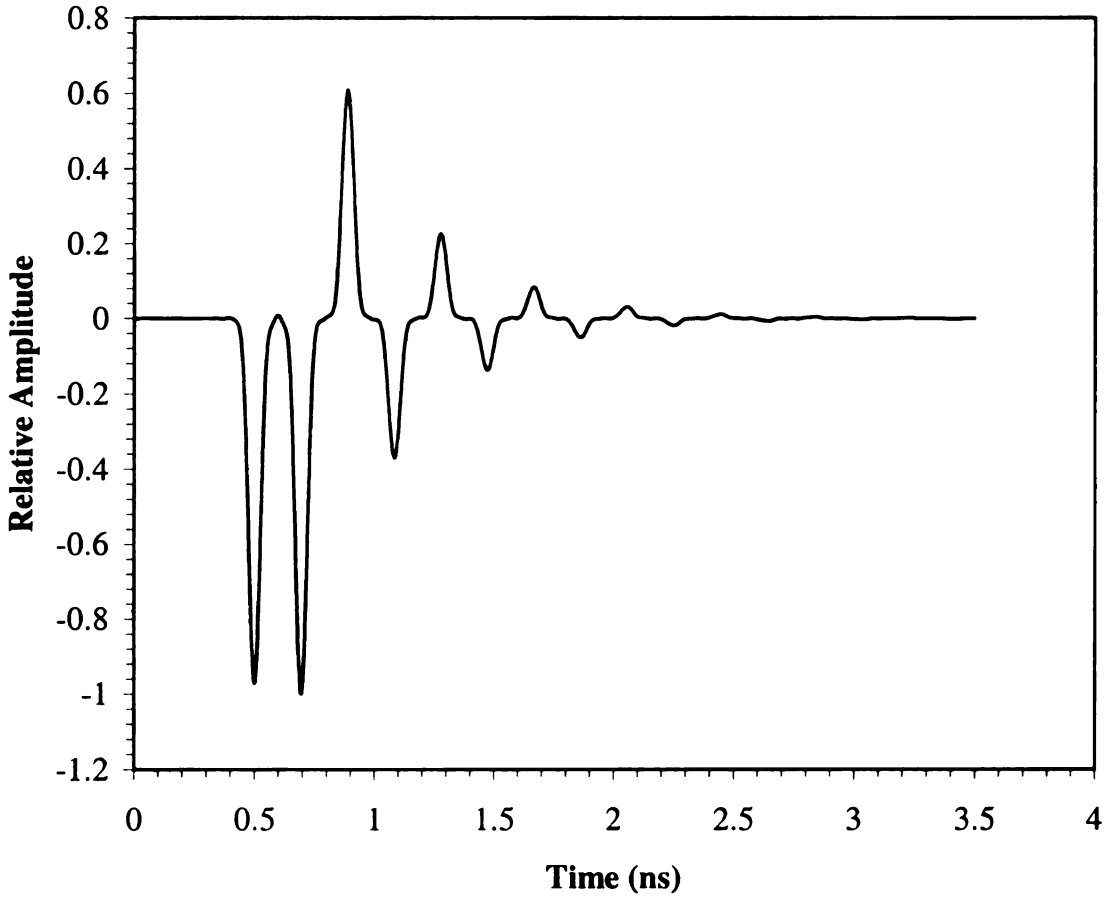

Figure 2-28 Response waveform for material 'SS'.

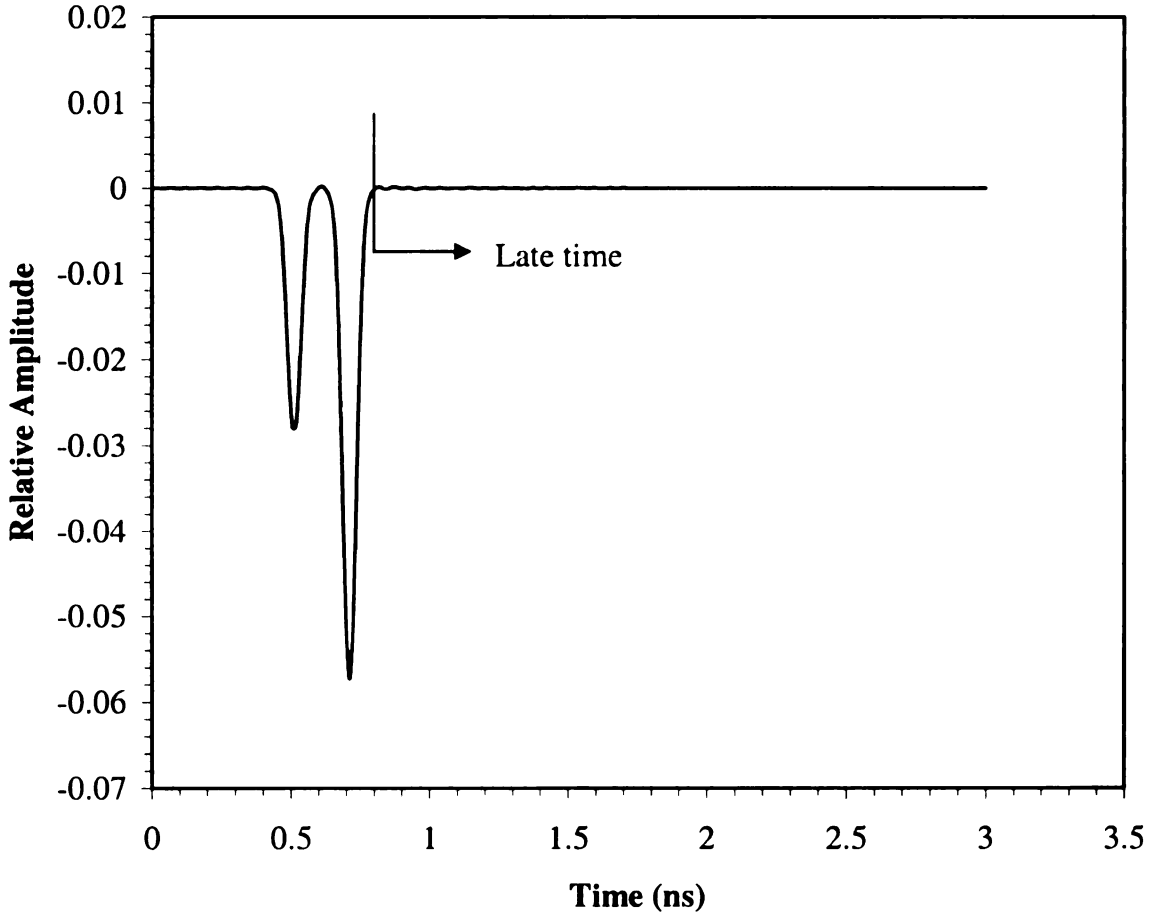

Figure 2-29 Convolution of material 'A' response with baseline E-pulse.

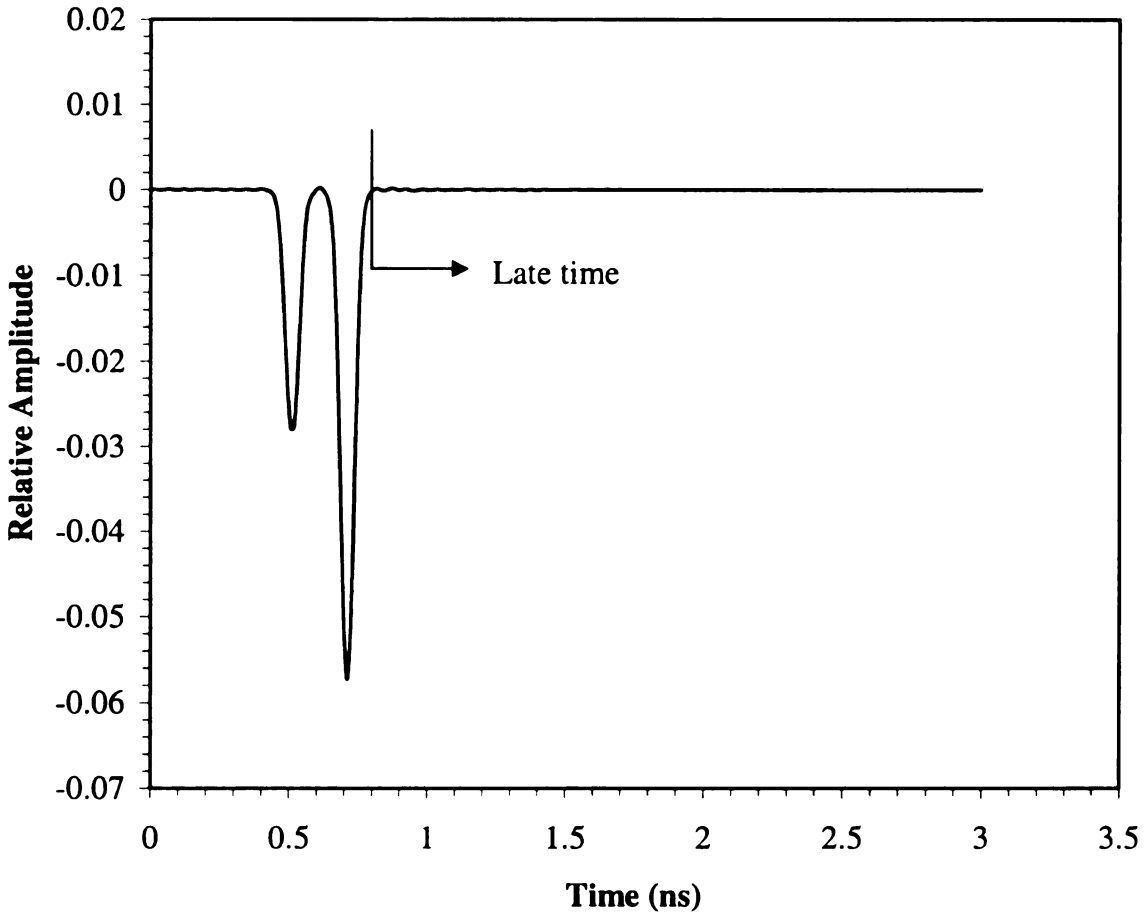

Figure 2-30 Convolution of material 'AA' response with baseline E-pulse.

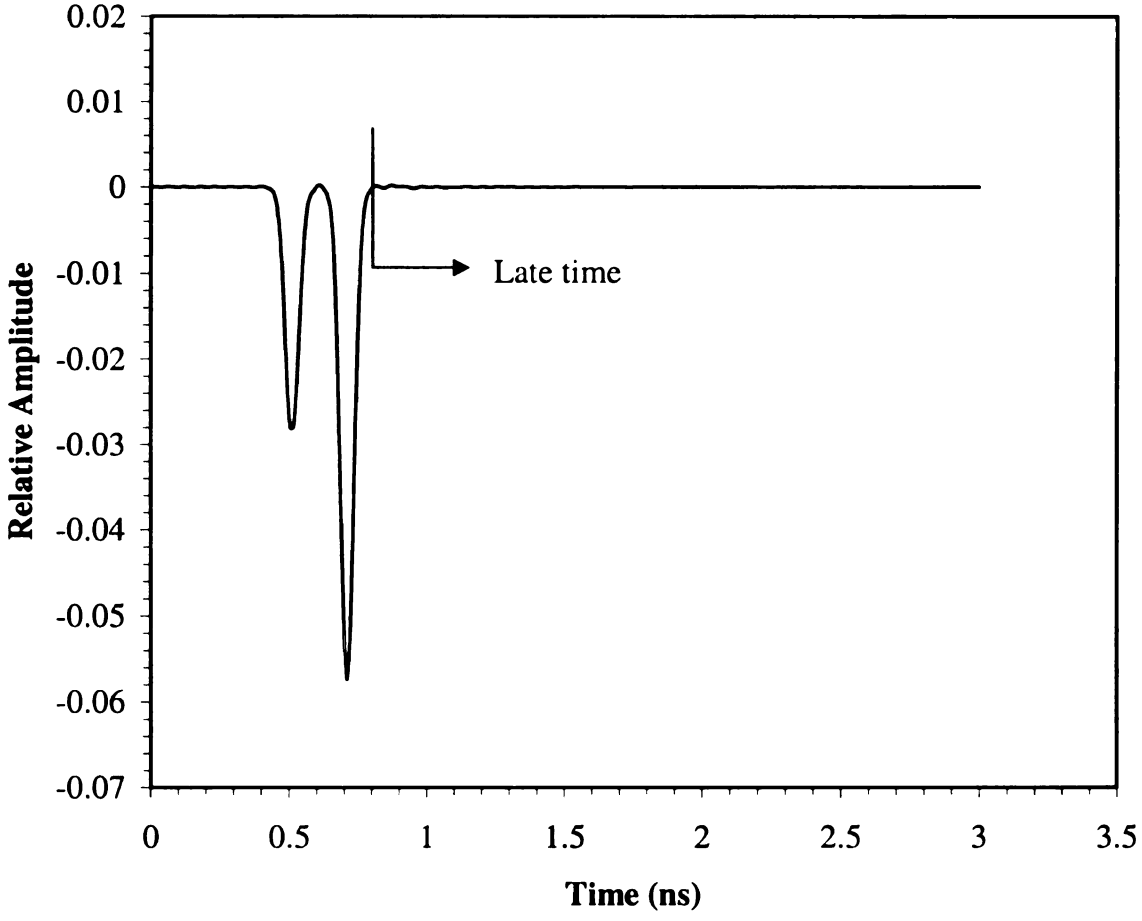

Figure 2-31 Convolution of material 'F' response with baseline E-pulse.

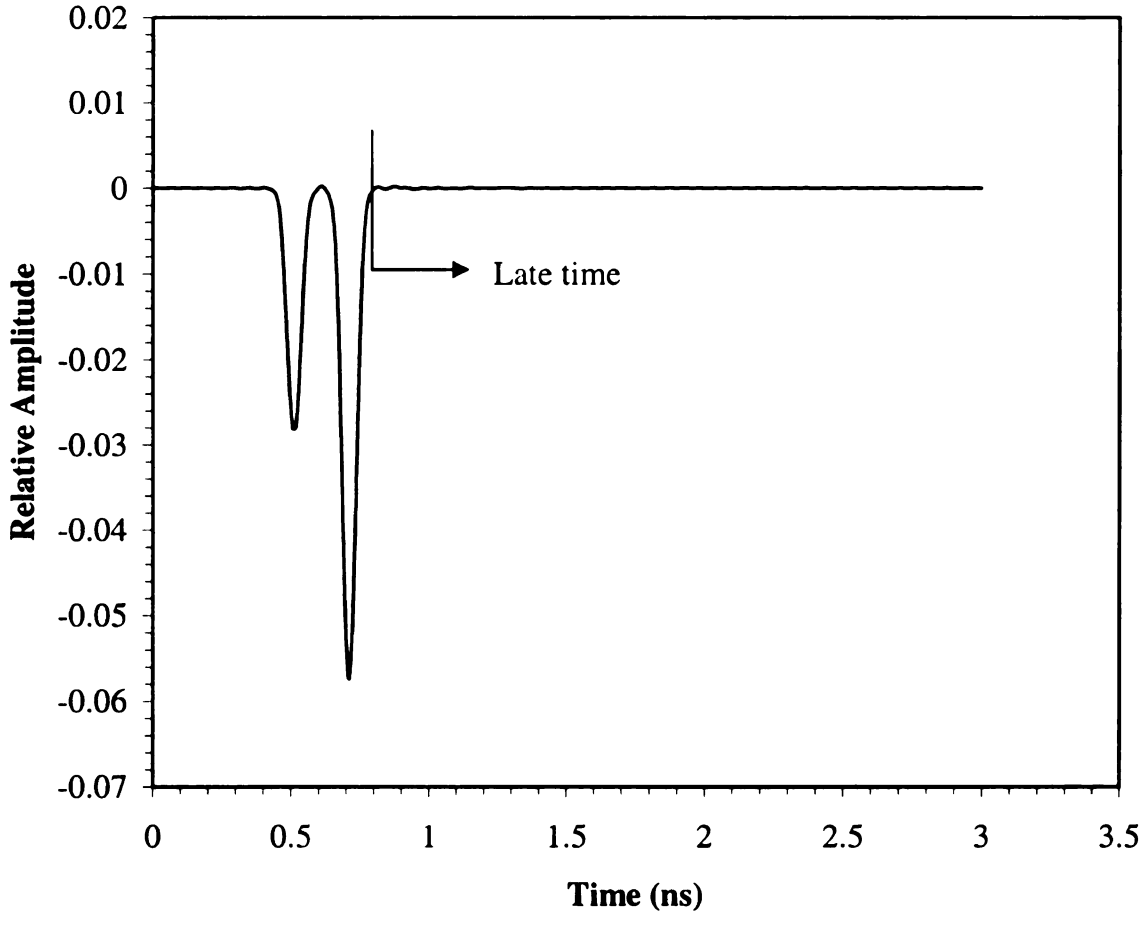

Figure 2-32 Convolution of material 'FF' response with baseline E-pulse.

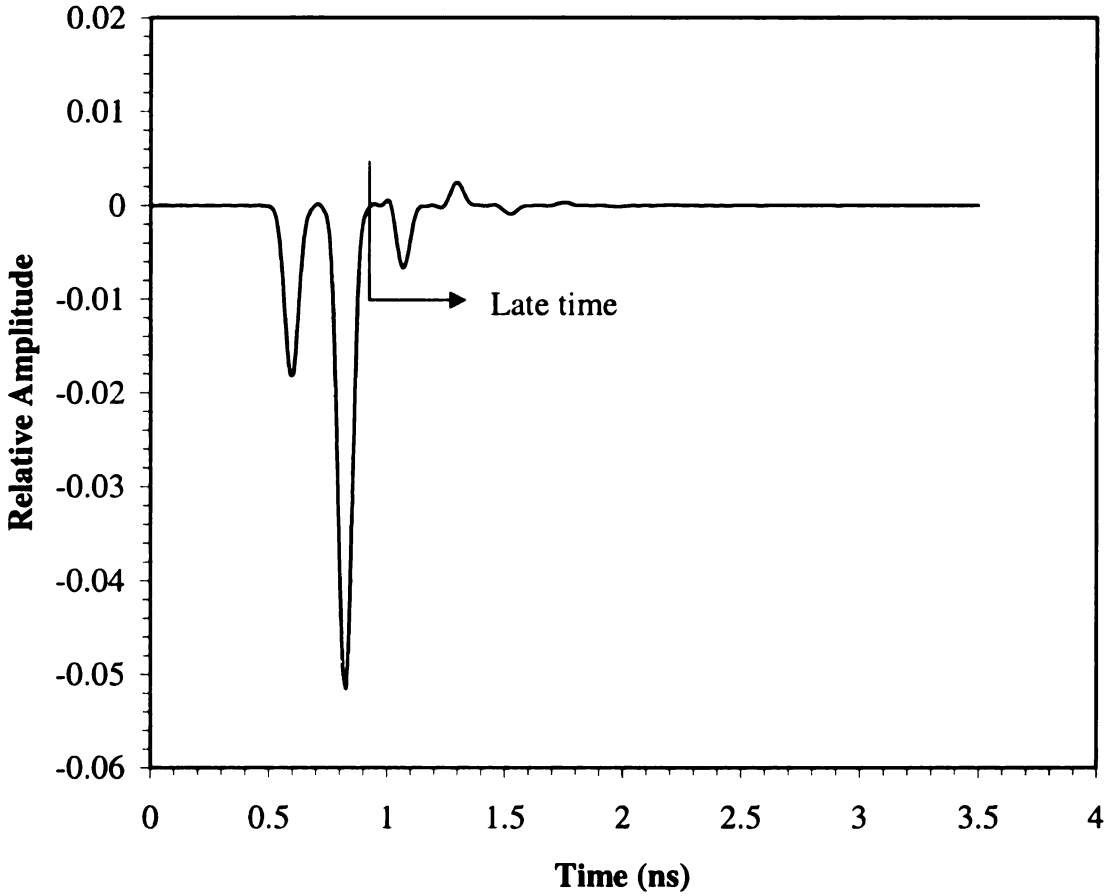

Figure 2-33 Convolution of material 'S' response with baseline E-pulse.

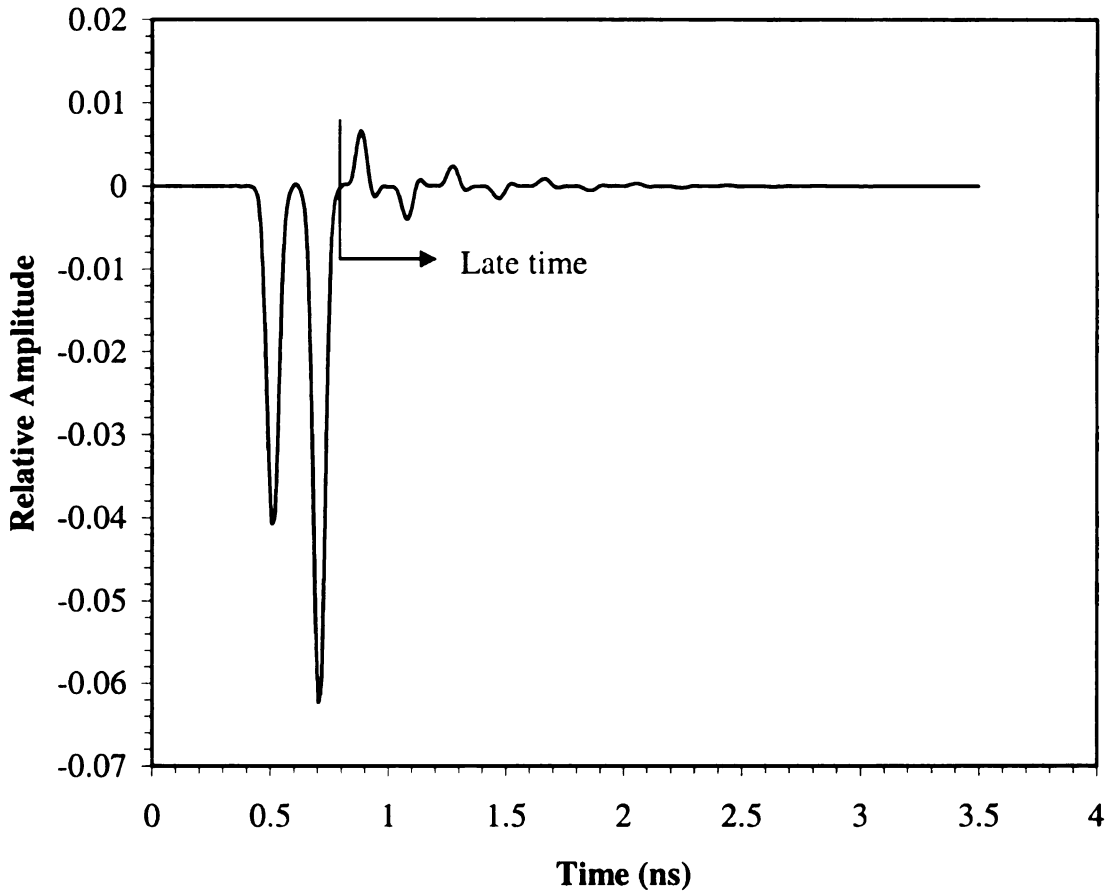

Figure 2-34 Convolution of material 'SS' response with baseline E-pulse.

Table 2-8 shows the calculations for EDNa versus aspect angle for parallel polarization and Table 2-9 shows the calculations for EDNa versus aspect angle for perpendicular polarization. A plot of the EDNa values for both polarizations is shown in Figure 2-35. It can be seen in the plot that there is minimal change in the EDNa value up to 10°-15° (depending on the definition of minimal). This suggests that a moderate change in aspect angle is tolerable. Typical applications of the E-pulse technique for layered material evaluation would generally be such that minimal deviation in aspect angle from the baseline angle would be seen. A measurement device built to implement this technique could easily be designed to limit changes in the aspect angle of less than a couple of degrees. Thus, the problem of the aspect angle dependent nature of the EDNa could be eliminated.

Material	Aspect Angle, θ_i	EDNa
A	0	3.70E-07
B	1	3.72E-07
C	2	3.78E-07
D	3	3.90E-07
E	4	4.13E-07
F	5	4.51E-07
G	6	5.11E-07
H	7	6.02E-07
I	8	7.32E-07
J	9	9.14E-07
K	10	1.16E-06
L	15	3.88E-06
M	20	1.08E-05
N	25	2.48E-05
P	30	4.93E-05
Q	35	8.75E-05
R	40	1.43E-04
S	45	2.17E-04

Table 2-8 EDNa calculations for change in aspect angle for parallel polarization.

Material	Aspect Angle, θ_i	EDNa
AA	0	3.70E-07
BB	1	3.72E-07
CC	2	3.78E-07
DD	3	3.92E-07
EE	4	4.15E-07
FF	5	4.55E-07
GG	6	5.17E-07
HH	7	6.10E-07
II	8	7.45E-07
JJ	9	9.31E-07
KK	10	1.18E-06
LL	15	3.99E-06
MM	20	1.13E-05
NN	25	2.69E-05
PP	30	5.58E-05
QQ	35	1.06E-04
RR	40	1.87E-04
SS	45	3.17E-04

Table 2-9 EDNa calculations for change in aspect angle for perpendicular polarization.

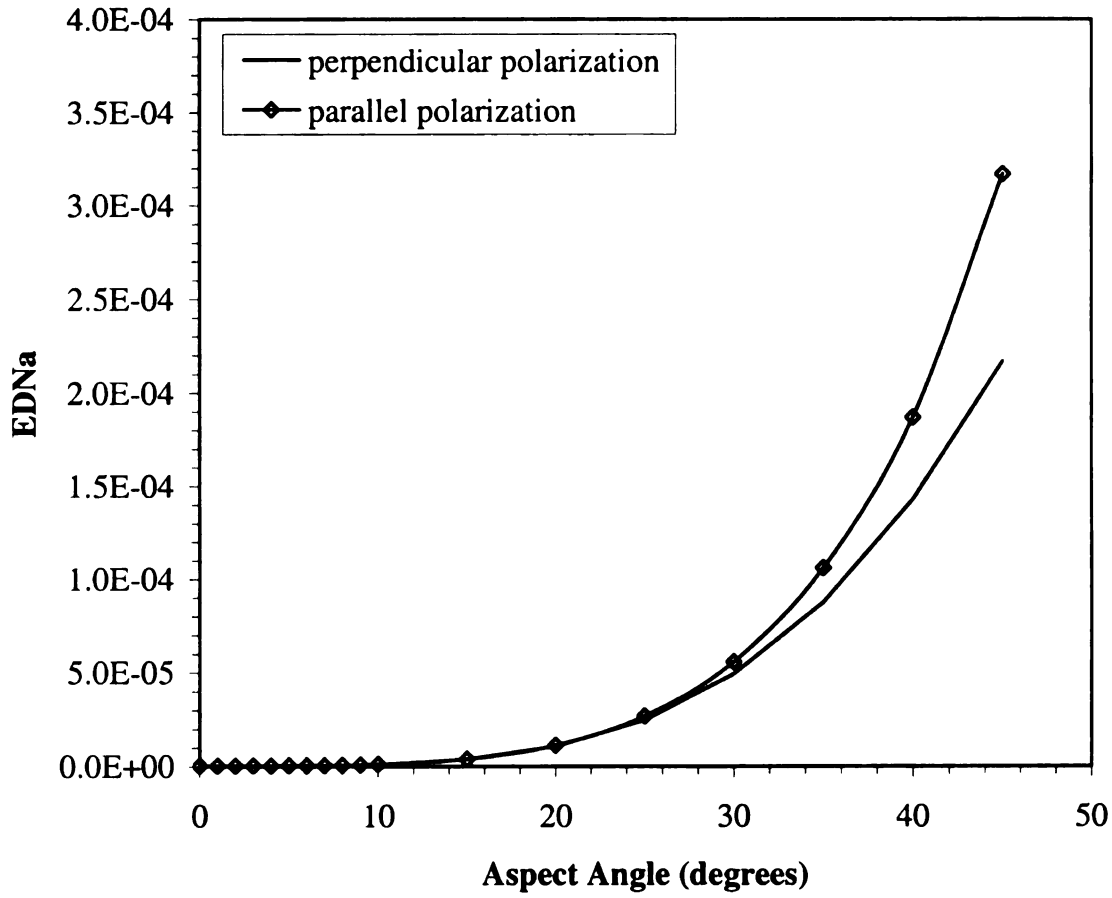

Figure 2-35 EDNa vs. change in aspect angle for single lossless layer.

2.2.4 Change in the Number of Natural Modes

The final parameter to be investigated for the noise-free data is the number of natural modes, or natural frequencies, that are used to generate the E-pulse. As shown by (2.10), there are an infinite number of natural frequencies, or modes, that can be calculated for a layered material. It is obvious that only a finite number of these modes can be used to reconstruct a response and generate an E-pulse. Therefore, it is necessary to determine the optimum number of modes to use. Because using the natural modes to reconstruct the response waveform is an estimation, it is most likely that using a greater number of modes would yield a more accurate estimate. However, not only do the modes reconstruct the response, they are also used to generate the E-pulse. Presently, the investigation is to determine the optimum number of modes used to generate an E-pulse which will give the most accurate EDNa calculations.

To determine the optimum number of modes needed to generate an E-pulse, a baseline response will be convolved with many natural E-pulses that have been generated with KPNAT.for using different numbers of modes. Table 2-1 shows the material properties used to reconstruct a baseline response waveform using (1.1) and MLPREF.for. Figure 2-4 shows a plot of this waveform. Ten different E-pulses were generated, each with a different number of modes, as shown in Table 2-10. Examples of three of these E-pulses are shown in Figure 2-36, Figure 2-37, an Figure 2-38. Figure 2-36 shows an E-pulse generated with only one mode, Figure 2-37 shows an E-pulse generated with 5 modes, and Figure 2-38 shows an E-pulse generated with 10 modes. As the number of modes increases the E-pulses are seen to become narrower and when

convolved with the response waveform yield a smaller value of the convolution. The convolution of the baseline response with these three E-pulses can be seen in Figure 2-39, Figure 2-40, and Figure 2-41, respectively.

E-pulse	Number of Modes
A	1
B	2
C	3
D	4
E	5
F	6
G	7
H	8
I	9
J	10

Table 2-10 E-pulses generated using different modes.

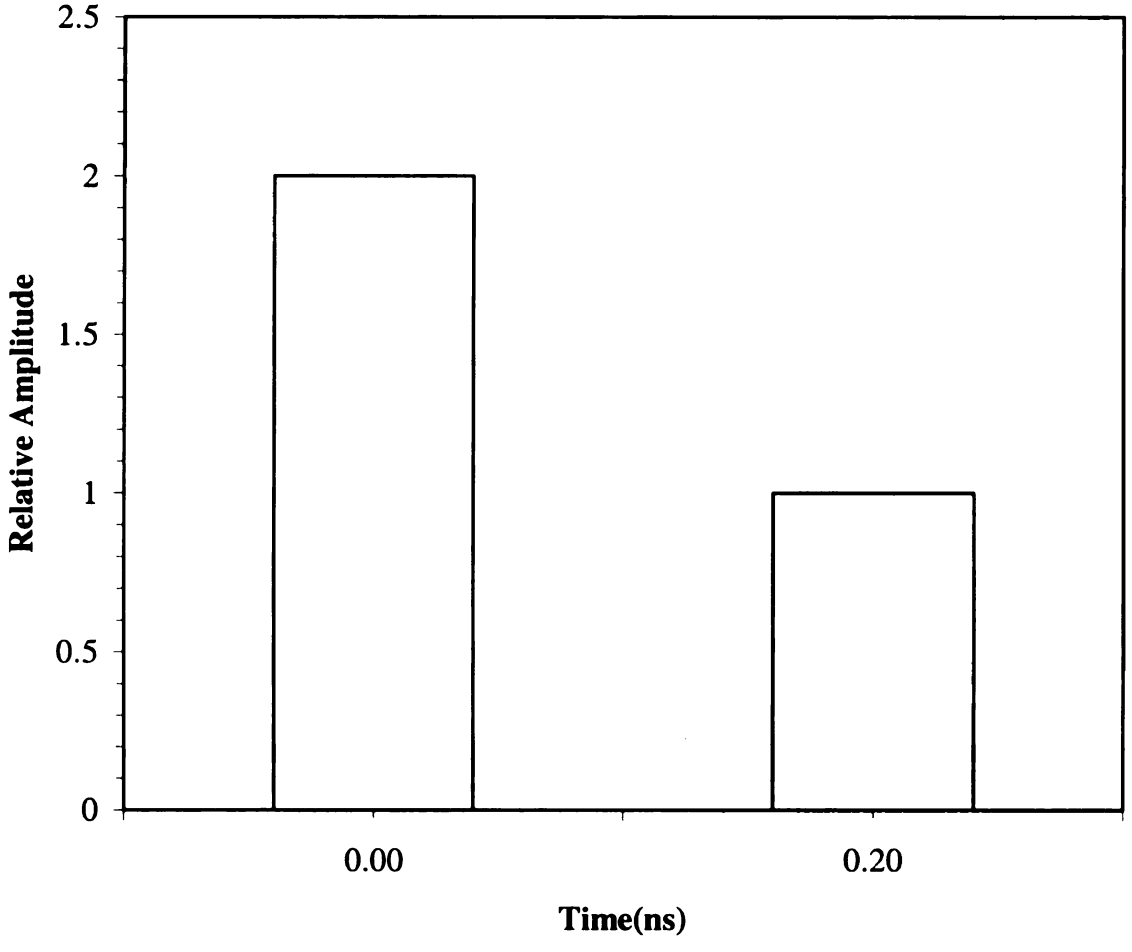

Figure 2-36 E-pulse generated using 1 mode.

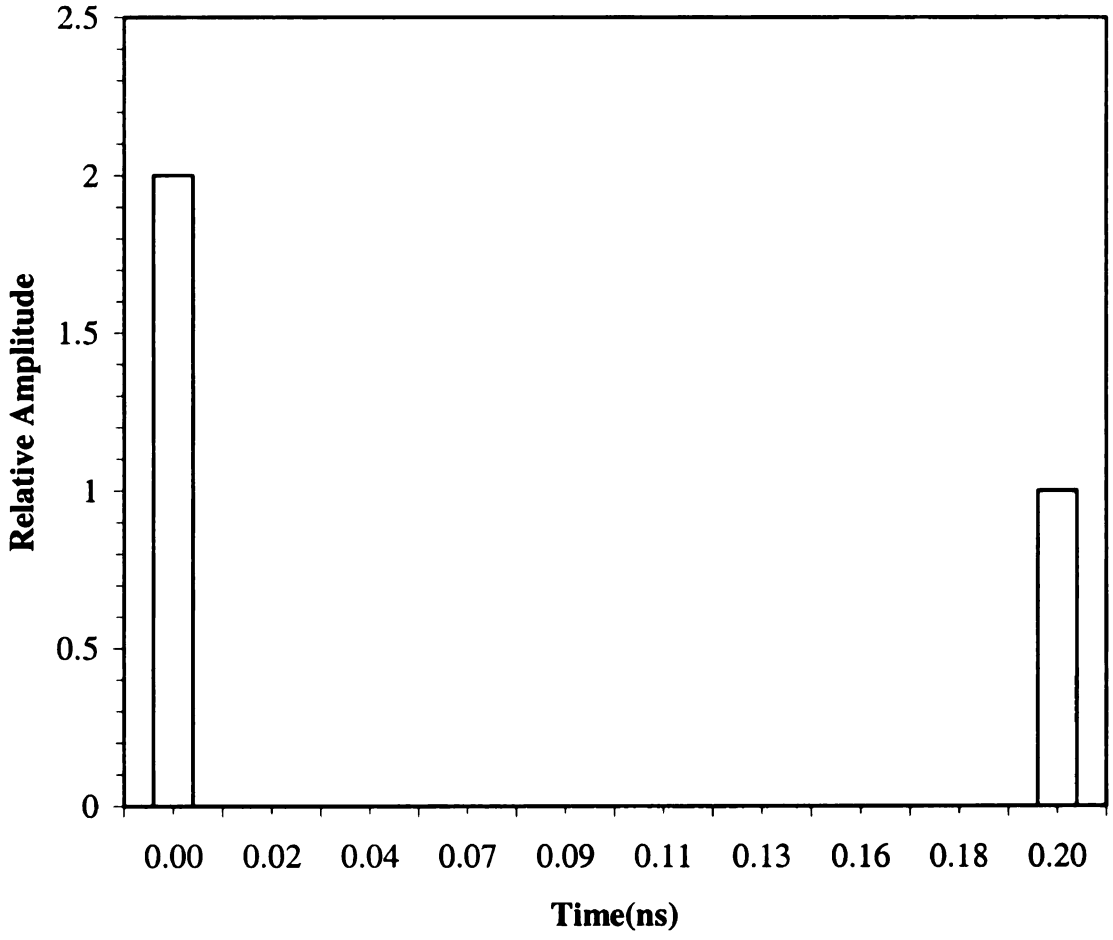

Figure 2-37 E-pulse generated using 5 modes.

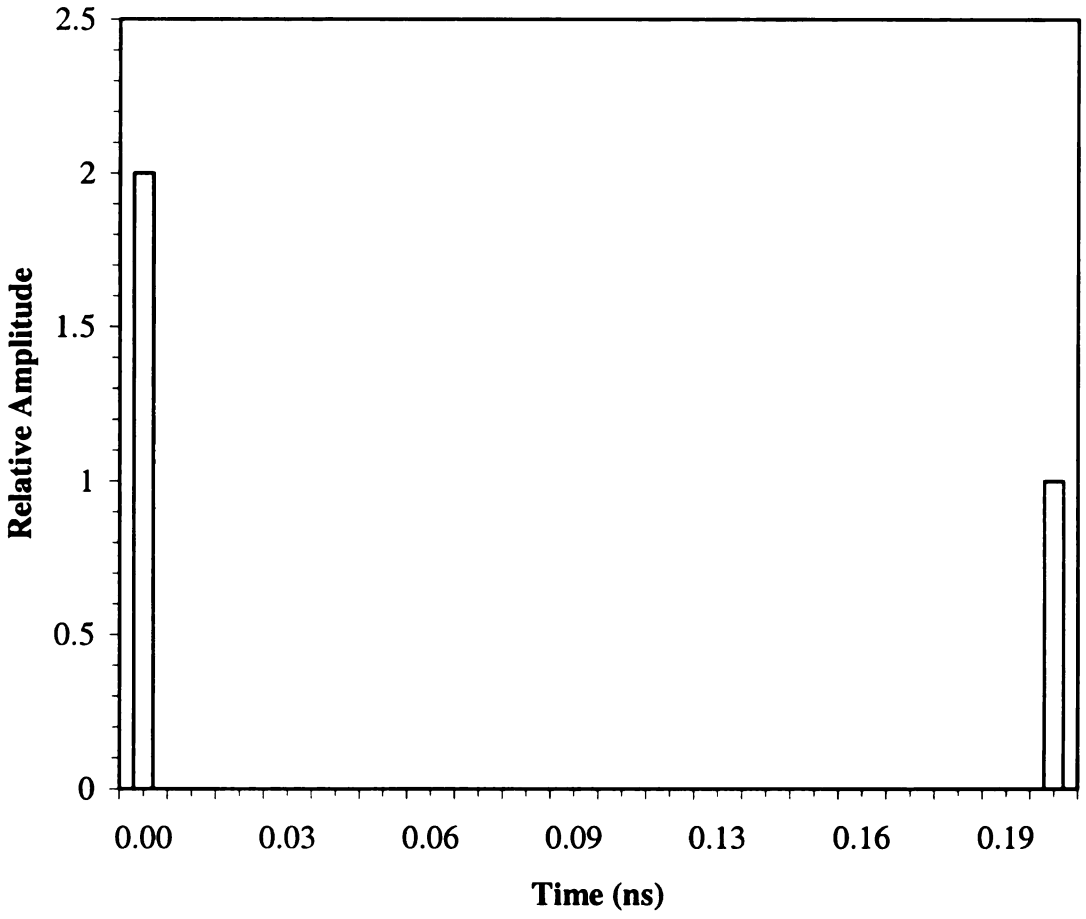

Figure 2-38 E-pulse generated using 10 modes.

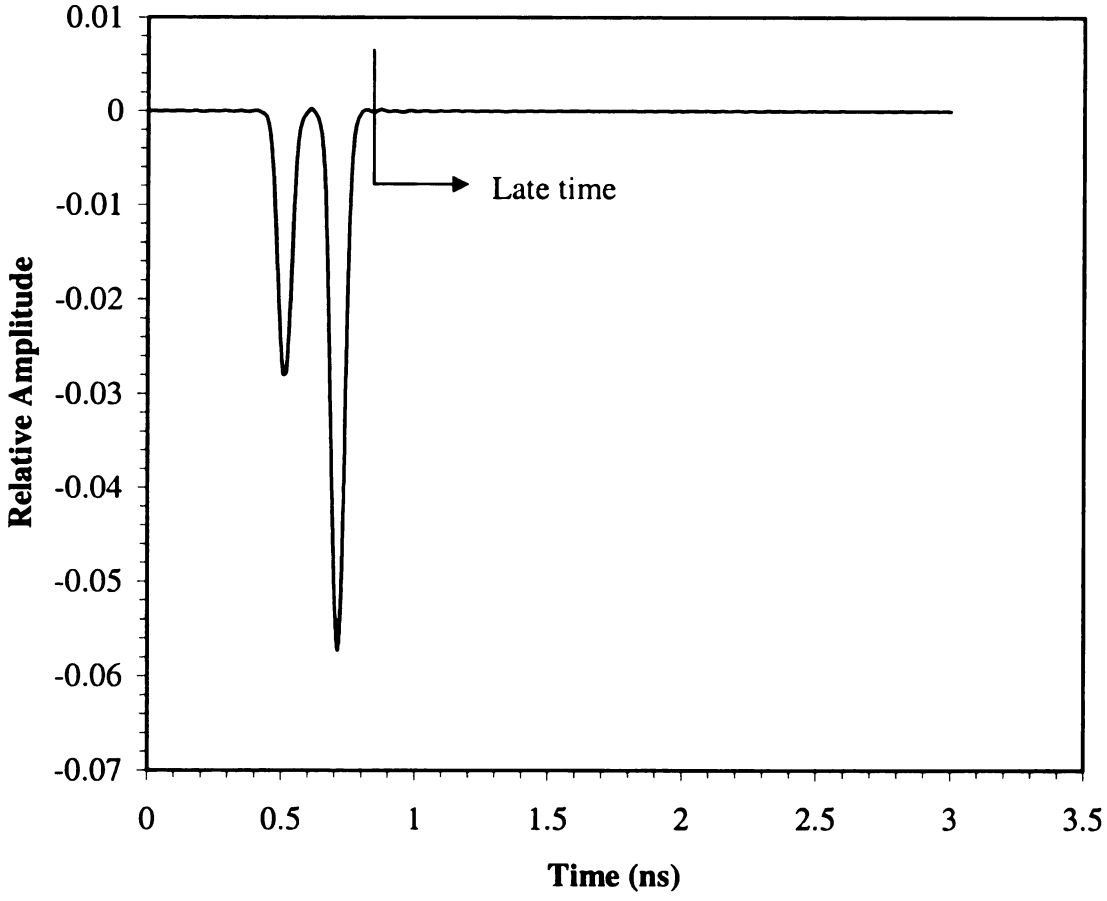

Figure 2-40 Convolution of baseline response with E-pulse 'E'.

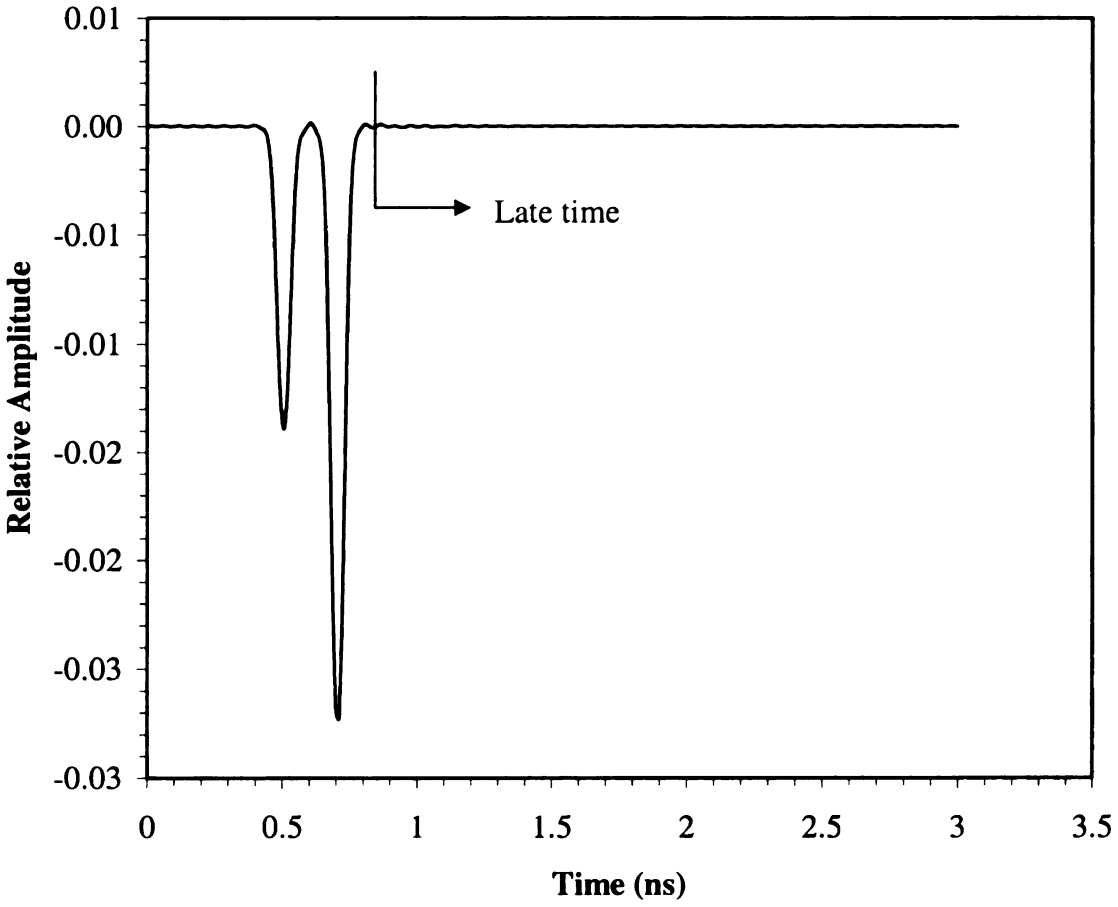

Figure 2-41 Convolution of baseline response with E-pulse 'J'.

As done previously, evaluation begins by tabulating the EDNa values, as seen in Table 2-11. These EDNa values are plotted against the number of modes in Figure 2-42. It can be seen from both Table 2-11 and Figure 2-42 that all of the E-pulses except the one generated using only one mode give a value very close to zero. This evidence suggests that using 5 modes to generate the E-pulses is more than sufficient.

A quick way to check that the proper number of modes is being used is to compare the imaginary parts of the natural frequencies, ω_n, to the frequency range used to generate the responses. By comparing the natural frequencies in Table 1-1 to the windowed frequency data in Figure 2-3 it can quickly be seen that only the first 5 modes are within the frequency range of the response data.

E-pulse	Number of Modes	EDNa
A	1	3.32E-02
B	2	2.12E-04
C	3	3.26E-06
D	4	6.63E-07
E(baseline)	5	3.70E-07
F	6	2.76E-07
G	7	2.27E-07
H	8	1.95E-07
I	9	1.72E-07
J	10	1.55E-07

Table 2-11 EDNa calculations for change in the number of modes.

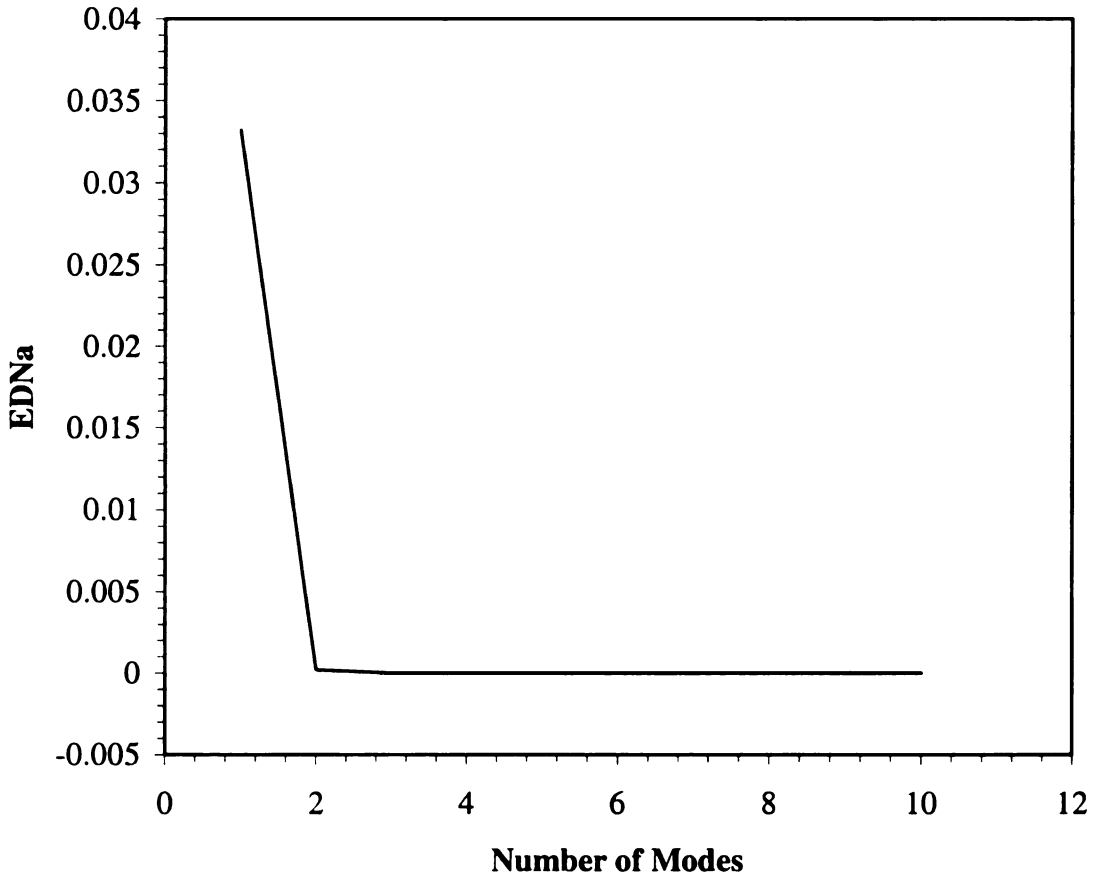

Figure 2-42 EDNa vs. change in the number of natural modes in the E-pulse.

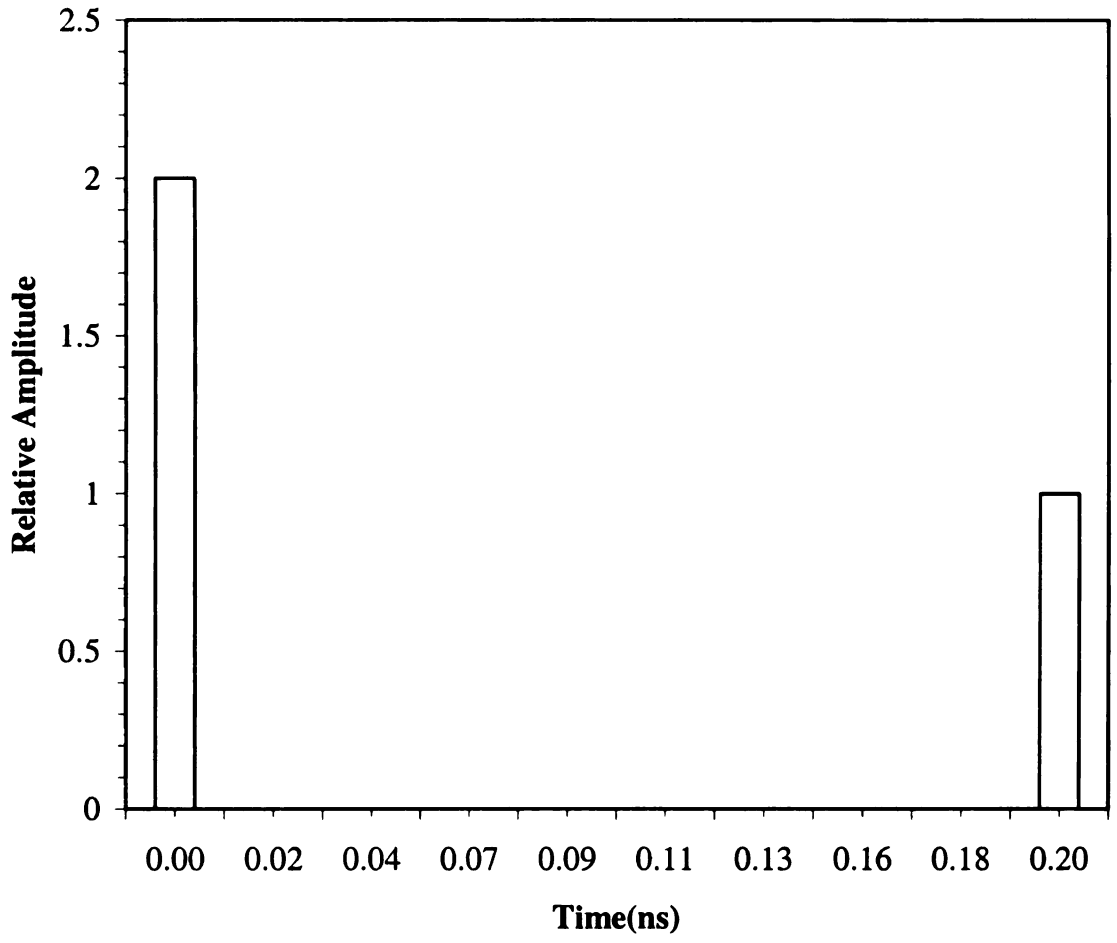

Figure 2-37 E-pulse generated using 5 modes.

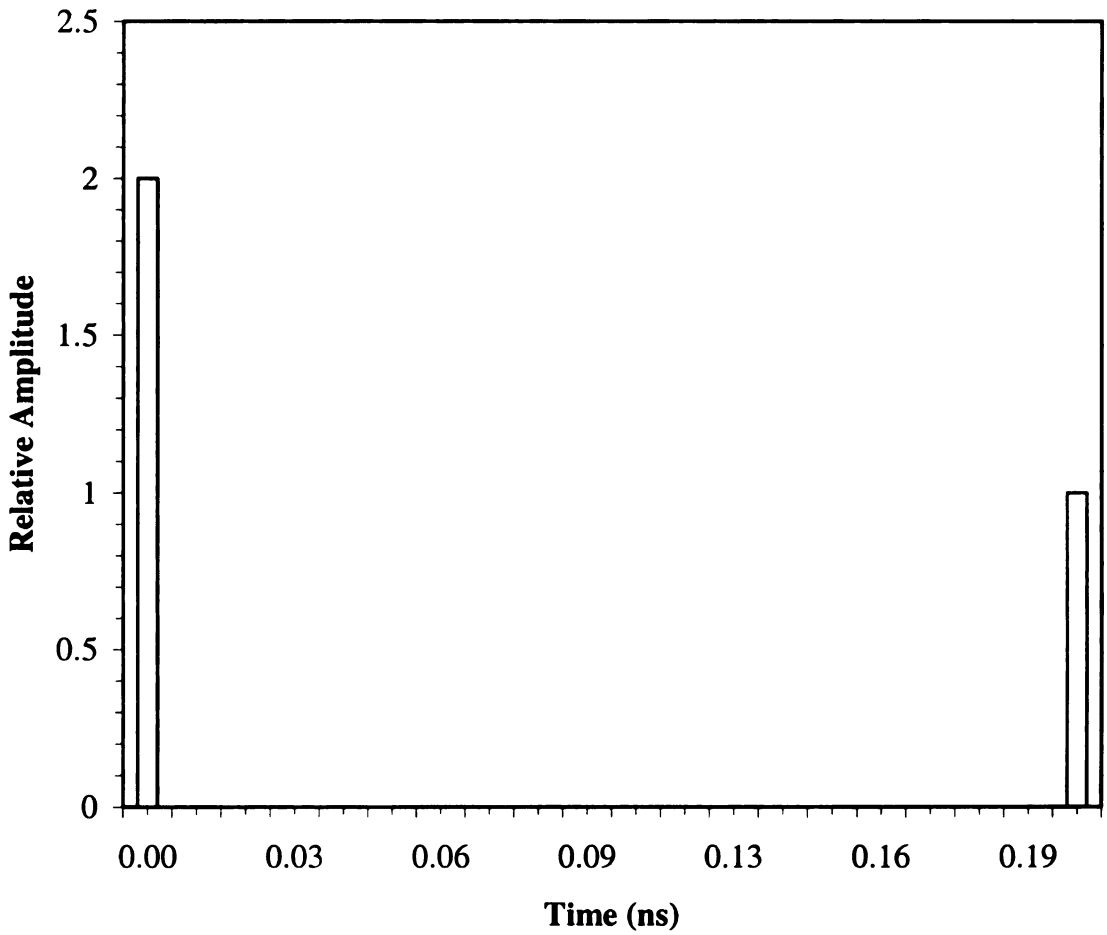

Figure 2-38 E-pulse generated using 10 modes.

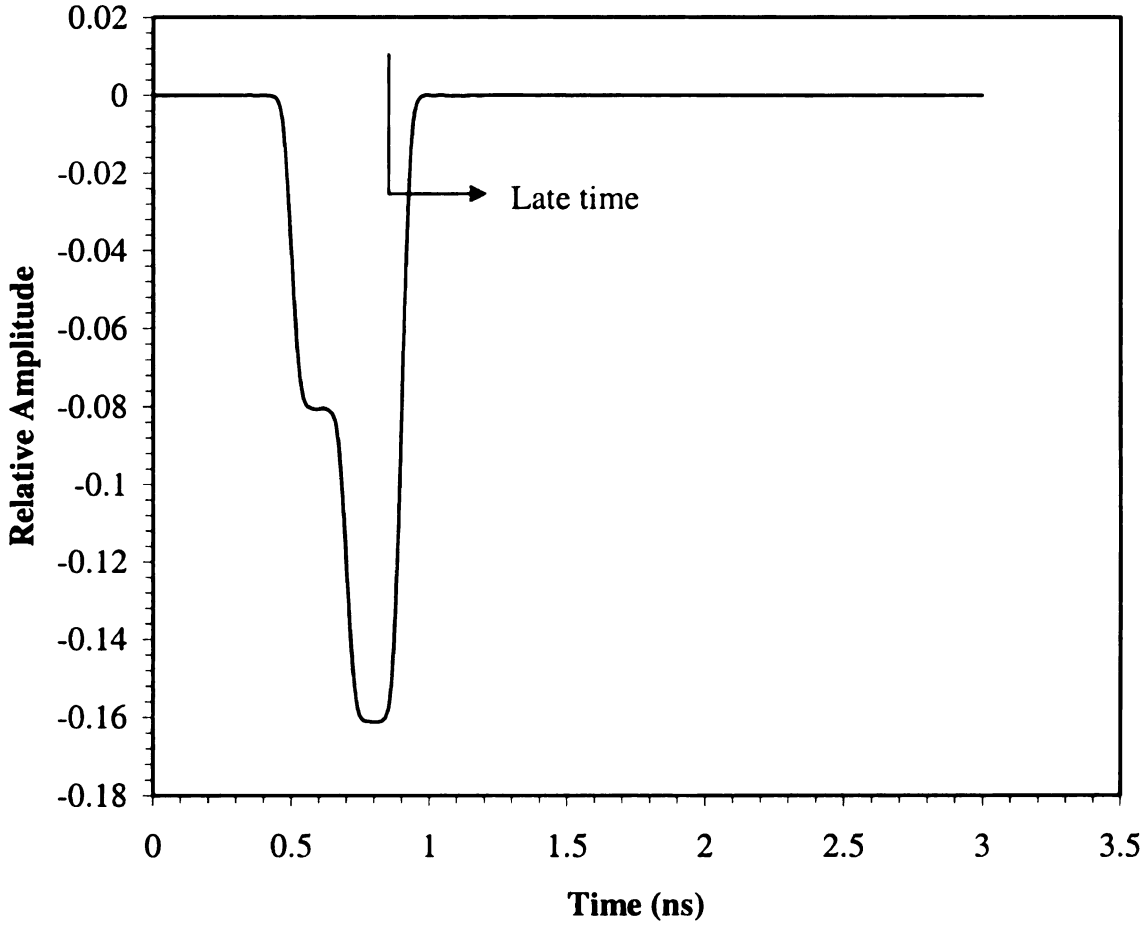

Figure 2-39 Convolution of baseline response with E-pulse 'A'.

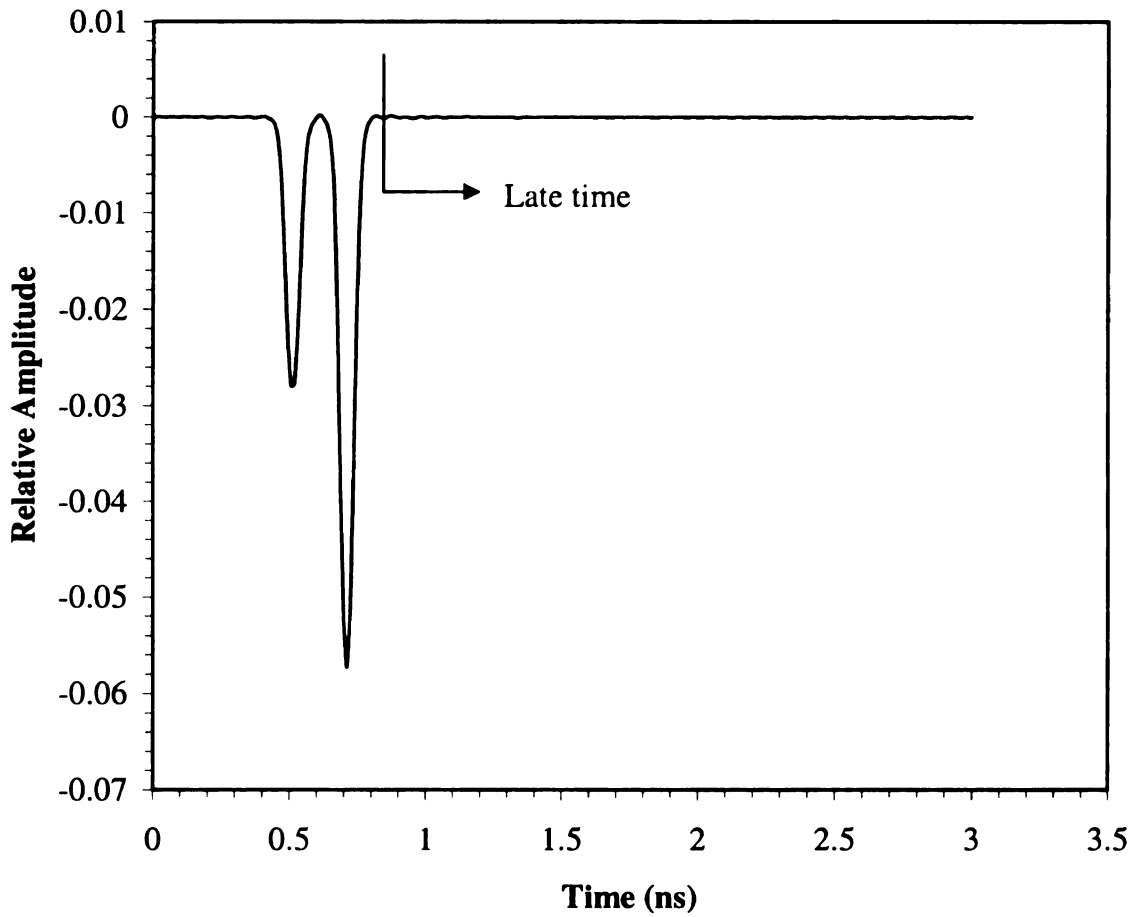

Figure 2-40 Convolution of baseline response with E-pulse 'E'.

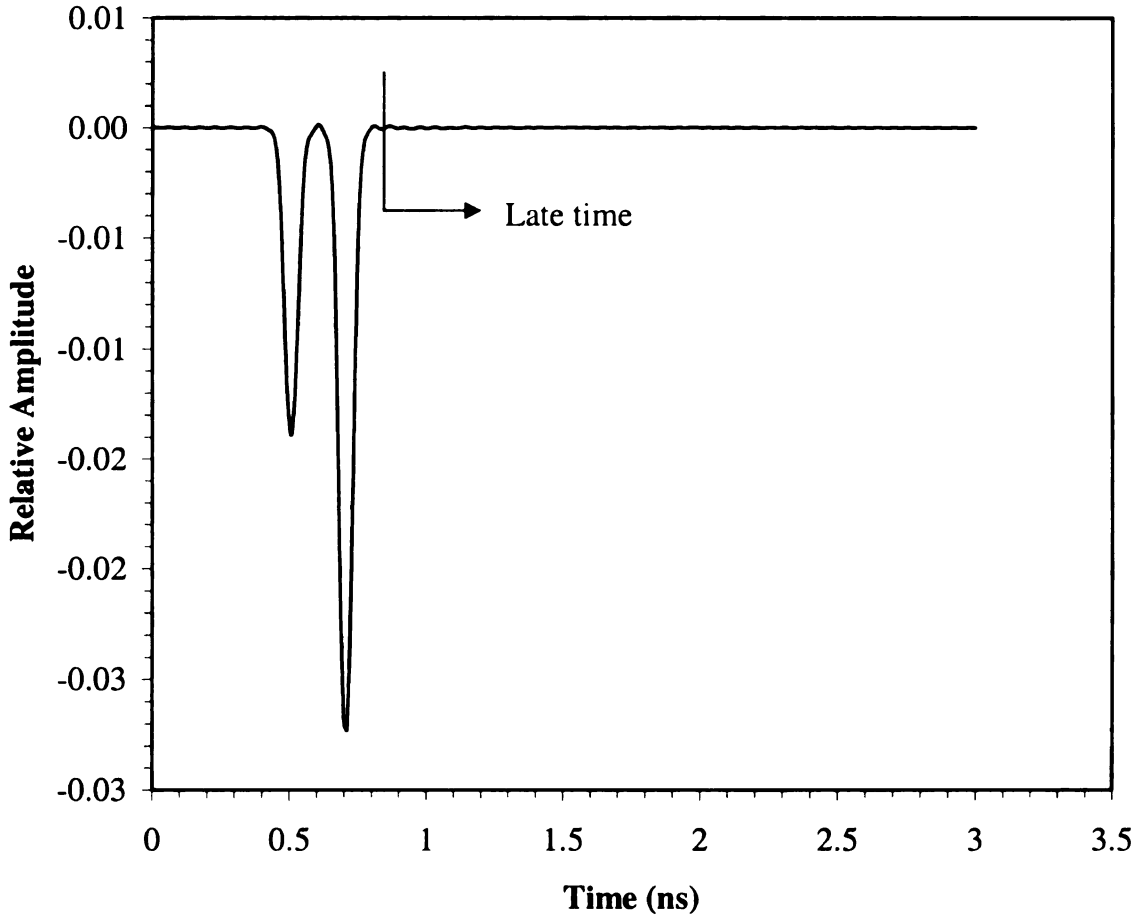

Figure 2-41 Convolution of baseline response with E-pulse 'J'.

As done previously, evaluation begins by tabulating the EDNa values, as seen in Table 2-11. These EDNa values are plotted against the number of modes in Figure 2-42. It can be seen from both Table 2-11 and Figure 2-42 that all of the E-pulses except the one generated using only one mode give a value very close to zero. This evidence suggests that using 5 modes to generate the E-pulses is more than sufficient.

A quick way to check that the proper number of modes is being used is to compare the imaginary parts of the natural frequencies, ω_n, to the frequency range used to generate the responses. By comparing the natural frequencies in Table 1-1 to the windowed frequency data in Figure 2-3 it can quickly be seen that only the first 5 modes are within the frequency range of the response data.

E-pulse	Number of Modes	EDNa
A	1	3.32E-02
B	2	2.12E-04
C	3	3.26E-06
D	4	6.63E-07
E(baseline)	5	3.70E-07
F	6	2.76E-07
G	7	2.27E-07
H	8	1.95E-07
I	9	1.72E-07
J	10	1.55E-07

Table 2-11 EDNa calculations for change in the number of modes.

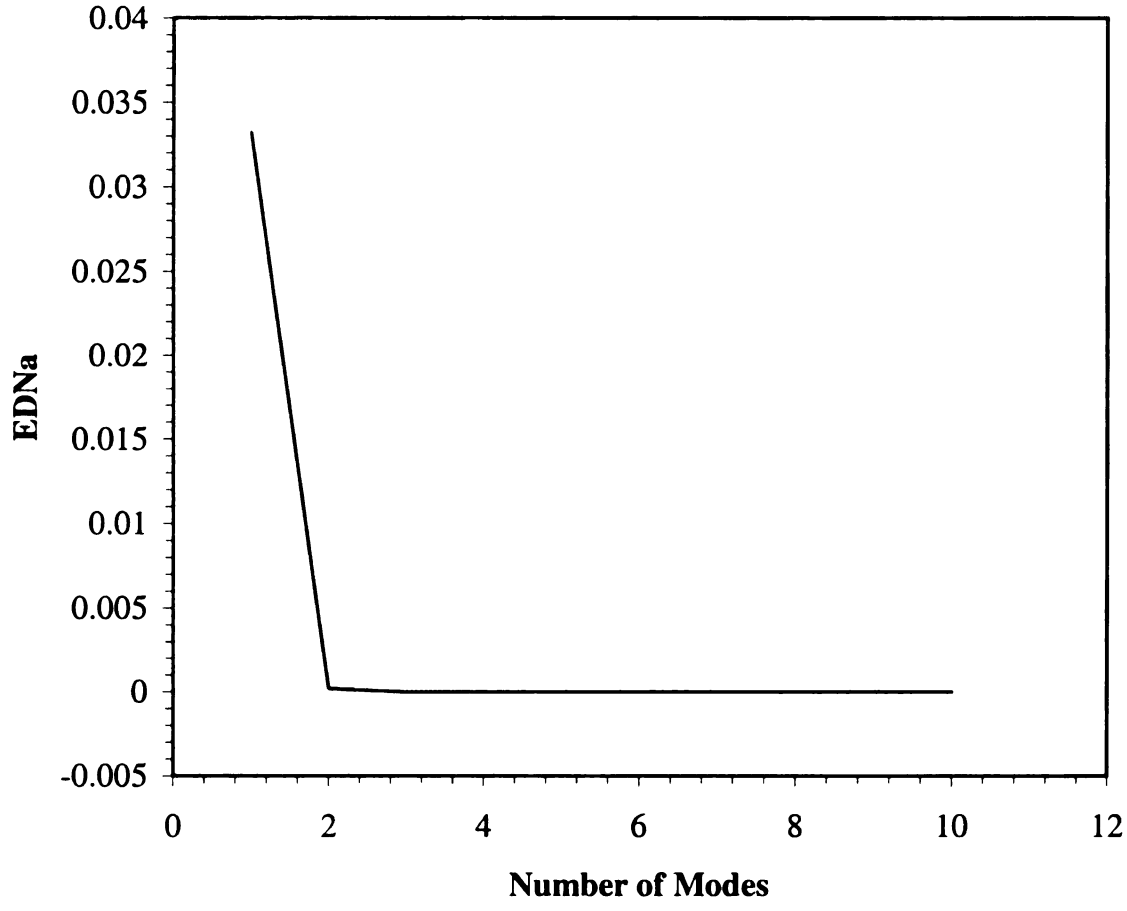

Figure 2-42 EDNa vs. change in the number of natural modes in the E-pulse.

2.3 Effects of Noise on EDNa

So far it has been shown that the E-pulse technique can diagnose changes in material properties for noise-free models. Practical measurements, however, are not noise-free. Thermal noise from the test equipment as well as background noise from the atmosphere are typical sources of interference that must be considered.

The noise model applied to the simulation data is discussed. Then this noise model is used to evaluate how well the E-pulse technique works to diagnose changes in layer thickness and permittivity using noisy response data.

2.3.1 Noise Model

A zero-mean gaussian noise model with probability density function,

$$f_X(x) = \frac{1}{\sqrt{2\pi\sigma^2}} e^{x^2/2\sigma^2}, \quad -\infty < x < \infty \ \ and \ \ \sigma > 0, \tag{2.15}$$

where σ^2 is the variance, was used to corrupt the response data. In the case of zero-mean gaussian noise, σ^2 is also called the time average power [8]. For transient signals we define the time-average power as,

$$Signal\ power = \frac{\int_W s^2(t)\,dt}{W}, \tag{2.16}$$

where $s(t)$ is the noise-free response signal and W is chosen as the minimum duration time window that contains 99% of the total energy of the noise-free data. Thus, the signal-to-noise ratio (SNR) is defined as,

$$SNR(dB) = 10\log_{10}\left\{\frac{Signal\ power}{\sigma^2}\right\}. \tag{2.17}$$

Using (2.17) to determine the time-average power of the noise , σ^2, yields,

$$\sigma^2 = \frac{\frac{\int s^2(t)\,dt}{W}}{10^{SNR/10}}. \tag{2.18}$$

By substituting values for the SNR, the time-average power of the noise can be determined.

It should be noted that in order to improve the statistics and ensure an accurate Gaussian model, 500 random samples of noise data were generated using (2.18). Each of these samples was then added to the response data and, following convolution, the EDNa resulting from each noisy response was calculated. The mean of these 500 EDNa values was then calculated and used as the EDNa.

2.3.2 EDNa/EDRa vs. Signal-to-Noise Ratio

Since the effects of changing the material properties on the EDNa using noise-free data was shown in previous sections, the major discussion here will be to show the effects of noise on the EDNa. The effects of noise on the data for EDNa versus change in thickness and EDNa versus change in permittivity will be shown. However, the number of data points presented will be limited (e.g., only 5 layer thicknesses will be evaluated compared to 15 in the noise free case). This is in consideration of the amount of data that would be generated to evaluate every data point as in the case of the noise free data.

For both the change in thickness and the change in permittivity the same baseline response will be used as an example. Seven different levels of noise were added to this baseline response waveform, seen in Figure 2-43. The levels of noise that were added to this response are shown in Table 2-12. The baseline response waveform is the same one

shown in Figure 2-4. One fact to note is that the duration of the response waveform in Figure 2-43 is less than the response waveform in Figure 2-4. The duration is determined such that the response waveform contains 99% of the energy contained in the original waveform. Plots of the noise corrupted response waveforms for three of the SNR values shown in Table 2-12 are shown as examples. Figure 2-44, Figure 2-45, and Figure 2-46 show the baseline response corrupted by noise such that the SNR is 30dB, 15dB, and 2dB, respectively. An E-pulse generated from the natural frequencies of the baseline response is shown in Figure 2-8. The resulting waveforms generated by convolving these three responses with this E-pulse are shown in Figure 2-47, Figure 2-48, and Figure 2-49. As expected, the late-time convolutions of the noise corrupted waveforms contain more energy. As the SNR decreases the late-time energy increases.

It is intuitively obvious that as more noise is added to the data, it will become harder to detect changes in the thickness or even to identify a response with no changes. It is possible to detect changes in thickness or permittivity up to a certain level of noise corruption.

As an illustration of how noise can affect a convolution waveform for a material, other than the baseline, consider Figure 2-50, Figure 2-51, and Figure 2-52. Figure 2-50 shows a plot of the noise-free convolution of material 'D' from Table 2-2 in section 2.2.1 with the baseline E-pulse. Figure 2-51 and Figure 2-52 show the same convolution with SNR of 15dB and 2dB, respectively. The effects of noise are evident in the figures. As the noise increases it becomes increasingly more difficult to determine whether the late-time energy is caused by a change in material properties or by noise.

Response Waveform	Signal-to-Noise (SNR)
A	Noise-free
B	30
C	25
D	20
E	15
F	10
G	5
H	2

Table 2-12 SNR of response waveforms.

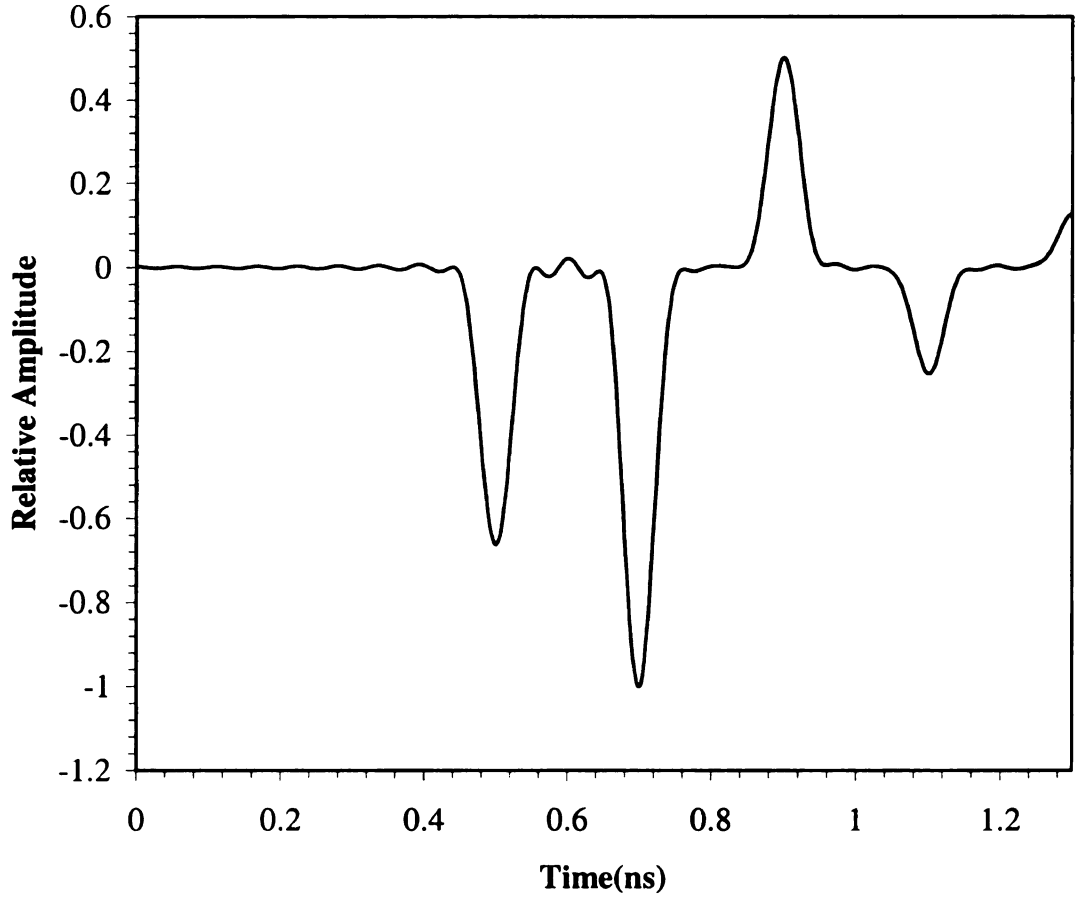

Figure 2-43 Response waveform 'A'.

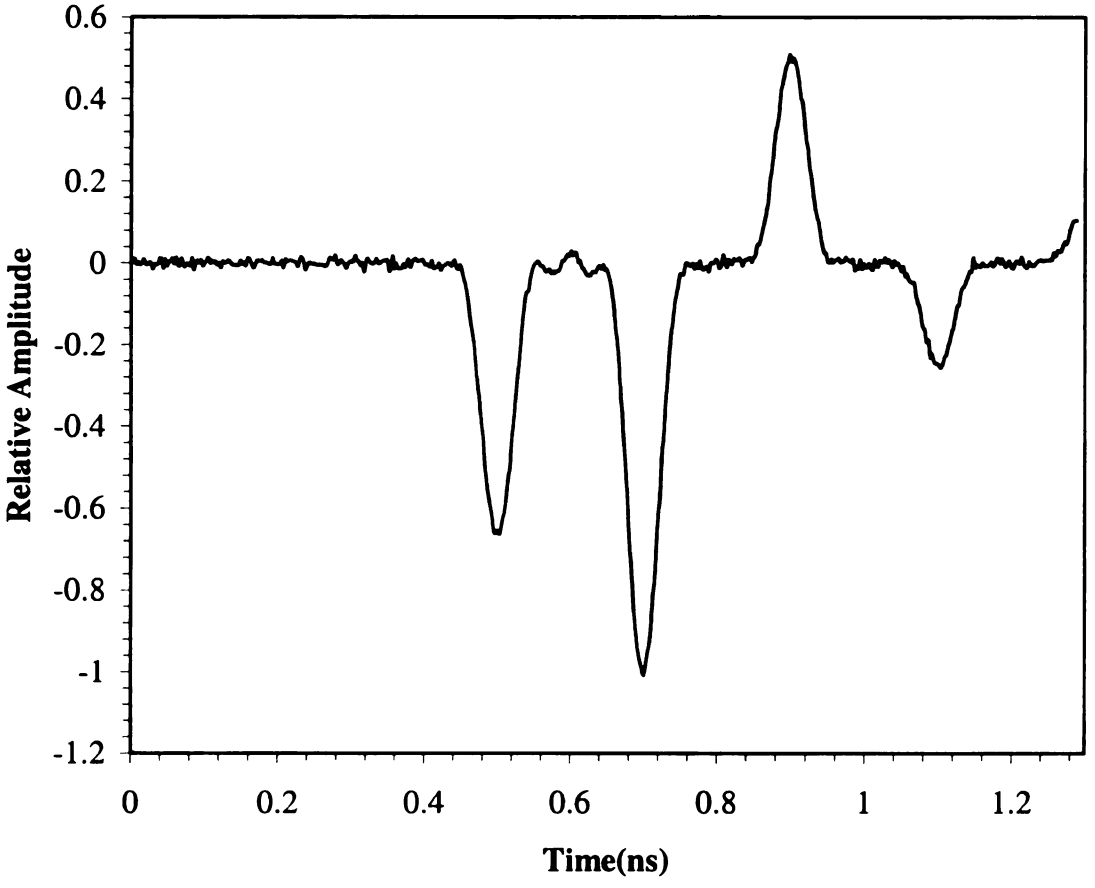

Figure 2-44 Response waveform 'B'.

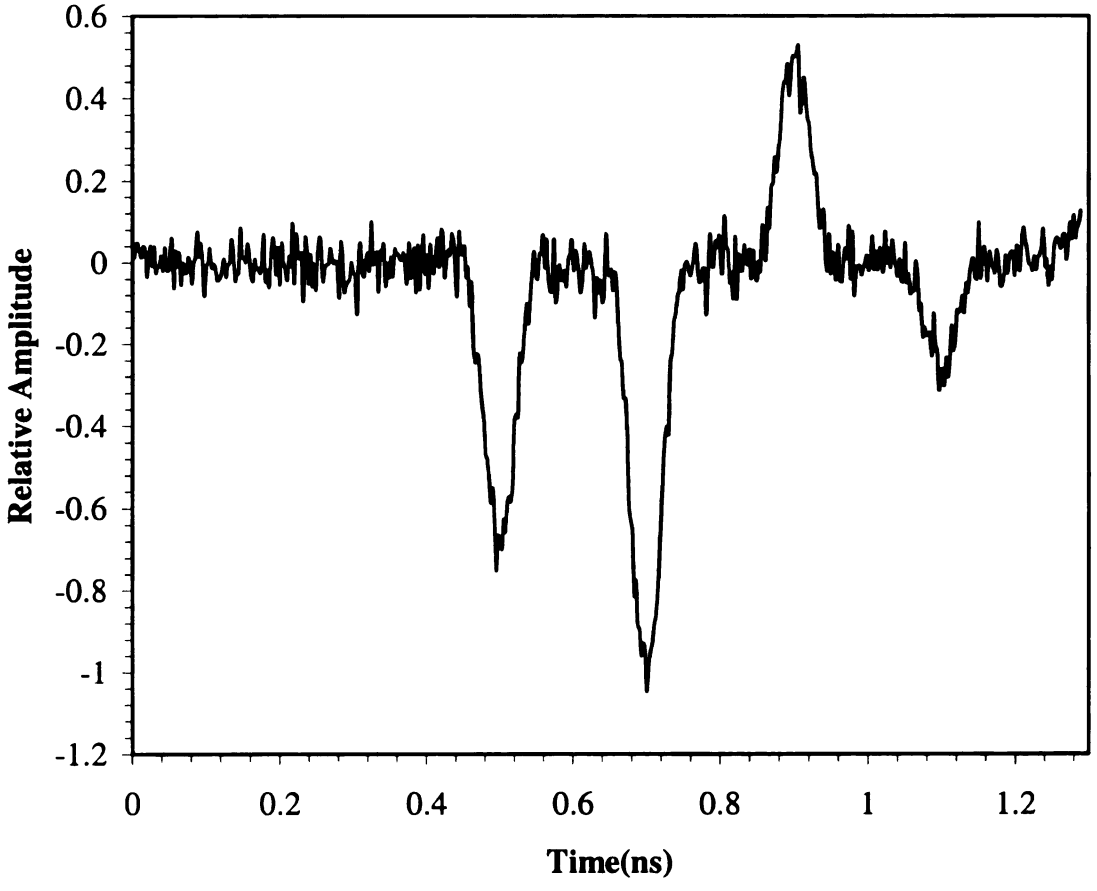

Figure 2-45 Response waveform 'E'.

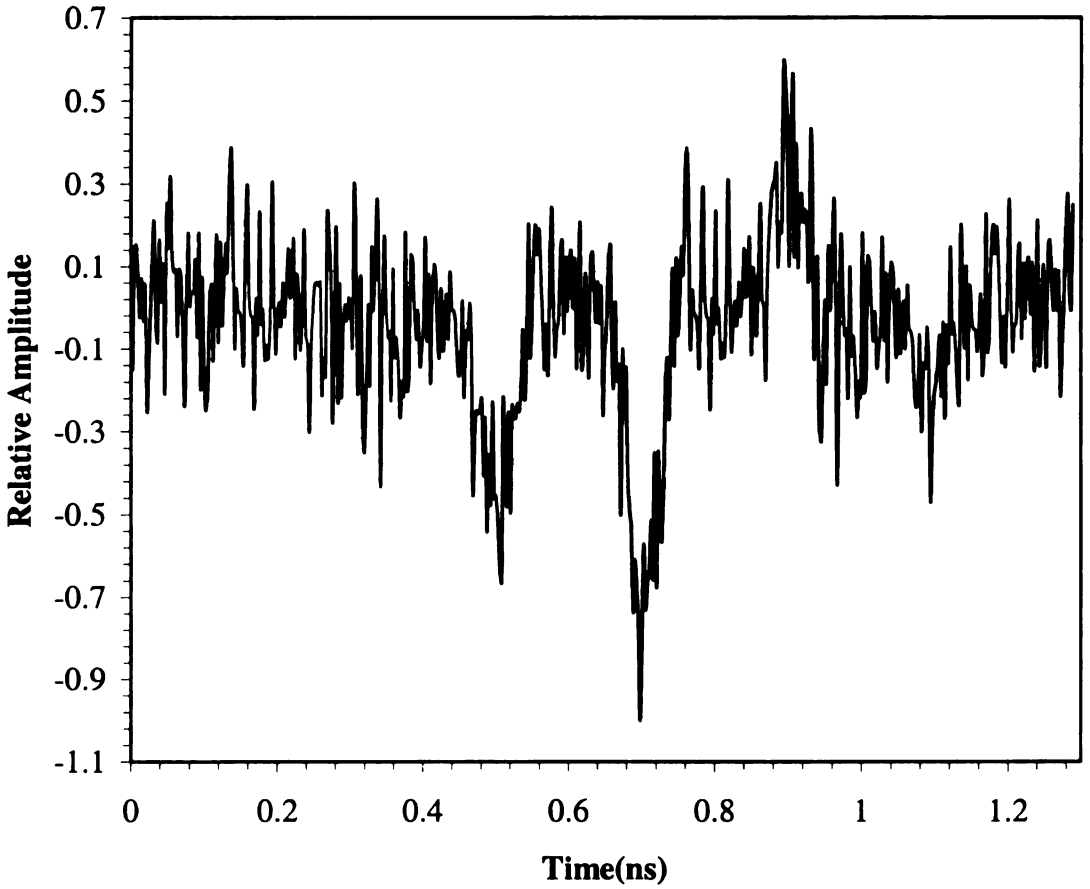

Figure 2-46 Response waveform 'H'.

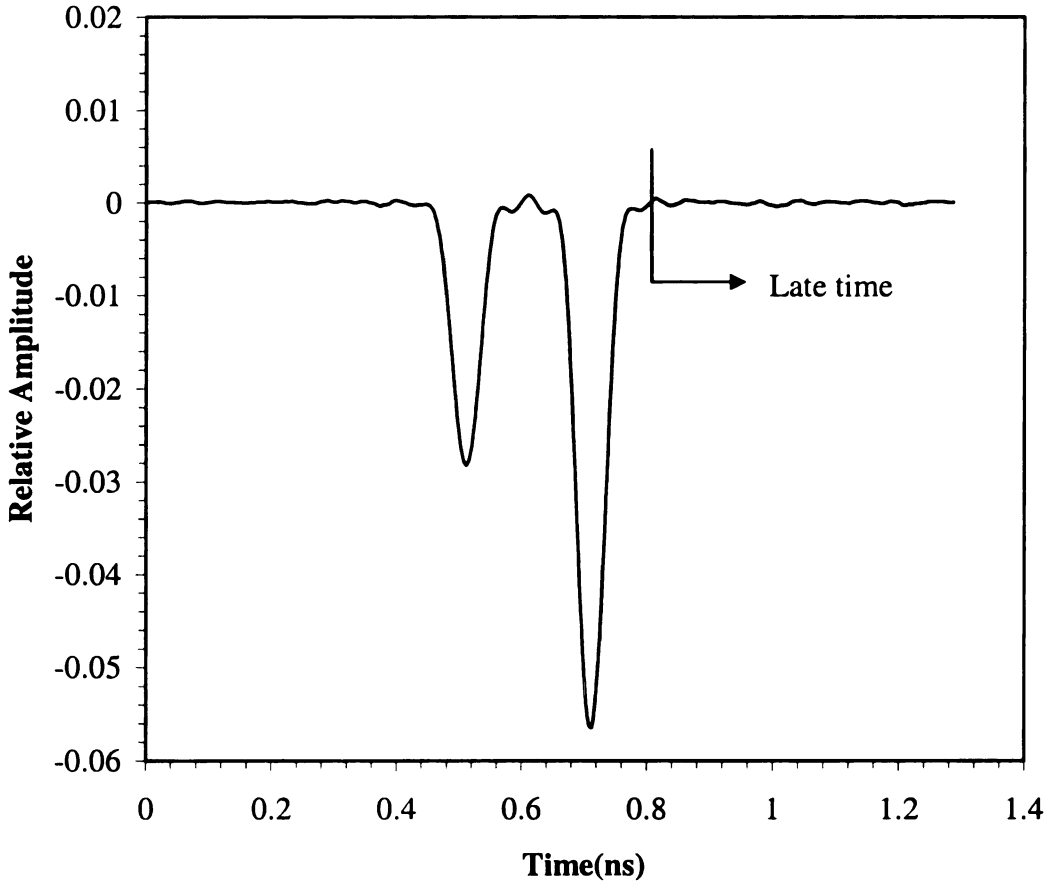

Figure 2-47 Convolution of response waveform 'B' with baseline E-pulse.

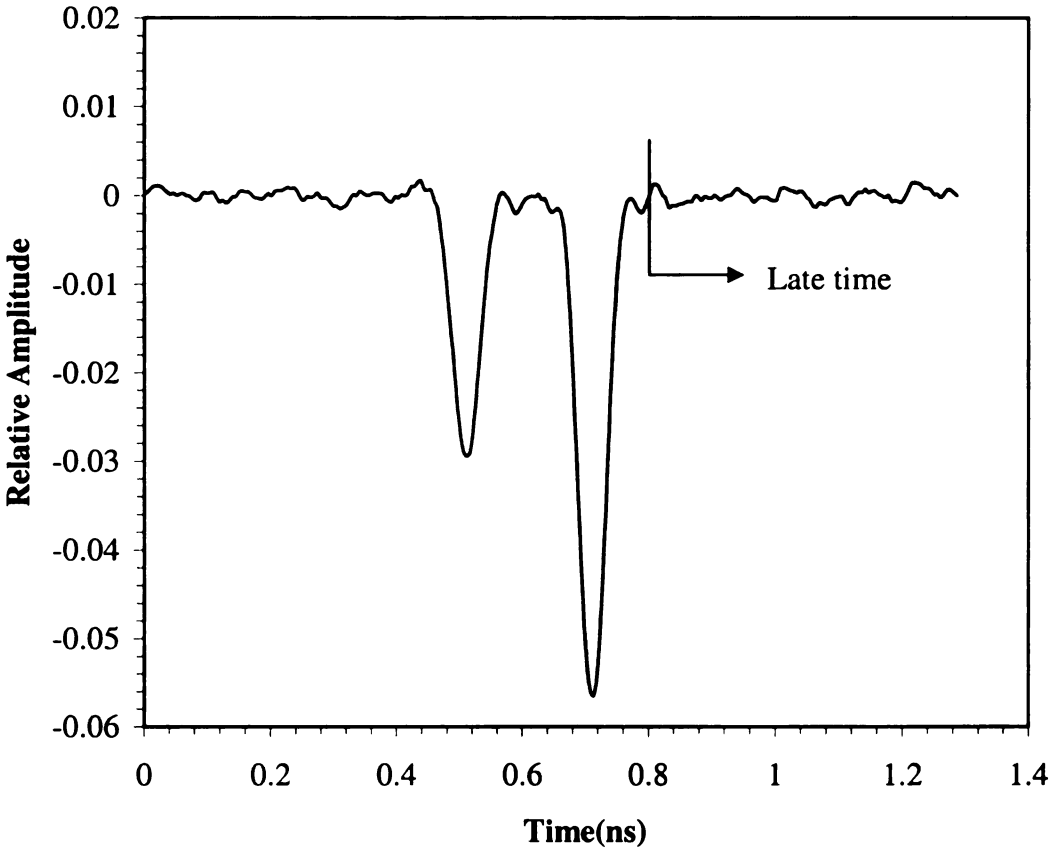

Figure 2-48 Convolution of response waveform 'E' with baseline E-pulse.

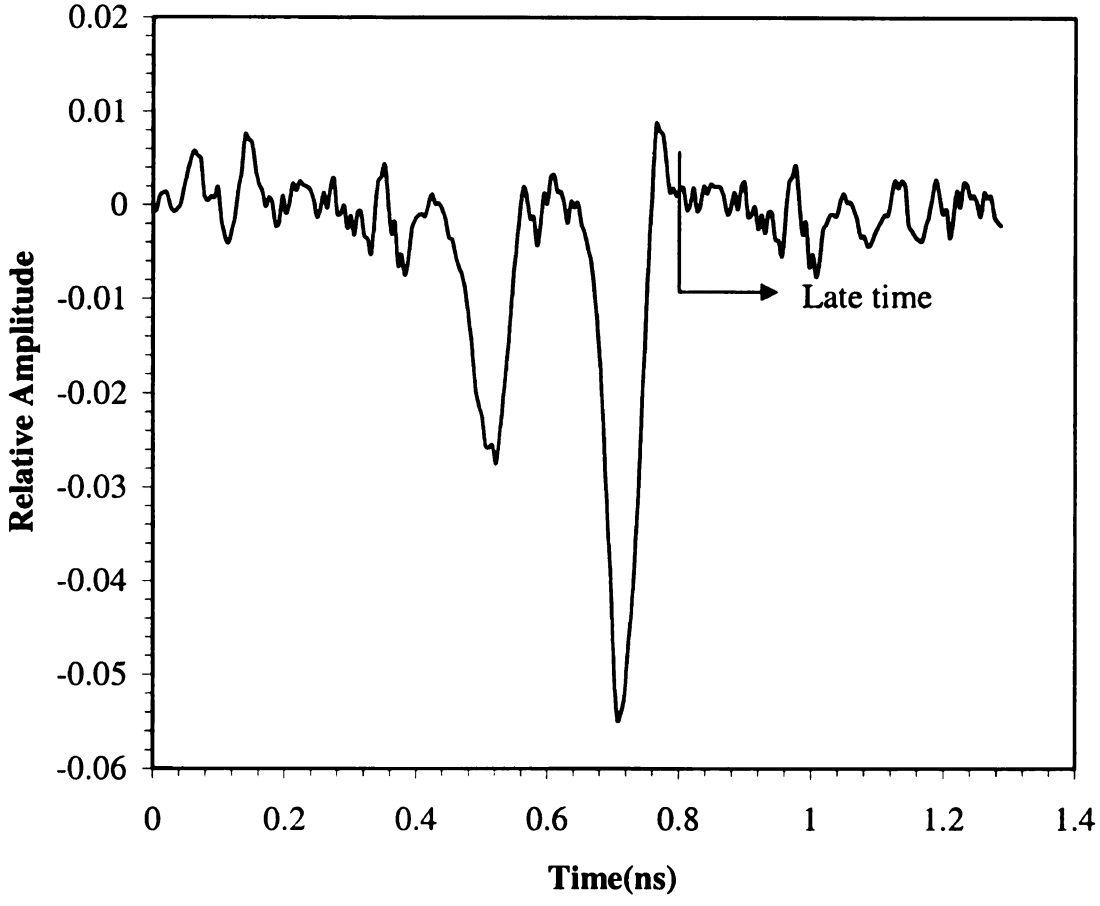

Figure 2-49 Convolution of response waveform 'H' with baseline E-pulse.

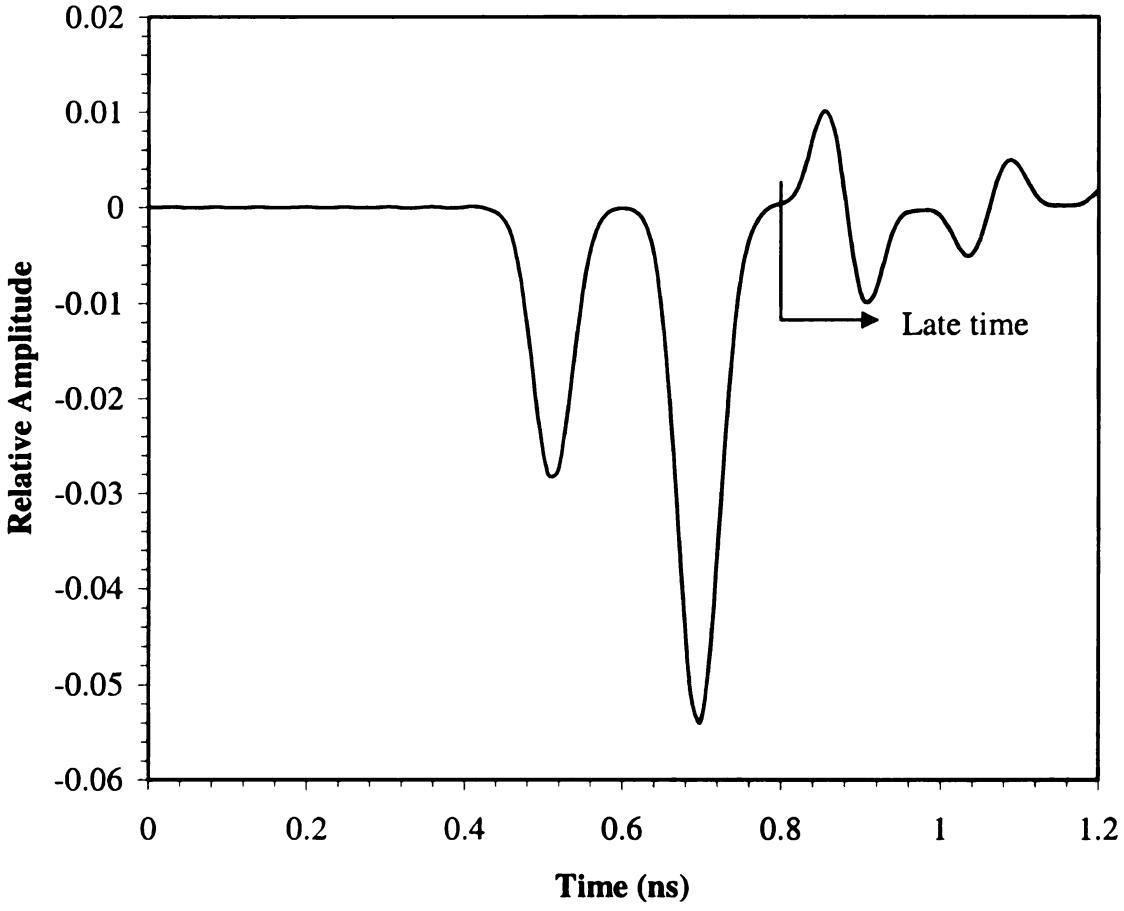

Figure 2-50 Noise-free convolution of material 'D' with baseline E-pulse.

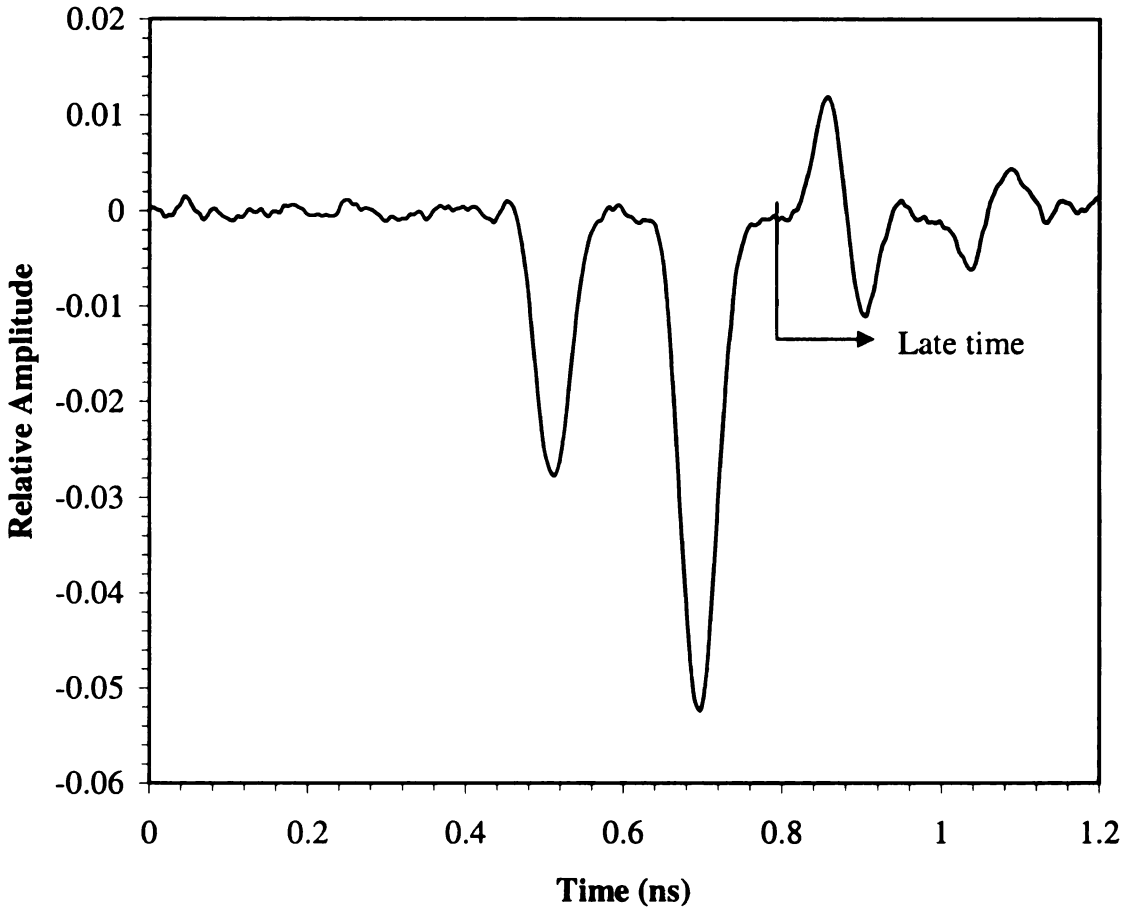

Figure 2-51 Convolution of material 'D' with baseline E-pulse with SNR=15dB.

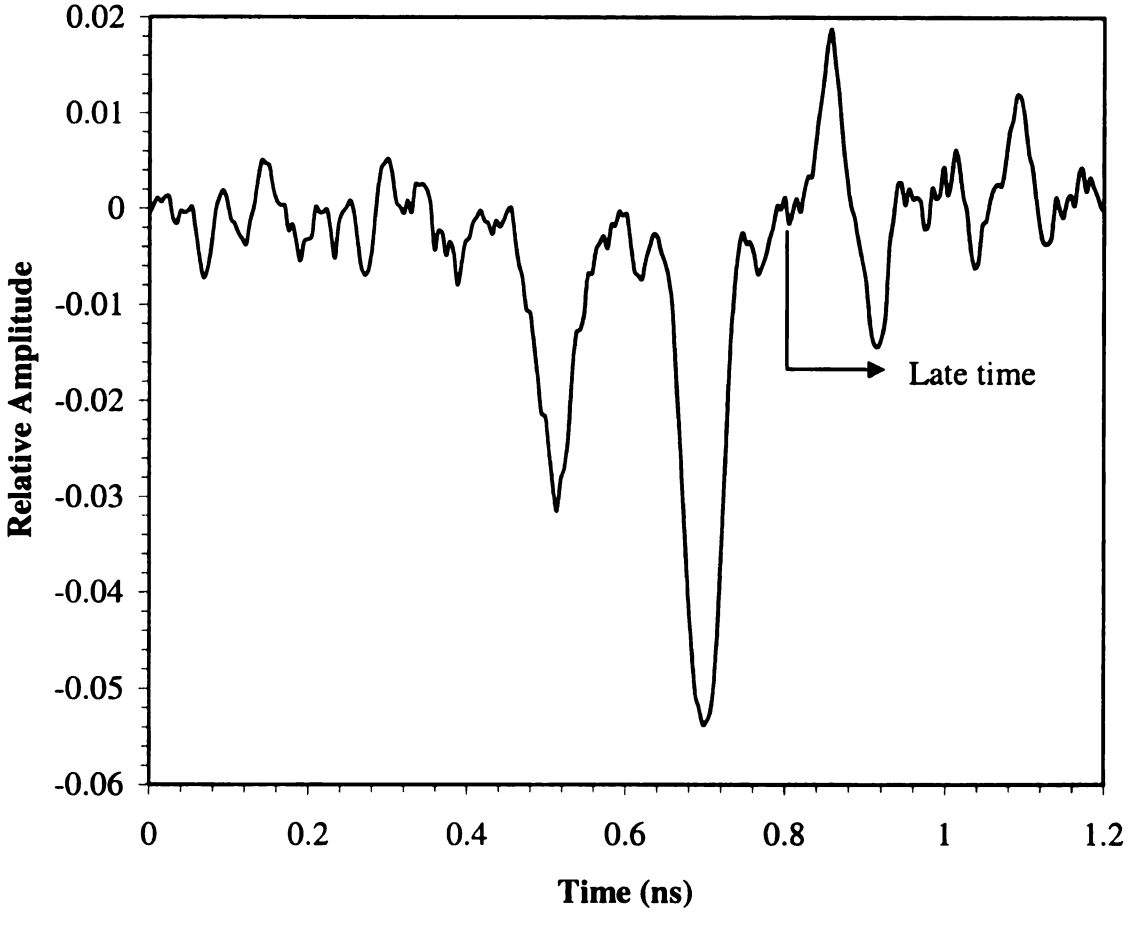

Figure 2-52 Convolution of material 'D' with baseline E-pulse with SNR=2dB.

Table 2-13 shows the EDNa values for several SNR and thicknesses. Table 2-14 shows the EDRa values calculated from those EDNa values in Table 2-13. Table 2-15 shows the EDNa values for several SNR and values of permittivity. Table 2-16 shows the EDRa values calculated from those EDNa values in Table 2-15. Following the tabulated EDNa and EDRa values are their plots. Figure 2-53 shows a plot of the EDNa versus SNR for several thicknesses and Figure 2-54 shows the EDRa versus SNR for several thicknesses. Figure 2-55 shows a plot of the EDNa versus SNR for several values of the permittivity and Figure 2-56 shows the EDRa versus SNR for several values of permittivity.

It can be seen in the EDNa plots, Figure 2-53 and Figure 2-55, that as the SNR increases, the EDNa value for the baseline case approaches zero while the EDNa values for the other cases get larger. This shows that as the SNR improves it becomes easier to detect changes in the thickness and permittivity. In the EDRa plots, Figure 2-54 and Figure 2-56, a similar observation can be made. As the SNR increases, the EDRa value for all of the cases except the baseline increases. The baseline case, of course, will always have an EDRa of zero. Again, this increase in EDRa suggests that as the SNR improves it becomes easier to detect changes in the thickness or permittivity.

A particular amount of change in the thickness or permittivity would determine an EDRa threshold value. For example, if it was desired to detect a change of 1mm or greater in thickness one could use Figure 2-54 to determine what threshold value of EDRa to set for a particular SNR. While it is possible to detect changes in material properties for good SNR, it is anticipated that at very low SNR it will be impossible to

detect small changes.

Thickness (mm)	2dB SNR	5dB SNR	10dB SNR	15dB SNR	20dB SNR	25dB SNR	30dB SNR
8	2.49E-03	2.92E-03	3.34E-03	3.51E-03	3.58E-03	3.60E-03	3.60E-03
9	1.09E-03	1.13E-03	1.18E-03	1.21E-03	1.22E-03	1.22E-03	1.22E-03
10	3.50E-04	2.07E-04	8.47E-05	2.89E-05	1.01E-05	4.28E-06	2.31E-06
11	1.13E-03	1.17E-03	1.19E-03	1.21E-03	1.22E-03	1.22E-03	1.22E-03
12	2.61E-03	3.03E-03	3.41E-03	3.57E-03	3.63E-03	3.64E-03	3.65E-03

Table 2-13 EDNa for numerous SNR and thicknesses.

Thickness (mm)	2dB SNR	5dB SNR	10dB SNR	15dB SNR	20dB SNR	25dB SNR	30dB SNR
8	8.52	1.15E+01	1.60E+01	2.08E+01	2.55E+01	2.92E+01	3.19E+01
9	4.93	7.37E+00	1.14E+01	1.62E+01	2.08E+01	2.45E+01	2.72E+01
10	0.00	0.00	0.00	0.00	0.00	0.00	0.00
11	5.09	7.52E+00	1.15E+01	1.62E+01	2.08E+01	2.45E+01	2.72E+01
12	8.73	1.17E+01	1.60E+01	2.09E+01	2.56E+01	2.93E+01	3.20E+01

Table 2-14 EDRa for numerous SNR and thicknesses.

ε_r	2dB SNR	5dB SNR	10dB SNR	15dB SNR	20dB SNR	25dB SNR	30dB SNR
7	1.11E-03	1.25E-03	1.38E-03	1.43E-03	1.45E-03	1.46E-03	1.46E-03
8	4.96E-04	4.52E-04	3.98E-04	3.99E-04	3.92E-04	3.90E-04	3.89E-04
9	2.28E-04	2.03E-04	8.11E-05	2.92E-05	1.02E-05	3.57E-06	2.22E-06
10	6.12E-04	5.24E-04	4.43E-04	4.08E-04	3.96E-04	3.93E-04	3.92E-04
11	1.23E-03	1.36E-03	1.31E-03	1.36E-03	1.36E-03	1.38E-03	1.37E-03

Table 2-15 EDNa for numerous SNR and values of relative permittivity.

ε_r	2dB SNR	5dB SNR	10dB SNR	15dB SNR	20dB SNR	25dB SNR	30dB SNR
7	6.87	7.89E+00	1.23E+01	1.69E+01	2.15E+01	2.61E+01	2.82E+01
8	3.38	3.48E+00	6.91E+00	1.14E+01	1.58E+01	2.04E+01	2.24E+01
9	0.00	0.00E+00	0.00E+00	0.00E+00	0.00E+00	0.00E+00	0.00E+00
10	4.29	4.12E+00	7.37E+00	1.15E+01	1.59E+01	2.04E+01	2.25E+01
11	7.32	8.26E+00	1.21E+01	1.67E+01	2.12E+01	2.59E+01	2.79E+01

Table 2-16 EDRa for numerous SNR and values of relative permittivity.

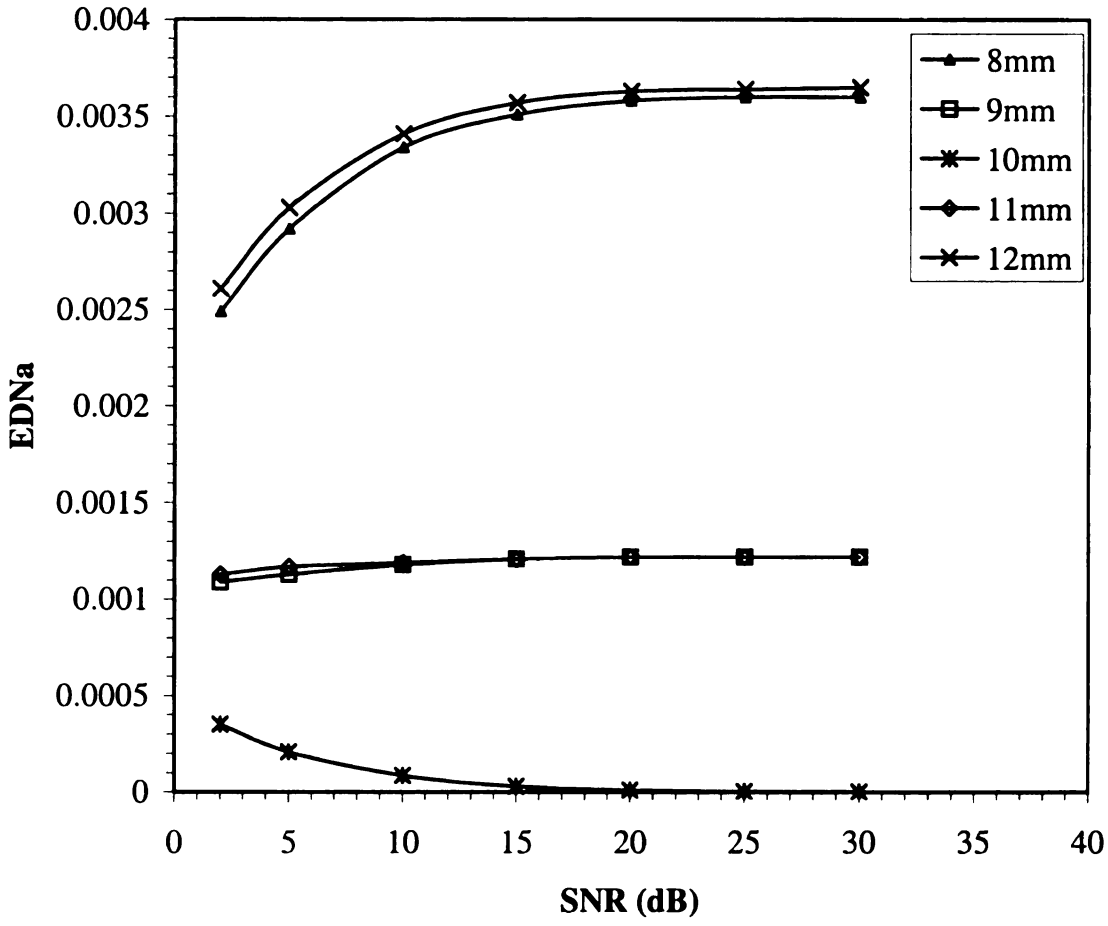

Figure 2-53 Comparison of EDNa vs. SNR for several thickness.

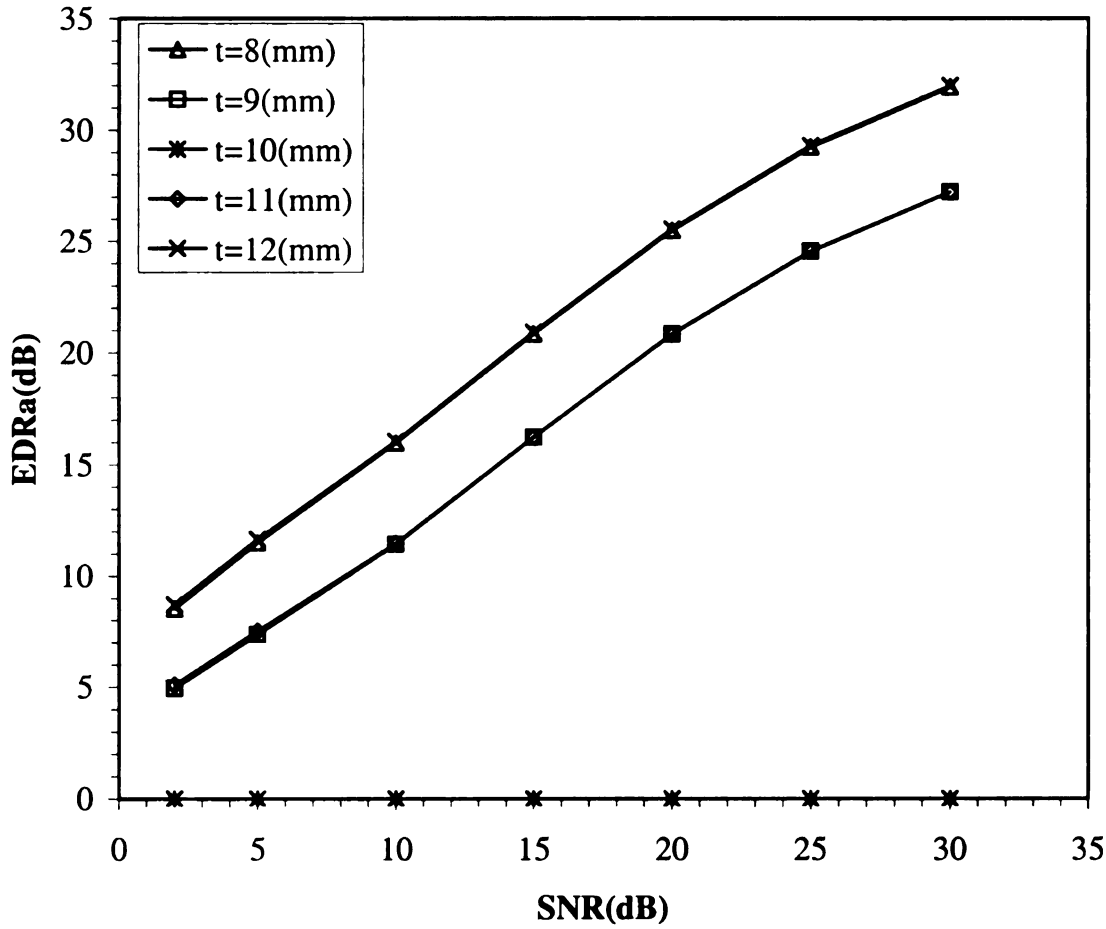

Figure 2-54 Comparison of EDRa vs. SNR for several thicknesses.

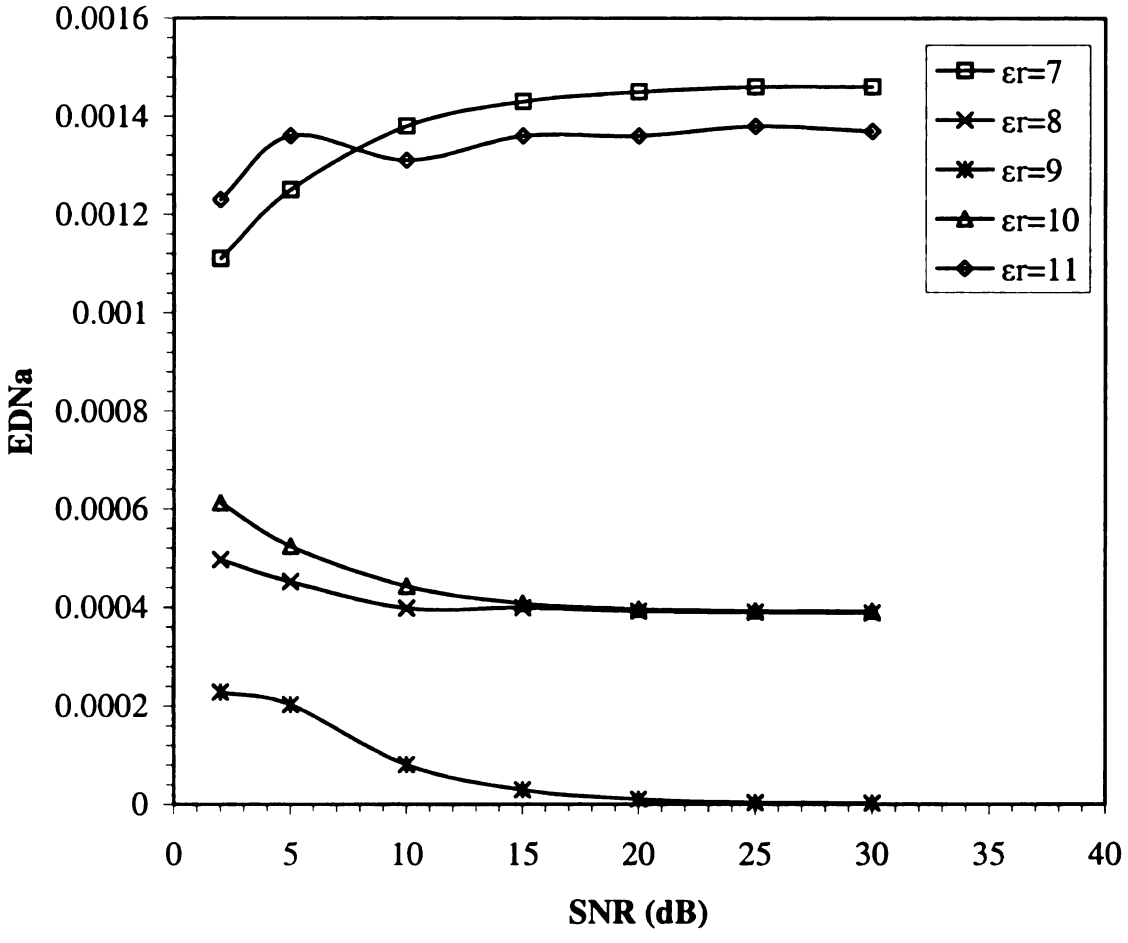

Figure 2-55 Comparison of EDNa vs. SNR for several values of permittivity.

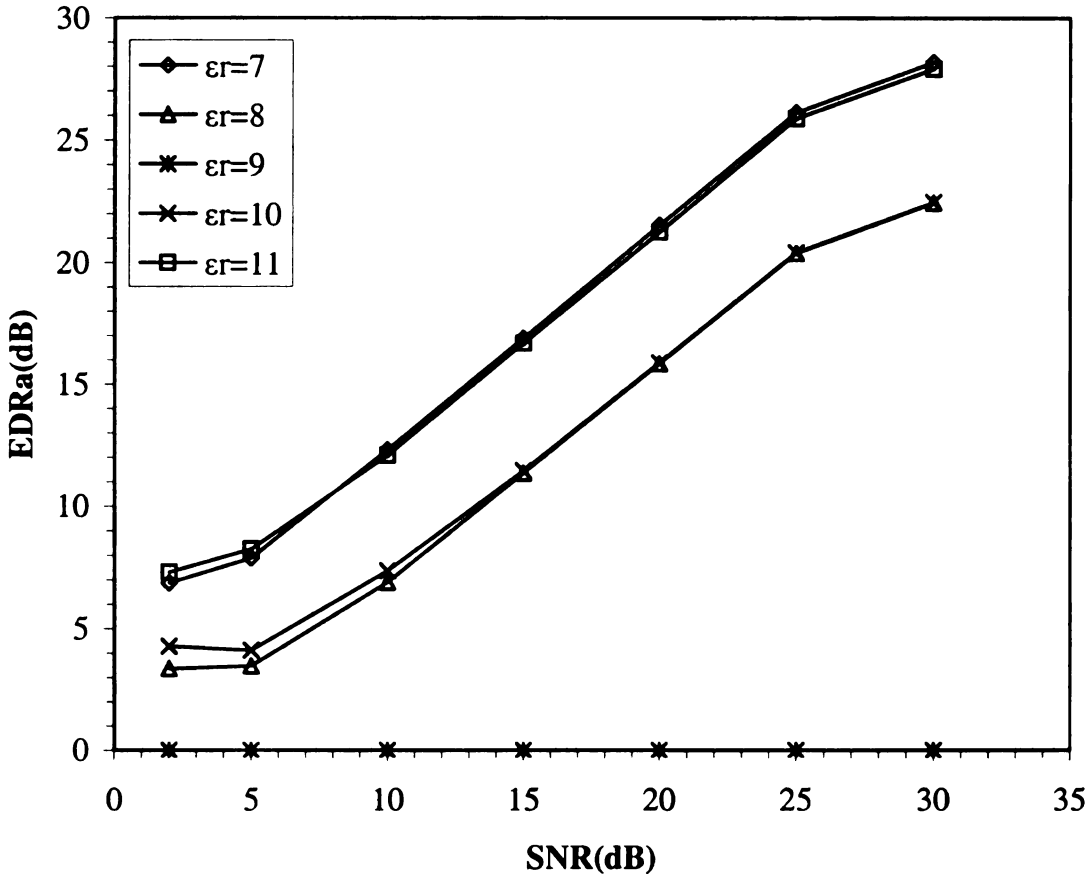

Figure 2-56 Comparison of EDRa vs. SNR for several values of permittivity.

Chapter 3

Single Lossy Layer

The goal of this chapter is to explore how the conductivity of the material layer affects our ability to determine changes in layered material properties. The chapter begins with an explanation of how to determine the natural frequencies of conductive material. A similar approach to that used in chapter 2 is used, the difference being that for conductive material the permittivity is complex. The remainder of the chapter shows the results of using the E-pulse to determine changes in the thickness, permittivity, angle of incidence, and conductivity for noise-free data. The last section will show the effects of noise on the use of the EDNa.

3.1 Theoretical Determination of Natural Frequencies of Conductive Material

To calculate the natural frequencies for materials with conductivity not equal to zero requires a slightly different evaluation. Begin by letting

$$\varepsilon_1(\omega) = \varepsilon_0\varepsilon_{1r} - j\frac{\sigma}{\omega} \quad \ldots\sigma \neq \sigma(\omega) \tag{3.1}$$

or,

$$\varepsilon_1(s) = \varepsilon_0\varepsilon_{1r} + \frac{\sigma}{s}. \tag{3.2}$$

Therefore,

$$Z_1 = \begin{cases} \dfrac{\eta_0}{\sqrt{\varepsilon_{1r} + \dfrac{\sigma}{s\varepsilon_0} - \sin^2\theta_i}}, & \ldots perpendicular\ polarization \\ \eta_0 \dfrac{\sqrt{\varepsilon_{1r} + \dfrac{\sigma}{s\varepsilon_0} - \sin^2\theta_i}}{\varepsilon_{1r} + \dfrac{\sigma}{s\varepsilon_0}}, & \ldots parallel\ polarization \end{cases} \tag{3.3}$$

Once again, the poles of (1.50) determine the natural frequencies. Therefore,

$$1 - \Gamma(s) e^{-s\tau(s)} = 0 \tag{3.4}$$

where

$$\tau(s) = \frac{2d}{c} \sqrt{\varepsilon_{1r} + \frac{\sigma}{s\varepsilon_0} - \sin^2\theta_i} \tag{3.5}$$

$$= \frac{2d}{c} F(s) \tag{3.6}$$

where

$$F(s) = \sqrt{\varepsilon_{1r} + \frac{\sigma}{s\varepsilon_0} - \sin^2\theta_i}\ . \tag{3.7}$$

Substituting (1.34) into (3.4) gives,

$$1 - \frac{Z_1(s) - Z_0}{Z_1(s) + Z_0} e^{-s\tau(s)} = 0 \tag{3.8}$$

or

$$Z_1(s) + Z_0 - \left(Z_1(s) - Z_0\right) e^{-s\tau(s)} = 0 \tag{3.9}$$

The solution to (3.9) for the natural frequencies depends on the polarization of the incident wave. Given the incident wave has perpendicular polarization produces the following expressions;

$$Z_1(s) = \frac{\eta_0}{F(s)}, \tag{3.10}$$

$$Z_0 = \frac{\eta_0}{\cos\theta_i}, \tag{3.11}$$

$$Z_1(s) + Z_0 - \left(Z_1(s) - Z_0\right)e^{-s\tau(s)} = 0. \tag{3.12}$$

Thus,

$$\frac{\eta_0}{F(s)} + \frac{\eta_0}{\cos\theta_i} - \left(\frac{\eta_0}{F(s)} - \frac{\eta_0}{\cos\theta_i}\right)e^{-s\tau(s)} = 0 \tag{3.13}$$

or

$$\boxed{\cos\theta_i + F(s) - \left(\cos\theta_i - F(s)\right)e^{-s\tau(s)} = 0}. \tag{3.14}$$

Given the incident wave has perpendicular polarization produces the following expressions;

$$Z_1(s) = \eta_0 \frac{F(s)}{G(s)}, \tag{3.15}$$

$$Z_0 = \eta_0 \cos\theta_i, \tag{3.16}$$

$$G(s) = \varepsilon_{1r} + \frac{\sigma}{s\varepsilon_0}, \tag{3.17}$$

$$Z_1(s) + Z_0 - \left(Z_1(s) - Z_0\right)e^{-s\tau(s)} = 0. \tag{3.18}$$

Thus,

$$\eta_0 \frac{F(s)}{G(s)} + \eta_0\cos\theta_i - \left(\eta_0 \frac{F(s)}{G(s)} - \eta_0\cos\theta_i\right)e^{-s\tau(t)} = 0 \tag{3.19}$$

or

$$\boxed{F(s) + G(s)\cos\theta_i - \left(F(s) - G(s)\cos\theta_i\right)e^{-s\tau(s)} = 0} \tag{3.20}$$

If the incident angle of the excitation is zero, then

$$H(s) = F(s)\big|_{\theta_i = 0} = \sqrt{G(s)} \tag{3.21}$$

and (3.14) and (3.20) reduce to the identical expression

$$\boxed{1 + H(s) - \left[1 - H(s)\right] e^{-s\tau'(s)}} \tag{3.22}$$

where

$$\tau'(s) = \frac{2d}{c} H(s). \tag{3.23}$$

Equation (3.14), (3.20), and (3.22) cannot be solved in closed form but can be solved numerically. The numerical solution to these equations is performed using the software program NFSIG.for, included in appendix E, written by Dr. Ed Rothwell.

3.2 Computation of EDNa and EDRa

Quantifying the results in chapter 3 is done exactly the same way as was done in chapter 2. The EDNa is used to quantify the results for the noise-free data and the EDRa is used to quantify the results for the noise-corrupted data.

3.2.1 Change in Layer Thickness

The material analyzed in this section is essentially the same material analyzed in section 2.2.1. The difference is that the material analyzed in this chapter has a non-zero conductivity ($\sigma = 0.5$). The properties of the materials evaluated are shown in Table 3-1. The thickness ranges from 5mm to 15mm with the baseline material having a thickness of 10mm. The baseline material is used to generate the E-pulse and is the material used for comparison in determining any changes in the thickness.

Keeping in mind the number of plots that would be required to illustrate all of the material configurations, only a representative sample was chosen. The two extreme cases

of change in thickness as well as the two cases with minimal change in thickness were chosen to illustrate the response curves and the convolution curves. Figure 3-1 and Figure 3-2 show the response waveforms of the extreme cases while Figure 3-3 shows a comparison of the responses of the two cases with thickness nearest to the baseline with the baseline response. It can be seen that when the thickness changes by more than 5mm in either direction the response waveform changes significantly. A good example of the effects of the conductivity can be seen by comparing Figure 3-2 with Figure 2-6. The response waveform in Figure 2-6 is that of a material with zero conductivity, but with all of the same properties otherwise as the material whose response waveform is shown in Figure 3-2. This comparison clearly shows that the material with conductivity exhibits signal loss as the pulse travels through the material.

As mentioned, the baseline material properties were used to generate the E-pulse, shown in Figure 3-4. This E-pulse was convolved with all of the response waveforms and the late-time energy of the convolution waveforms were used to determine the EDNa. Convolution of the E-pulse with the baseline response waveform is shown in Figure 3-5. It can be seen that, as expected, the late-time energy is near zero. The fact that it is not exactly zero can be attributed to the use of the number of modes to generate the E-pulse as well as round-off error. The convolutions of the E-pulse with the remaining illustrated cases are shown in Figure 3-6, Figure 3-7, Figure 3-8, and Figure 3-9. The materials with large deviation in thickness show a significant amount of late-time energy in their convolutions. In addition, late-time energy is seen in the Figure 3-8 and Figure 3-9 for the cases where the thickness was only slightly changed.

Material	ε	μ	σ	Thickness (mm)	Polarization	Angle of incidence, θ_i
A	$9\varepsilon_0$	μ_0	0.5	5	Parallel	0
B	$9\varepsilon_0$	μ_0	0.5	6	Parallel	0
C	$9\varepsilon_0$	μ_0	0.5	7	Parallel	0
D	$9\varepsilon_0$	μ_0	0.5	8	Parallel	0
E	$9\varepsilon_0$	μ_0	0.5	9	Parallel	0
F	$9\varepsilon_0$	μ_0	0.5	9.5	Parallel	0
G	$9\varepsilon_0$	μ_0	0.5	9.75	Parallel	0
H (baseline)	$9\varepsilon_0$	μ_0	0.5	10	Parallel	0
I	$9\varepsilon_0$	μ_0	0.5	10.25	Parallel	0
J	$9\varepsilon_0$	μ_0	0.5	10.5	Parallel	0
K	$9\varepsilon_0$	μ_0	0.5	11	Parallel	0
L	$9\varepsilon_0$	μ_0	0.5	12	Parallel	0
M	$9\varepsilon_0$	μ_0	0.5	13	Parallel	0
N	$9\varepsilon_0$	μ_0	0.5	14	Parallel	0
P	$9\varepsilon_0$	μ_0	0.5	15	Parallel	0

Table 3-1 Material properties for changing thickness.

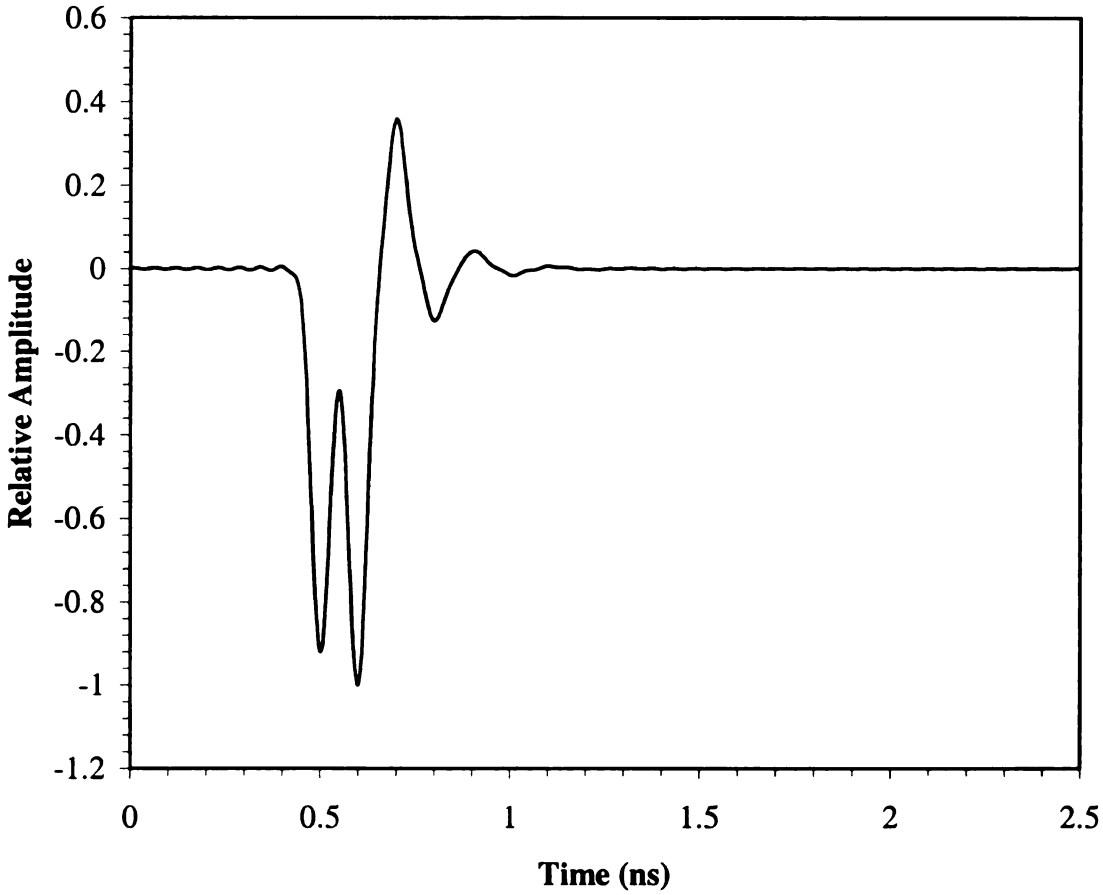

Figure 3-1 Response waveform for material 'A'

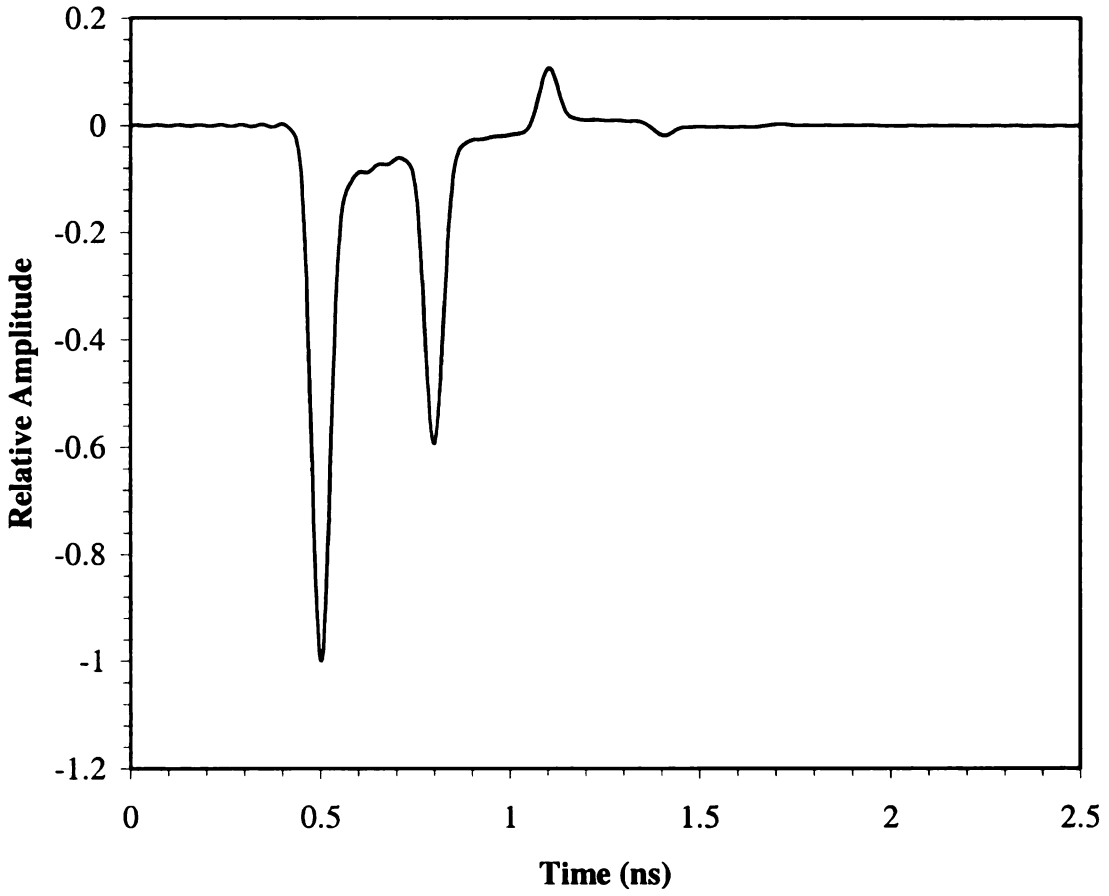

Figure 3-2 Response waveform for material 'P'

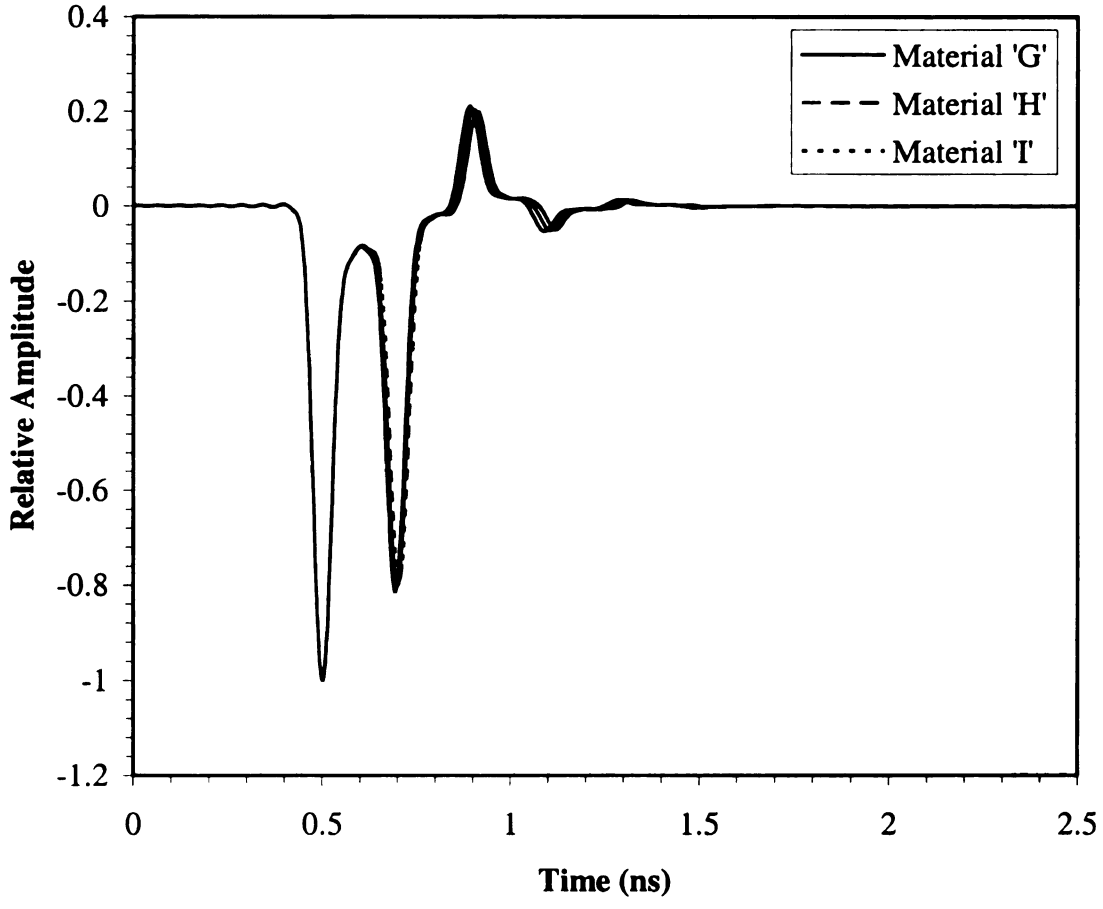

Figure 3-3 Comparison of response waveform for materials 'G', 'H', and 'I'.

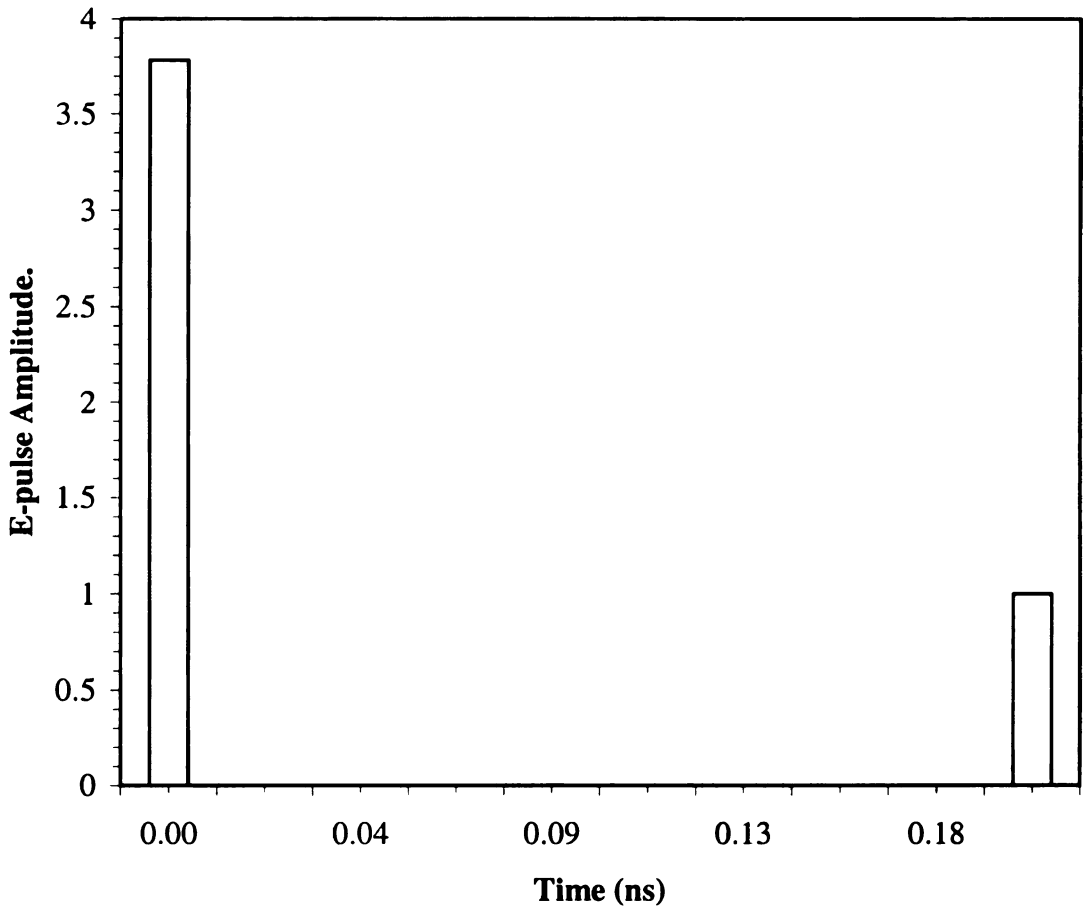

Figure 3-4 E-pulse generated from the baseline material properties.

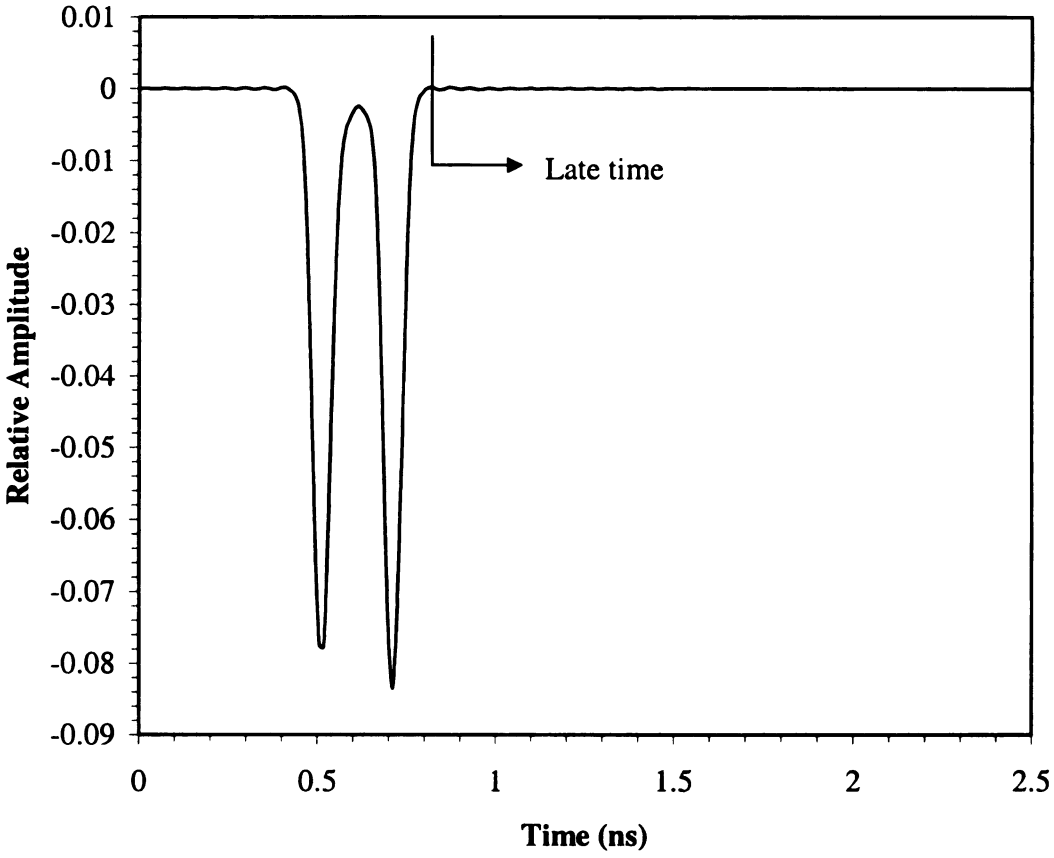

Figure 3-5 Convolution of baseline response with baseline E-pulse.

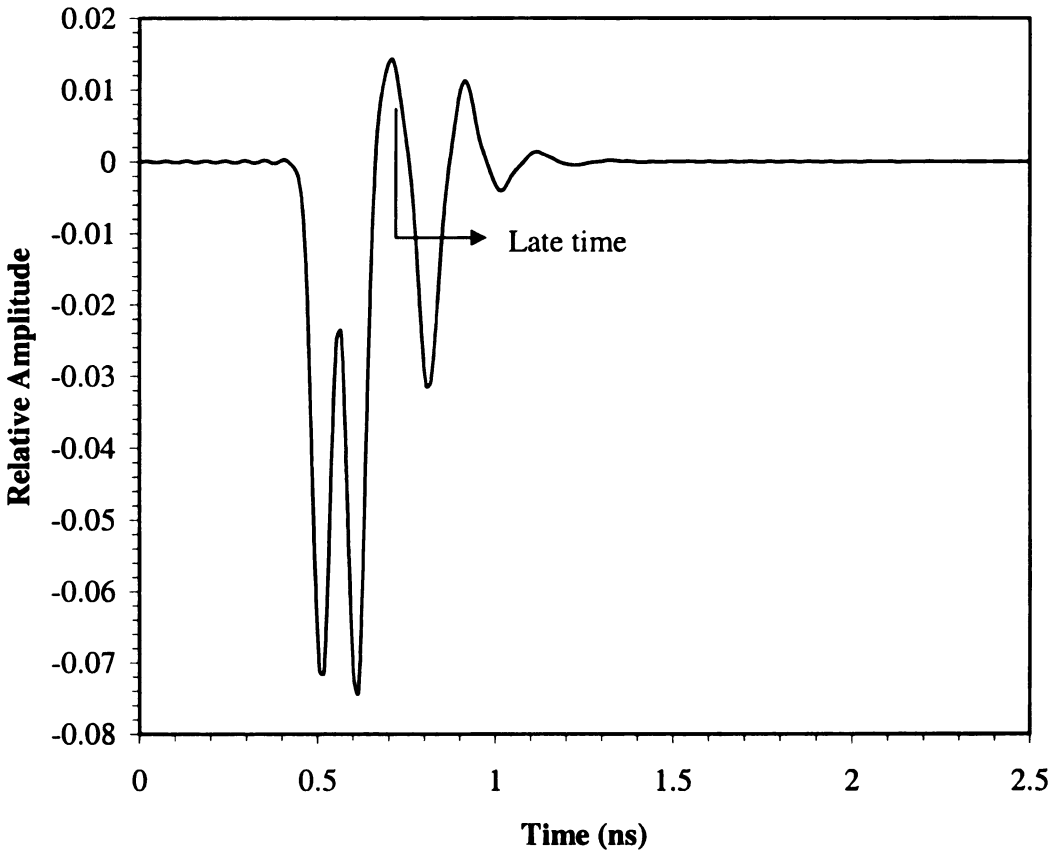

Figure 3-6 Convolution of material 'A' response with baseline E-pulse.

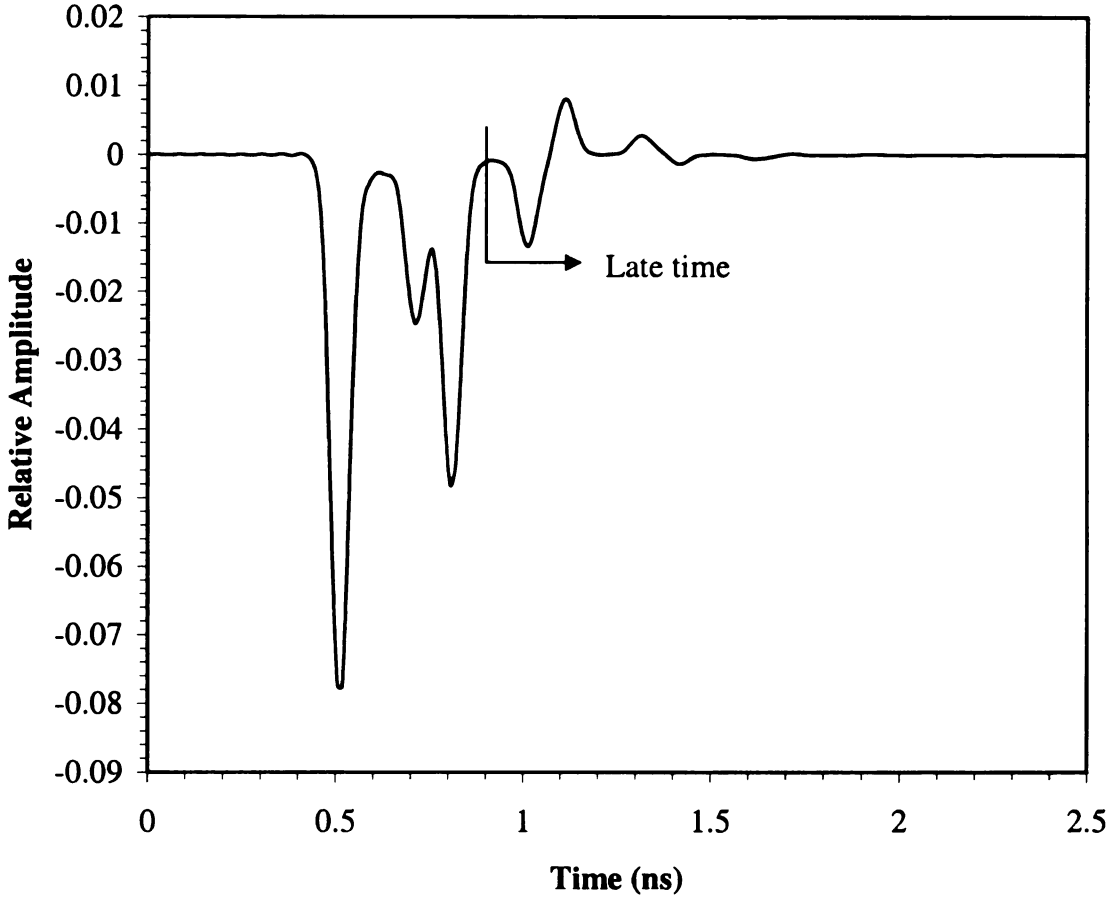

Figure 3-7 Convolution of material 'P' response with baseline E-pulse.

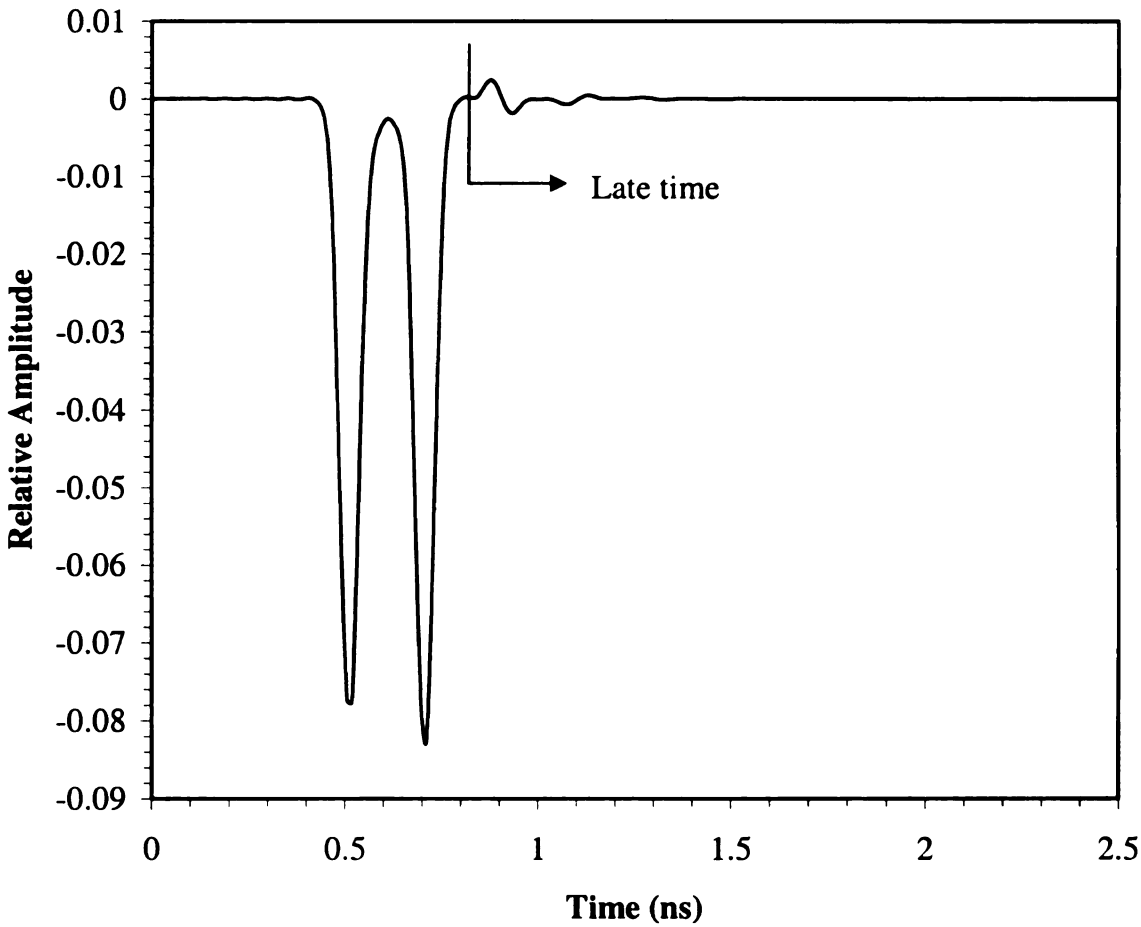

Figure 3-8 Convolution of material 'G' response with baseline E-pulse.

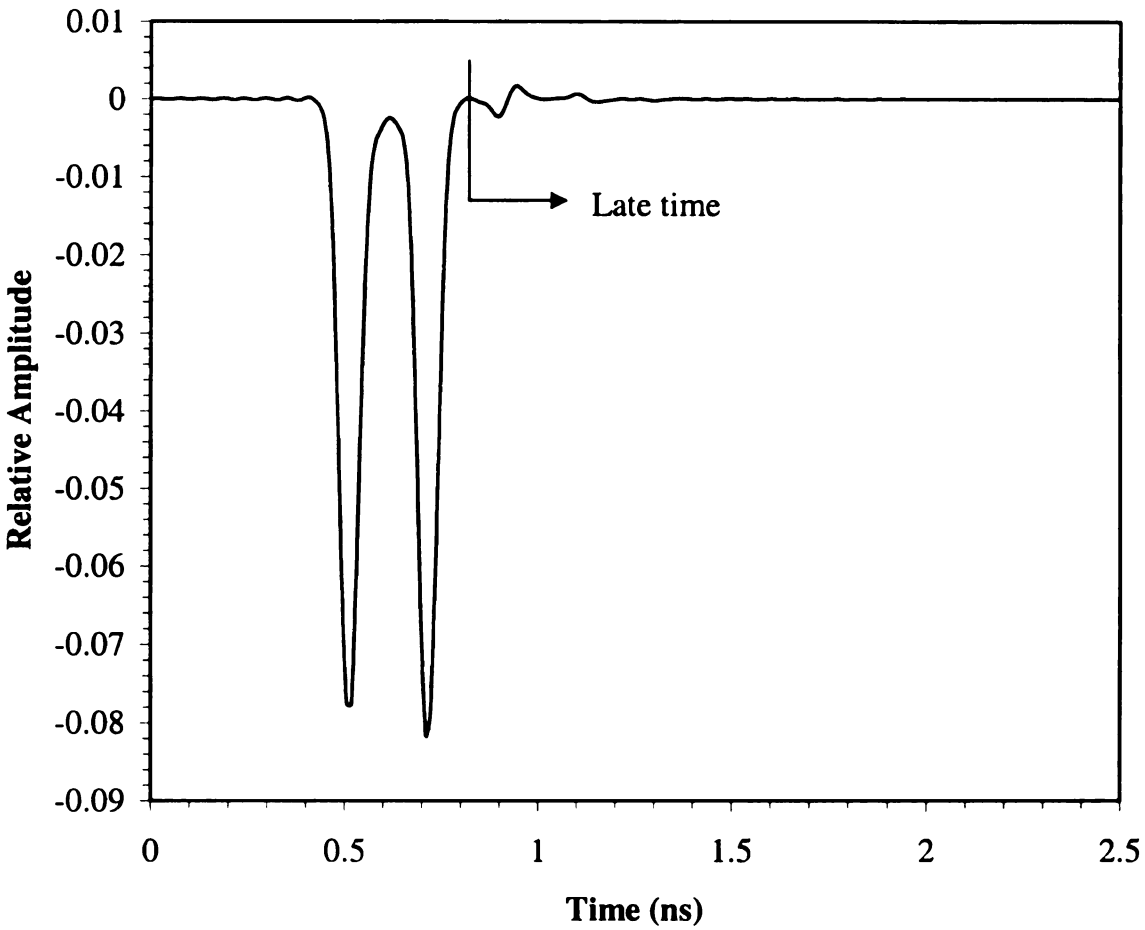

Figure 3-9 Convolution of material 'I' response with baseline E-pulse.

To quantify the results of the convolution late-time energy, the EDNa method of section 2.2 was used. Using (2.12), the EDNa values were calculated for all of the materials in Table 3-1. The resulting EDNa values are shown in Table 3-2. As expected, the baseline material had the smallest EDNa and as the thickness deviated from further from the baseline the EDNa increased. The EDNa values are plotted against the thickness in Figure 3-10. One distinction to note is the asymmetric property of the plot. This is due to the loss of the signal caused by the material. As the material becomes thicker the loss increases and thus the late-time response energy decreases. This results in a decrease in the late-time energy and thus a lower EDNa value. Figure 3-11 shows a comparison of the EDNa values calculated in this section to those calculated in section 2.2.1 for change in thickness of lossless material ($\sigma = 0$). Again, the effects of the material loss can be seen in the EDNa. When the material causes signal loss the EDNa values decrease overall. This fact will become very important in chapter 4 when magram materials are discussed.

Material	Thickness	EDNa
A	5	1.92E-03
B	6	1.66E-03
C	7	1.30E-03
D	8	6.82E-04
E	9	1.84E-04
F	9.5	4.59E-05
G	9.75	1.16E-05
H	10	2.16E-07
I	10.25	9.98E-06
J	10.5	3.83E-05
K	11	1.35E-04
L	12	3.76E-04
M	13	5.33E-04
N	14	5.69E-04
P	15	5.41E-04

Table 3-2 EDNa calculations for change in thickness of lossy material.

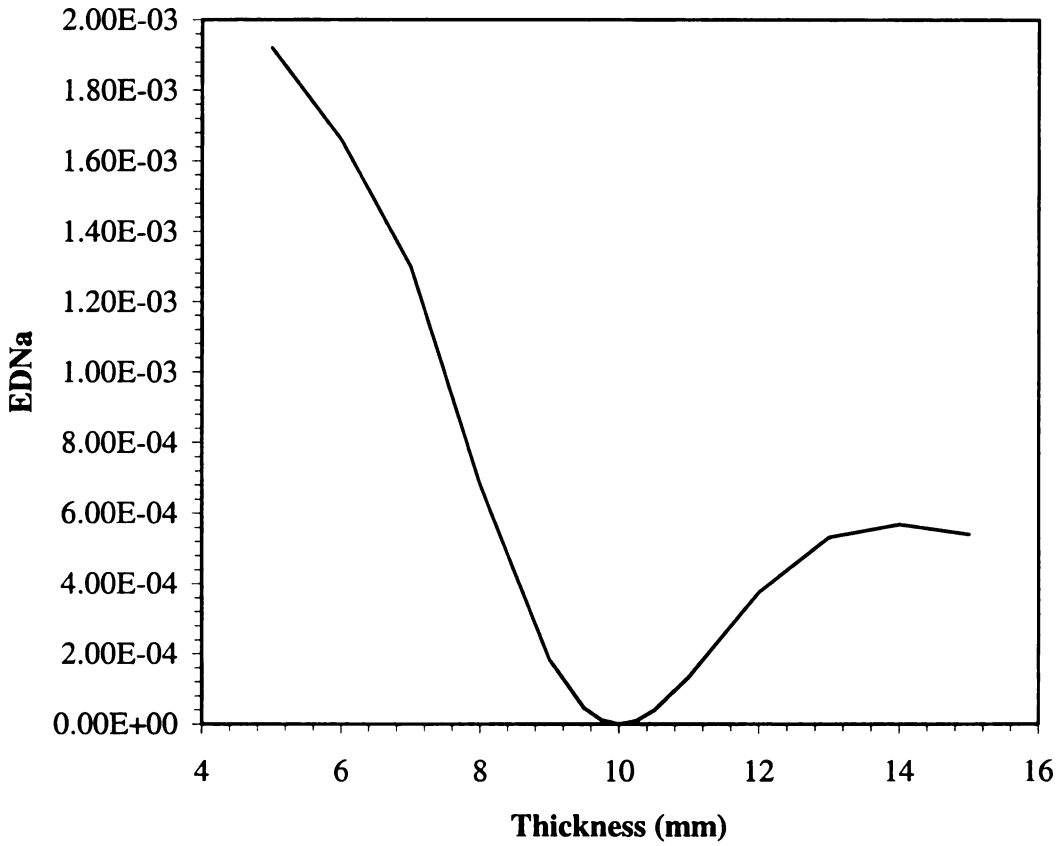

Figure 3-10 EDNa vs. change in thickness for a single lossy layer.

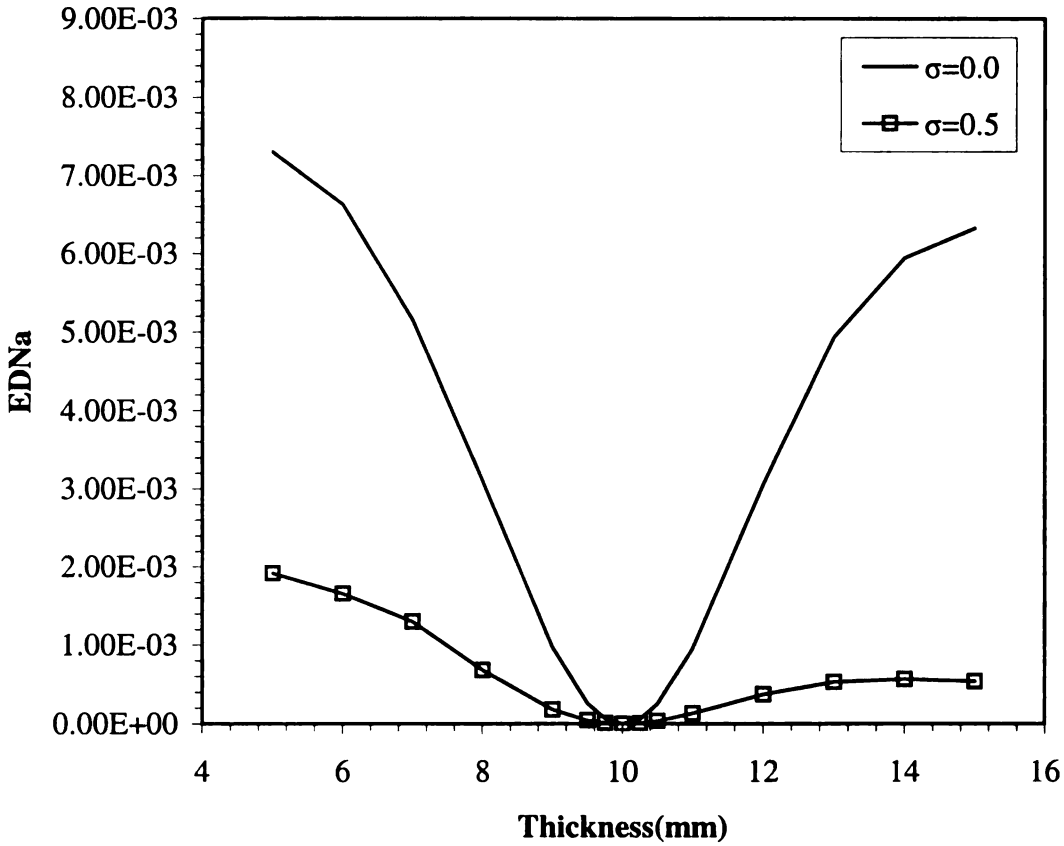

Figure 3-11 EDNa vs. change in thickness for lossless and lossy layers.

3.2.2 Change in Layer Relative Permittivity

Once again, the materials analyzed in this section are similar to those in section 2.2.2 except this section examines lossy materials ($\sigma = 0.5$). The material properties for the samples in this section are shown in Table 3-3. The relative permittivity of the material samples range from 4 to 14. The baseline material used to generate the E-pulse and used for comparison has a relative permittivity of 9. The materials used to illustrate the response and convolution waveforms are the extreme values 4 and 14 as well as the values immediate to the baseline value, 8.75 and 9.25. Figure 3-12 and Figure 3-13 show the response waveforms for the extreme values, materials 'A' and 'P'. For the smaller value, the permittivity is approaching that of air. Thus, the response is nearer to what would be expected from a metal plate. The initial reflection is off the material layer and air interface. This is followed by a reflection from the metal backing. Since the permittivity is low, most of the energy of the pulse is reflected by these two reflections. Any remaining energy within the layer is quickly able to escape the material layer. The layer with the higher permittivity initially reflects more energy at the material layer and air interface. Energy that enters the material layer takes longer to escape, hence the additional reflections that are seen. Figure 3-14 shows a comparison of the baseline response to the responses from materials with the smallest deviation in permittivity, materials 'G' and 'I'. Virtually no difference can be seen in these response waveforms.

An E-pulse is generated using the baseline material properties. This is the same E-pulse generated in the previous section and can be seen in Figure 3-4. This E-pulse was convolved with each material response. Figure 3-15 shows the resulting convolution

using the baseline response. As expected, the late-time energy is nearly zero. Figure 3-16 and Figure 3-17 show the waveform resulting from the E-pulse being convolved with the responses of the extreme values of permittivity, materials 'A' and 'P'. The late-time energy in both of these instances is large because of the large change in permittivity. The last two convolutions are shown in Figure 3-18 and Figure 3-19. These are the E-pulse convolved with materials 'G' and 'I', the materials with the least change in permittivity. While the late-time energy is smaller than the extreme value convolutions, it is still evident by inspection.

Material	ε	μ	σ	Thickness (mm)	Polarization	Angle of incidence, θ_i
A	$4\varepsilon_0$	μ_0	0.5	10	Parallel	0
B	$5\varepsilon_0$	μ_0	0.5	10	Parallel	0
C	$6\varepsilon_0$	μ_0	0.5	10	Parallel	0
D	$7\varepsilon_0$	μ_0	0.5	10	Parallel	0
E	$8\varepsilon_0$	μ_0	0.5	10	Parallel	0
F	$8.5\varepsilon_0$	μ_0	0.5	10	Parallel	0
G	$8.75\varepsilon_0$	μ_0	0.5	10	Parallel	0
H (baseline)	$9\varepsilon_0$	μ_0	0.5	10	Parallel	0
I	$9.25\varepsilon_0$	μ_0	0.5	10	Parallel	0
J	$9.5\varepsilon_0$	μ_0	0.5	10	Parallel	0
K	$10\varepsilon_0$	μ_0	0.5	10	Parallel	0
L	$11\varepsilon_0$	μ_0	0.5	10	Parallel	0
M	$12\varepsilon_0$	μ_0	0.5	10	Parallel	0
N	$13\varepsilon_0$	μ_0	0.5	10	Parallel	0
P	$14\varepsilon_0$	μ_0	0.5	10	Parallel	0

Table 3-3 Material properties for change in relative permittivity.

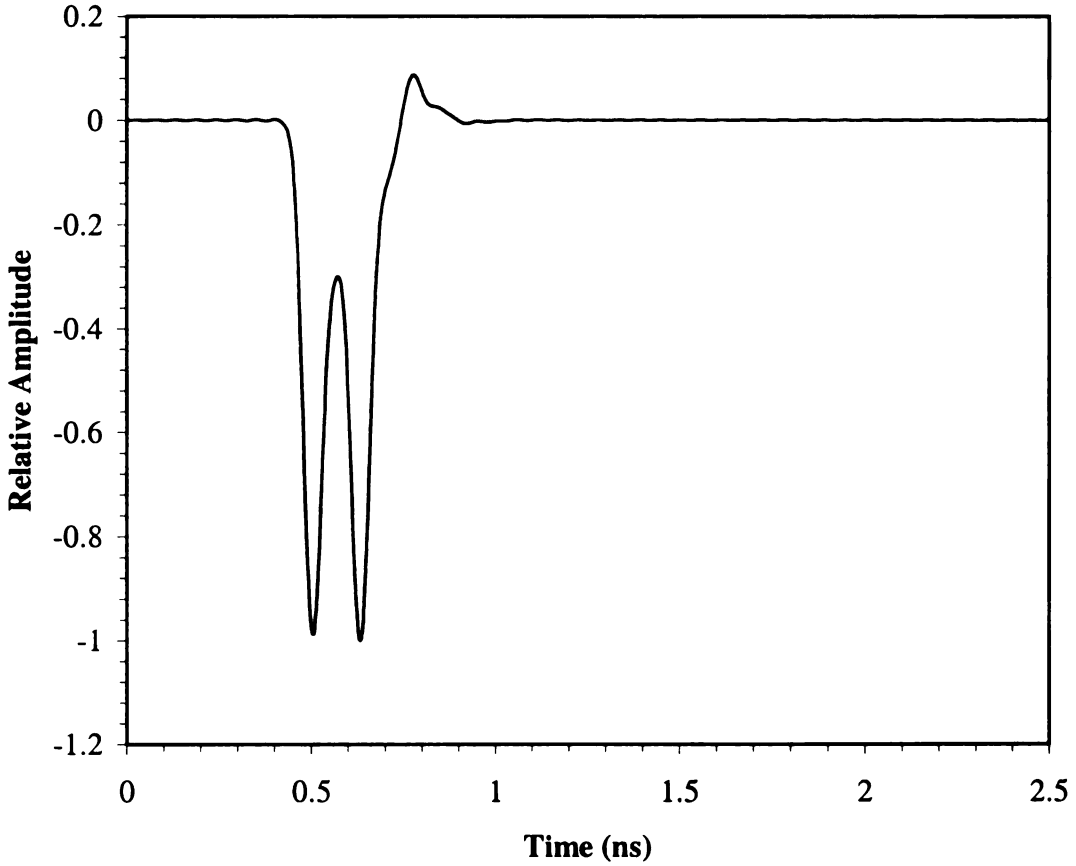

Figure 3-12 Response waveform for material 'A'.

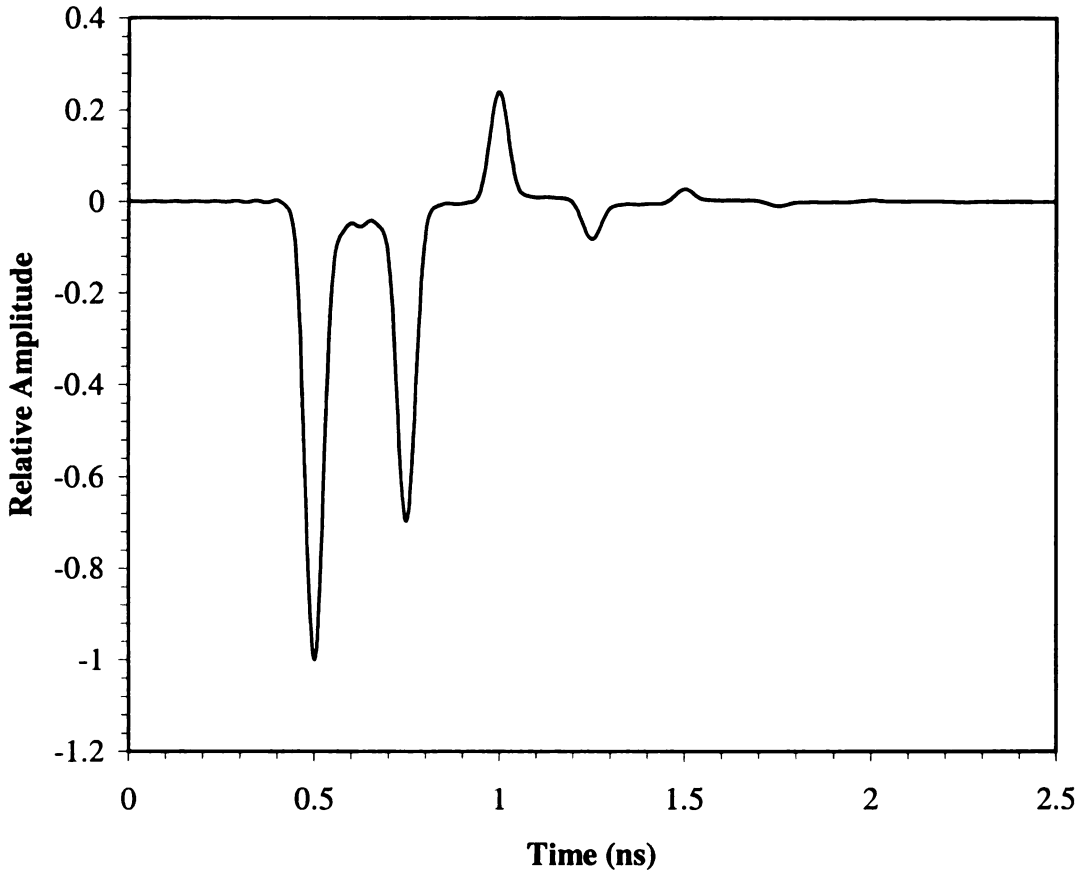

Figure 3-13 Response waveform for material 'P'.

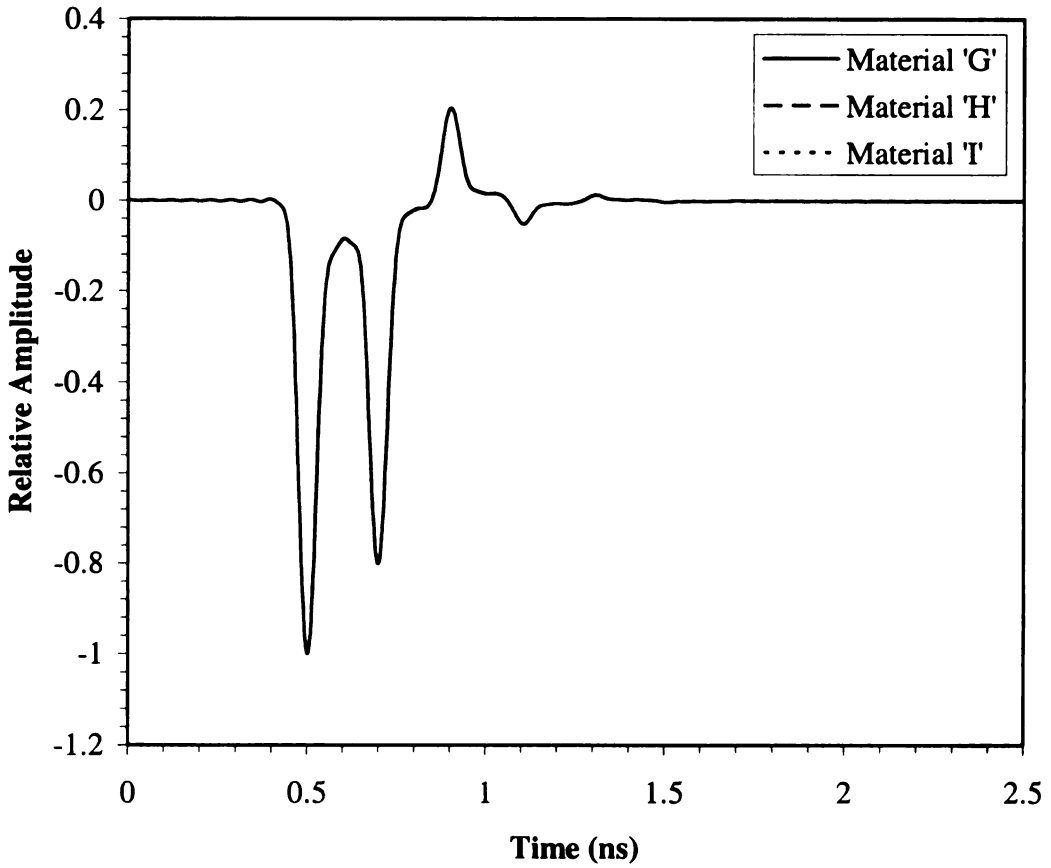

Figure 3-14 Comparison of response waveform for materials 'G', 'H', and 'I'.

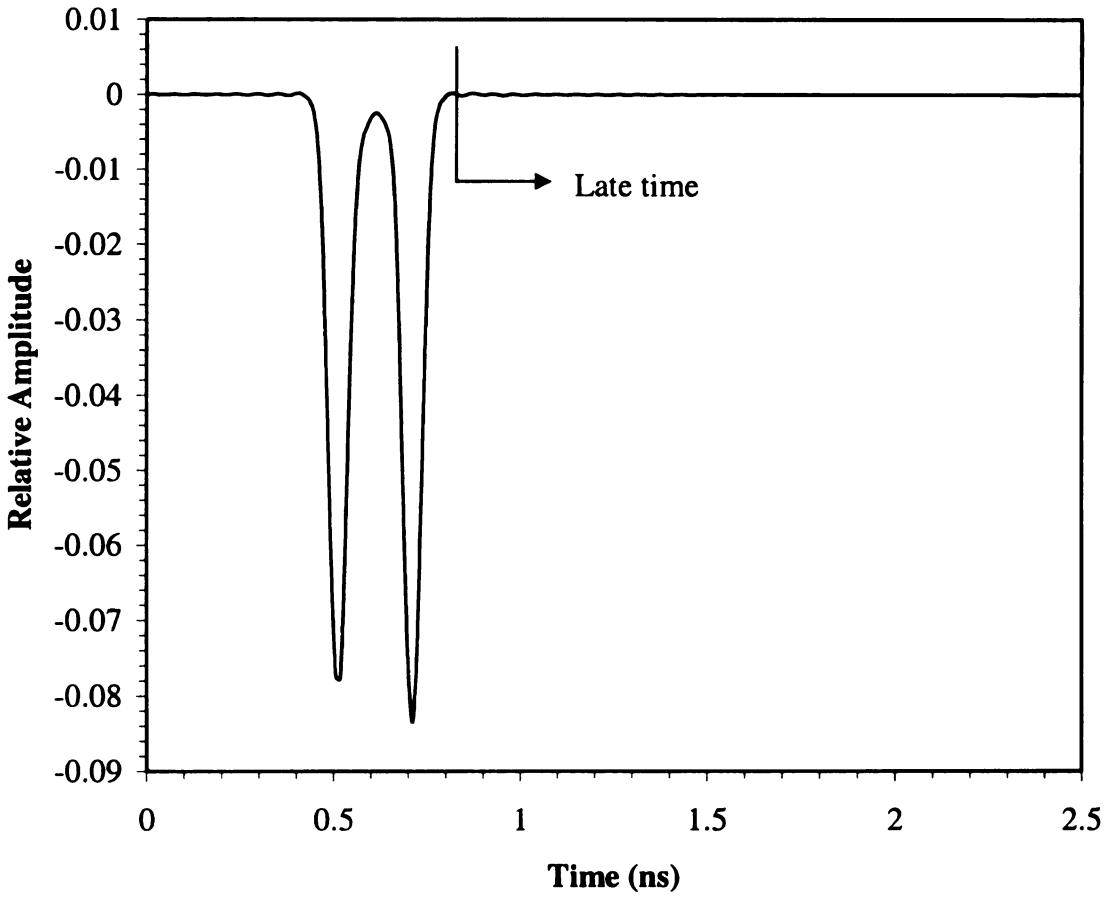

Figure 3-15 Convolution of baseline response with baseline E-pulse.

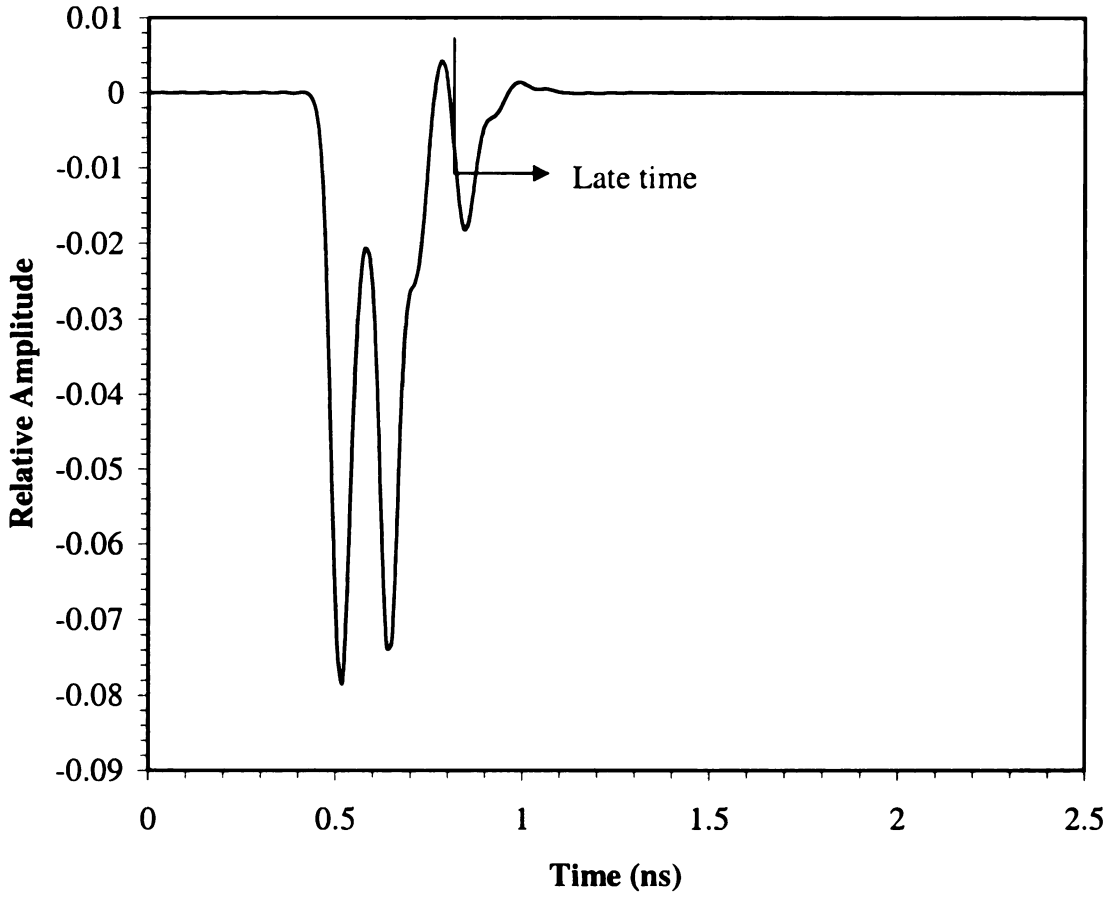

Figure 3-16 Convolution of material 'A' with baseline E-pulse.

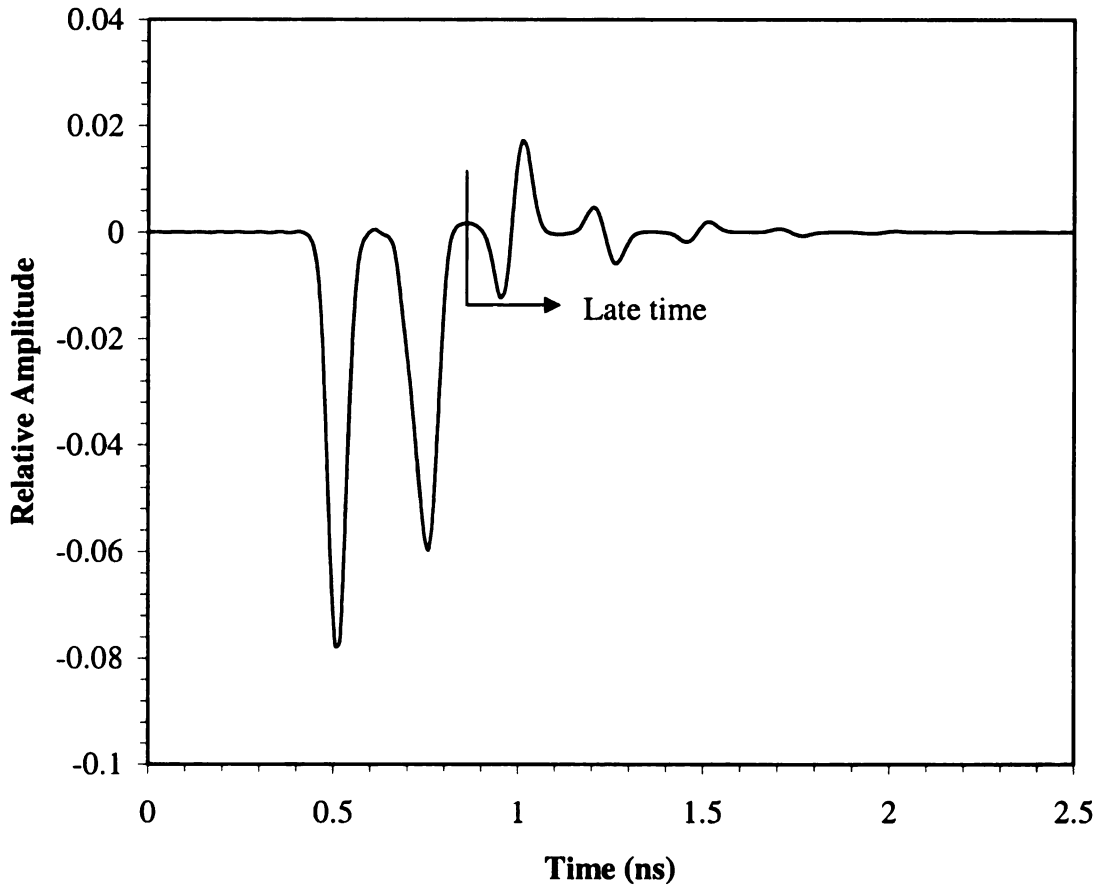

Figure 3-17 Convolution of material 'P' with baseline E-pulse.

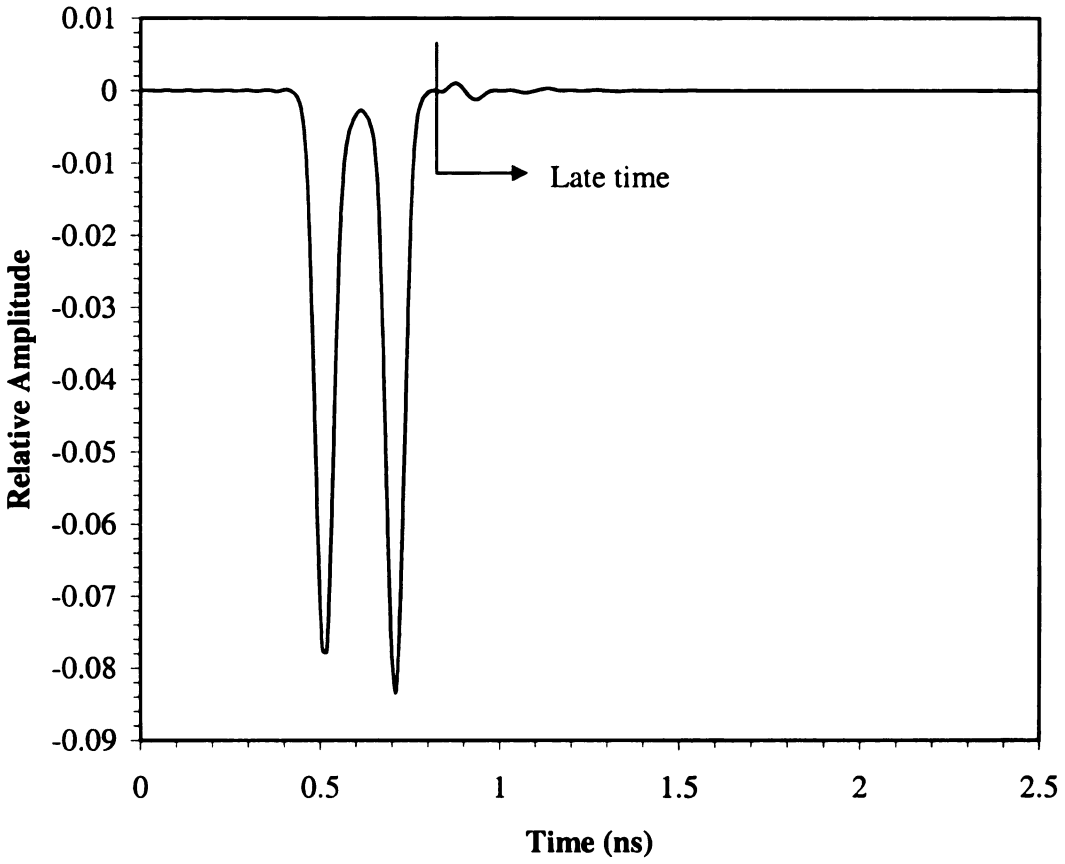

Figure 3-18 Convolution of material 'G' with baseline E-pulse.

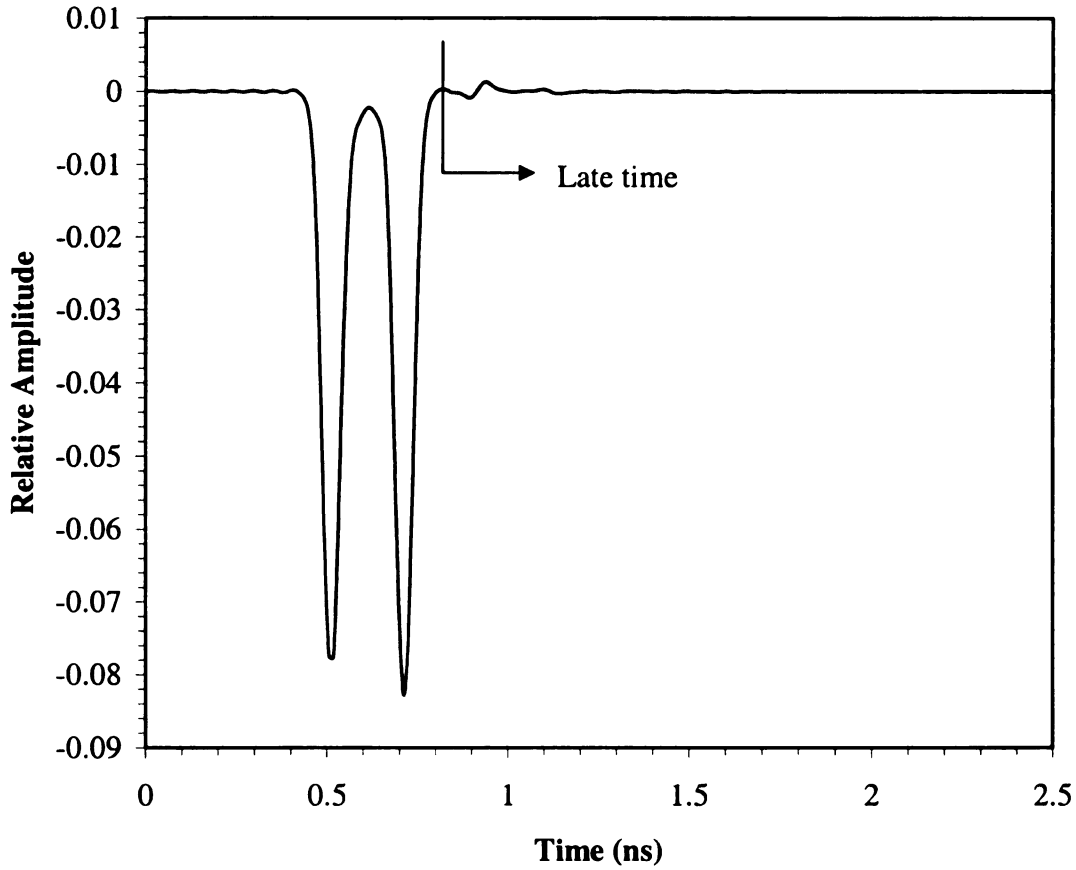

Figure 3-19 Convolution of material 'I' with baseline E-pulse.

The late-time energy contained in the convolution waveforms is quantified using the EDNa. Table 3-4 shows the values of EDNa calculated for each material configuration. It can be seen that the material with the lowest EDNa value is the baseline material 'H'. Figure 3-20 shows the EDNa values plotted against the permittivity. An asymmetry exists in the plot similar to that in the EDNa plot for changing thickness. This is due to the ability of the energy to more easily escape the material layer with low permittivity causing a lower late-time energy relative to the convolution late-time energy of the materials with high permittivity. Figure 3-21 shows a comparison of this EDNa plot with that of the EDNa plot versus permittivity for the lossless case, shown in Figure 2-22. This plot shows the material loss effects the late-time energy for the change in permittivity just as it did for the change in thickness. Again, this fact will be further considered in chapter 4.

Material	Permittivity	EDNa
A	4	6.01E-04
B	5	4.73E-04
C	6	3.22E-04
D	7	1.69E-04
E	8	4.77E-05
F	8.5	1.24E-05
G	8.75	3.39E-06
H	9	2.16E-07
I	9.25	2.95E-06
J	9.5	1.18E-05
K	10	4.71E-05
L	11	1.78E-04
M	12	3.64E-04
N	13	5.69E-04
P	14	7.66E-04

Table 3-4 EDNa calculations for change in permittivity of lossy material.

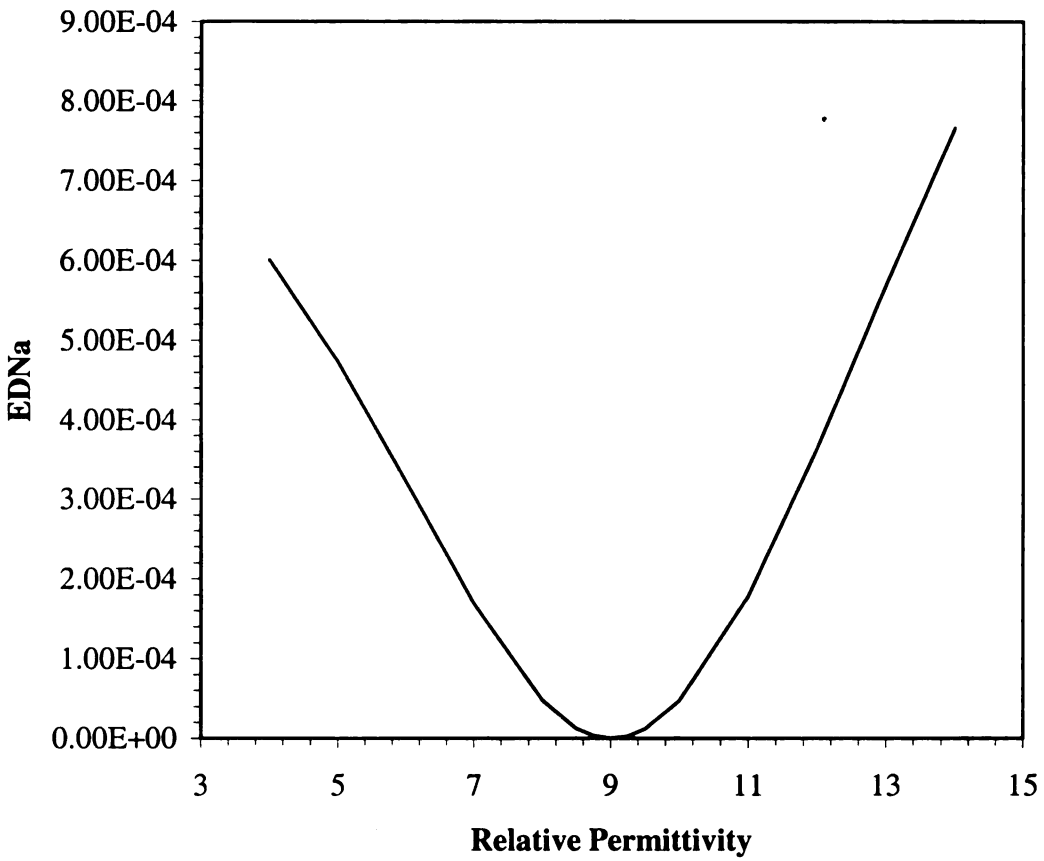

Figure 3-20 EDNa vs. change in relative permittivity for lossy layer.

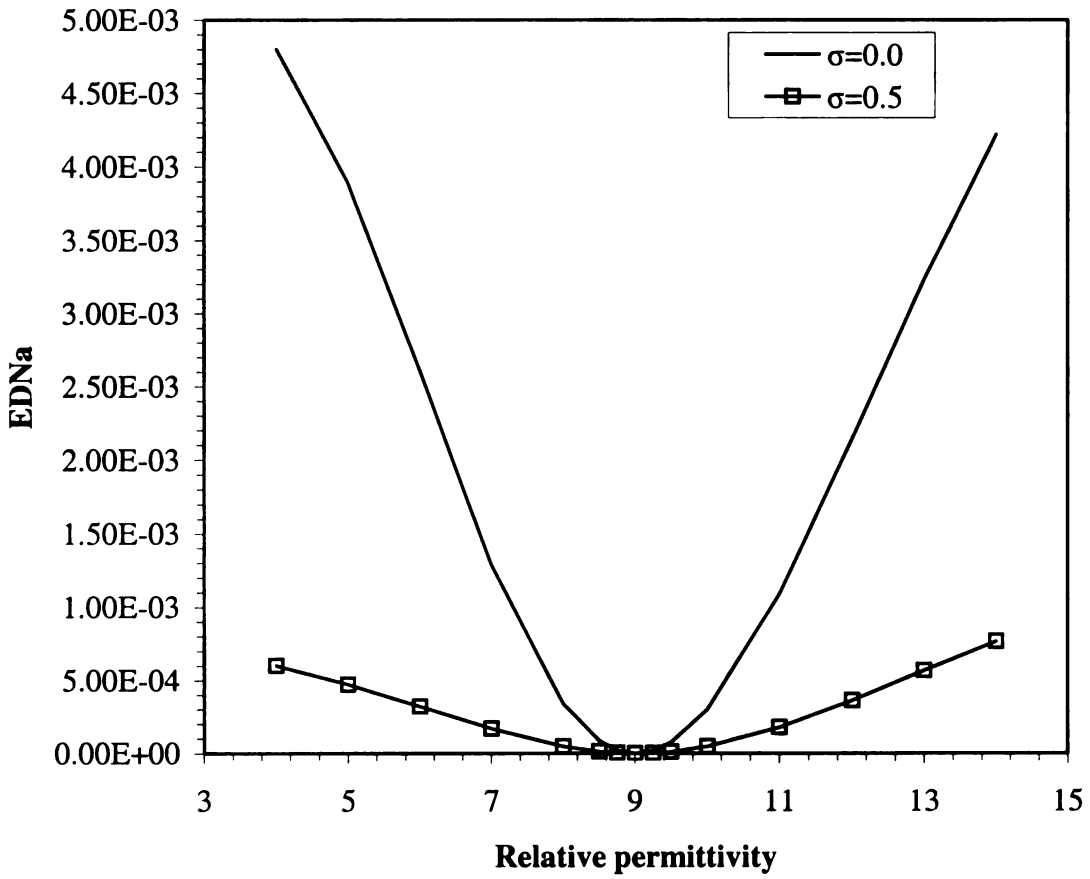

Figure 3-21 EDNa vs. change in relative permittivity for lossless and lossy layers.

3.2.3 Change in Aspect Angle

This section will discuss the effects of angle of incidence on the EDNa for lossy material layers. Table 3-5 shows the properties of the material layers investigated when the incident field had parallel polarization and Table 3-6 shows the properties when the field had perpendicular polarization. The angle of incidence was tested to a maximum of 45° for both polarizations. These material properties are the same as those in section 2.2.3 with the exception being the conductivity is not zero in this section.

Three different angles of incidence are used to illustrate the response and convolution waveforms. Figure 3-22 and Figure 3-23 show the response waveforms for 0° angle of incidence for both parallel and perpendicular polarization, respectively. Figure 3-24 and Figure 3-25 show the response waveforms for 5° angle of incidence. Finally, Figure 3-26 and Figure 3-27 show the response waveforms for 45° angle of incidence. All of the response waveforms appear very similar, and thus indicate there is not a large effect to the response from the angle of incidence. However, the real test will be the difference in the EDNa values. Each response waveform was convolved with the E-pulse shown in Figure 3-4 and the late-time energy was determined. The convolution waveforms for the example responses are shown in Figure 3-28 through Figure 3-33. Figure 3-28 and Figure 3-29 show the convolution of the E-pulse with the response waveforms for material 'A' and 'AA'. Figure 3-30 and Figure 3-31 show the convolution of the E-pulse with the response waveforms for material 'F' and 'FF'. And finally, Figure 3-32 and Figure 3-33 show the convolution of the E-pulse with the response waveforms for materials 'S' and 'SS'. While the extreme cases of 45° angle of

incidence shows a significant amount of late-time energy the baseline case and the case of 5° angle of incidence show near zero late-time energy. By inspection it would not be possible to discriminate the 0° and 5° convolutions. The EDNa values will show the difference in the late-time energies.

Material	ε	μ	σ	Thickness (mm)	Polarization	Angle of incidence, θ_i
A(baseline)	$9\varepsilon_0$	μ_0	0.5	10	Parallel	0
B	$9\varepsilon_0$	μ_0	0.5	10	Parallel	1
C	$9\varepsilon_0$	μ_0	0.5	10	Parallel	2
D	$9\varepsilon_0$	μ_0	0.5	10	Parallel	3
E	$9\varepsilon_0$	μ_0	0.5	10	Parallel	4
F	$9\varepsilon_0$	μ_0	0.5	10	Parallel	5
G	$9\varepsilon_0$	μ_0	0.5	10	Parallel	6
H	$9\varepsilon_0$	μ_0	0.5	10	Parallel	7
I	$9\varepsilon_0$	μ_0	0.5	10	Parallel	8
J	$9\varepsilon_0$	μ_0	0.5	10	Parallel	9
K	$9\varepsilon_0$	μ_0	0.5	10	Parallel	10
L	$9\varepsilon_0$	μ_0	0.5	10	Parallel	15
M	$9\varepsilon_0$	μ_0	0.5	10	Parallel	20
N	$9\varepsilon_0$	μ_0	0.5	10	Parallel	25
P	$9\varepsilon_0$	μ_0	0.5	10	Parallel	30
Q	$9\varepsilon_0$	μ_0	0.5	10	Parallel	35
R	$9\varepsilon_0$	μ_0	0.5	10	Parallel	40
S	$9\varepsilon_0$	μ_0	0.5	10	Parallel	45

Table 3-5 Material properties for changing angle, parallel polarization.

Material	ε	μ	σ	Thickness (mm)	Polarization	Angle of incidence, θ_i
AA(baseline)	$9\varepsilon_0$	μ_0	0.5	10	Perpendicular	0
BB	$9\varepsilon_0$	μ_0	0.5	10	Perpendicular	1
CC	$9\varepsilon_0$	μ_0	0.5	10	Perpendicular	2
DD	$9\varepsilon_0$	μ_0	0.5	10	Perpendicular	3
EE	$9\varepsilon_0$	μ_0	0.5	10	Perpendicular	4
FF	$9\varepsilon_0$	μ_0	0.5	10	Perpendicular	5
GG	$9\varepsilon_0$	μ_0	0.5	10	Perpendicular	6
HH	$9\varepsilon_0$	μ_0	0.5	10	Perpendicular	7
II	$9\varepsilon_0$	μ_0	0.5	10	Perpendicular	8
JJ	$9\varepsilon_0$	μ_0	0.5	10	Perpendicular	9
KK	$9\varepsilon_0$	μ_0	0.5	10	Perpendicular	10
LL	$9\varepsilon_0$	μ_0	0.5	10	Perpendicular	15
MM	$9\varepsilon_0$	μ_0	0.5	10	Perpendicular	20
NN	$9\varepsilon_0$	μ_0	0.5	10	Perpendicular	25
PP	$9\varepsilon_0$	μ_0	0.5	10	Perpendicular	30
QQ	$9\varepsilon_0$	μ_0	0.5	10	Perpendicular	35
RR	$9\varepsilon_0$	μ_0	0.5	10	Perpendicular	40
SS	$9\varepsilon_0$	μ_0	0.5	10	Perpendicular	45

Table 3-6 Material properties for changing angle, perpendicular polarization.

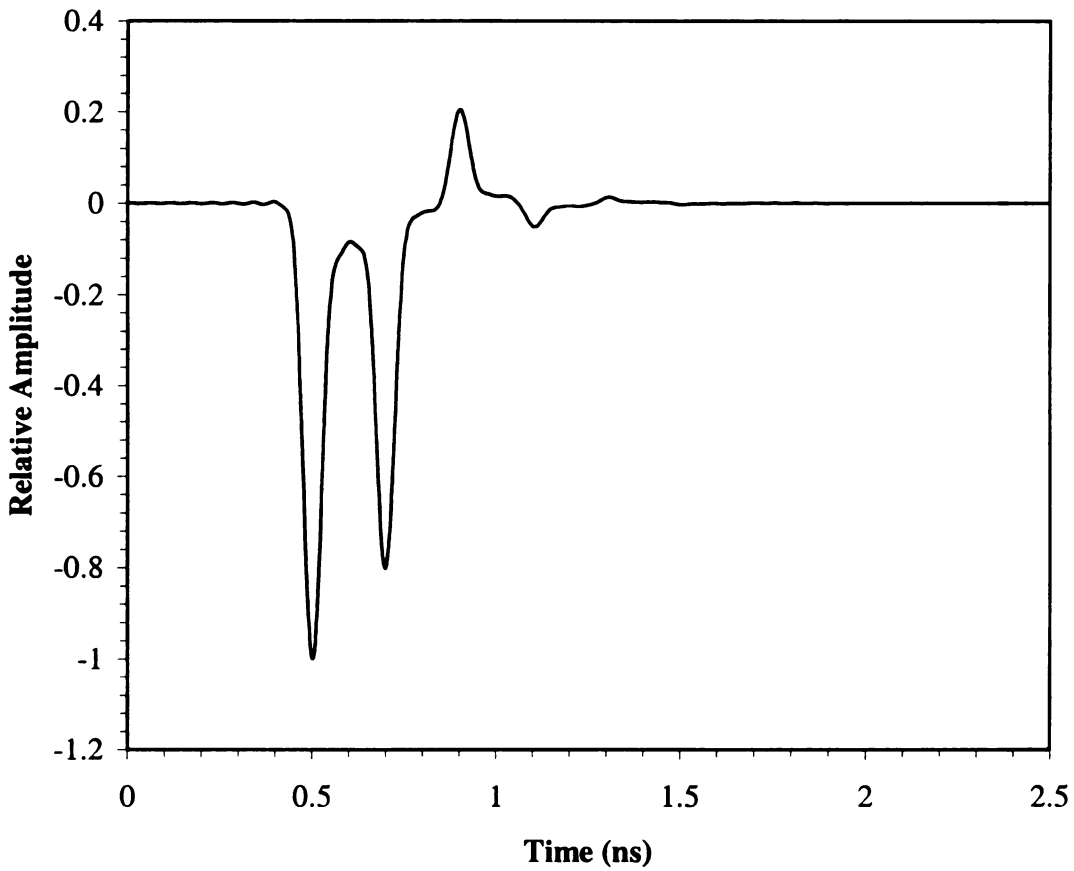

Figure 3-22 Response waveform for material 'A'.

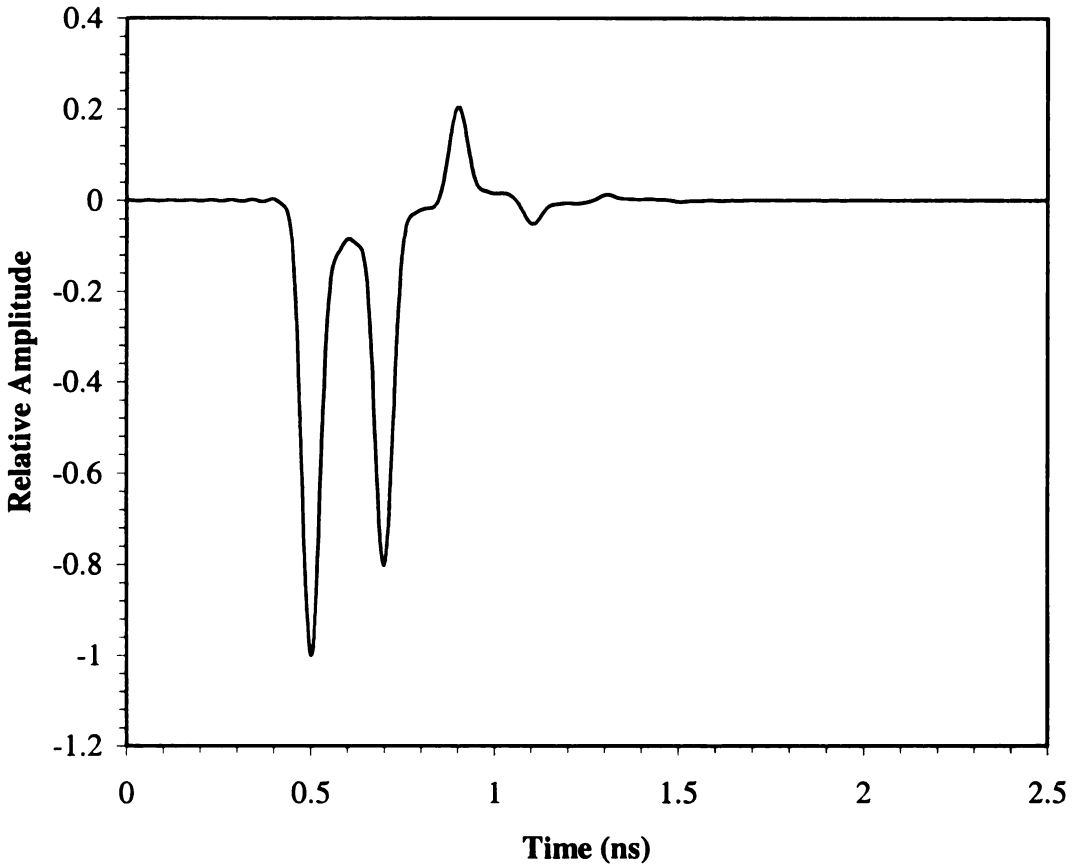

Figure 3-23 Response waveform for material 'AA'.

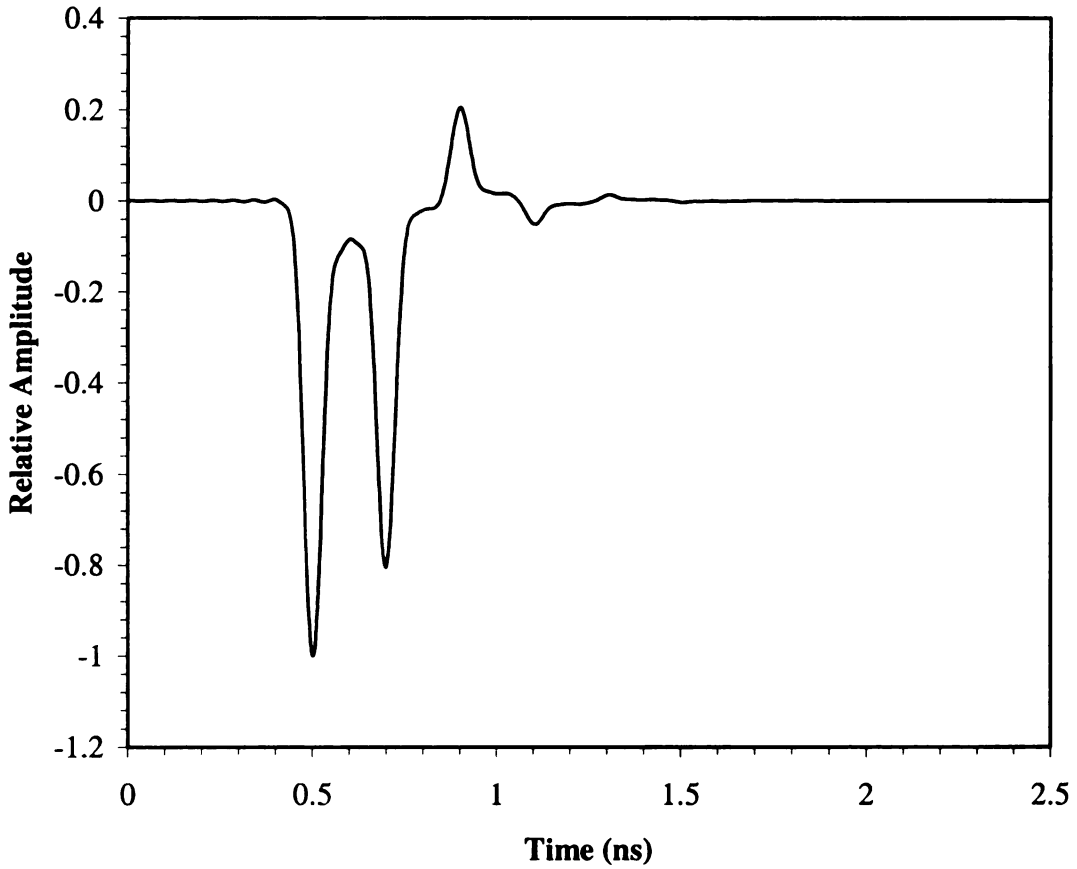

Figure 3-24 Response waveform for material 'F'.

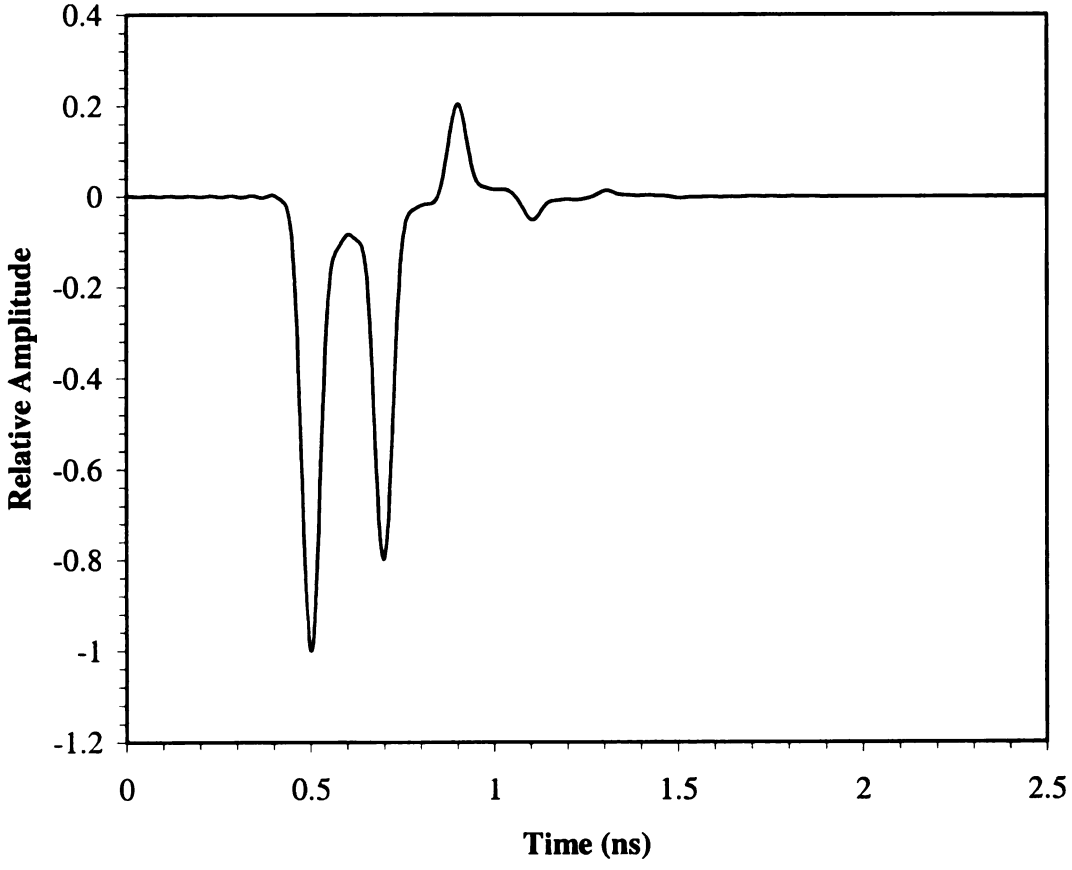

Figure 3-25 Response waveform for material 'FF'.

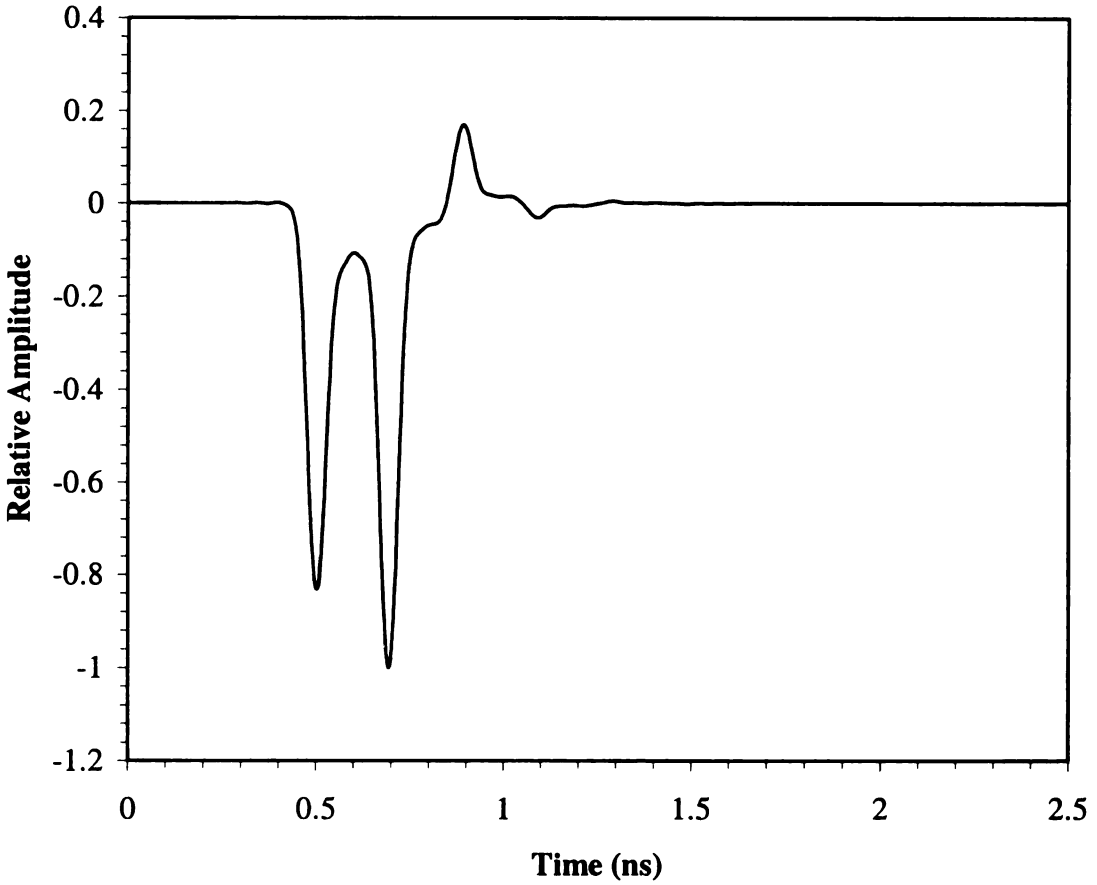

Figure 3-26 Response waveform for material 'S'.

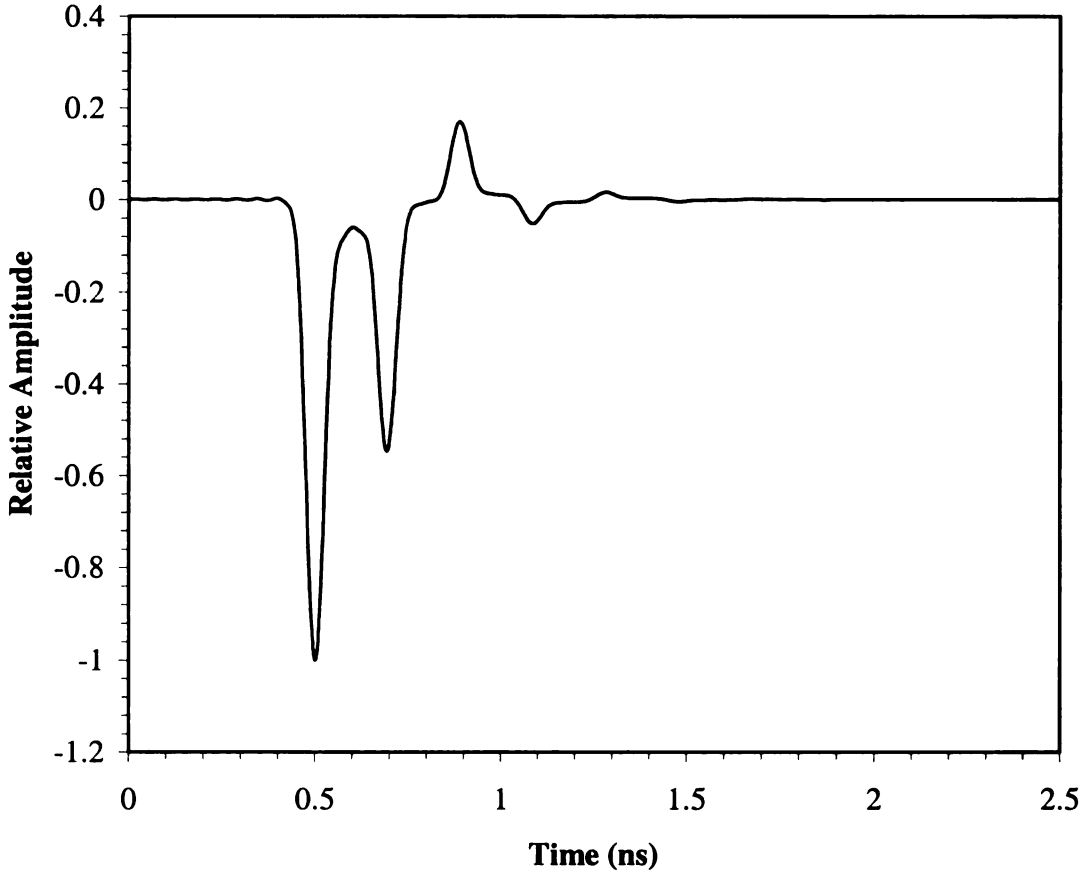

Figure 3-27 Response waveform for material 'SS'.

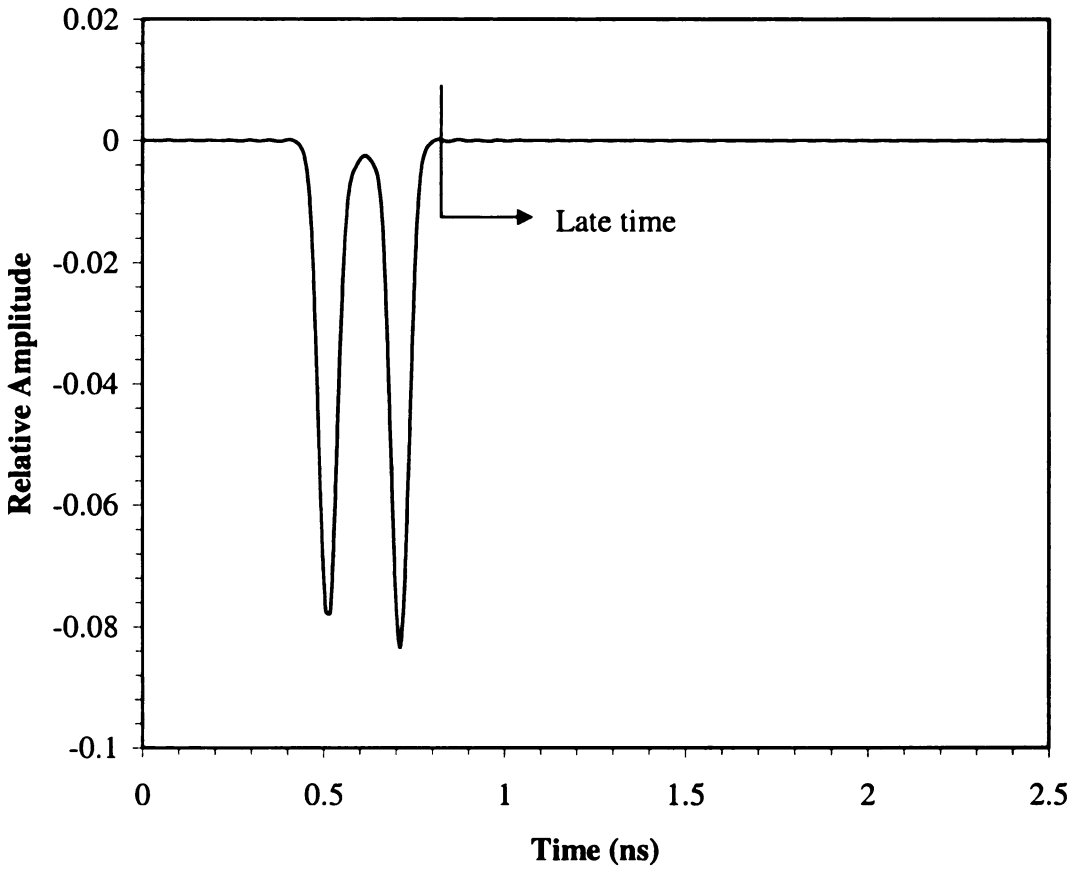

Figure 3-28 Convolution of material 'A' with baseline E-pulse.

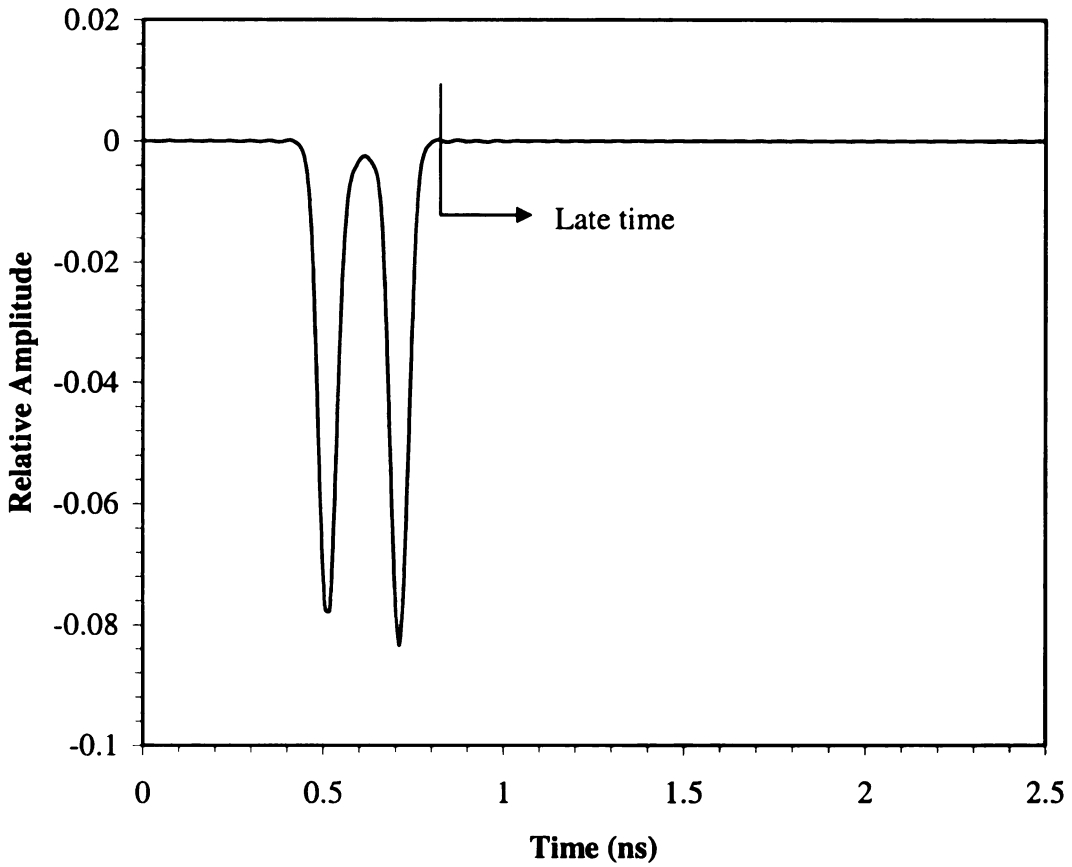

Figure 3-29 Convolution of material 'AA' with baseline E-pulse.

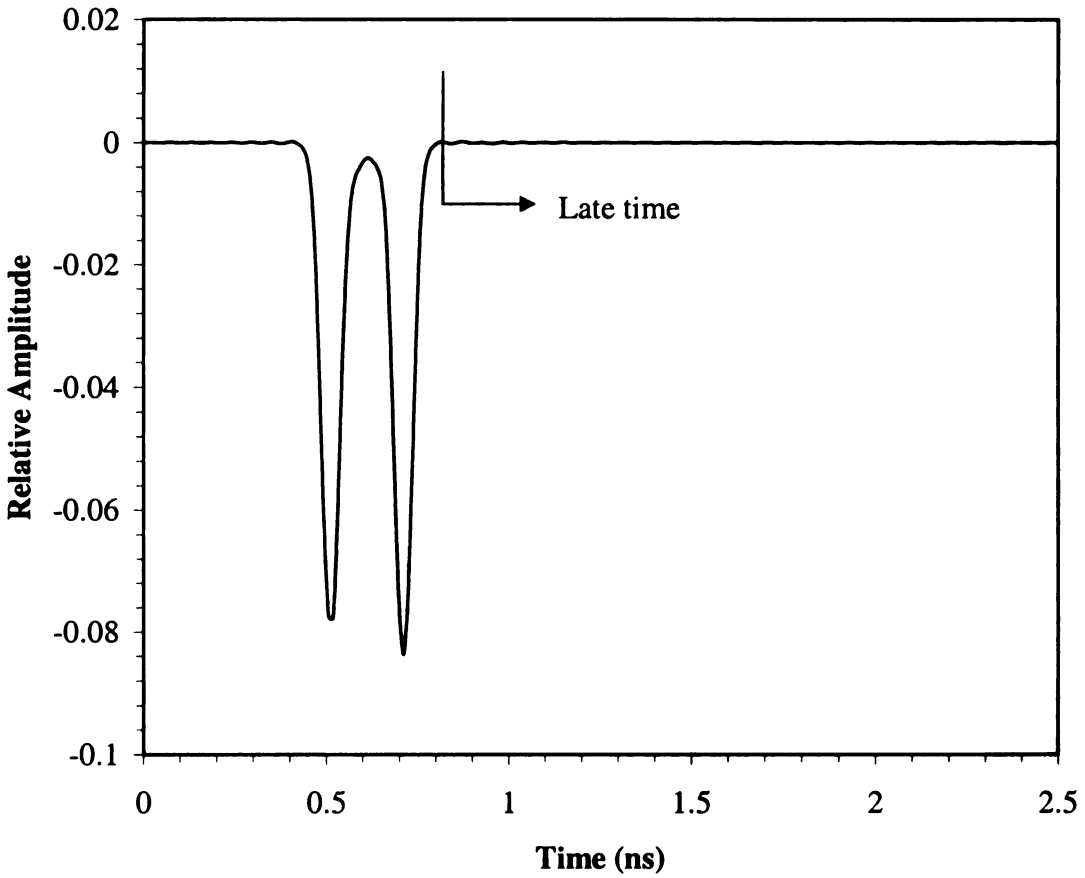

Figure 3-30 Convolution of material 'F' with baseline E-pulse.

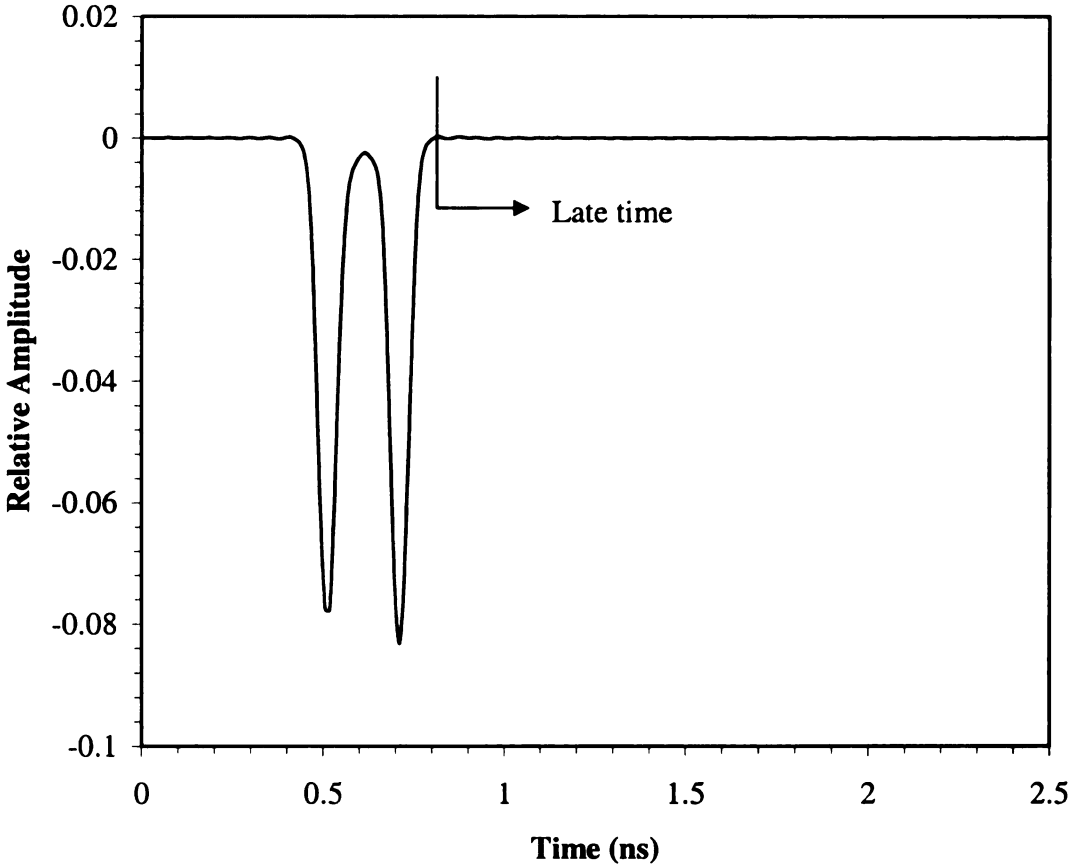

Figure 3-31 Convolution of material 'FF' with baseline E-pulse.

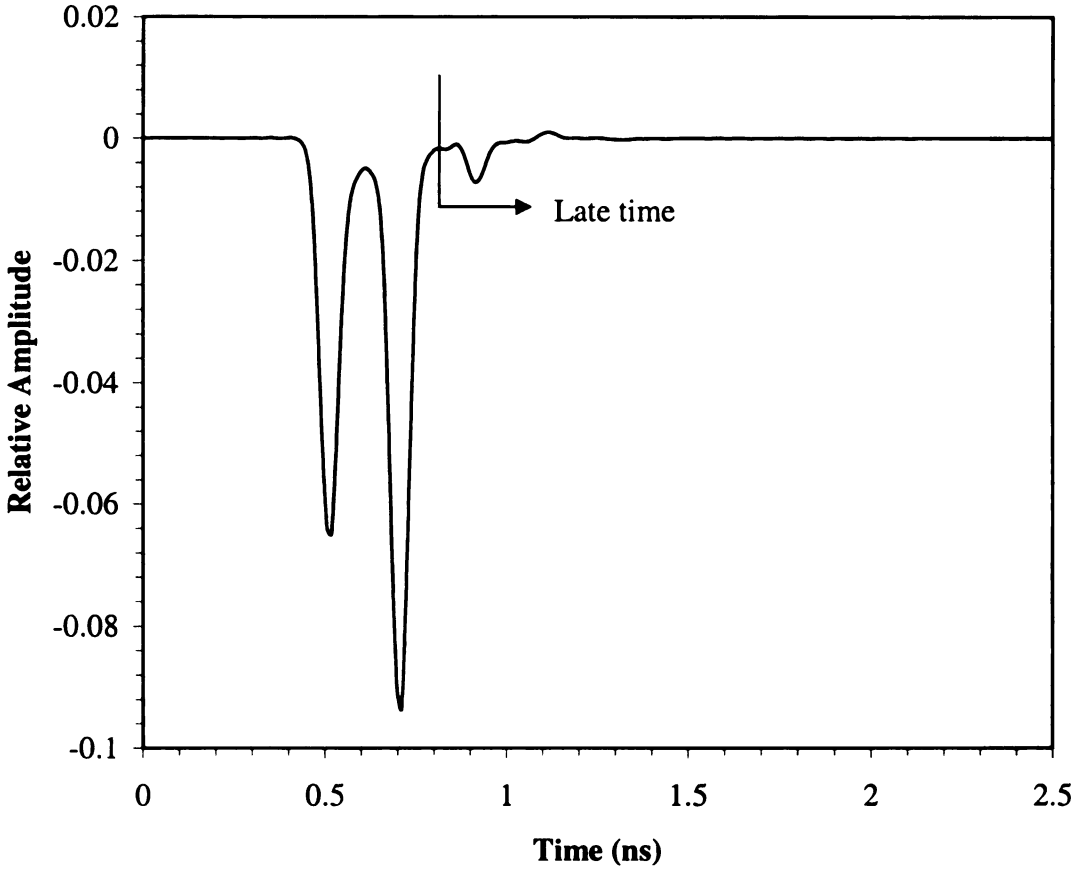

Figure 3-32 Convolution of material 'S' with baseline E-pulse.

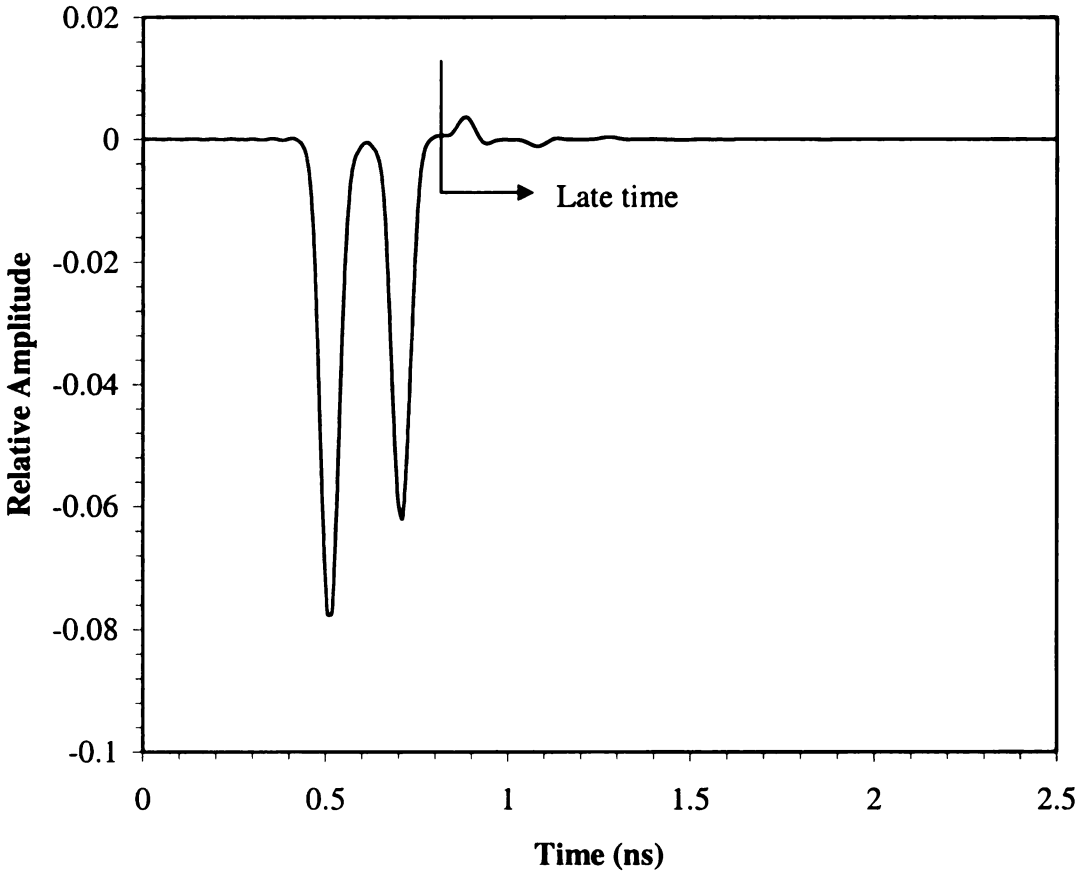

Figure 3-33 Convolution of material 'SS' with baseline E-pulse.

Quantification of the late-time energy was accomplished using the EDNa values. Table 3-7 and Table 3-8 show the EDNa values for each aspect angle for both the parallel and perpendicular polarization. These tables show that there is very little difference in the EDNa values up to 10°. A graphical representation of this data is shown in Figure 3-34. Here again the data shows relatively little change in the EDNa up to 10°. Figure 3-35 shows a comparison of the EDNa values calculated in this section for lossy materials to those calculated in section 2.2.3 for lossless materials. Consistent with previous discussions on the lossy material EDNa values, this comparison shows that the lossy material results in lower EDNa values overall compared to the lossless material values.

Material	Aspect Angle, θ_i	EDNa
A	0	2.16E-07
B	1	2.16E-07
C	2	2.18E-07
D	3	2.20E-07
E	4	2.25E-07
F	5	2.34E-07
G	6	2.47E-07
H	7	2.68E-07
I	8	2.98E-07
J	9	3.39E-07
K	10	3.96E-07
L	15	1.04E-06
M	20	2.80E-06
N	25	6.67E-06
P	30	1.43E-05
Q	35	2.83E-05
R	40	5.30E-05
S	45	9.61E-05

Table 3-7 EDNa calculations for change in aspect angle for parallel polarization.

Material	Aspect Angle, θ_i	EDNa
AA	0	2.16E-07
BB	1	2.16E-07
CC	2	2.17E-07
DD	3	2.18E-07
EE	4	2.21E-07
FF	5	2.26E-07
GG	6	2.35E-07
HH	7	2.48E-07
II	8	2.69E-07
JJ	9	2.98E-07
KK	10	3.39E-07
LL	15	7.91E-07
MM	20	1.94E-06
NN	25	4.18E-06
PP	30	7.89E-06
QQ	35	1.33E-05
RR	40	2.04E-05
SS	45	2.88E-05

Table 3-8 EDNa calculations for change in aspect angle for perpendicular polarization.

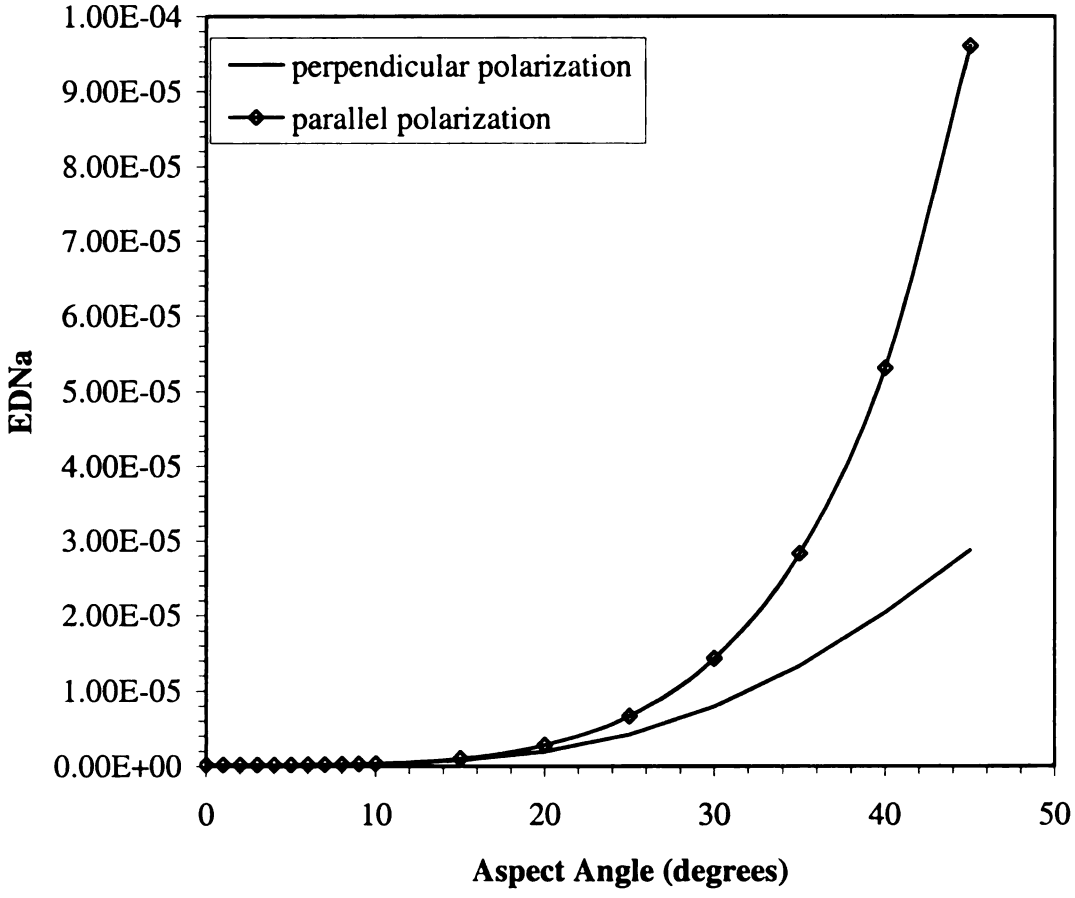

Figure 3-34 EDNa vs. change in aspect angle for lossy layer.

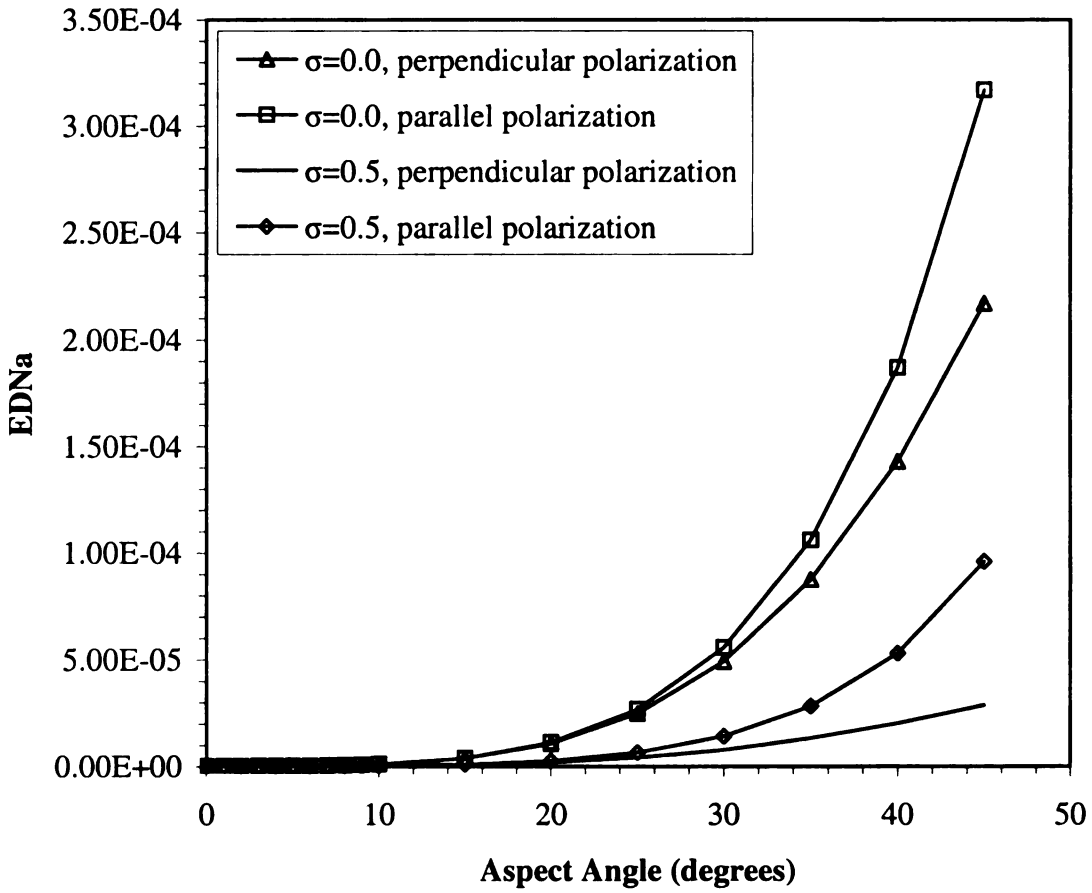

Figure 3-35 Comparison of EDNa vs. aspect angle for lossless and lossy layers.

3.2.4 Change in Conductivity

This section will explore whether a change in the conductivity of the material layer can be detected using the EDNa values. The material properties of the various sample materials evaluated are shown in Table 3-9. The response and convolution waveforms for five values of conductivity are shown as examples. The response waveform for the baseline material, material 'I', is shown in Figure 3-37. The response waveforms for the extreme cases of change in conductivity, materials 'A' and 'S' are shown in Figure 3-39 and Figure 3-36. There is an obvious difference between the baseline material response and these responses so this should reflect a difference in EDNa. It can be seen in Figure 3-38 that when the conductivity gets as high as 5, virtually all of the incident pulse gets reflected by the material layer and air interface. The material layer acts nearly as though it were a conductive plate. Lastly, Figure 3-40 and Figure 3-38 show the response waveforms for the materials with the least change in conductivity from the baseline, materials 'H' and 'J'. The response waveforms look very similar to the baseline response so the EDNa values should be closer. The EDNa values are calculated using the late-time energy in the convolution waveforms. Thus, each material response is convolved with a baseline E-pulse. The baseline E-pulse used is shown in Figure 3-4. The convolution of the baseline E-pulse with the baseline response is shown in Figure 3-41 and as expected the late-time energy is near zero. Figure 3-42 and Figure 3-43 show the convolution of the baseline E-pulse with the response waveforms for materials 'A' and 'S'. In the first figure it can be seen that the late-time energy is relatively large while in the second it is not so obvious. Figure 3-44 and Figure

3-45 show the convolution of the baseline E-pulse with materials 'H' and 'J'. Again, by inspection it is not clear how large the late-time energy might be in relation to the baseline. Thus it is necessary to calculate and compare EDNa values.

Material	ε	μ	σ	Thickness (mm)	Polarization	Angle of incidence, θ_i
A	$9\varepsilon_0$	μ_0	0	10	Parallel	0
B	$9\varepsilon_0$	μ_0	2e-5	10	Parallel	0
C	$9\varepsilon_0$	μ_0	2e-2	10	Parallel	0
D	$9\varepsilon_0$	μ_0	0.1	10	Parallel	0
E	$9\varepsilon_0$	μ_0	0.2	10	Parallel	0
F	$9\varepsilon_0$	μ_0	0.3	10	Parallel	0
G	$9\varepsilon_0$	μ_0	0.4	10	Parallel	0
H	$9\varepsilon_0$	μ_0	0.45	10	Parallel	0
I (baseline)	$9\varepsilon_0$	μ_0	0.5	10	Parallel	0
J	$9\varepsilon_0$	μ_0	0.55	10	Parallel	0
K	$9\varepsilon_0$	μ_0	0.6	10	Parallel	0
L	$9\varepsilon_0$	μ_0	0.7	10	Parallel	0
M	$9\varepsilon_0$	μ_0	0.8	10	Parallel	0
N	$9\varepsilon_0$	μ_0	0.9	10	Parallel	0
P	$9\varepsilon_0$	μ_0	1.5	10	Parallel	0
Q	$9\varepsilon_0$	μ_0	2.0	10	Parallel	0
R	$9\varepsilon_0$	μ_0	2.5	10	Parallel	0
S	$9\varepsilon_0$	μ_0	5	10	Parallel	0

Table 3-9 Material properties for changing conductivity.

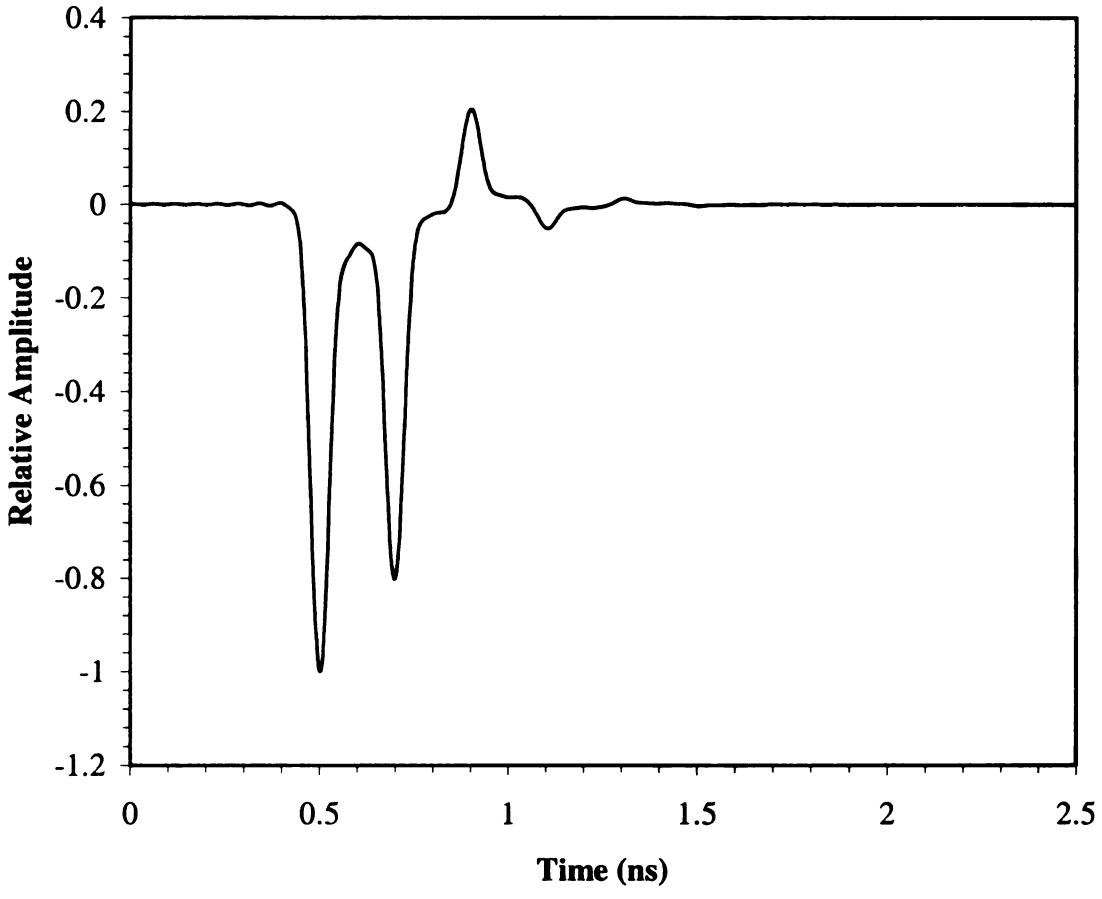

Figure 3-36 Response waveform for material 'I'.

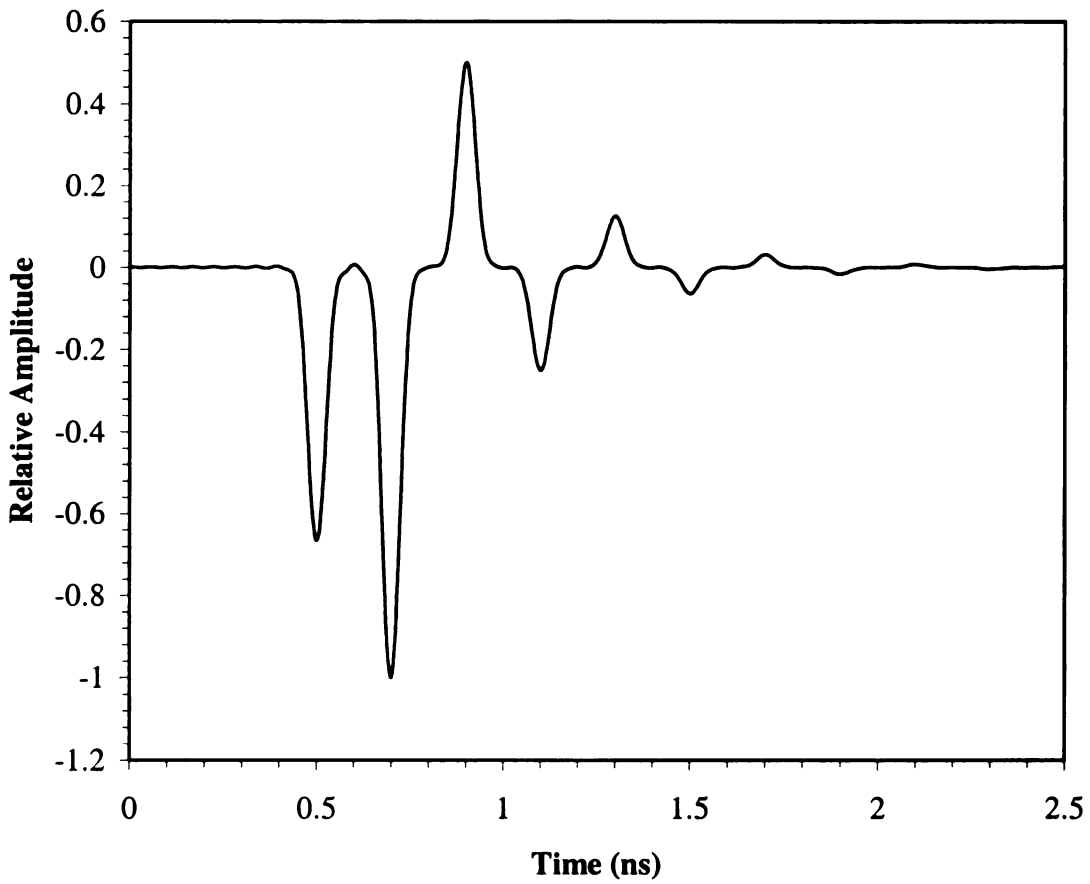

Figure 3-37 Response waveform for material 'A'.

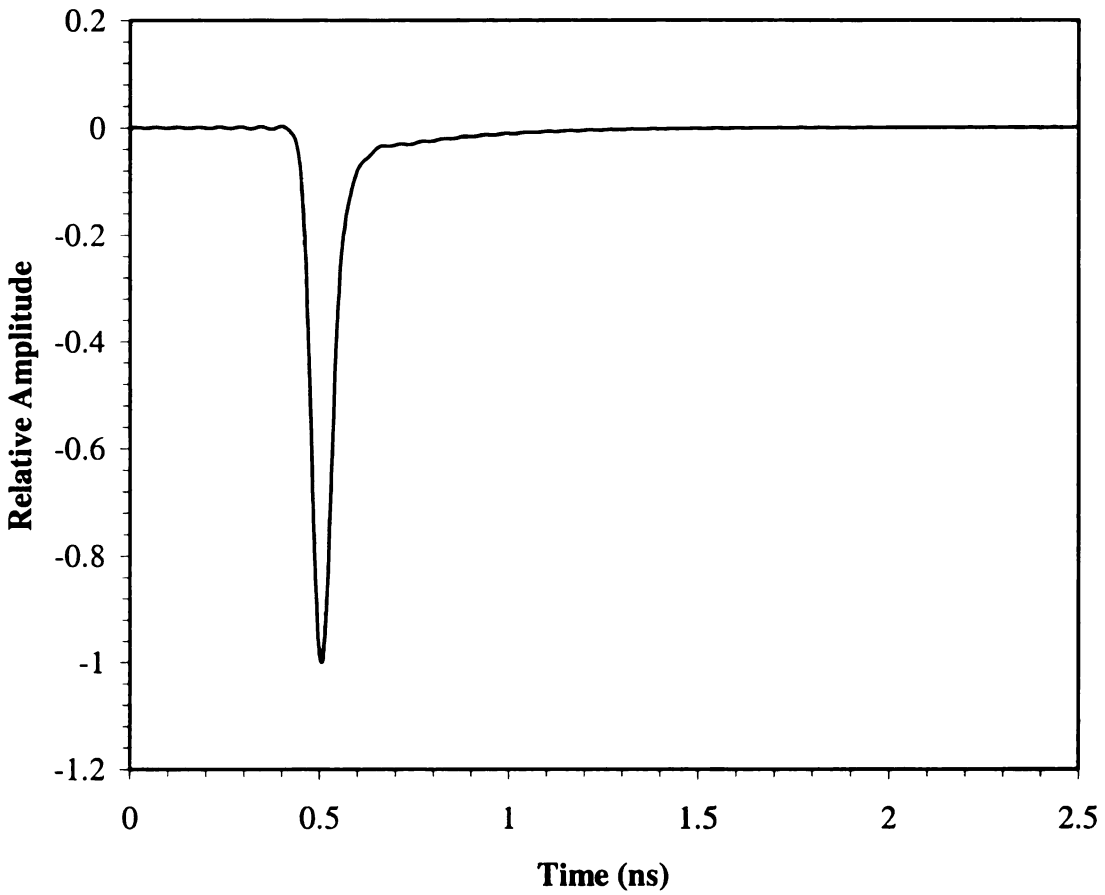

Figure 3-38 Response waveform for material 'S'.

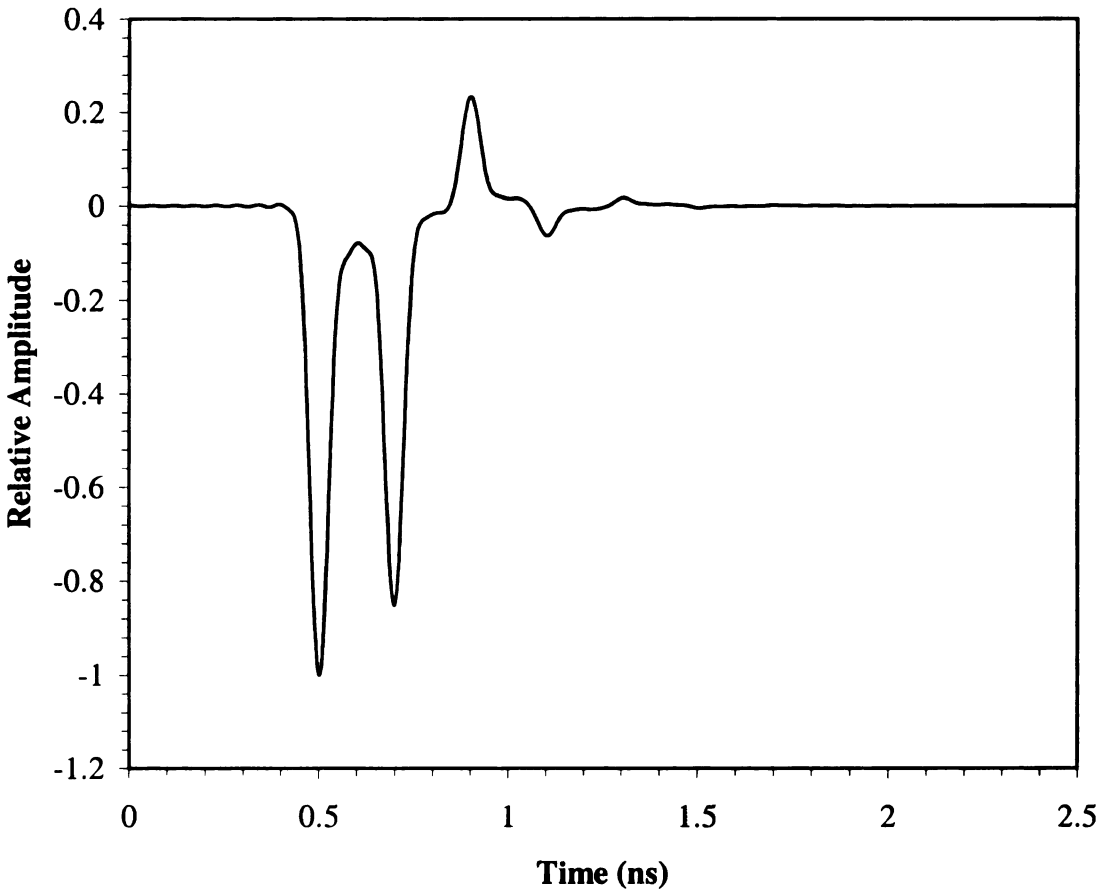

Figure 3-39 Response waveform for material 'H'.

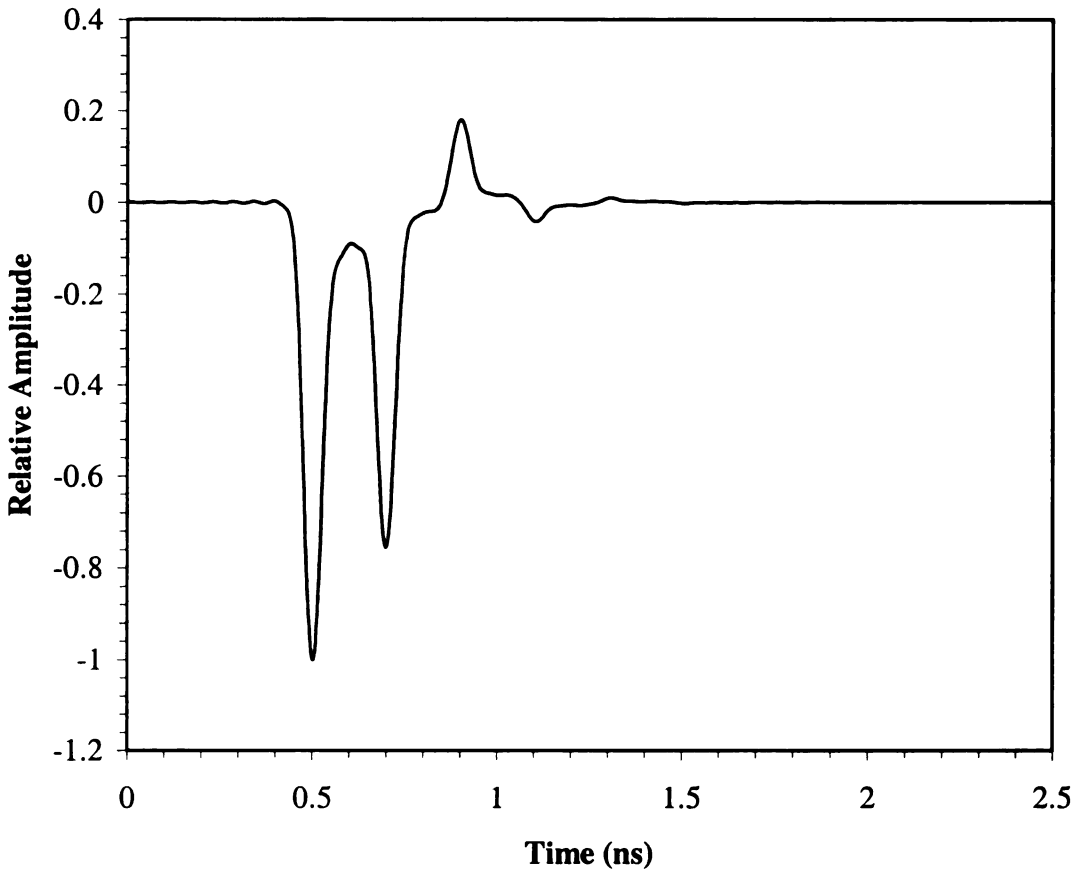

Figure 3-40 Response waveform for material 'J'.

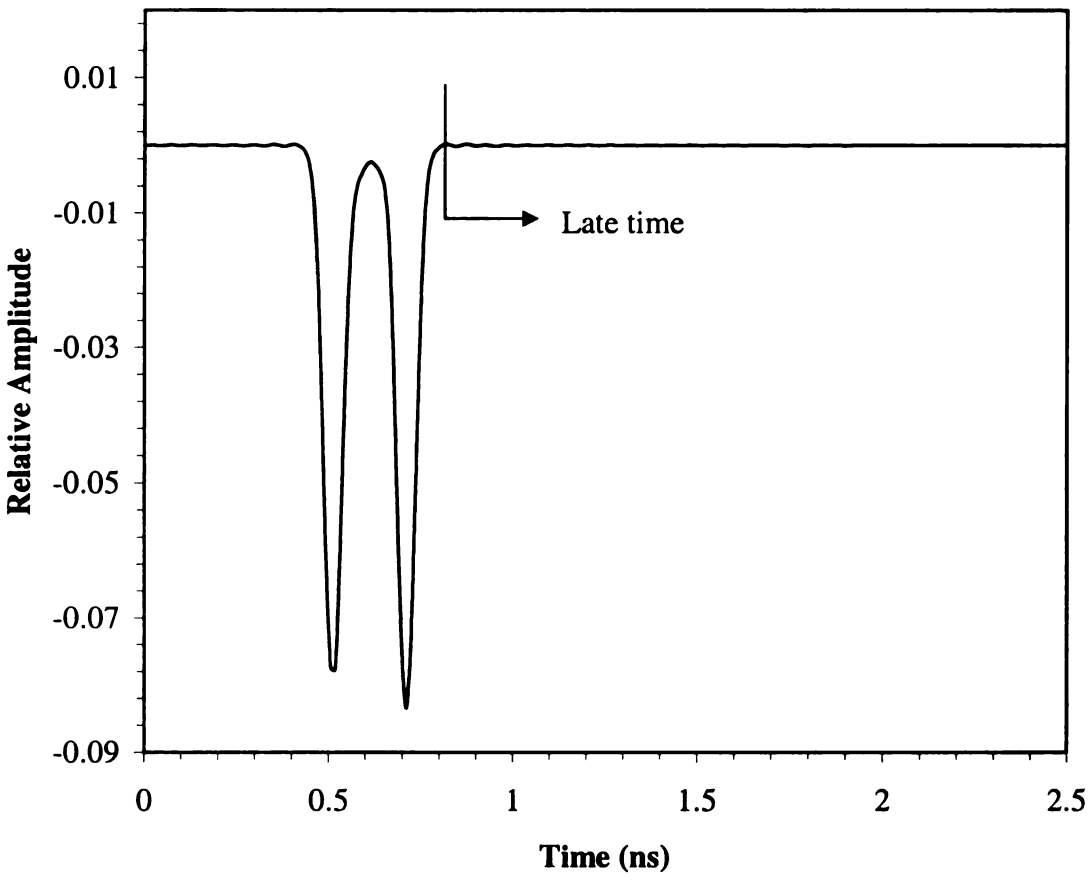

Figure 3-41 Convolution of the baseline response with the baseline E-pulse.

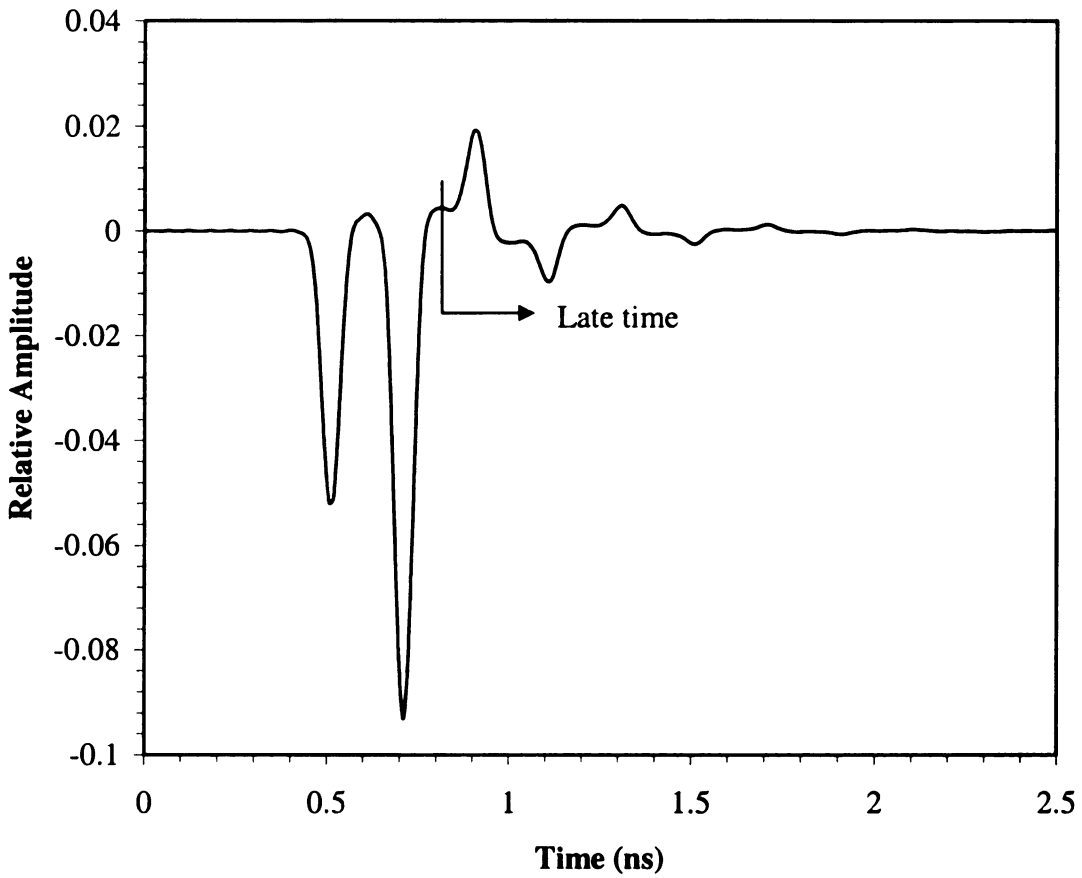

Figure 3-42 Convolution of material 'A' response with the baseline E-pulse.

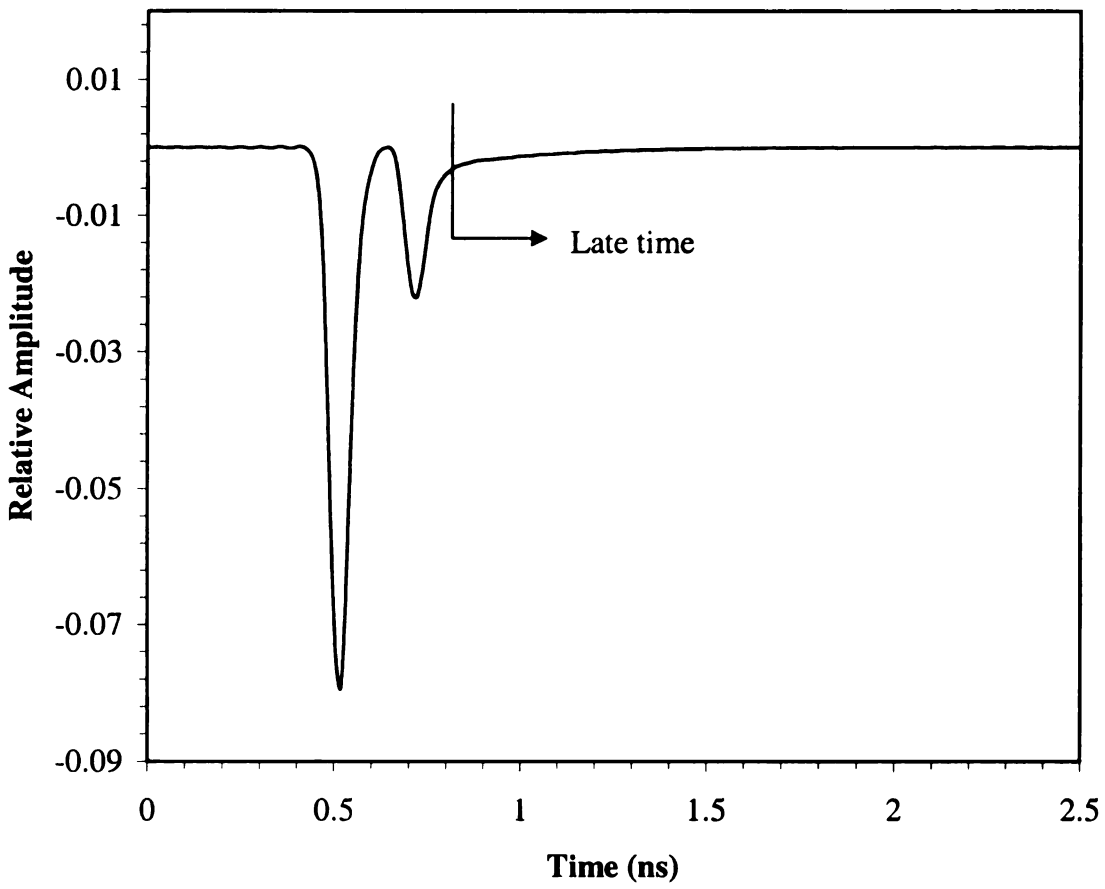

Figure 3-43 Convolution of material 'S' response with the baseline E-pulse.

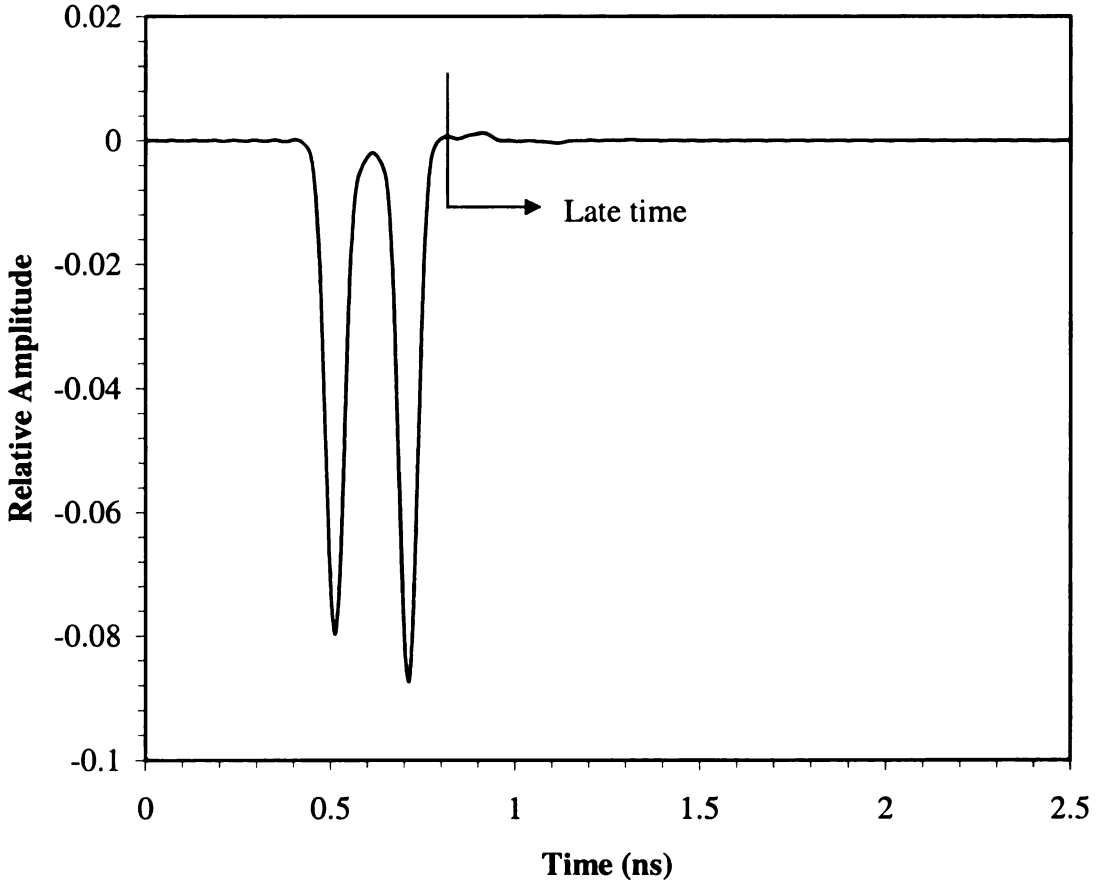

Figure 3-44 Convolution of material 'H' response with the baseline E-pulse.

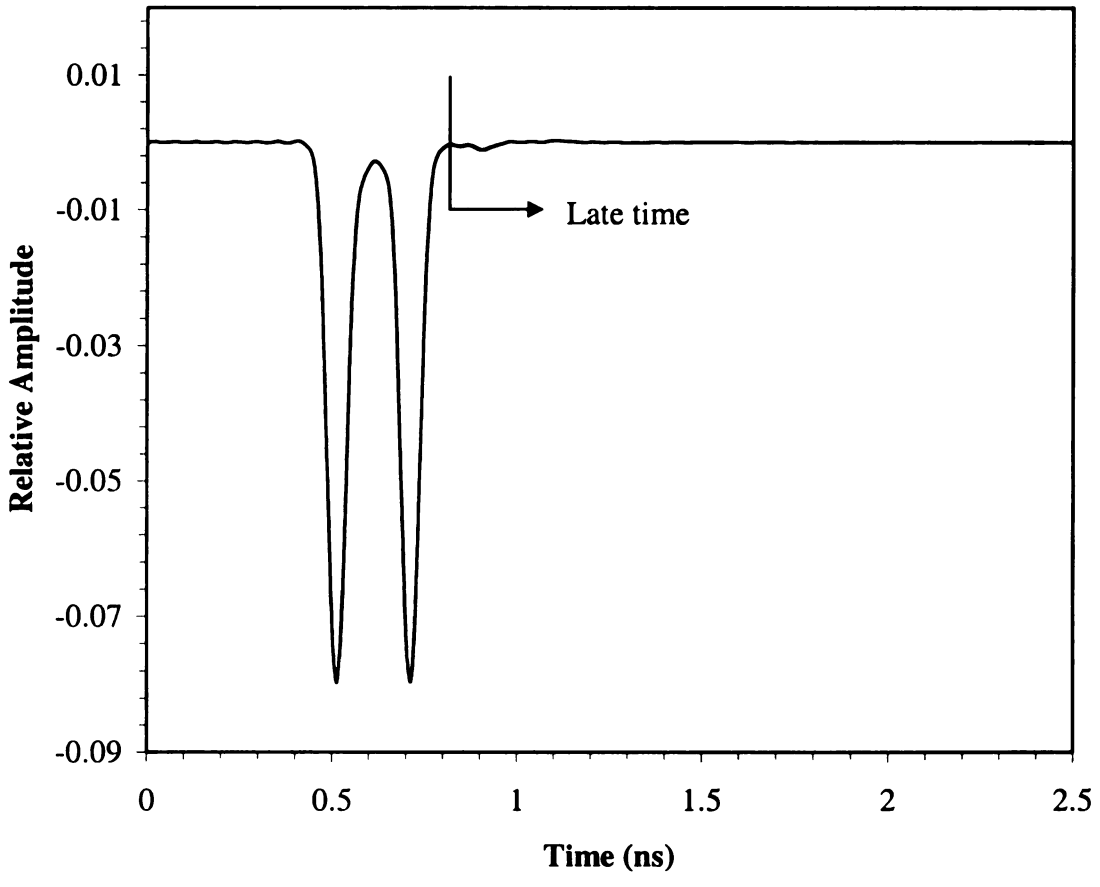

Figure 3-45 Convolution of material 'J' response with the baseline E-pulse.

Table 3-10 shows the EDNa values calculated for the various values of conductivity. It is not so evident as in previous EDNa tables how effective the EDNa is in this instance. These EDNa values are seen plotted in Figure 3-46. While at first glance it might appear that the EDNa effectively discriminates changes in conductivity, by comparing these EDNa values to those in previous EDNa plots, there is in fact a much smaller change in EDNa for changes in conductivity. This would imply that for small changes in conductivity (e.g., from a baseline of 0.5 to 0.75), it might be very difficult to detect a change. A very low EDNa threshold would have to be set relative to those that might be set to detect changes in thickness or permittivity. This will become more evident in the next chapter when noise is added to the data.

Material	Conductivity, $\sigma(S/m)$	EDNa
A	0	9.48E-04
B	2e-5	9.48E-04
C	2e-2	8.39E-04
D	0.1	4.92E-04
E	0.2	2.24E-04
F	0.3	8.03E-05
G	0.4	1.64E-05
H	0.45	2.84E-06
I	0.5	2.16E-07
J	0.55	3.78E-06
K	0.6	1.00E-05
L	0.7	3.23E-05
M	0.8	5.82E-05
N	0.9	8.35E-05
P	1.5	1.67E-04
Q	2.0	1.71E-04
R	2.5	1.55E-04
S	5.0	8.05E-05

Table 3-10 EDNa calculations for change in conductivity of material.

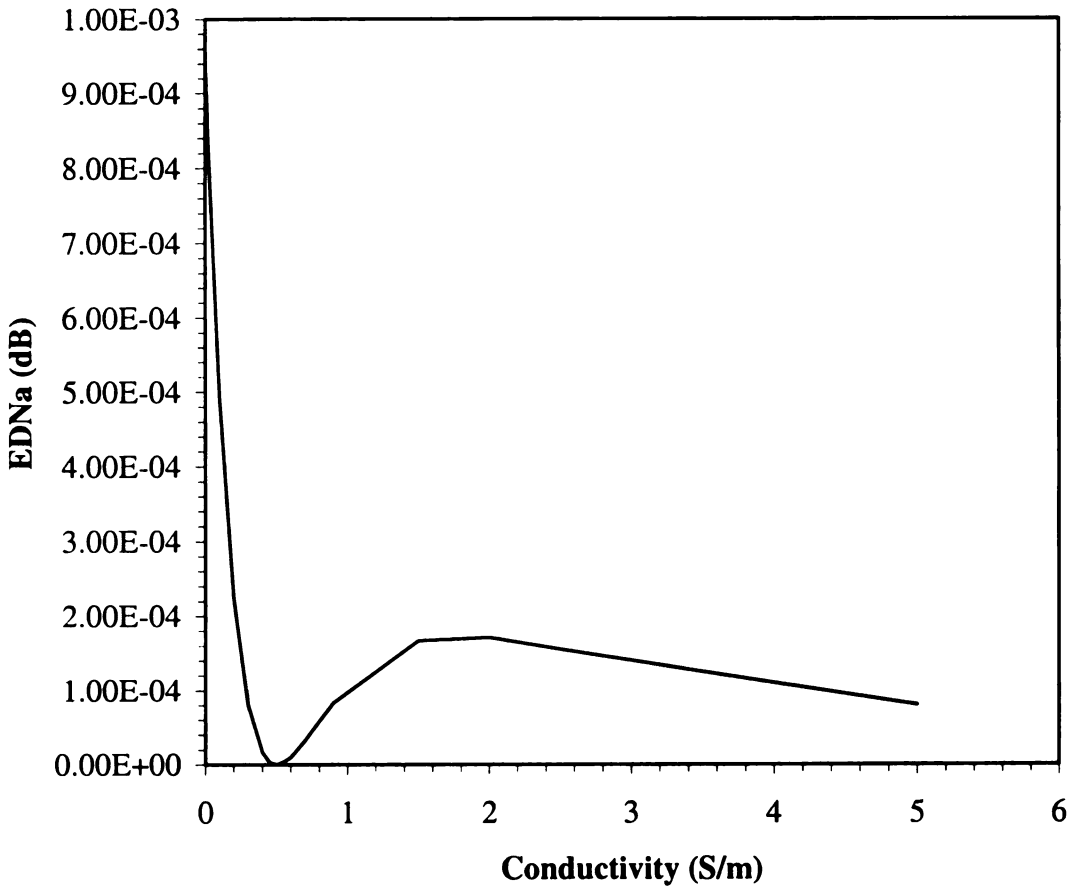

Figure 3-46 EDNa vs. change in conductivity.

3.3 Effects of Noise on EDNa

The same noise model as that used in chapter 2 for lossless materials was applied to the lossy materials discussed in this chapter. The noise was added to the response waveforms before convolution and for each case 500 different samples were generated and then averaged to arrive at the EDNa. Since noise corrupts all of the signals, including the baseline, none of the convolutions are expected to have zero late-time energy. To allow consistent comparisons of changes in the EDNa, the EDRa was calculated and used as the quantitative tool for noisy data.

3.3.1 EDRa vs. Signal-to-Noise Ratio

The goal of using the EDRa values is to be able to determine changes in material properties even in data with low SNR. Ideally, we would like to be able to identify changes in properties regardless of noise, but that is obviously not practical. The discussion in chapter 2 on noise corruption showed examples of the noise corrupted response waveforms and resulting convolutions. The response waveforms and convolutions are essentially the same so the these examples will not be shown in this chapter. Instead, the focus of discussion will be the EDRa values and their plots. The three properties examined are the thickness, permittivity, and conductivity. It has been shown thus far in this chapter that when the material layer is lossy the EDNa values calculated are lower than when the material is lossless. With the addition of noise it is expected that discrimination of material property changes will become increasingly more difficult. Table 3-11 shows the EDRa values for changes in thickness. The baseline material has a thickness of 10mm and thus its EDRa is zero for all SNR, as it should be

according to (2.13). Consistent with discussion on noise corruption in chapter 2, SNR's of 2, 5, 10, 15, 20, 25, and 30dB were considered. Table 3-12 shows the EDRa values for changes in permittivity and Table 3-13 shows the EDRa values for changes in conductivity. One interesting thing to note about Table 3-13 is that some of the EDRa values are negative. This means that the EDNa value for the baseline was not the smallest value for that particular configuration of SNR and conductivity. This implies that the changes in the material properties cannot be detected at this particular level of noise. The EDRa values are shown plotted in Figure 3-47, Figure 3-48, and Figure 3-49. Figure 3-47 shows the EDRa versus SNR for changing thicknesses. It can be seen that for all SNR's investigated some threshold EDRa value could be set to determine changes in the thickness. Figure 3-48 shows the EDRa versus SNR for changing values of permittivity. Again, it can be seen that a threshold EDRa value could be set to determine changes in permittivity. Where the difficulty begins it with Figure 3-49 which shows the EDRa versus SNR for changing conductivity. What this plot shows is that as the SNR decreases it becomes more difficult, even impossible, to determine small changes in the conductivity. It should be noted that for larger changes in conductivity (e.g., a change from σ=0.5 to σ=0.4) it is still possible to set a threshold to detect changes.

Thickness (mm)	2dB SNR	5dB SNR	10dB SNR	15dB SNR	20dB SNR	25dB SNR	30dB SNR
8	2.90	4.42	8.45	13.3	18.1	22.7	27.4
9	1.72	1.76	4.31	8.17	12.6	17.1	21.7
10	0	0	0	0	0	0	0
11	1.15	1.09	3.49	7.12	11.4	15.8	20.4
12	2.09	3.03	6.49	10.9	15.6	20.1	24.8

Table 3-11 EDRa vs. SNR for several thicknesses.

Permittivity	2dB SNR	5dB SNR	10dB SNR	15dB SNR	20dB SNR	25dB SNR	30dB SNR
7	0.757	1.69	3.93	7.47	11.9	16.4	21.2
8	0.176	0.657	1.65	3.52	6.94	11.1	15.9
9	0	0	0	0	0	0	0
10	0.848	1.29	2.03	3.96	7.23	11.2	15.9
11	1.09	2.44	4.75	7.94	12.3	16.7	21.6

Table 3-12 EDRa vs. SNR for several values of permittivity.

Conductivity (S/m)	2dB SNR	5dB SNR	10dB SNR	15dB SNR	20dB SNR	25dB SNR	30dB SNR
0.3	1.46	1.57	3.05	5.25	9.17	13.9	18.2
0.4	0.865	0.522	1.05	1.91	3.97	7.73	11.6
0.45	0.478	0.451	0.765	0.798	1.51	3.46	6.0
0.5	0	0	0	0	0	0	0
0.55	0.285	0.0158	0.336	0.228	0.899	2.68	5.22
0.6	0.561	-0.129	0.537	0.788	2.61	6.06	9.71
0.7	-0.572	-0.0159	0.875	2.58	5.76	10.2	14.4

Table 3-13 EDRa vs. SNR for several values of conductivity.

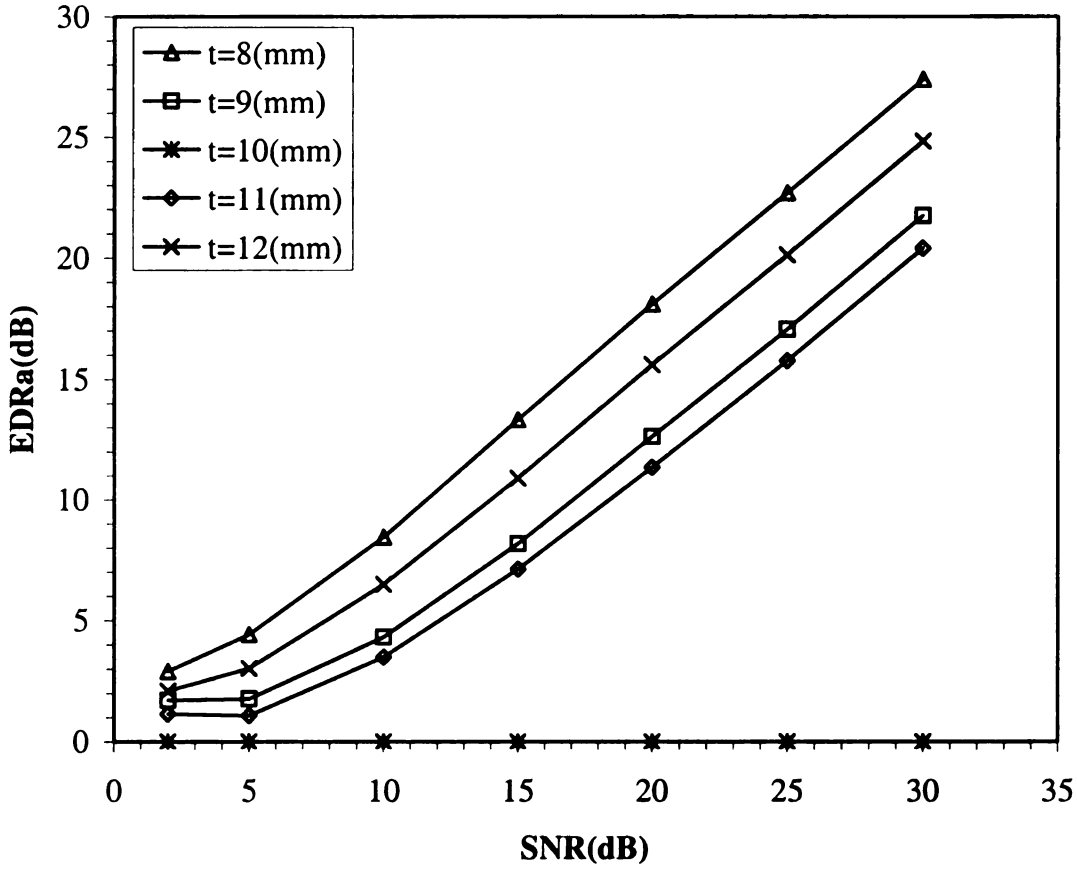

Figure 3-47 Comparison of EDRa vs. SNR for several thicknesses.

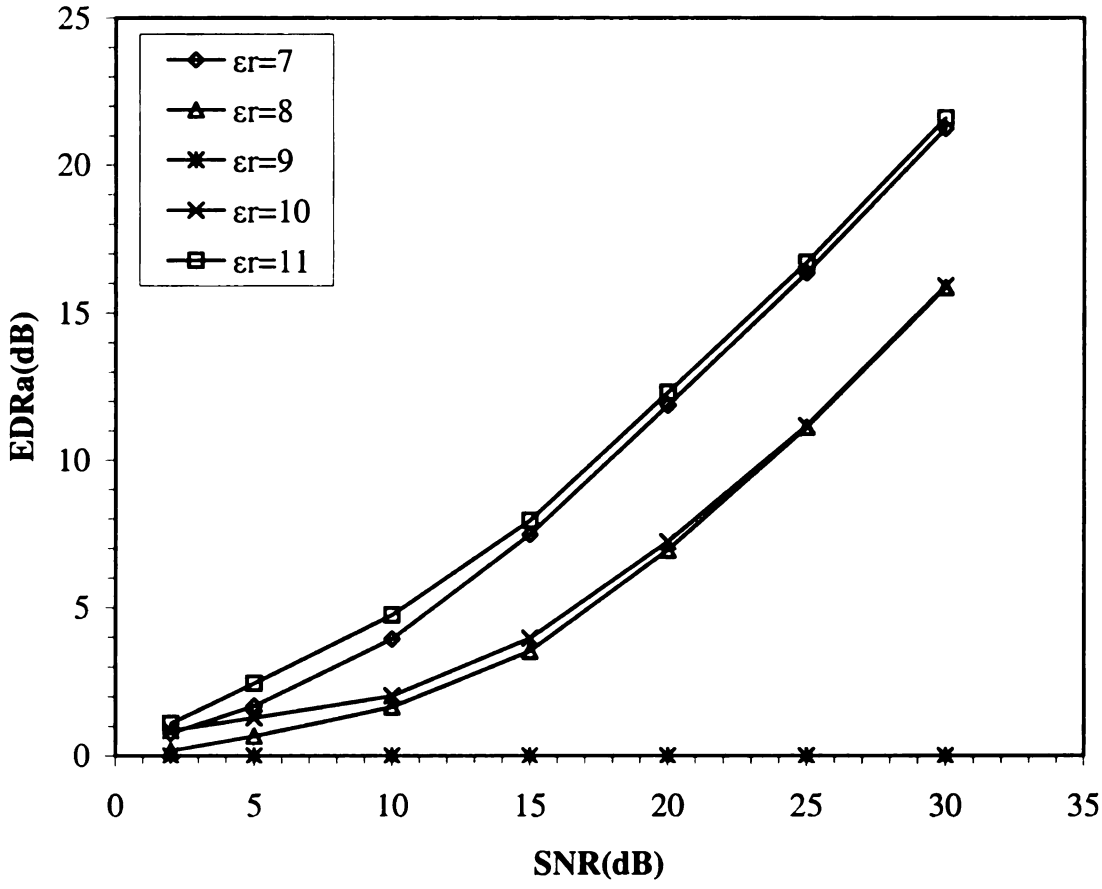

Figure 3-48 Comparison of EDRa vs. SNR for several values of permittivity.

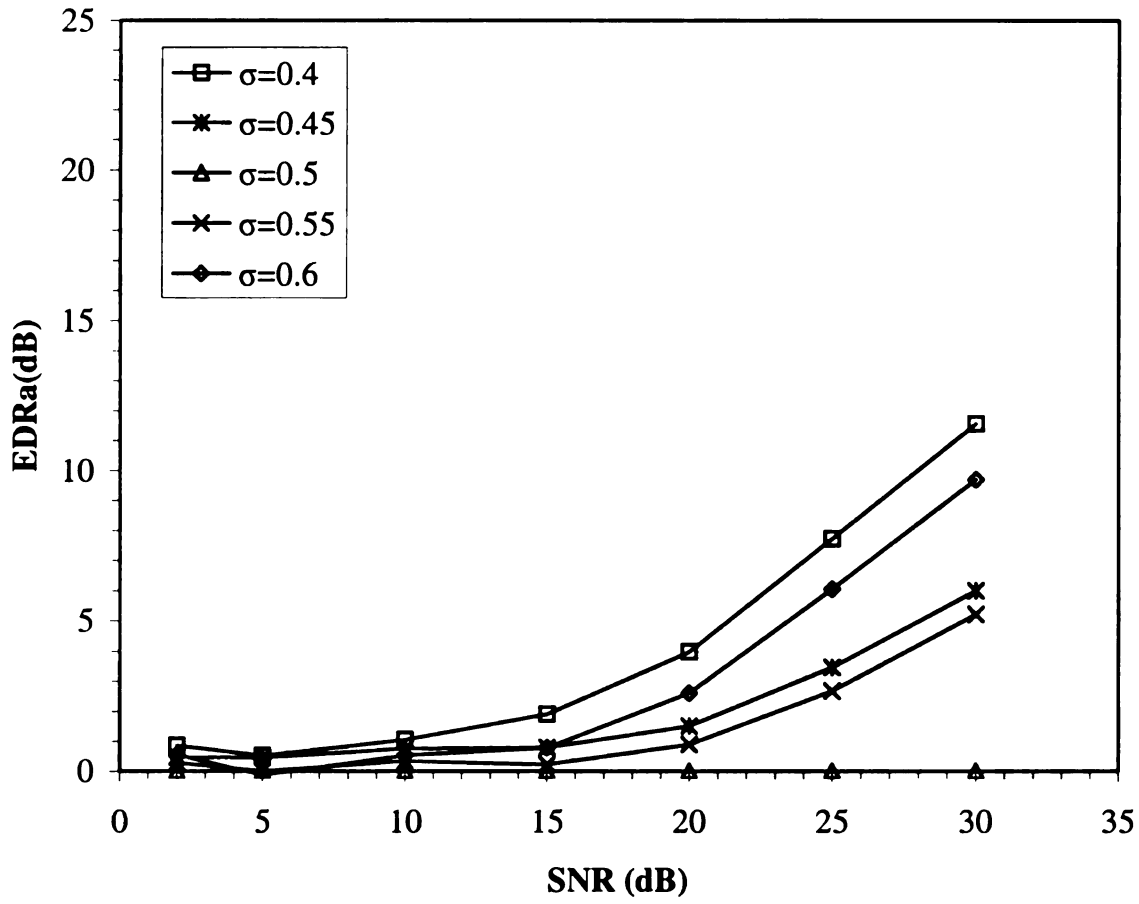

Figure 3-49 Comparison of EDRa vs. SNR for various values of conductivity.

Chapter 4

Magram - Single Layer

The previous chapters investigated the use of the E-pulse in diagnosing simple, single layered materials. Extending the E-pulse technique to more complicated layered materials will be discussed in this chapter and in chapter 5. The focus of this chapter will be on single layered Magram materials. Analysis of material properties using the E-pulse is dependent on the natural frequencies of the scattered response waveform. For simple layered materials where the properties were known it was possible to theoretically determine the natural frequencies. Given the scattered response of a layered material without knowledge of the material properties, the natural frequencies must be extracted from the response waveform numerically.

4.1 Extraction of the Natural Frequencies and E-Pulses from Response Waveforms

A solution of (1.22) for $e(t)$ is only possible given that the natural frequencies are already known. When the natural frequencies are unknown they must be extracted from the experimental response waveform. We begin by expanding the E-pulse into a sum of basis functions,

$$e(t) = \sum_{m=1}^{M} A_m f_m(t), \tag{4.1}$$

where $\{f_m(t)\}$ is an appropriate set of basis functions and A_m is the amplitude of the m'th basis function. Substituting (4.1) into (1.2) gives,

$$c(t) = \sum_{m=1}^{M} A_m f_m(t) * r^e(t), \quad t > T_L + T_e \tag{4.2}$$

$$= \int_0^{T_e} \sum_{m=1}^{M} A_m f_m(\tau) r^e(t-\tau)\, d\tau = 0, \quad t > T_L + T_e\,, \tag{4.3}$$

where $r^e(t)$ is the experimental response waveform. A solution to (4.3) for $\{A_m\}$ can be found using the moment method technique. Taking the inner product of (4.3) with a set of weighting function $\{w_m\}$ gives,

$$\sum_{m=1}^{M} A_m \int_0^{T_e} \int_{T_L+T_e}^{T_w} f_m(\tau) r^e(t-\tau) w_k(t)\, dt d\tau = 0, \quad k = 1,2,3,\cdots,K\,. \tag{4.4}$$

Here $f_m(t)$ is chosen to be a set of sub-sectional basis functions in the E-pulse expansion,

$$f_m(t) = \begin{cases} 1, & (m-1)\Delta \le t \le m\Delta \\ 0, & otherwise \end{cases}\,. \tag{4.5}$$

where Δ is the pulse width. The solution to (4.3) for $\{A_m\}$ is not unique. In fact, depending on the choice of M, there are infinitely many solutions. By choosing $M = K = 2N$, (4.4) becomes a set of homogeneous linear equations, and the resulting E-pulse is the "natural" E-pulse discussed previously. Sets of E-pulse amplitudes, $\{A_m\}$, that result in $c(t) = 0$, occur only at discrete values of T_e. By choosing $M = 2N+1$, $K = 2N$, (4.4) results in a set of linear equations that depend on a forcing function and the E-pulse is the "forced" E-pulse discussed previously. Since $c(t) = 0$ does not depend

on the determinant matrix being zero, solutions for $\{A_m\}$ occur for any T_e except those that give solutions for the "natural" E-pulse.

Numerous E-pulses with different T_e are generated by forcing (4.2) to be zero. Within this set of E-pulses there exists one which will allow the most accurate discrimination. In other words, many E-pulses are generated that force (1.2) to be very nearly equal to zero, but not exactly zero. As will be shown, the natural frequencies extracted are merely estimates with some degree of error. To find the optimum E-pulse, first the natural frequencies are extracted from each E-pulse and a set of estimated response waveforms, $\{\hat{r}(t)\}$ are created using (1.1). Next, a comparison of each $\hat{r}(t)$ to the original response, $r^e(t)$ using a least squared error technique gives the $\hat{r}(t)$ that most nearly represents $r^e(t)$. Given this $\hat{r}(t)$, the corresponding E-pulse used to generate it is then the most optimum for that specific response waveform, $r^e(t)$.

Assuming a "natural" E-pulse has been generated, extraction of the natural frequencies from the generated E-pulses begins by taking the Laplace transform of (4.1),

$$\mathfrak{L}\{e(t)\} = \mathfrak{L}\left\{\sum_{m=1}^{M} A_m f_m(t)\right\}, \tag{4.6}$$

$$E(s_n) = \sum_{m=1}^{M} A_m F_m(s_n), \quad n = 1,2,3,\ldots,N. \tag{4.7}$$

It was shown in section 1.1.2 that $E(s_n) = E\left(s_n^*\right) = 0$ to satisfy $c(t) = 0$. Therefore, by finding the roots of (4.7), the natural frequencies $s_n = \sigma_n + j\omega_n$ can be determined. Using the Laplace transform (1.3),

$$F_m(s) = \int_0^\infty f_m(t) e^{-st} dt \,, \tag{4.8}$$

where $f_m(t)$ was defined by (4.5). Thus

$$F_m(s_n) = \int_{(m-1)\Delta}^{m\Delta} 1 e^{-s_n t} dt \tag{4.9}$$

$$= \frac{e^{-s_n\Delta} - 1}{s_n} e^{-s_n m\Delta} \,. \tag{4.10}$$

Substituting (4.10) into (4.7) gives,

$$E(s_n) = \frac{\left(e^{-s_n\Delta} - 1\right)}{s_n} \sum_{m=1}^{M} A_m e^{-s_n m\Delta} = 0 \,, \tag{4.11}$$

the roots of which are found by solving the polynomial equation,

$$\sum_{m=1}^{M} A_m Z_n^m = 0 \,, \tag{4.12}$$

where

$$Z_n = e^{-s_n\Delta} \,. \tag{4.13}$$

Knowing Z_n allows one to solve for the natural frequencies,

$$s_n = -\frac{1}{\Delta} \ln(Z_n) \,, \tag{4.14}$$

where the pulse width, Δ, has been shown [2] to equal,

$$\Delta = \frac{p\pi}{\omega_k}, \quad p = 1, 2, 3, \cdots, \quad 1 \le k \le N \,. \tag{4.15}$$

These natural frequencies can then be substituted into (1.1) to determine the estimated response, $\hat{r}(t)$, for each E-pulse.

Once a set of estimated responses is found for each E-pulse, they can all be compared to the original response waveform to determine the optimum E-pulse. This is done by minimizing the squared error,

$$\varepsilon = \left| r(t) - \hat{r}(t) \right|^2 = \sum_i \left| r(t_i) - \hat{r}(t_i) \right|^2 , \tag{4.16}$$

where the sum is over sampled values in the late-time of the responses. This squared error is the error between the original response waveform and the set of estimated response waveforms reconstructed from the generated E-pulses. The reconstructed response which gives the minimum error determines the optimum E-pulse.

4.2 Magram Materials – Experimental Results

This section deals with the scattered response waveforms from Magram materials. The goal is to extract the natural frequencies from the scattered response waveforms, generate an E-pulse from these natural frequencies, and determine if the generated E-pulses are sufficient to detect changes in the magram material properties. Due to the proprietary nature of magram materials it was not possible to obtain any for testing. However, the scattered response frequency domain data from three unknown Magram material samples was provided for analysis. These samples will be referred to as sample A, sample B, and sample C. For each sample the magnitude and phase data was provided in the frequency range of 2-18 GHz. Figure 4-1 shows the magnitude plots of the scattered response from each sample and Figure 4-2 shows the phase plots from each sample. The magnitude plots can be compared to the magnitude plot for the single layer lossless materials shown in Figure 2-1 and the magnitude plots for the single layer lossy materials shown in Figure 4-3. It can be seen that the Magram responses show decreased

response for certain selective frequencies while the other materials do not exhibit this frequency selection. Magram materials behave similar to frequency selective surfaces.

A difference in the frequency responses that was addressed is the frequency range of the experimental data, 2-18GHz. This differed from the range of the theoretical data which had a frequency range of 0-18 GHz. This additional discontinuity at 2 GHz contributes additional error when the IFFT function is performed. To eliminate this error and to keep the results consistent with previous frequency domain responses, the experimental data was extrapolated to 0 GHz. This extrapolation was performed using the Microsoft Excel spreadsheet program. The results of these extrapolations are shown in Figure 4-4 and Figure 4-5.

To extract the natural frequencies from the response data, the frequency domain data was transformed into the time domain. This procedure was performed using the IFFT program in UTIL2B.exe. Before running the IFFT program a Gaussian modulated cosine windowing function was applied with width, $\tau = 0.06$, and center frequency of 2 GHz for the original data and 0 GHz for the extrapolated data. Both the original data and the extrapolated data were processed with the IFFT function and the resulting time domain waveforms are shown in Figure 4-6 and Figure 4-7. Figure 4-6 shows the time domain response waveforms for the original data. The error due to the discontinuity at 2 GHz is seen by the rise in amplitude before the initial reflection from the layer. This waveform should be zero until the first reflection. Figure 4-7 shows the time domain response waveform from the extrapolated data and it shows that this error has been improved, but there is still some error present.

Generating E-pulses from these time domain scattered response waveforms turns out not to work using the program EP.for. While the program does generate an E-pulse, the result does not give the proper results when trying to discriminate between scattered responses. Figure 4-8 shows an E-pulse generated from the sample A scattered response waveform using 5 modes. Each sample's response waveform was convolved with this E-pulse to see if the resulting convolution waveform would show an ability to discriminate between the three sample responses. Figure 4-9 shows the convolution of the sample A response waveform with the E-pulse. It is obvious that the late-time energy in the convolution is not zero as we would expect. Figure 4-10 shows the convolution of the sample B response waveform with the E-pulse. Figure 4-11 shows the convolution of the sample C response waveform with the E-pulse. All three of the convolution waveforms contain a large amount of energy and are all very similar in shape. The EDNa values were calculated for each convolution and can be seen in Table 4-1. It is evident that the EDNa is not an appropriate way to determine changes to Magram materials.

The reason that the E-pulse does not work for Magram materials is most likely due to the nature of the material. It is designed to absorb energy at certain frequencies. Since the Magram materials absorb the incident wave, seemingly very efficiently, there is not enough scattered response to allow extraction of the natural frequencies. In addition, the very frequency range from which we are trying extract the natural frequencies from is the same range these particular sample responses are designed to absorb energy in.

For example, in the single lossless layer case, the natural frequencies that were calculated and used to generate the E-pulse for one particular case can be seen in Table 4-2. The frequency range of the scattered response investigated was 0-18 GHz and

according to Table 4-2 each natural mode in the E-pulse is within that range. Therefore, when the E-pulse is convolved with the scattered response these natural frequencies cancel. However, in the case of the Magram materials, there is not enough scattered response signal to extract the correct natural frequencies and even though EP.for generates an E-pulse, it is not made up of the correct frequencies with which to cancel the scattered response frequencies and thus the convolution is not zero and the technique does not work.

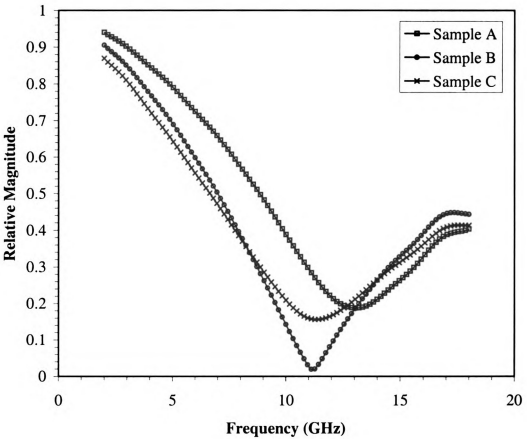

Figure 4-1 Magnitude plot of scattered response from unknown Magram materials.

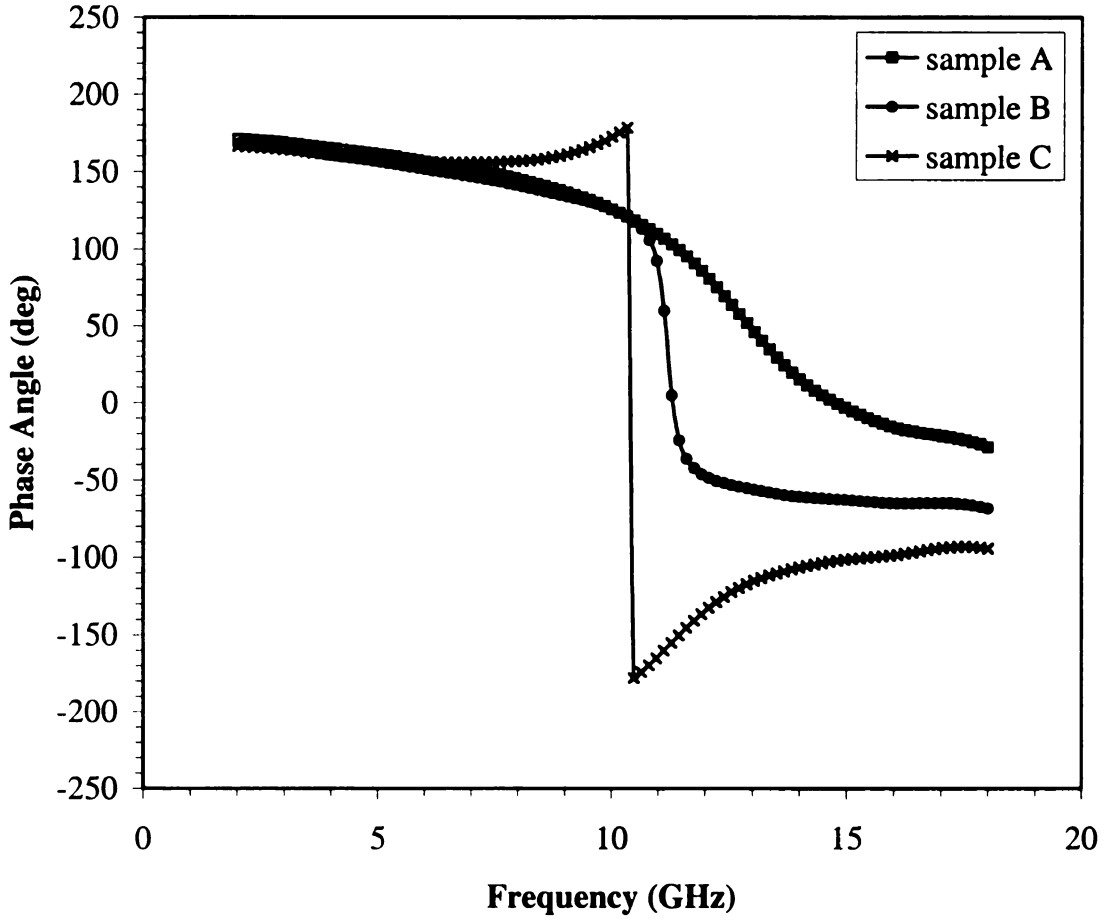

Figure 4-2 Phase plot of scattered response from unknown Magram materials.

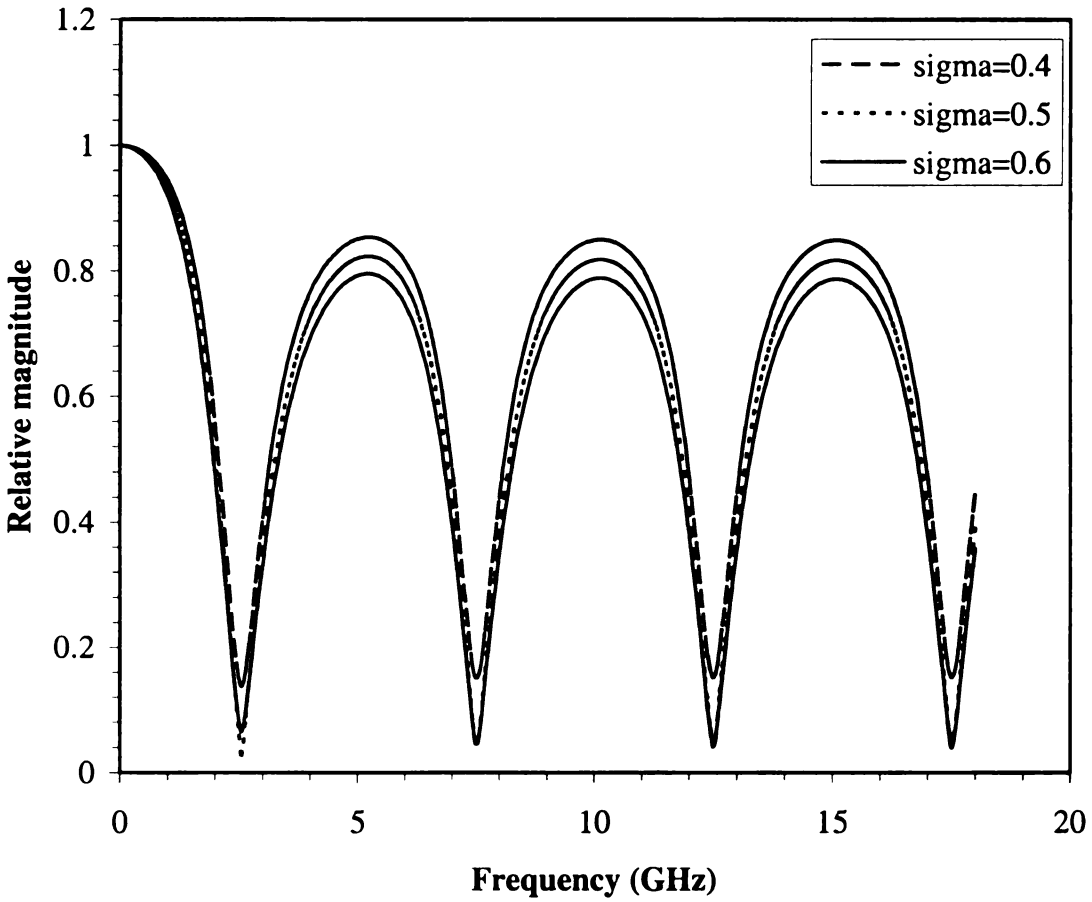

Figure 4-3 Frequency domain response plots for single layer lossy materials.

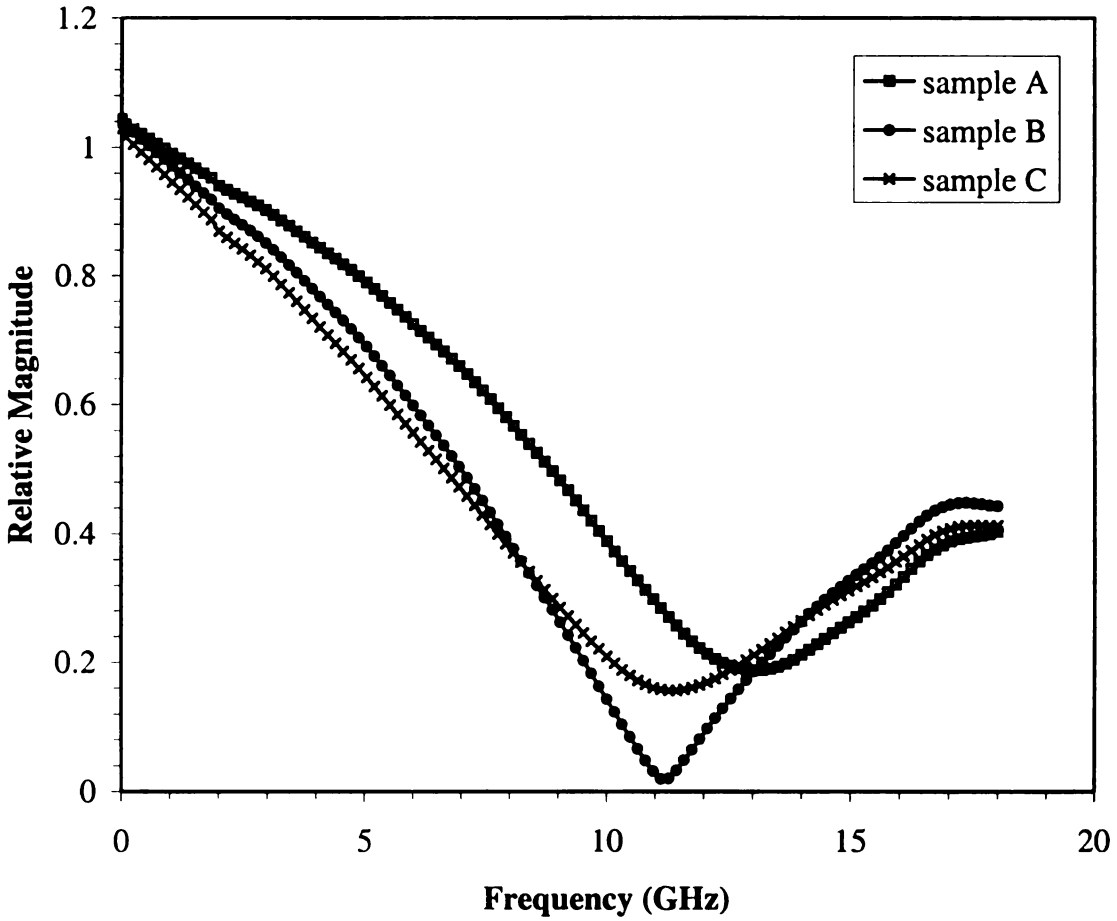

Figure 4-4 Extrapolated magnitude plots of scattered responses.

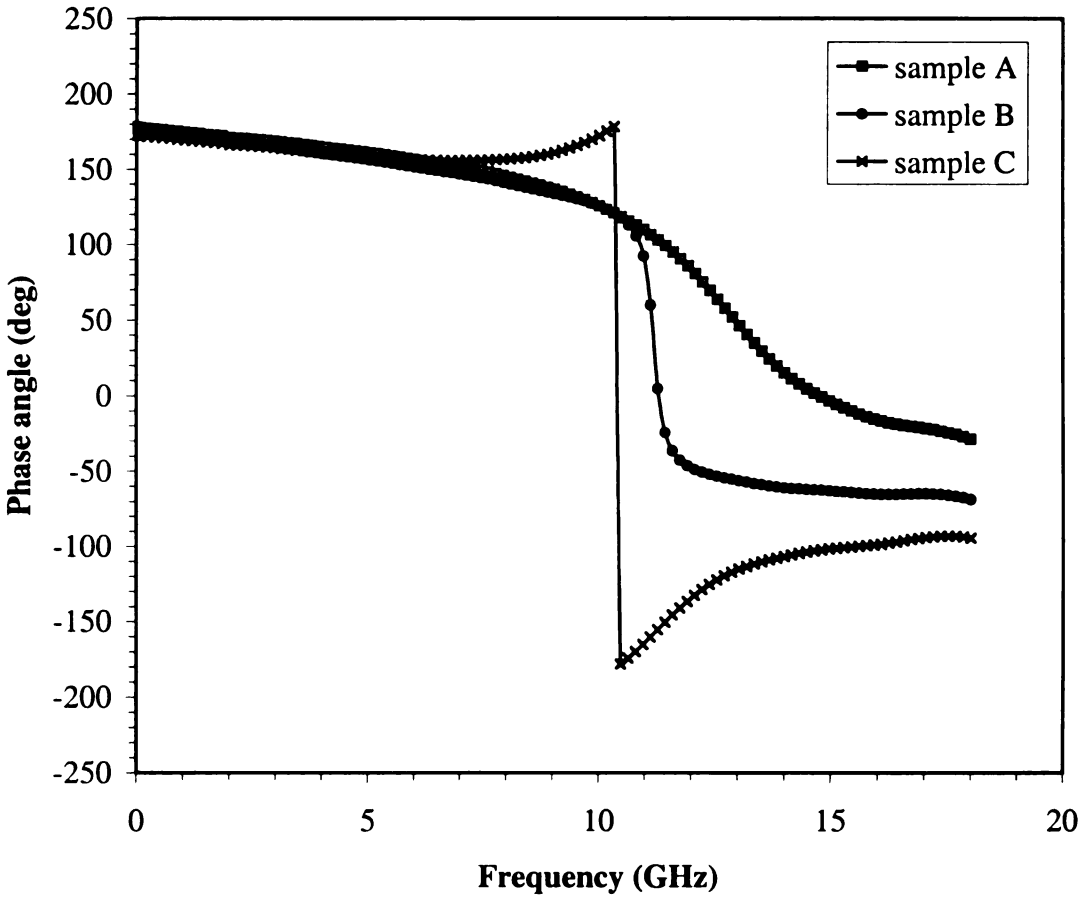

Figure 4-5 Extrapolated phase plots of scattered responses.

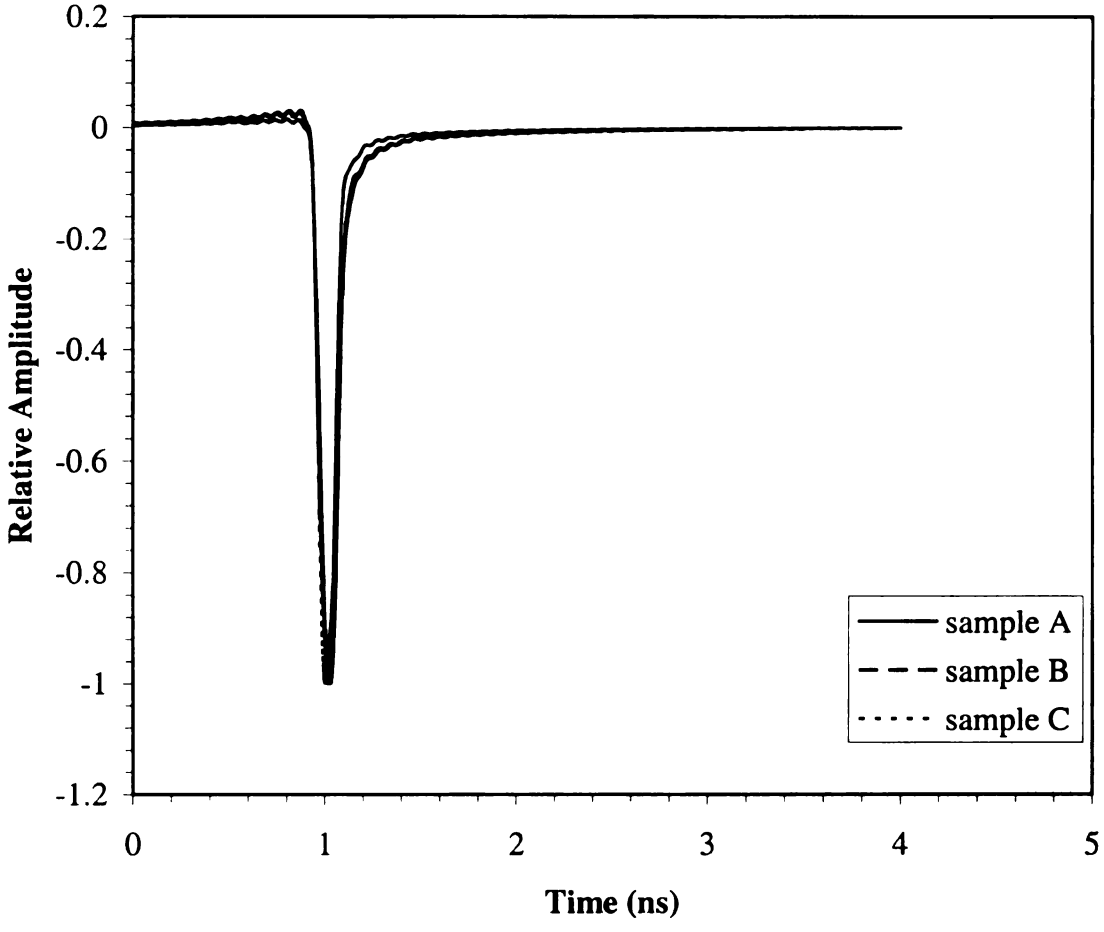

Figure 4-6 Time domain response of unknown Magram samples.

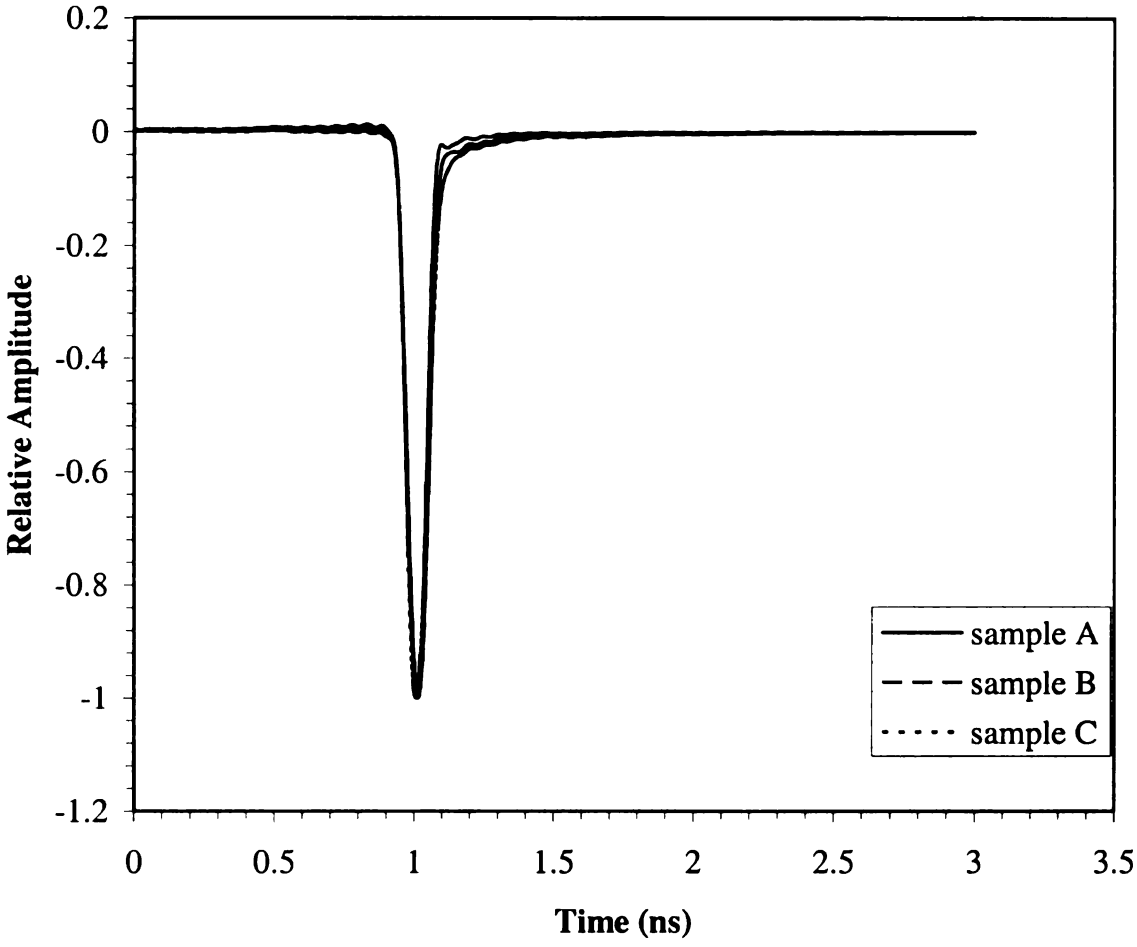

Figure 4-7 Time domain response for extrapolated data.

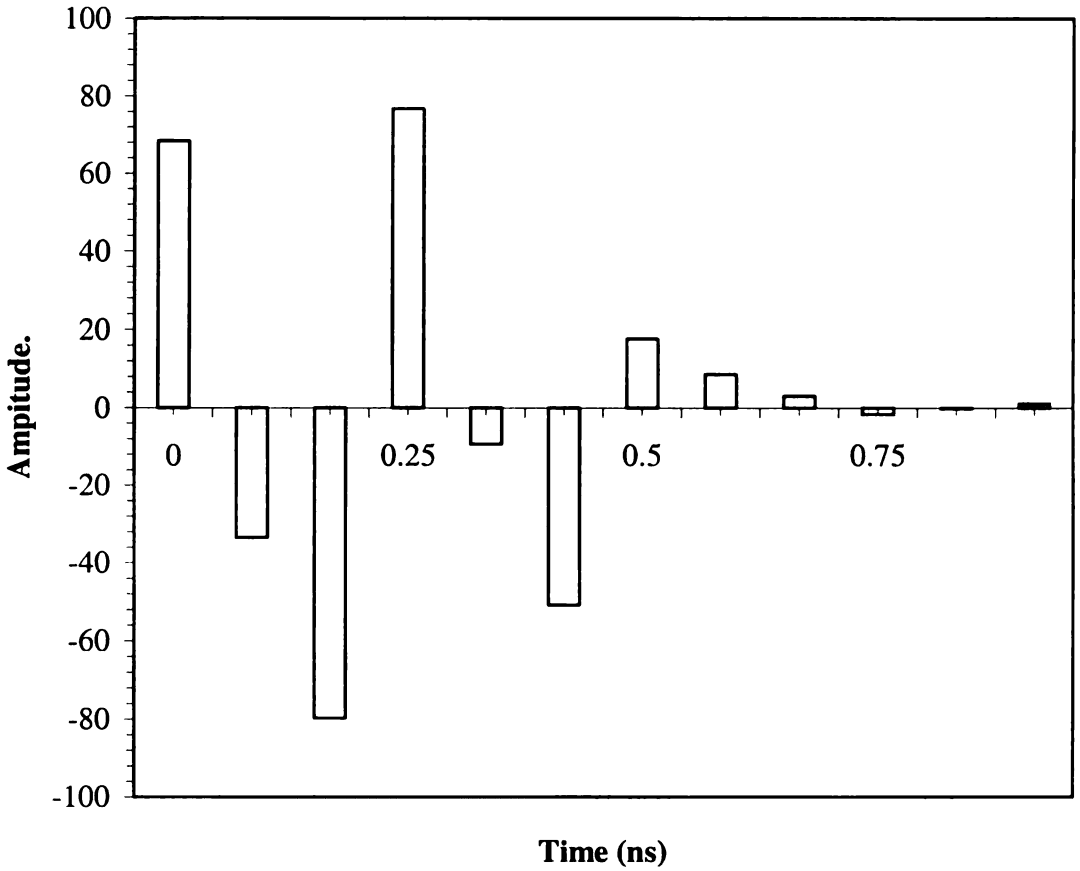

Figure 4-8 E-pulse generated from Sample A response using 5 modes.

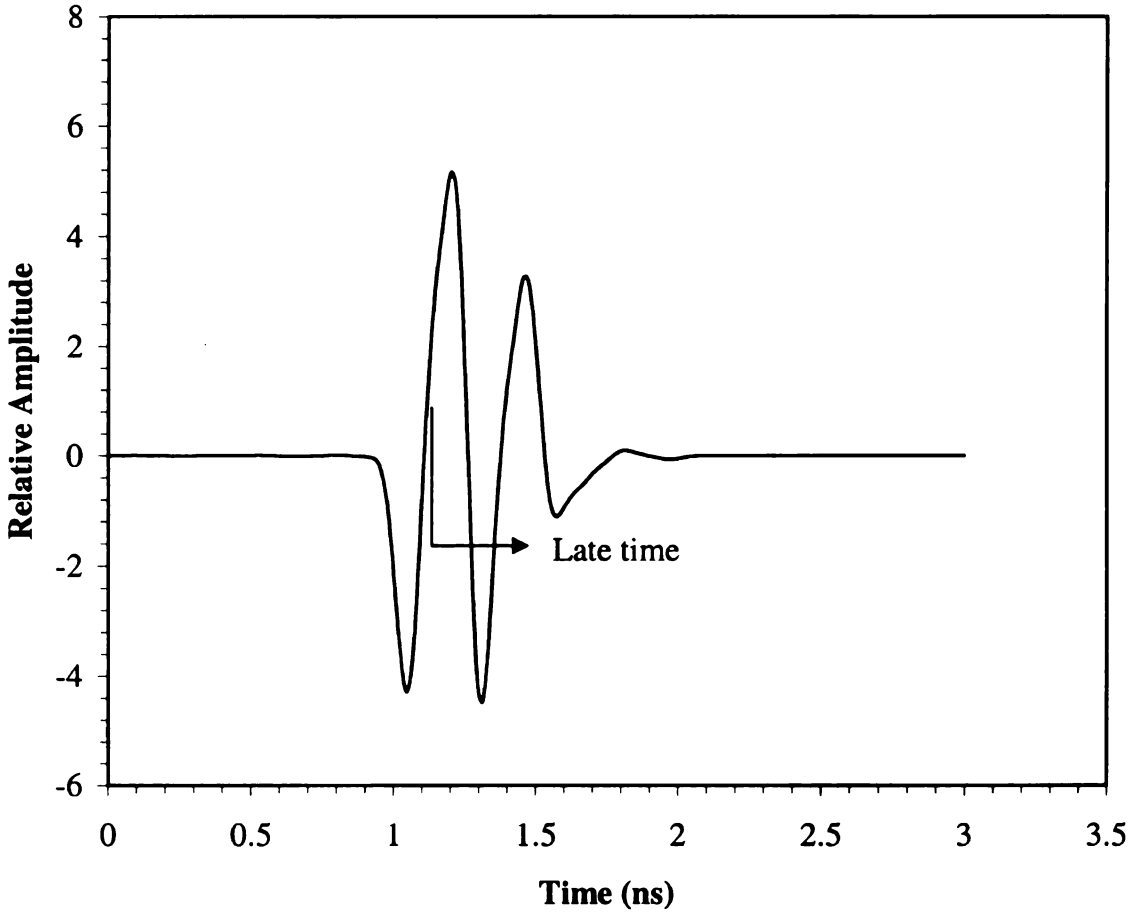

Figure 4-9 Convolution of the sample A response with the sample A E-pulse.

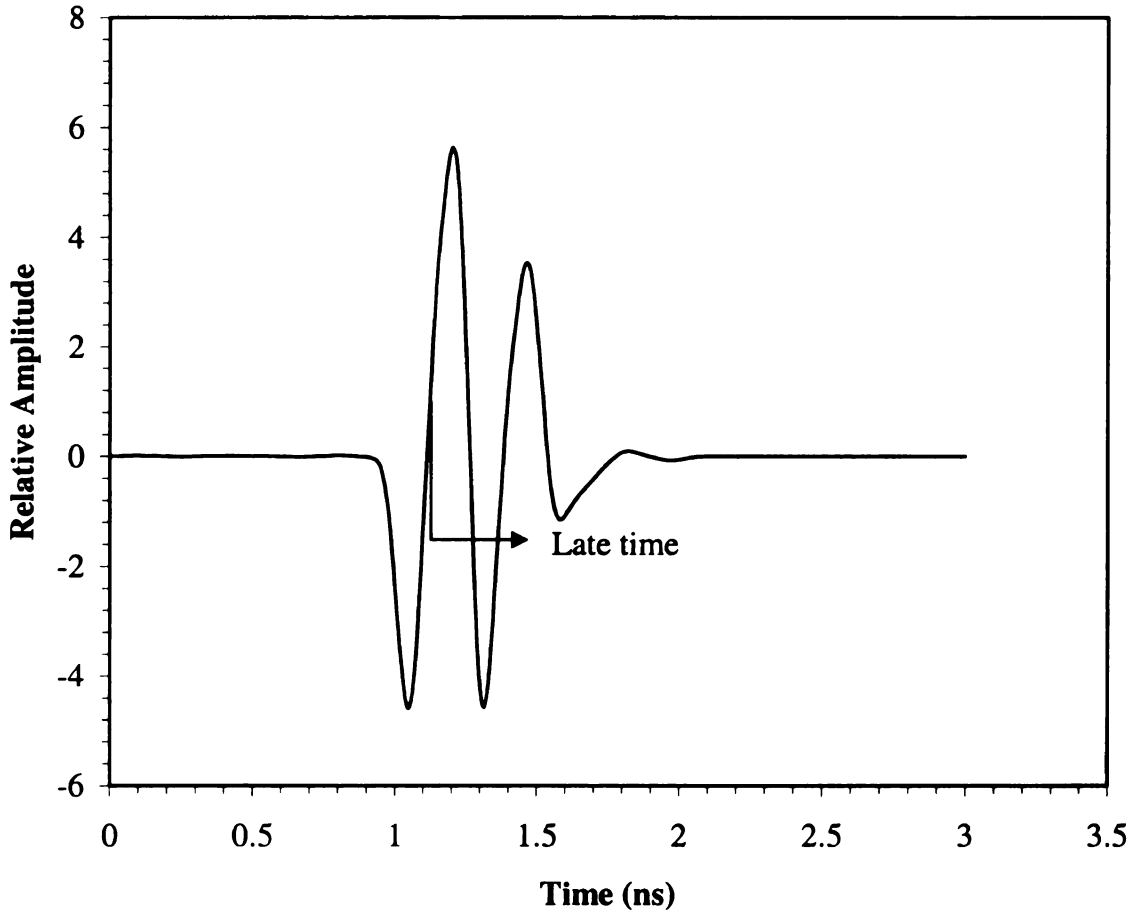

Figure 4-10 Convolution of the sample B response with the sample A E-pulse.

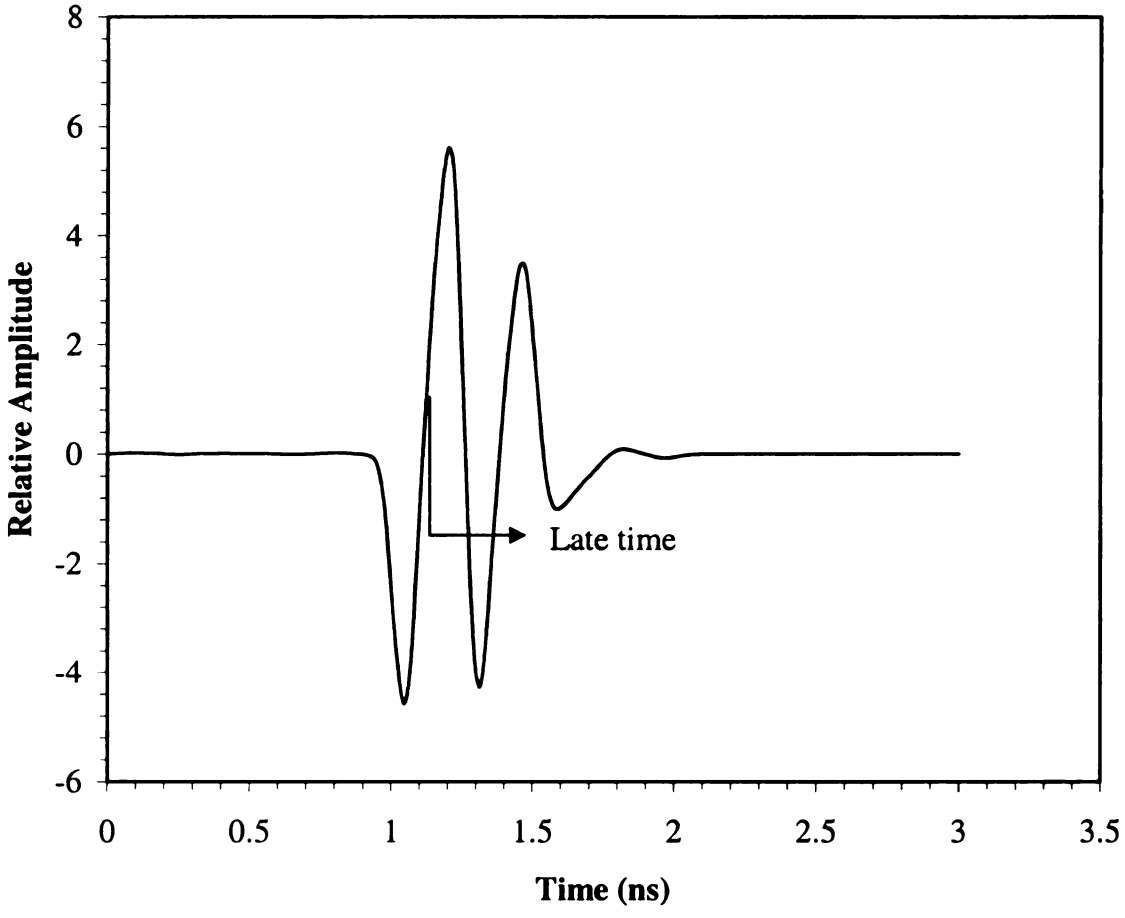

Figure 4-11 Convolution of the sample C response with the sample A E-pulse.

Sample	EDNa
A	3.80e-2
B	3.70e-2
C	3.54e-2

Table 4-1 EDNa values for the three Magram samples.

Mode	σ (S/m)	ω (Grads/sec)	f (GHz)
1	-3.466	15.71	2.5
2	-3.466	47.12	7.5
3	-3.466	78.54	12.5
4	-3.466	110.0	17.5
5	-3.466	141.3	22.5

Table 4-2 Natural frequencies for single lossless layered case.

Chapter 5

Impedance Sheet Over Single Layer

Previous chapters have discussed single layer conductor backed materials. The discussion will now explore a single layer conductor backed material with a thin resistive sheet placed on the surface of the layer. This thin sheet, or impedance sheet, will help reduce the backscatter from the layered materials at certain frequencies and is called a Salisbury Screen [12]. The surface resistance of the impedance sheet is defined in terms of the thickness and conductivity of the sheet,

$$R_s = \frac{1}{\sigma t}, \tag{5.1}$$

where σ is the conductivity in Siemens per meter and t is the thickness of the impedance sheet in meters. The purpose of this chapter will be to show how changes in the surface resistance of the impedance sheet will effect the EDNa. Several scattered response waveforms for layered materials with impedance sheets with different surface resistances will be simulated using the program MLPREF.for. The changes in surface resistance will be due to changes in the conductance; thus, the thickness of the impedance sheet will remain constant.

5.1 Theoretical Determination of Natural Frequencies

The first step in using the E-pulse as a means to identify changes in material properties is to determine the natural frequencies. Previous cases did not consider the configuration of a layered material with an impedance sheet, so the mathematics for this configuration must first be verified to be consistent with previous findings. Figure 5-1

shows the path of the wave in a layered material with an impedance sheet. To find the natural frequencies of the scattered response begin with the time domain scattered response given by,

$$R(t) = \Gamma_1 f(t) + T_1(-1)T_2 f(t-2T) + T_1(-1)\Gamma_2(-1)T_2 f(t-4T) + \cdots, \qquad (5.2)$$

where T is the transit time across region 1. The transmission coefficients T_1 and T_2 are the transmission coefficients into and out of the impedance sheet, respectively, while Γ_1 and Γ_2 are the respective reflection coefficients. The function $f(t)$ is the incident pulse that is used to excite the material. Equation (5.2) can be rewritten as

$$R(t) = \Gamma_1 f(t) + T_1 T_2 \sum_{n=1}^{\infty} (-1)^n \Gamma_2^n f(t-2nT) \qquad (5.3)$$

or

$$R(t) = f(t) * h(t), \qquad (5.4)$$

where

$$h(t) = \Gamma_1 \delta(t) + T_1 T_2 \sum_{n=1}^{\infty} (-1)^n \Gamma_2^n \delta(t-2nT) \qquad (5.5)$$

is the unit impulse function of the layered material [13]. By letting

$$\begin{aligned} (-1)^n \Gamma_2^n \delta(t-2nT) &= (-\Gamma_2)^n \delta(t-2nT) = e^{\alpha t}\delta(t-2nT) \\ &= \left(e^{2\alpha T}\right)^n \end{aligned} \qquad (5.6)$$

then

$$e^{2\alpha T} = -\Gamma_2 \qquad (5.7)$$

and solving for alpha gives

$$\alpha = \frac{1}{2T}\ln(-\Gamma_2). \tag{5.8}$$

Equation (5.8) can then be substituted into (5.5) giving

$$h(t) = \Gamma_1\delta(t) + T_1T_2e^{\alpha t}\sum_{n=1}^{\infty}\delta(t-2nT). \tag{5.9}$$

Using

$$\sum_{n=1}^{\infty}\delta(t-2nT) = u(t-2T)\sum_{n=-\infty}^{\infty}\delta(t-2nT) \tag{5.10}$$

and the Poisson-Sum formula [6]

$$\sum_{n=-\infty}^{\infty}\delta(t+n\tau) = \frac{1}{\tau}\sum_{n=-\infty}^{\infty}e^{jn\omega_o t} \tag{5.11}$$

where $\omega_o = \frac{2\pi}{\tau}$, (5.9) then becomes

$$h(t) = \Gamma_1\delta(t) + T_1T_2e^{\alpha t}\left[u(t-2T)\frac{1}{2T}\sum_{n=-\infty}^{\infty}e^{jn\frac{\pi}{T}t}\right] \tag{5.12}$$

$$= \Gamma_1\delta(t) + \frac{T_1T_2}{2T}u(t-2T)\sum_{n=-\infty}^{\infty}e^{(\alpha_n + j\omega_n)t}, \tag{5.13}$$

where $\omega_n = \frac{n\pi}{T}$ and $\alpha_n = \alpha$. The impulse response, (5.13), can finally be expressed as

$$h(t) = \Gamma_1\delta(t) + \frac{T_1T_2}{2T}u(t-2T)\left(e^{\alpha t} + 2\sum_{n=1}^{\infty}e^{\alpha t}\cos(\omega_n t)\right), \tag{5.14}$$

and the natural frequencies are given by

$$\boxed{s_n = \alpha + j\omega_n = \frac{1}{2T}\ln(-\Gamma_2) + j\frac{n\pi}{T}}. \tag{5.15}$$

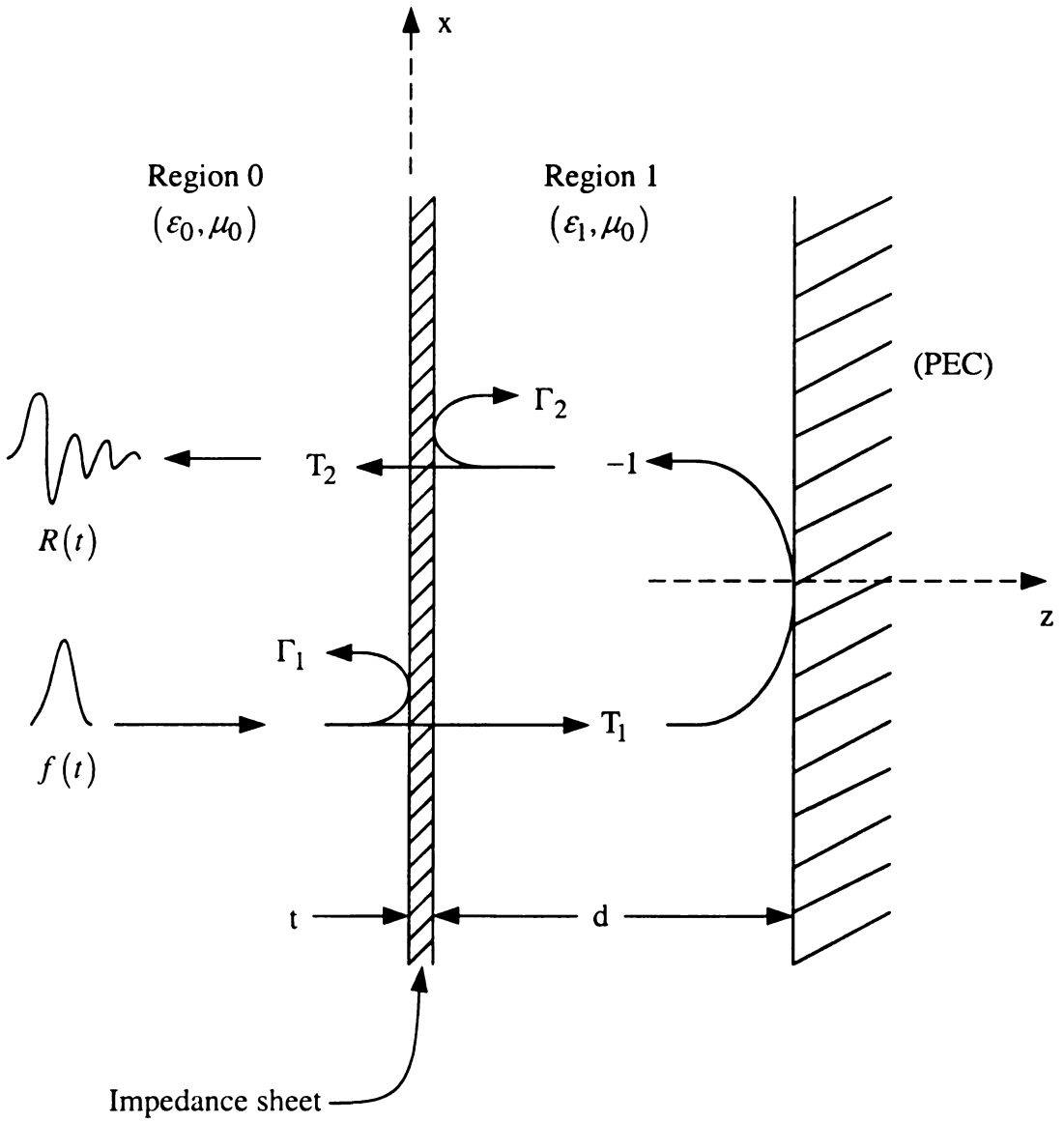

Figure 5-1 Layered material covered by impedance sheet.

5.2 Construction of the E-pulse

The current version the program EP.for does not implement the math in section 5.1 correctly and is unable to properly extract the natural frequencies and generate a correct E-pulse. In the interest of time, the E-pulse used to generate results in this chapter was generated heuristically.

Twenty-one layered materials with varying values of surface resistance were compared. IN each case region 1 is considered to be a foam layer with parameters of free space $(\varepsilon = \varepsilon_0, \mu = \mu_0, \sigma = 0)$. Table 5-1 shows the material properties of the impedance sheet for each layered material configuration. Material 'K', with a surface resistance of 377 $(\Omega / sq.)$, is considered the baseline material. The response waveform from material 'K' was used to generate the E-pulse and for comparison to determine changes in surface resistance. This baseline case is a Salisbury screen that produces a low reflected field at when the impedance sheet is located a quarter wavelength from the conductive backing, $d = \frac{\lambda}{4}$, or $f = 5.9\,GHz$. This is clearly seen in Figure 5-2 computed using MLPREF.for.

The purpose of the E-pulse is to give a zero result when it is convolved with a response waveform from which the E-pulse is generated. To get the correct E-pulse, first the ratio of consecutive reflections was determined. This ratio was used to determine the amplitudes of the E-pulse pulses. Each pair of consecutive reflections should have the same ratio, from (5.5), this ratio is seen to be $-\Gamma_2$. As an example, Figure 5-3 shows the time response for material 'K' with $f(t)$ resulting from windowing the frequency data generated by MLPREF.for using a Gaussian modulated cosine windowing function with

$\tau = 0.06\ ns$ and a center frequency of 0 GHz. In this figure, the ratio of reflection #2 to reflection #1 should be equal to the ratio of reflection #3 to reflection #2, and so on for each remaining pair. This ratio was determined to be, $-\Gamma_2 = 0.33$ for the baseline response. Therefore, an E-pulse with two pulses with amplitudes in this ratio was generated. The separation of the two pulses is equal to the separation of the reflections which again should be equal for each pair of reflections. This was determined to be 0.085 (ns) which is equal to twice the one-way transit time, T, through the layer. In order for the E-pulse to generate a zero late-time convolution the overlap area of each pulse with a reflection must cancel one another. Therefore, the second pulse of the E-pulse was made negative. The resulting E-pulse is shown in Figure 5-4. This E-pulse was convolved with the response waveform from each layered material configuration and the resulting EDNa were recorded.

Material	ε	μ	σ (S/m)	R_s (Ω/sq)	Impedance sheet thickness (mm)
A	ε_0	μ_0	400	50	0.05
B	ε_0	μ_0	200	100	0.05
C	ε_0	μ_0	133.3	150	0.05
D	ε_0	μ_0	100	200	0.05
E	ε_0	μ_0	80	250	0.05
F	ε_0	μ_0	66.7	300	0.05
G	ε_0	μ_0	57.1	350	0.05
H	ε_0	μ_0	55.6	360	0.05
J	ε_0	μ_0	54.1	370	0.05
K(baseline)	ε_0	μ_0	53.1	377	0.05
M	ε_0	μ_0	51.9	385	0.05
N	ε_0	μ_0	51.3	390	0.05
P	ε_0	μ_0	50	400	0.05
Q	ε_0	μ_0	44.4	450	0.05
R	ε_0	μ_0	40	500	0.05
S	ε_0	μ_0	36.4	550	0.05
T	ε_0	μ_0	33.3	600	0.05
U	ε_0	μ_0	30.8	650	0.05
V	ε_0	μ_0	28.6	700	0.05

Table 5-1 Material properties of impedance sheet.

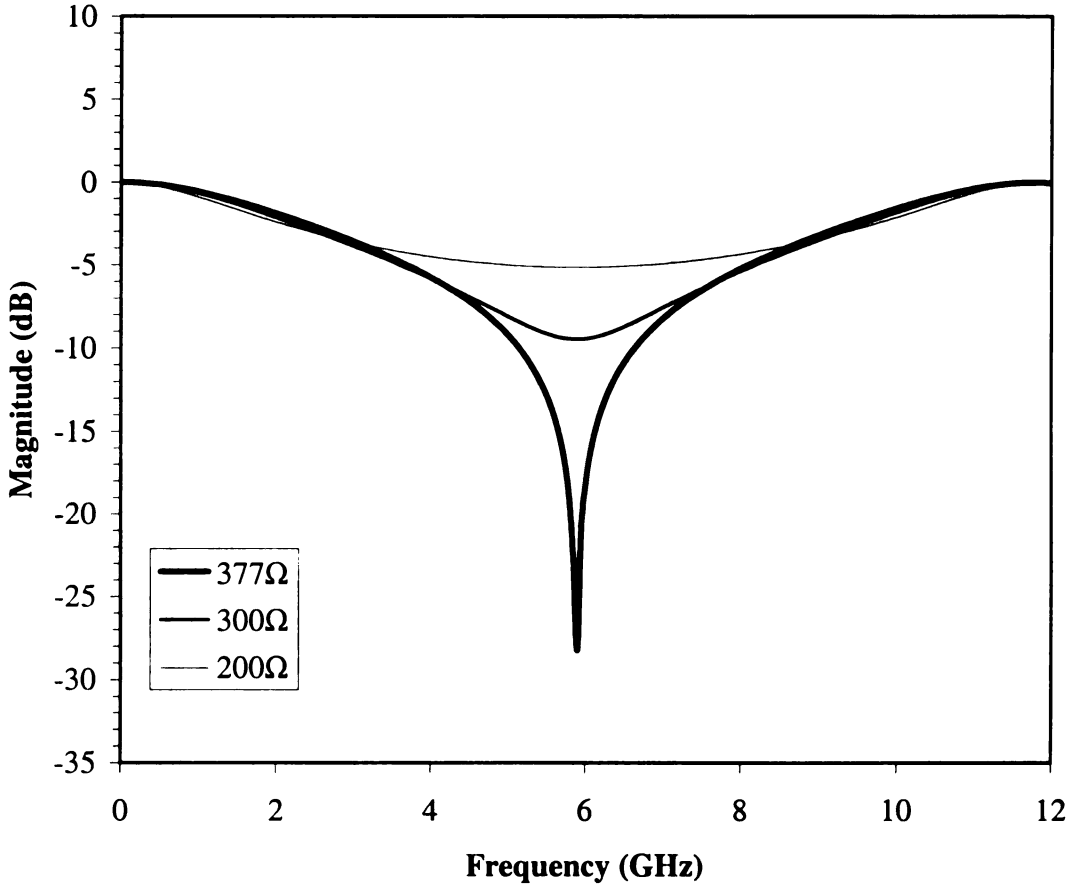

Figure 5-2 Frequency domain scattered response of Salisbury screen.

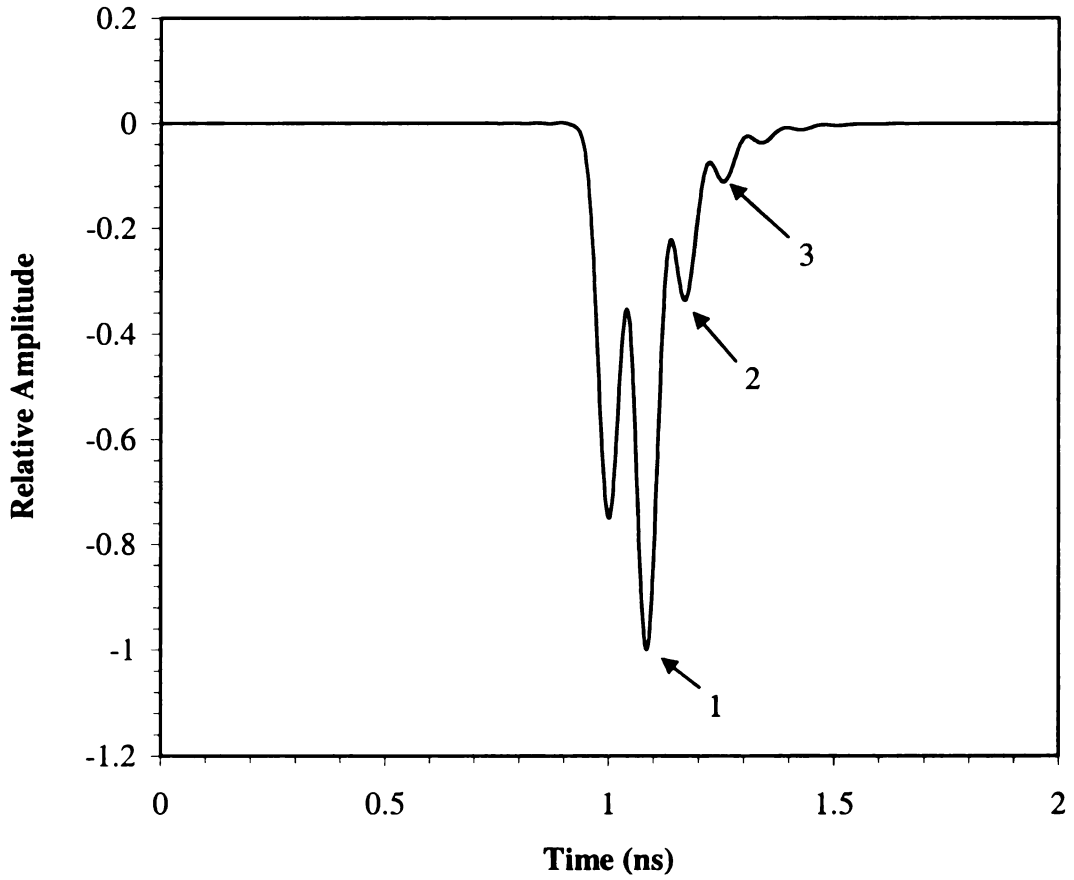

Figure 5-3 Response waveform for baseline material.

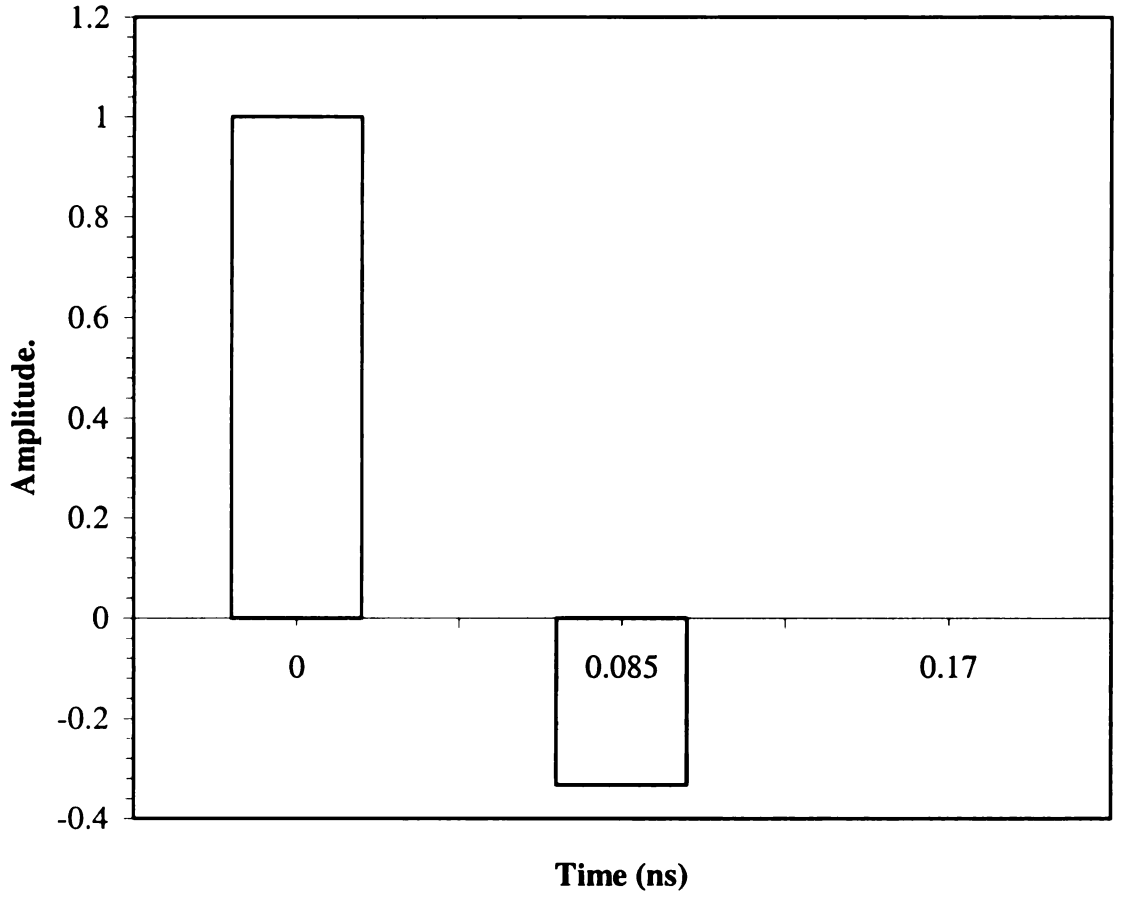

Figure 5-4 E-pulse generated for impedance sheet response.

5.2.1 Change in Surface Resistance

Of the twenty-one material configurations shown in Table 5-1, the response and convolution waveforms for five configurations will be shown as examples. The baseline material is material 'K' with a surface resistance, $R_s = 377\Omega$. The scattered response for this material is shown in Figure 5-3. In comparison, Figure 5-5 and Figure 5-6 show the extreme cases of change in surface resistance. Figure 5-5 shows the scattered response waveform for material 'A' with $R_s = 50\Omega$ and Figure 5-6 shows the waveform for material 'V' with $R_s = 700\Omega$. From (5.1), as the conductivity becomes smaller, the surface resistance becomes larger. It can be seen in Figure 5-5 that when the surface resistance is small (σ is large) the impedance sheet acts as a good conductor and reflects a large portion of the incident energy at the first reflection. This first large reflection is followed by many smaller reflections as the wave dies out. As seen in Figure 5-6, when the surface resistance is large (σ is small) the impedance sheet acts as a poor conductor and very little energy is reflected initially. Also, very little energy is confined within the space between the conductive backing and impedance sheet. Most of the energy is reflected off of the conductive backing which is seen in the second reflection of Figure 5-6. One can assume that the large difference between these responses and the baseline response will yield large differences in the EDNa values.

In contrast to the extreme changes in surface resistance, Figure 5-7 shows a comparison of the baseline response to the responses of material 'J' and 'M' which have minor changes in surface resistance, $R_s = 370\Omega$ and $R_s = 385\Omega$, respectively, from the baseline. As can be seen, these waveforms are very similar and nearly indistinguishable

from one another. It is expected that there will be little difference in the value of EDNa between these responses.

Using PCONV2.for, each of the responses for the materials listed in Table 5-1 were convolved with the constructed E-pulse and the EDNa was calculated from the late-time energy of the resulting convolution waveform. Figure 5-8 shows the convolution of material 'K', the baseline material, with the E-pulse. This can be compared to Figure 5-9, the convolution of material 'A' with the E-pulse, and Figure 5-10, the convolution of material 'V' with the E-pulse. It is evident that there is more late-time energy in the latter two convolutions, as expected. This difference in late-time energy is not evident in Figure 5-11 and Figure 5-12. These are the convolution waveforms for materials 'J' and 'M', respectively. No large difference in EDNa is discernable from these figures. For that matter, it would be a challenge even to determine which convolution was from the baseline material. To determine this, the EDNa values that were calculated are shown in Table 5-2. While there is little difference in the EDNa values between 'J', 'K', and 'M' one could easily determine which was the baseline material from these numbers. The EDNa values are plotted in Figure 5-13. This plot shows that the E-pulse does have the ability to discriminate changes in the surface resistance to a certain degree.

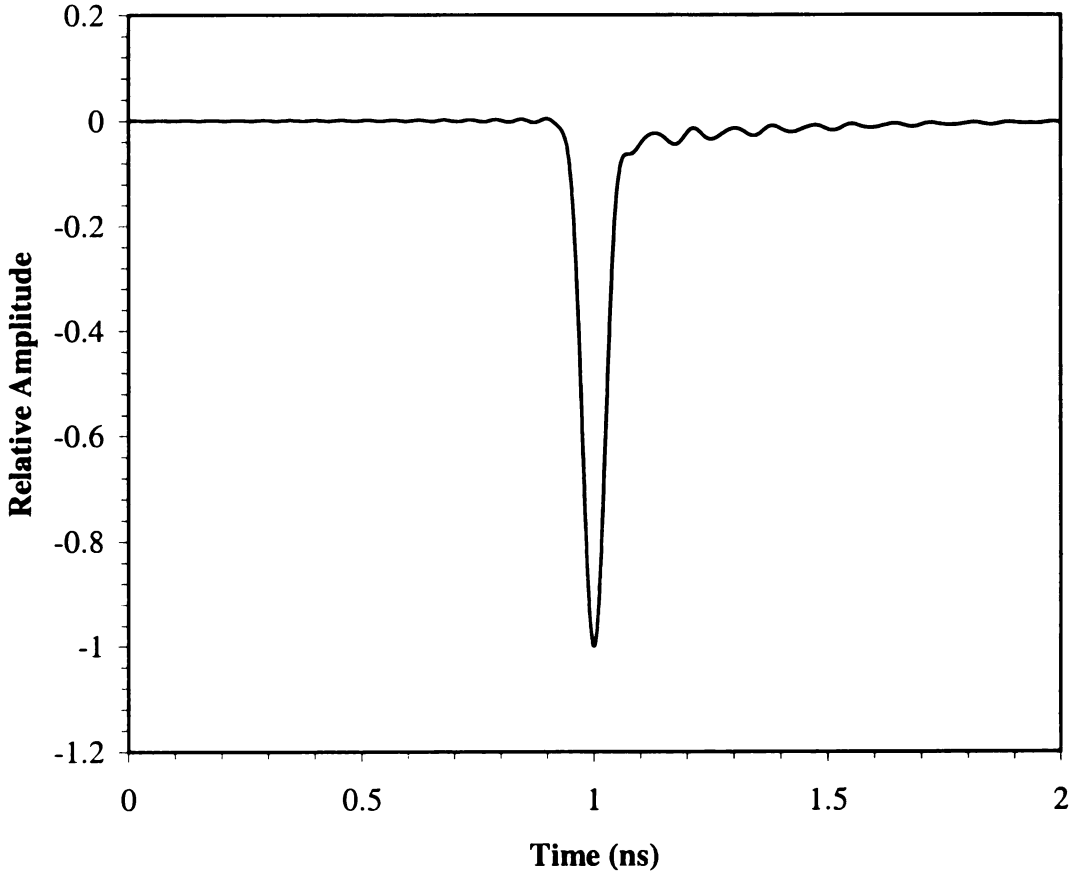

Figure 5-5 Response waveform from material 'A'.

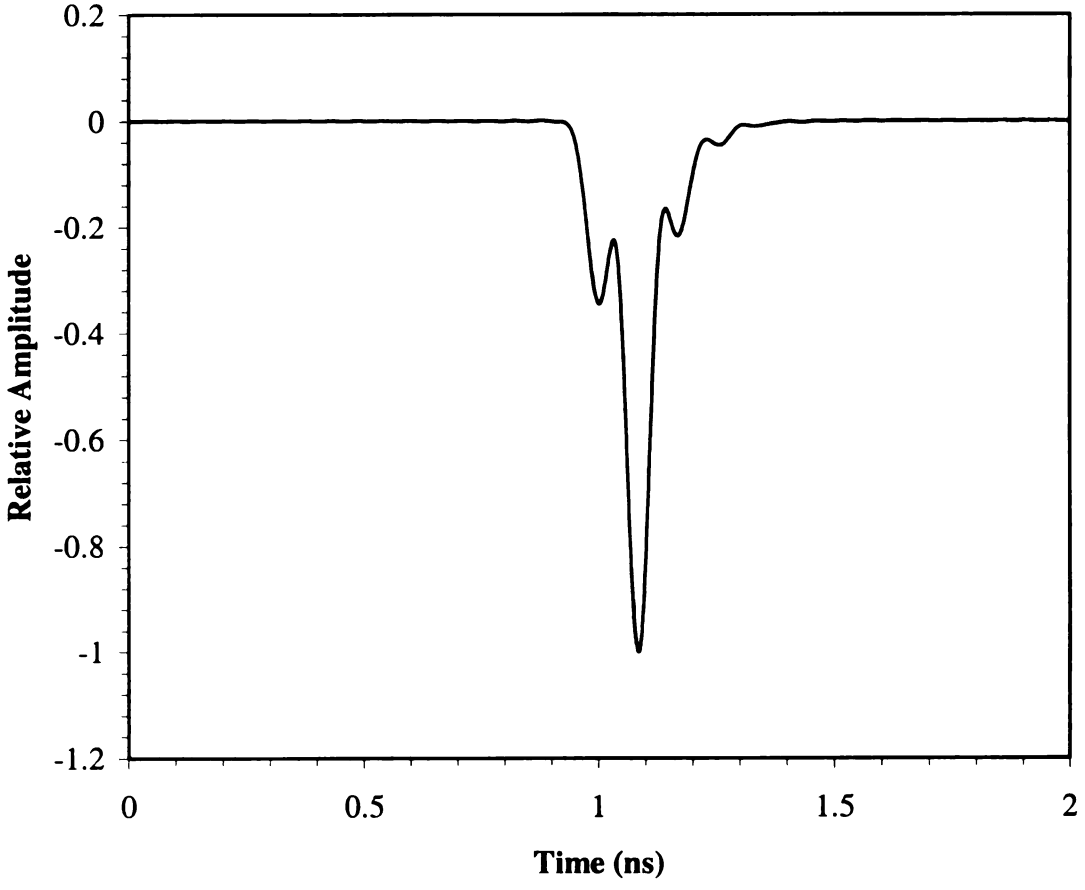

Figure 5-6 Response waveform from material 'V'.

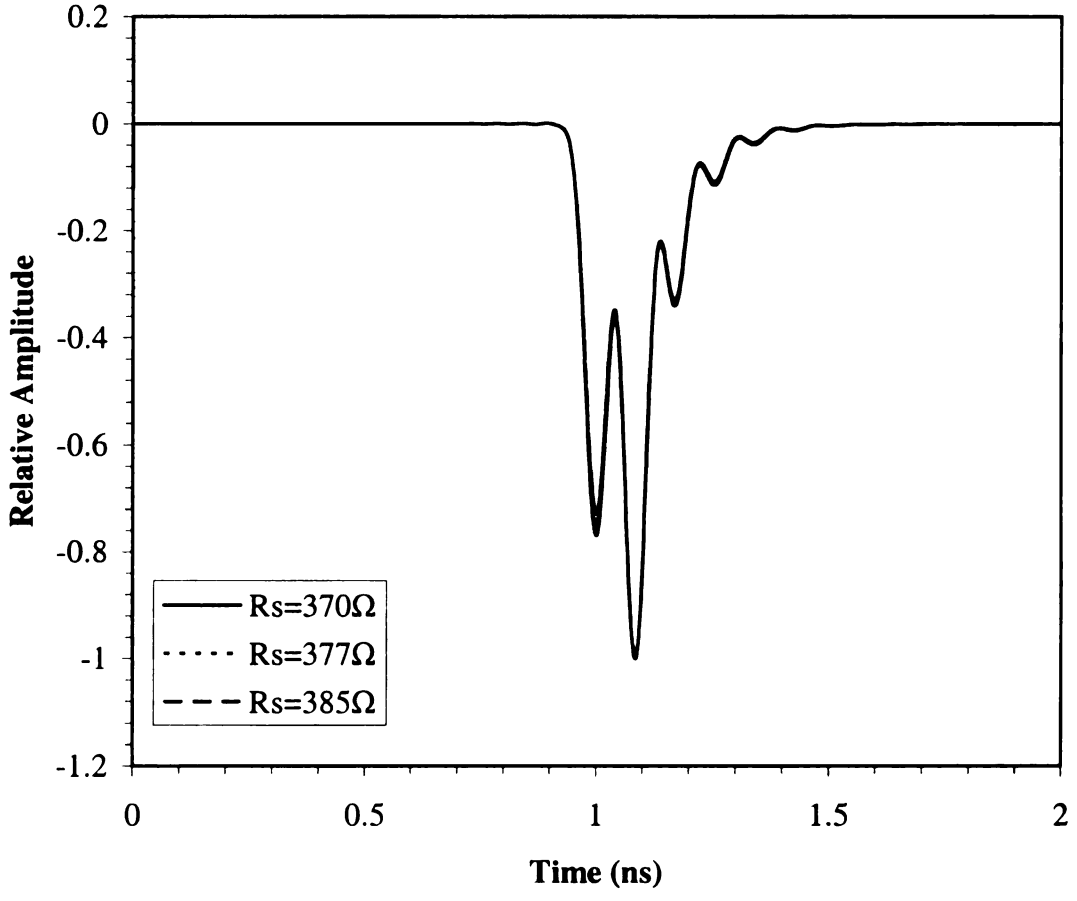

Figure 5-7 Comparison of response waveforms from materials 'J', 'K', and 'M'.

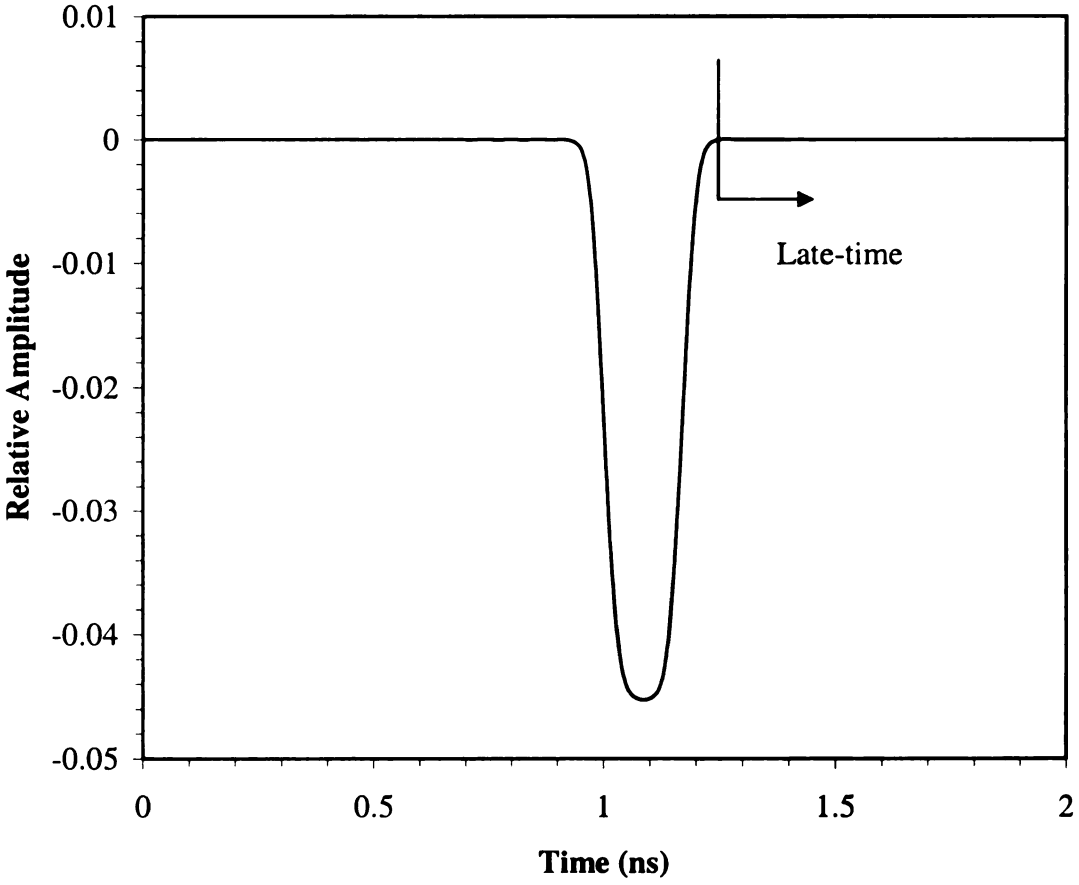

Figure 5-8 Convolution of response from material 'K' with the E-pulse.

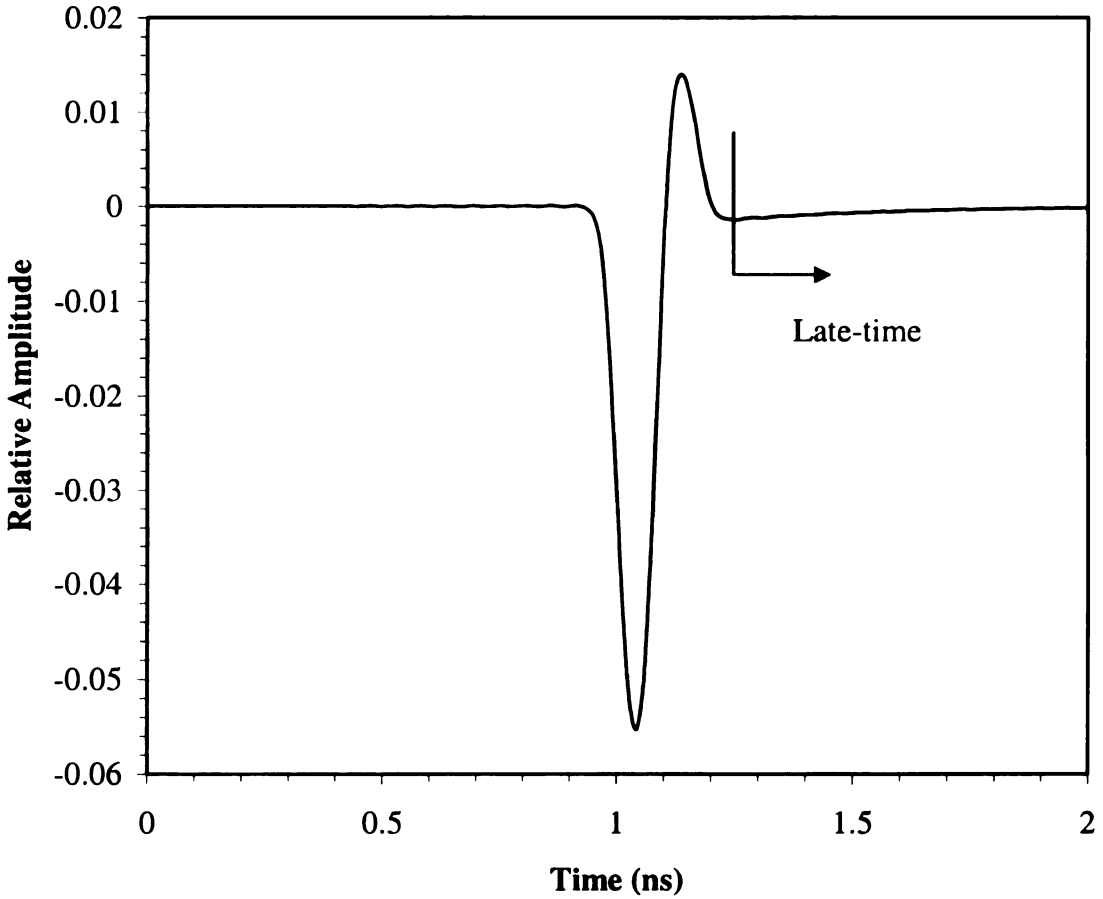

Figure 5-9 Convolution of response from material 'A' with the E-pulse.

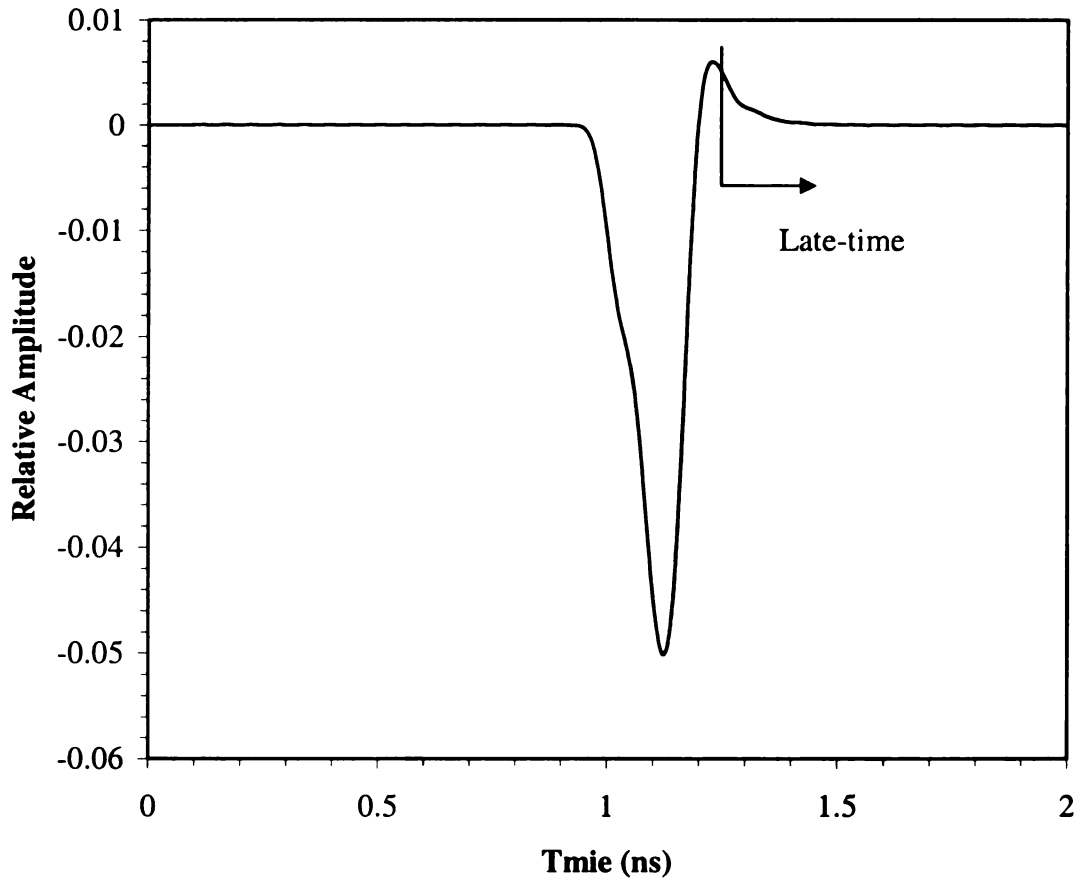

Figure 5-10 Convolution of response from material 'V' with the E-pulse.

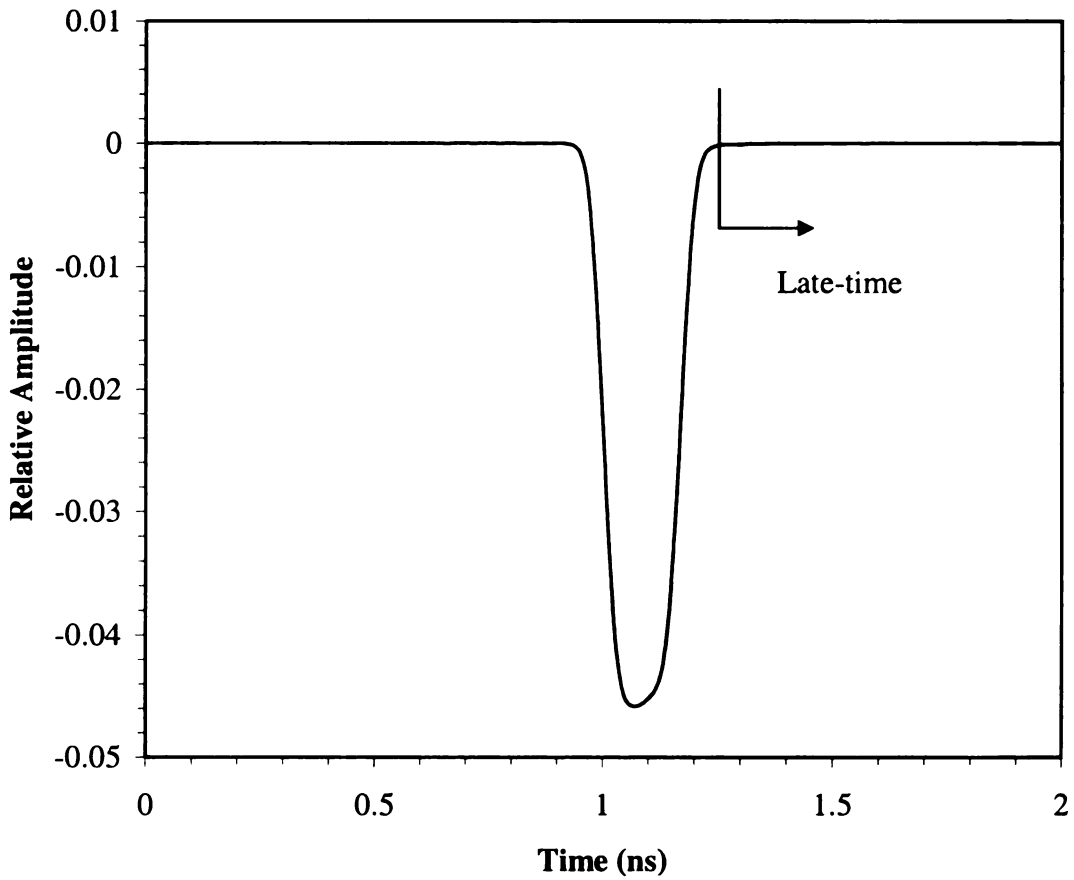

Figure 5-11 Convolution of response from material 'J' with the E-pulse.

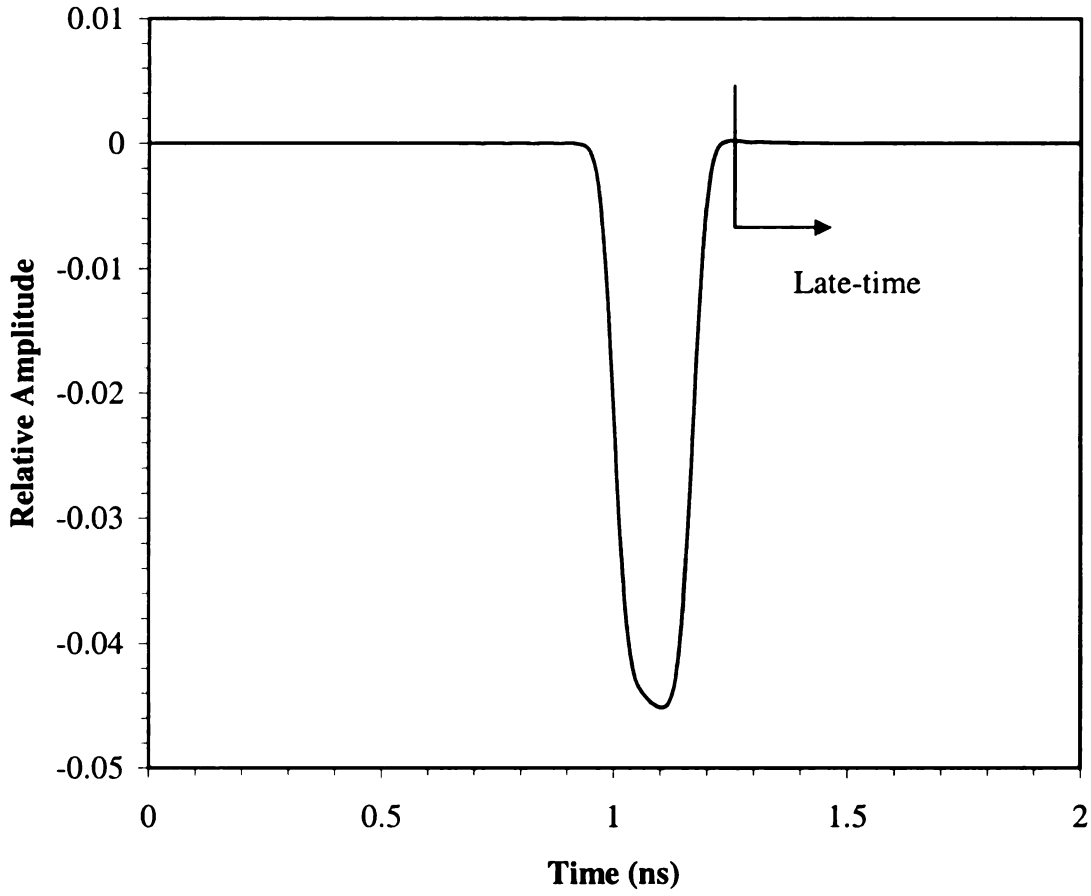

Figure 5-12 Convolution of response from material 'M' with the E-pulse.

Material	Surface Resistance, $R_s(\Omega/sq)$	EDNa
A	50	8.95E-05
B	100	2.28E-04
C	150	2.44E-04
D	200	1.73E-04
E	250	8.92E-05
F	300	3.00E-05
G	350	3.14E-06
H	360	1.17E-06
J	370	1.70E-07
K	377	1.34E-08
M	385	1.84E-08
N	390	7.18E-08
P	400	3.37E-07
Q	450	7.99E-07
R	500	2.28E-06
S	550	1.88E-05
T	600	4.55E-05
U	650	7.76E-05
V	700	1.12E-04

Table 5-2 EDNa for change in surface resistance of the impedance sheet.

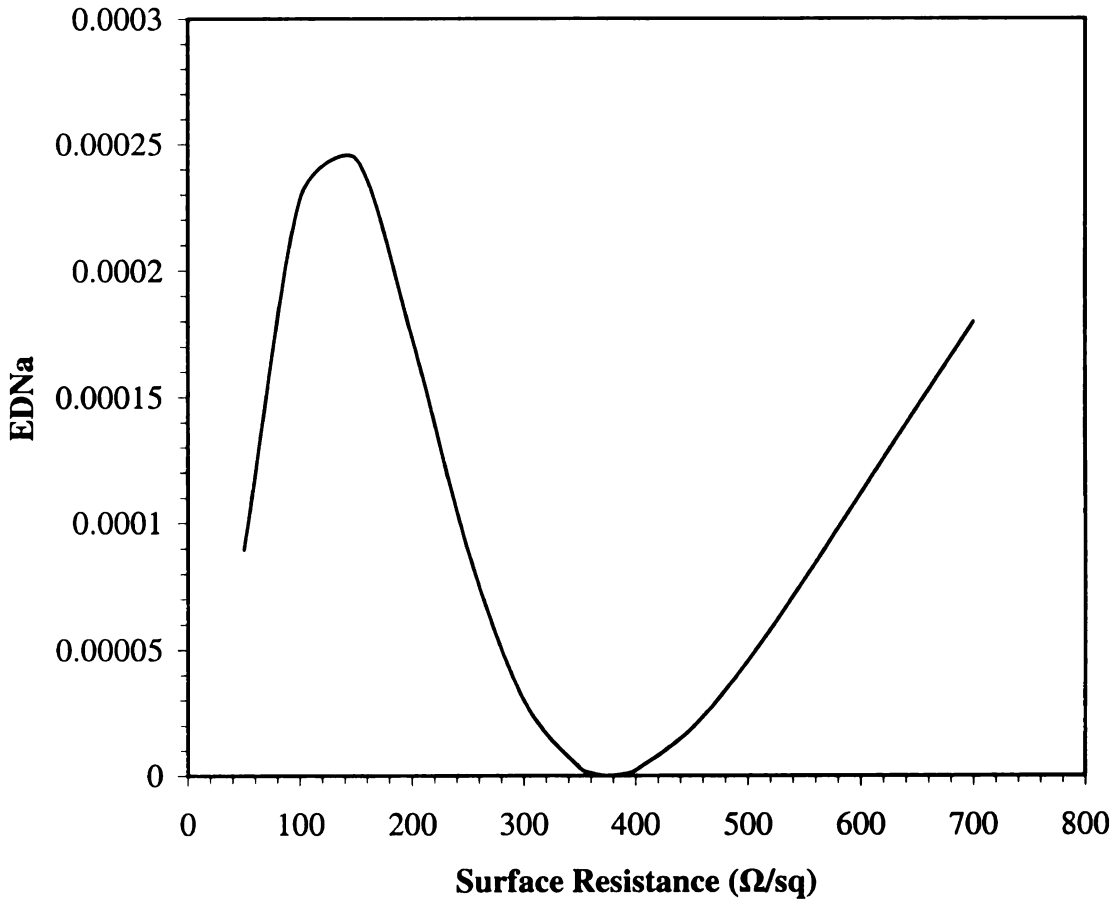

Figure 5-13 EDNa vs. surface resistance.

Chapter 6

Conclusion

6.1 Summary and Conclusions

This thesis has demonstrated the effectiveness of the E-pulse in detecting changes in the material properties of simple layered materials. Not only was the E-pulse effective for noise-free responses it was shown to be effective when the scattered responses were corrupted by noise. Many configurations of simple layered materials were investigated in this thesis. They included single lossless layered materials, single lossy layered materials, and a single lossless layered material with an impedance sheet. For the simple cases it has been shown that the E-pulse can be used for determining changes in certain properties. These properties included the layer thickness, relative permittivity, conductivity, and surface resistance of the impedance sheet.

Just as importantly, this thesis has demonstrated the ineffectiveness of the E-pulse for detecting changes in Magram material properties. The cause of failure of the E-pulse for the Magram material was due to the effective design of the material. Magram material is designed as a radar absorber, its purpose being to absorb the radiated energy of incident waves. Although the effect is somewhat narrow-band, the temporal response is primarily specular, and lacks the multiple reflections needed for useful E-pulse discrimination.

It has also been shown that the angle of incidence and the polarization of the incident field do not adversely effect the E-pulse technique. One important practical

issue addressed in this thesis was the effect of noise on the E-pulse technique. It was shown that for moderate levels of noise the EDRa is very effective tool in quantifying the late-time energy. .

6.2 Future Work

Some ideas to consider for future research include determining the effectiveness of the E-pulse in determining changes in material properties for multiple layered materials. The impedance sheet layered material can be investigated for changes in the thickness of the impedance sheet and for changes in the thickness of the layer itself. A combination of the multiple layer and the impedance sheet can be considered. Some work has been done with a Salisbury screen covered by a loaded core. One last area to be investigated would be the use of statistical decision theory in combination with the E-pulse to help determine changes in material properties in the presence of significant levels of noise.

APPENDICES

A. Overview – NAT_FREQ.cpp

This program determines the natural frequencies of a layered material given the material properties. The material properties given as inputs are the thickness, the relative permittivity and the angle of incidence. The user can define the number of frequencies to calculate and write them to a file.

A.1 Source Code – NAT_FREQ.cpp

```
//*********************************************************************
// Garrett J Stenholm
// Date: 6/7/01
// Name: nat_freq
//
// Purpose: This program will determine the natural frequencies of a single layer,
conductor backed slab
//
// Input:       Slab thickness, t
//              Material dielectric constant, Er
//              Angle of incidence, Qi
//              User defined filename for output, file
//              Number of frequencies to calculate, num_freq
//
// Output: A file with the natural frequencies written in a two column, num_freq rows
format
//
//*********************************************************************

#include <fstream>
#include <iomanip>
#include <iostream>
#include <cmath>
#include <valarray>

using namespace std;
```

```
char file[30], answer;
ifstream in, exist;
ofstream out;
int num_freq, check=1;
double thickness, epsilon_r, inc_angle, tau, gamma, sigma;
const double c=2.998e8, pi=3.14159265359;

void main()
{
// user input
        cout << "\nEnter the slab thickness (in mm): ";
        cin  >> thickness;
        thickness = thickness * 1e-3;
        cout <<         "\nEnter the dielectric constant: ";
        cin  >> epsilon_r;
        cout << "\nEnter the angle of incidence: ";
        cin  >> inc_angle;
        cout << "\nEnter the number of frequencies to calculate: ";
        cin  >> num_freq;
        valarray<double> omega(num_freq);

// calculate natural frequencies
        // calculate tau
        tau = (2 * thickness * sqrt(epsilon_r - pow( sin(inc_angle),2) )) / c;

        // calculate gamma
        gamma = (sqrt(1 - pow(sin(inc_angle),2) ) - sqrt(epsilon_r -
        pow(sin(inc_angle),2) )) / ( sqrt(1 - pow(sin(inc_angle),2) ) + sqrt(epsilon_r -
        pow(sin(inc_angle),2) ) );

        // calculate sigma
        if(gamma<0)
        {
        gamma = gamma * -1;
        }
        sigma = (1/tau)*log(gamma);
        // calculate omega
        for(int n=0; n<=num_freq-1; n++)
        {
        omega[n] = ((2*n+1)*pi)/tau;
        }

// write frequencies to file

        // check for existing file and open file
        while(check==1)
```

```
        {
        cout << "\nEnter the name of the output file: ";
        cin  >> file;
        exist.open(file);
        if(exist.good())
                {
                cout << "\nThis file already exist, do you want to overwrite(y/n)? ";
                cin >> answer;
                if(answer=='y')
                {
                check=0;
                exist.close();
                exist.clear();
                out.open(file);
                }
                else
                {
                check=1;
                exist.close();
                exist.clear();
                }
                }
                else
                {
                check=0;
                exist.close();
                exist.clear();
                out.open(file);
                }
        }

// write to file
        for(int i=0; i<=omega.size()-1; i++)
        {
        out << fixed << showpoint << setprecision(3);
        out << sigma*1e-9 << " " << omega[i]*1e-9 << endl;
        }

        // close file
        out.close();
}
```

B. Overview – KPNAT.for

This program generates a natural E-pulse from the natural frequencies. The program reads the natural frequencies from a data file and outputs an E-pulse to a file.

B.1 Source Code - KPNAT.for

```
  program kpnat
    parameter (mmx=15, nmx=32)
c
    character*30 fnm, ftype
    real b(nmx), diag(nmx)
    integer ipvt(nmx)
c
    common /sfill/ a(nmx,nmx), nmodes, nb, dt, iexcit, nexcit, idc
    common /freqs/ qm(mmx), sg(mmx)
c
    pi = 4.*atan(1.)
c
    write(*,*) '*****************************************************'
    write(*,*) '**  Program : KPNAT.FOR                        **'
    write(*,*) '**                                             **'
    write(*,*) '**  Purpose : Construct natural E/S Pulse from  **'
    write(*,*) '**          natural frequencys.                **'
    write(*,*) '**                                             **'
    write(*,*) '**  Update : March 19, 1991                     **'
    write(*,*) '**                                             **'
    write(*,*) '**  Programmers : Dr. E.J. Rothwell            **'
    write(*,*) '**               Ponniah Ilavarasan            **'
    write(*,*) '**               John E. Ross III              **'
    write(*,*) '*****************************************************'
    write(*,*)
c
    write(*,*) 'Natural frequency file name ?'
    read (*,5) fnm
 5  format(a)
c
    call rdfrq(fnm, n)
    nmodes = n
c
    write(*,*) 'Enter option # :'
    write(*,*) '  0. E-pulse'
    write(*,*) '  1. Sine S-pulse'
    write(*,*) '  2. Cosine S-pulse'
```

```
      write(*,*) '  3. Combined S-pulse'
      read(*,*) iexcit
c
      nexcit = 0
      if(iexcit .eq. 0) goto 200
c
c  Display modes
c
      write(*,*) '*******************************************'
      write(*,*) '       #       sigma          omega'
       do 195 i = 1, nmodes
       write(*,*) i, sg(i), qm(i)
 195  continue
      write(*,*) '*******************************************'
c
      write(*,*) 'Enter number of mode to excite'
      read(*,*) nexcit
      sigma = sg(nexcit)
      omega = qm(nexcit)
c
 200  write(*,*) 'Kill dc (1=y 0=n) ?'
      Read(*,*) idc
c
c  Find highest frequency given
c
      imode = 1
      qmmax = qm(imode)
      do 205 i = 1, nmodes
       if(qm(i).gt.qmmax) then
        qmmax = qm(i)
        imode = i
       endif
 205  continue
c
c  Set degeneracy of modes (ie number of multiple modes)
c  No degeneracy if mmode = 1.
c
      mmode = 1
c
c  Calculate time interval and number of basis functions
c
      dt = mmode*pi/qm(imode)
      nb = 2*nmodes-1
      if(iexcit .eq. 0) nb = nb+1
      if(iexcit .eq. 3) nb = nb-1
      if(idc .eq. 1) nb = nb+1
```

```
c
      call fill
c
      nsize = nb-1
      istart = imode
      if(iexcit .eq. 2 .or. iexcit .eq. 3) istart = istart-1
      do 100 i = istart, nsize
        do 90 j = 1, nb
          a(i,j) = a(i+1,j)
 90     continue
 100  continue
c
      do 110 n = 1, nb
        b(n) = -a(n,nb)
 110  continue
c
      call decomp(nsize,a,ipvt,diag)
      call solve(nsize,a,ipvt,b)
      b(nb) = 1.
c
      call normal(b,nb,dt,iexcit,nexcit)
c
      pdur = dt*float(nb)
c
      write(*,*)
      write(*,*) 'Pulse duration = ',pdur
      write(*,*) 'Number of basis functions = ',nb
      dtpul = pdur / nb
      write(*,*) '        #         Amplitude'
c
      do 210 i = 1, nb
        write(*,*) i, b(i)
 210  continue
c
      if(nexcit.eq.0) ftype = 'Time'
      if(nexcit.ne.0) ftype = 'Spulse'
c
      write(*,*) 'Filename for results'
      read(*,5) fnm
c
      call wrdata(fnm,ftype,dtpul,nb,sigma,omega,b)
c
      end
c
c--------------------------------------------------------------------------
c
```

```
c  RDFRQ - Reads in the natural frequencies from a disk file.
c
      subroutine rdfrq(fnm, nmodes)
      parameter (lun=10, mmx=15)
c
      character*30 fnm
c
      common /freqs/ qm(mmx), sg(mmx)
c
      open (unit=lun, file=fnm, status='old')
c
      i = 1
 10   read(lun,*,end=99,err=999) sg(i), qm(i)
      i = i + 1
      goto 10
c
 99   nmodes = i-1
      close(lun)
      return
c
 999  write(*,*) '***  Error in RDFRQ ***'
      close(lun)
      stop
c
      end
c
c-------------------------------------------------------------------------
c
c  WRDATA - writes data to disk in ndf format
c
      subroutine wrdata(fnm,ftype,dt,np,sigma,omega,b)
      parameter (lun=10, nmx=32)
c
      character*30 fnm, ftype
      real b(nmx)
c
      open(lun, file=fnm, status='unknown')
c
      write(lun,5) ftype
 5    format (a)
c
      if (ftype.eq.'Spulse') write(lun,*) sigma, omega

      write(lun,5) '0.0'
c
      write(lun,*) dt
```

```
c
      do 20 i = 1, np
 20     write(lun,*) b(i)
c
      close(lun)
      return
c
      end
c
c-------------------------------------------------------------------------
c
c  FILL - Fills the coefficient matrix
c
      subroutine fill
      parameter (mmx=15, nmx=32)
c
      common /sfill/ a(nmx,nmx),nmodes,nb,dt,iexcit,nexcit,idc
      common /freqs/ qm(mmx),sg(mmx)
c
      nm2 = 2*nmodes
      do 110 n = 1,nmodes
        do 100 m =1, nb
          tl = float(m-1)*dt
          tu = tl + dt
          a(n,m) = rcos(n,tu) - rcos(n,tl)
          a(n+nmodes,m) = rsin(n,tu) - rsin(n,tl)
 100    continue
 110  continue
c
      if(iexcit .eq. 0) goto 500
      if(iexcit .eq. 2) goto 190
c
      nr = nmodes + nexcit
      nt = nm2 - 1
      do 150 n = nr, nt
        do 140 m = 1, nb
          a(n,m) = a(n+1,m)
 140    continue
 150  continue
c
 190  if(iexcit .eq. 1) goto 500
c
      nr = nexcit
      nt = nm2 - 1
      do 250 n = nr, nt
        do 240 m = 1, nb
```

```
        a(n,m) = a(n+1,m)
 240    continue
 250  continue
c
 500  if(idc .eq. 0) goto 600
c
      do 520 m = 1, nb
       a(nb,m) = 1.
 520  continue
c
 600  return
      end
c
c-------------------------------------------------------------------------
c
c  RSIN - Evaluate integral of exp(x)*sin(x)
c
      real function rsin(n,x)
      parameter (mmx=15, nmx=32)
c
      common /freqs/ qm(mmx) ,sg(mmx)
c
      rsin  = exp(-sg(n)*x)*(-sg(n)*sin(qm(n)*x) - qm(n)*cos(qm(n)*x))
c
      return
      end
c
c-------------------------------------------------------------------------
c
c  RCOS - Evaluate integral of exp(x)*sin(x)
c
      real function rcos(n,x)
      parameter (mmx=15, nmx=32)
c
      common /freqs/ qm(mmx) ,sg(mmx)
c
      rcos  = exp(-sg(n)*x)*(-sg(n)*cos(qm(n)*x) + qm(n)*sin(qm(n)*x))
c
      return
      end
c
c-------------------------------------------------------------------------
c
c  NORMAL - normalizes E-Pulses
c
      subroutine normal(b,nb,dt,iexcit,nexcit)
```

```
      parameter (nmx=32)
c
      real b(nmx)
c
      if((iexcit .eq. 0).or.(iexcit.eq.3)) goto 500
c
      rnorm = 0.
      do 50 l = 1, nb
        tl = float(l-1)*dt
        tu = tl + dt
        if(iexcit .eq. 2) rnorm = rnorm+b(l) *
     &       (rcos(nexcit,tu) - rcos(nexcit,tl))
        if(iexcit .eq. 1) rnorm = rnorm+b(l)*
     &      (rsin(nexcit,tu) - rsin(nexcit,tl))
 50   continue
c
      do 100 l = 1, nb
        b(l) = b(l)/rnorm
 100  continue
c
 500  return
      end
c
c-------------------------------------------------------------------------
c
c SOLVE - solves matrix eqn ax=b with decomposed by decomp

      subroutine solve(n,a,ipvt,b)
      parameter (nmx=32)
c
      integer n,ipvt(nmx)
      integer nm1,k,kb,kp1,km1,m,i
      reala(nmx,nmx),b(nmx),s
c
c  Forward elimination
c
      if (n.eq.1) goto 30
      nm1 = n - 1
      do 10 k = 1, nm1
        kp1 = k + 1
        m = ipvt(k)
        s = b(m)
        b(m) = b(k)
        b(k) = s
        do 10 i = kp1, n
 10       b(i) = b(i) + a(i,k)*s
```

```
c
c  Back substitution
c
      do 20 kb = 1, nm1
        km1 = n - kb
        k = km1 + 1
        b(k) = b(k)/a(k,k)
        s = -b(k)
        do 20  i = 1, km1
 20       b(i) = b(i) + a(i,k)*s
c
 30   b(1) = b(1)/a(1,1)
c
      return
      end
c
c-------------------------------------------------------------------------------
c
c  DECOMP - decomposes matrix a to triangular form
c  From : Linear Algebra by Gilbert Strang
c
      subroutine decomp(n,a,ipvt,diag)
      parameter (nmx=32)
c
      integer n, ipvt(nmx)
      integer nm1, i, j, k, kp1, m
      real a(nmx,nmx), diag(nmx)
      real p, t
c
      ipvt(n) = 1
      if (n .eq. 1) Go to 70
      nm1 = n-1
c
      do 60 k = 1, nm1
        kp1 = k+1
c
c  Find pivot p
c
        m = k
        do 10 I = kp1, n
 10       if (abs(a(i,k)) .gt. abs(a(m,k))) m = i
        ipvt(k) = m
        if (m .ne. k) ipvt(n) = -ipvt(n)
        p = a(m,k)
        a(m,k) = a(k,k)
        a(k,k) = p
```

```
      diag(k) = p
      if (p .eq. 0.0) goto 60
c
c  Compute mutipliers
c
 20    do 30 i = kp1, n
 30      a(i,k) = -a(i,k)/p
c
c  Interchange rows and columns
c
      do 50 j = kp1, n
        t = a(m,j)
        a(m,j) = a(k,j)
        a(k,j) = t
        if (t .eq. 0.0) goto 50
        do 40 i = kp1, n
          a(i,j) = a(i,j) + a(i,k)*t
 40       continue
 50     continue
 60   continue
c
 70   diag(n) = a(n,n)*float(ipvt(n))
c
     return
     end
c
c-------------------------------------------------------------------------------
c
```

C. Overview – PCONV2.for

This program is the program which does most of the work when using the E-pulse technique. It convolves the scattered response waveforms with the E-pulses. It gives the user the ability to either use noise-free response signals or add noise to the signal. It outputs the value of the EDNa and writes the convolution waveform to a file.

C.1 Source Code – PCONV2.for

```
  PROGRAM PCONV2
C
C  PERFORMS TRAPEZOIDAL RULE CONVOLUTION OF DATA SET
C  AND PULSE FUNCTION BASED E-PULSE
```

```
C
C  VERSION OF 29 May 2001
C       Revised by Garrett J Stenholm
C
      REAL hah(2050,2050)
          REAL H(2050,2050) ,T(2050), AN(2050), EDNA(512), SNR(512), Er
          REAL ED(32), EPS(32), th(32), ang(32), TEMP1(32), TEMP2(32), d, ai
      CHARACTER*32 FILENAM, dummy, NOISE1, NOISE2, temp, EPULSE,
RESPON
          character*32 filnam(20), filnamc(20), COMMA, array
          CHARACTER*32 FILE, blah
          integer in, FILES, CH, pos, size, file_flag, update, element
C
      COMMON /BLOCK1/ RM(2050),B(2050),DT,DLT,AL(50),NP
      COMMON /BLOCK2/ CON(2050),TCON(2050),DTC
C
          IJ=1
          in    = 500
          FILES  = 1
c         EPULSE = 'epuls10h.ndf'
c         RESPON = 'resp10h.ndf'
c         Ttr   = 0.1
c         Tp    = 0.1
c         Tb    = 0.5
          NC    = 250
c         INOISE = 1

Ccccccccccccccccccccccccccccccccccccccccccccccccccc
C  Create files for (response + noise) signal
Ccccccccccccccccccccccccccccccccccccccccccccccccccc
          filnam(1) = 'r'
          filnam(2) = 'respb.dat'
          filnam(3) = 'respc.dat'
          filnam(4) = 'respd.dat'
          filnam(5) = 'respe.dat'
          filnam(6) = 'respf.dat'
          filnam(7) = 'respg.dat'
          filnam(8) = 'resph.dat'
          filnam(9) = 'respi.dat'
          filnam(10) = 'respj.dat'

          filnamc(1) = 'c'
          filnamc(2) = 'convb.dat'
          filnamc(3) = 'convc.dat'
          filnamc(4) = 'convd.dat'
          filnamc(5) = 'conve.dat'
```

```
        filnamc(6) = 'convf.dat'
        filnamc(7) = 'convg.dat'
        filnamc(8) = 'convh.dat'
        filnamc(9) = 'convi.dat'
        filnamc(10) = 'convj.dat'
C
    WRITE (*,*) 'ENTER NAME OF E-PULSE FILE (.ndf)'
    READ  (*,1) EPULSE
 1   format(a)
    OPEN (10,FILE=EPULSE,STATUS='UNKNOWN')
C
    read  (10,1) dummy
    read  (10,*) start
    read  (10,*) dd
    np=1
5     READ  (10,*,end=10) AL(np)
    np=np+1
    go to 5
10   np=np-1
    write (*,*) 'no. pulses=',np
    tk=np*dd
    write (*,*) 'tk=',tk
    CLOSE (10)

Ccccccccccccccccccccccccccccccccccccccccccccccccccccccccccccccccc
C       Determine the energy in the E-pulse
Ccccccccccccccccccccccccccccccccccccccccccccccccccccccccccccccccc
        Ee=0
        do 11 J=1,np
        Ee=Ee+dd*(AL(J)**2)
11      continue
        write (*,*) 'E-pulse energy =',Ee
        print 1
C
    SIZE  = 1.
    WRITE (*,*) 'ENTER NAME OF RESPONSE FILE (.ndf)'
    READ  (*,1) RESPON
    OPEN (10,FILE=RESPON,STATUS='UNKNOWN')
C
    read (10,1) dummy
    read (10,*) start
    READ(10,*) DT
    I = 1
15   READ(10,*,END=20) H(1,I)
        T(I) = FLOAT(I-1)*DT
    I = I+ 1
```

```
      GO TO 15
20    NPTS = I-1
      WRITE(*,*) 'NPTS = ',NPTS
      CLOSE (10)

Ccccccccccccccccccccccccccccccccccccccccccccccccccccc
C  Determine the energy in the response file
Ccccccccccccccccccccccccccccccccccccccccccccccccccccc
        Er=0
        do 21 I=1,NPTS
        Er=Er+DT*(H(1,I)**2)
21      continue

Ccccccccccccccccccccccccccccccccccccccccccccccccccccccccccccccccccccccccccccc
C  Enter times to determine the late-time,TL, for convolution energy calculation
Ccccccccccccccccccccccccccccccccccccccccccccccccccccccccccccccccccccccccccccc
        write (*,*) 'Enter the one-way transit time: '
        read  (*,*) Ttr
        write (*,*) 'Enter timee delay: '
        read  (*,*) Tb
        write (*,*) 'Enter pulse width: '
        read  (*,*) Tp

Cccccccccccccccccccccccccccccccccccc
C  ADD NOISE IF DESIRED
Cccccccccccccccccccccccccccccccccccc
      WRITE(*,830)
 830  FORMAT(1X,'ADD NOISE?(1=Y 0=N):' $)
      READ(*,*) INOISE

Ccccccccccccccccccccccccccccccccccccccccccccccccccccccccccccccccccccccccccccc
C  Calculate 99% of energy in noise-free signal and re-determine the number of points
Ccccccccccccccccccccccccccccccccccccccccccccccccccccccccccccccccccccccccccccc
        if(INOISE .EQ. 1) then
         alimit=Er
         S=0
         K=0
 34      K=K+1
         S=S+DT*(H(1,K)**2)
         if(S .LT. alimit) goto 34
         NPTS=K
        endif

        write(*,*) 'alimit= ',alimit
        write(*,*) 'S= ',S
        write(*,*) 'NPTS= ',NPTS
```

```
C       WRITE (*,*) 'ENTER NO. PTS IN CONVOLUTION:'
C    READ(*,*) NC
C
     DLT = TK/FLOAT(NP)
     T1  = T(1)

Cccccccccccccccccccccccccccccccccccccccccccccccccccccccccccccccccc
C  SHIFT ORIGIN OF RESPONSE
Cccccccccccccccccccccccccccccccccccccccccccccccccccccccccccccccccc
     DO 30 I= 1,NPTS
      T(I)  = T(I)-T1
 30   CONTINUE

          IF (INOISE .EQ. 1) THEN
           write(*,*) 'Enter the desired SNR: '
           read(*,*) SR
           db=SR/10

Cccccccccccccccccccccccccccccccccccccccccccccccccccccccccccccccccc
C  Calculate the variance and standard deviation to
C  determine noise energy based on the response signal energy
Cccccccccccccccccccccccccccccccccccccccccccccccccccccccccccccccccc
           W=NPTS*DT
           var=Er/(W*(10**db))
           sigma=sqrt(var)

Cccccccccccccccccccccccccccccccccccccccccccccccccccccccccccccccccc
C  Add noise to the response signal and create 'in' number of samples
C  'seed' is the starting point for determining the random numbers used
C  to simulate gaussian noise
Cccccccccccccccccccccccccccccccccccccccccccccccccccccccccccccccccc
          WRITE(*,840)
 840  FORMAT(1X,'ENTER RANDOM DECIMAL SEED:' $)
        READ(*,*) SEED

          OPEN (30,FILE="temp.dat",STATUS='UNKNOWN')
          DO 53 IJ=1,in
           DO 50 I= 1,NPTS
            AN(I) = sigma*GAUSRV(SEED)
            hah(I,IJ)=AN(I)
            WRITE (30,*) hah(I,IJ)
            l=IJ+1
       H(l,I)  = H(1,I) + AN(I)
 50    CONTINUE
```

```
Ccccccccccccccccccccccccccccccccccccccccccccccccccccccccccccccccc
C  Calculate the noise energy and SNR calculated
C   from the generated random noise
Ccccccccccccccccccccccccccccccccccccccccccccccccccccccccccccccccc
        En=0
        do 710 J=1,NPTS
        En=En+DT*(AN(J)**2)
 710    continue
        SNR(IJ)=10*log10((S/En))
C       write (*,*) IJ,' Actual SNR= ', snr

Ccccccccccccccccccccccccccccccccccccccccccccccccccccccccccccccccc
C   Write the first 10 new noise-corrupted response signals to files
ccccccccccccccccccccccccccccccccccccccccccccccccccccccccccccccccc
        IF(IJ .LT. FILES+1) THEN
        OPEN (10,FILE=filnam(IJ),STATUS='UNKNOWN')
        DO 52 I= 1,NPTS
        WRITE (10,*) T(I), H(IJ+1,I)
 52     CONTINUE
        CLOSE(10)
    ENDIF
C
 53  CONTINUE
        CLOSE(30)
C
        ENDIF

Ccccccccccccccccccccccccccccccccccccccccccccccccccccccccccccccccc
C   CALCULATE LINEAR INTERPOLATION COEFICIENTS
Ccccccccccccccccccccccccccccccccccccccccccccccccccccccccccccccccc
        if(INOISE .EQ. 0) in=1
c       do 65 IJ=1,1
35   NPTSM1 = NPTS-1
    DO 60 I= 1,NPTSM1
     RM(I) = (H(1,(I+1))-H(1,I))/DT
     B(I)  = H(1,I)-RM(I)*FLOAT(I-1)*DT
60   CONTINUE
C
    TS    = 0.
    TE    = T(NPTS-1)
    DTC   = (TE-TS)/FLOAT(NC-1)
    TT    =TS

    DO 70 I= 1,NC
     TCON(I) = TT
     CON(I)  = R(TT)
```

```
      TT    = TT+DTC
70    CONTINUE

c        IF(IJ .GT. 1 .AND. IJ .LT. FILES+2) THEN
c     OPEN (10,FILE=filnamc(IJ-1),STATUS='UNKNOWN')
c     DO 275 J=1, NC
c        WRITE (10,*) TCON(J)+start,CON(J)
c275  CONTINUE
c        CLOSE(10)
c        ENDIF

Ccccccccccccccccccccccccccccccccccccccccc
C  Determine the late-time
Ccccccccccccccccccccccccccccccccccccccccc
         TL = 2*Ttr+Tb+Tp
         TLi = nint(TL/DTC)+1

         if(INOISE .EQ. 0) then
          write(*,*) 'Enter the name of the convolution output file: '
          read (*,*) FILENAM
c        FILENAM = 'conv.dat'
          OPEN (10,FILE=FILENAM,STATUS='UNKNOWN')
      DO 285 J=1, NC
           WRITE (10,*) TCON(J)+start,CON(J)
 285   CONTINUE
           CLOSE(10)
         endif

Ccccccccccccccccccccccccccccccccccccccccccccccccccccccccccccccccccccccccccccccc
C  Calculate the energy of the response and convolution waveform
Ccccccccccccccccccccccccccccccccccccccccccccccccccccccccccccccccccccccccccccccc
         Er=0
         do 621 J=1,NPTS
         Er=Er+DT*(H(IJ,J)**2)
621      continue

         Ec=0
         do 71 K=TLi,(NC-1)
         Ec=Ec+(TCON(K+1)-TCON(K))*(CON(K)**2)
71       continue

Ccccccccccccccccccccccccccccccccc
C        EDN calculation
Ccccccccccccccccccccccccccccccccc
         EDN = Ec / Ee
         EDNA(IJ) = Ec / (Ee * Er)
```

```
c       write (*,*) IJ,' Old EDN= ',EDN, ' New EDN= ',EDNA(IJ)
65      continue

Ccccccccccccccccccccccccccccccccccccccccccccccccccccccccccccccc
C       Write the ENDA 2x2 array to a file for comparison
Ccccccccccccccccccccccccccccccccccccccccccccccccccccccccccccccc
        write(*,*) 'Enter the name of the file to write the EDNA array to: '
        read(*,*) array

        open (10,FILE=array,STATUS='UNKNOWN')
        do 67 i=1,in
         write (10,*) EDNA(i+1)
67      continue
        close(10)

Ccccccccccccccccccccccccccccccccccccccccccccccccccccccccccccccc
C  Calculate the mean and standard deviation of the EDN
Ccccccccccccccccccccccccccccccccccccccccccccccccccccccccccccccc
        SUMsnr=0
        DO 760 I=2,in
        SUMsnr = SUMsnr+SNR(I)
760     CONTINUE

        AMEANsnr = SUMsnr/FLOAT(in-1)

        SUM=0
        DO 770 I=2,in
        SUM = SUM+EDNA(I)
770     CONTINUE

        AMEAN = SUM/FLOAT(in-1)

        SUMM=0
        DO 75 I=2, in
        SUMM = SUMM+(EDNA(I)-AMEAN)**2
75      CONTINUE

        VARI = SUMM/FLOAT(in-2)
        SD   = SQRT(VARI)

        if(INOISE .EQ. 1) then
         WRITE (*,*) 'Response file     = ', RESPON
         WRITE (*,*) 'Ttr               = ', Ttr
         WRITE (*,*) 'Number of samples  = ', in
         WRITE (*,*) 'Files written            = ', FILES
         WRITE (*,*) 'Mean SNR                       = ', AMEANsnr
```

```
        WRITE (*,*) 'Mean EDNA                    = ', AMEAN
        WRITE (*,*) 'Standard deviation     = ', SD

       elseif(INOSIE .EQ.0) then
        WRITE (*,*) 'Response file     = ', RESPON
        WRITE (*,*) 'Ttr            = ', Ttr
        WRITE (*,*) 'EDNA             = ', EDNA(1)
       endif

800    WRITE (*,*) 'DO YOU WANT TO WRITE THE EDNA TO A FILE? '
       WRITE (*,*) '1. EPSILON FILE'
       WRITE (*,*) '2. THICKNESS FILE'
       WRITE (*,*) '3. ANGLE FILE'
       WRITE (*,*) '4. DO NOT WRITE TO A FILE'
c      READ (*,*) CH
       ch=4
803    format(f10.2, a3, F15.10)

       IF(CH .EQ. 1) THEN
        WRITE (*,*) 'ENTER Er: '
        READ (*,*) Er
        I=1

ccccccccccccccccccccccccccccccccccccccccccccccccccccccccccccccccc
c  open file and read into memory
ccccccccccccccccccccccccccccccccccccccccccccccccccccccccccccccccc
       OPEN (10, FILE='DELTAE.DAT', STATUS='UNKNOWN')
805    READ (10,803,END=810) EPS(I), COMMA, ED(I)
       I=I+1
       GOTO 805
810    I=I-1
       CLOSE(10)
       size = I

ccccccccccccccccccccccccccccccccccccccccccccccccc
c  determine if the file existed or is new
ccccccccccccccccccccccccccccccccccccccccccccccccc

ccccccccccccccccccccccccccccccc
c  file is new
ccccccccccccccccccccccccccccccc
       IF(size .EQ. 0) THEN
        file_flag = 1
        OPEN (10, FILE='DELTAE.DAT', STATUS='UNKNOWN')
        WRITE(10,803) Er, ',', EDNA(1)
        CLOSE(10)
```

```
        ENDIF

ccccccccccccccccccccccccccccccc
c  file has already been created
ccccccccccccccccccccccccccccccc
        IF(I .NE. 0) THEN
         FILE='DELTAE.DAT'
         update =0
         do 815 i=1, size
          if(Er .eq. EPS(i) .and. update .eq. 0) THEN
           call replace(EPS, ED, Er, EDNA(1), i, size, FILE)
           update =1
          else if(Er .lt. EPS(i) .and. update .eq. 0) then
           call insert(EPS, ED, Er, EDNA(1), i, size, FILE)
           update =1
          else if(Er.gt.EPS(i).and.update.eq.0.and.Er.lt.EPS(i+1)) then
           call insert(EPS, ED, Er, EDNA(1), i+1, size, FILE)
           update =1
          else if(Er.gt.EPS(i).and.i.eq.size.and.update.eq.0) then
           call append(EPS, ED, Er, EDNA(1), i+1, size, FILE)
           update =1
          endif
815       continue
        ENDIF

        ELSE IF(CH .EQ. 2) THEN
         WRITE (*,*) '2 IS A BETTER CHOICE'
        WRITE (*,*) 'ENTER thickness: '
         READ (*,*) d
         I=1

ccccccccccccccccccccccccccccccccccccccccccccccccccccccc
c  open file and read into memory
ccccccccccccccccccccccccccccccccccccccccccccccccccccccc
        OPEN (10, FILE='DELTAT.DAT', STATUS='UNKNOWN')
820     READ (10,803,END=835) th(I), COMMA, ED(I)
        I=I+1
        GOTO 820
835     I=I-1
        CLOSE(10)
        size = I

ccccccccccccccccccccccccccccccccccccccccccccccccccccccc
c  determine if the file existed or is new
ccccccccccccccccccccccccccccccccccccccccccccccccccccccc
```

```
ccccccccccccccccccccccccccccccccccccc
c  file is new
ccccccccccccccccccccccccccccccccccccc
          IF(size .EQ. 0) THEN
           file_flag = 1
           OPEN (10, FILE='DELTAT.DAT', STATUS='UNKNOWN')
           WRITE(10,803) d, ',', EDNA(1)
           CLOSE(10)
          ENDIF

ccccccccccccccccccccccccccccccccccccc
c  file has already been created
ccccccccccccccccccccccccccccccccccccc
          IF(I .NE. 0) THEN
           FILE='DELTAT.DAT'
           update =0
           do 850 i=1, size
            if(d .eq. th(i) .and. update .eq. 0) THEN
             call replace(th, ED, d, EDNA(1), i, size, FILE)
             update =1
            else if(d .lt. th(i) .and. update .eq. 0) then
             call insert(th, ED, d, EDNA(1), i, size, FILE)
             update =1
            else if(d.gt.th(i).and.update.eq.0.and.d.lt.th(i+1)) then
             call insert(th, ED, d, EDNA(1), i+1, size, FILE)
             update =1
            else if(d.gt.th(i).and.i.eq.size.and.update.eq.0) then
             call append(th, ED, d, EDNA(1), i+1, size, FILE)
             update =1
            endif
850        continue
          ENDIF

         ELSE IF(CH .EQ. 3) THEN
          WRITE (*,*) '3 IS THE BEST CHOICE'

      WRITE (*,*) 'ENTER angle: '
          READ (*,*) ai
          I=1

ccccccccccccccccccccccccccccccccccccccccccccccccccccccccccccccc
c  open file and read into memory
ccccccccccccccccccccccccccccccccccccccccccccccccccccccccccccccc
          OPEN (10, FILE='DELTAA.DAT', STATUS='UNKNOWN')
860       READ (10,803,END=870) ang(I), COMMA, ED(I)
          I=I+1
```

```
        GOTO 860
870     I=I-1
        CLOSE(10)
        size = I

ccccccccccccccccccccccccccccccccccccccccccccccccccccccccccccc
c  determine if the file existed or is new
ccccccccccccccccccccccccccccccccccccccccccccccccccccccccccccc
c
ccccccccccccccccccccccccccccccccc
c  file is new
ccccccccccccccccccccccccccccccccc
        IF(size .EQ. 0) THEN
         file_flag = 1
         OPEN (10, FILE='DELTAA.DAT', STATUS='UNKNOWN')
         WRITE(10,803) ai, ',', EDNA(1)
         CLOSE(10)
        ENDIF

ccccccccccccccccccccccccccccccccc
c  file has already been created
ccccccccccccccccccccccccccccccccc
        IF(I .NE. 0) THEN
         FILE='DELTAA.DAT'
         update =0
         do 890 i=1, size
          if(ai .eq. ang(i) .and. update .eq. 0) THEN
           call replace(ang, ED, ai, EDNA(1), i, size, FILE)
           update =1
          else if(ai .lt. ang(i) .and. update .eq. 0) then
           call insert(ang, ED, ai, EDNA(1), i, size, FILE)
           update =1
          else if(ai.gt.ang(i).and.update.eq.0.and.ai.lt.ang(i+1)) then
           call insert(ang, ED, ai, EDNA(1), i+1, size, FILE)
           update =1
          else if(ai.gt.ang(i).and.i.eq.size.and.update.eq.0) then
           call append(ang, ED, ai, EDNA(1), i+1, size, FILE)
           update =1
          endif
890       continue
        ENDIF

        ELSE IF(CH .EQ. 4) THEN
         WRITE (*,*) 'OK, GOODBYE!'

        ELSE IF(CH.NE.1 .AND. CH.NE.2 .AND. CH.NE.3 .AND. CH.NE.4 ) THEN
```

```
        WRITE (*,*) 'NOT A VALID CHOICE'
        GOTO 800
       ENDIF
999  STOP
C
     END
C*********************************************************************
C
     FUNCTION R(TT)
C
C  CALCULATES CONVOLUTION AT TIME TT
C
     COMMON /BLOCK1/ RM(2050),B(2050),DT,DLT,AL(50),NP
C
     R     = 0.
C
     DO 90 N= 1,NP
C
      SUM   = 0.
      TL    = TT-FLOAT(N)*DLT
      IF (TL .LT. 0.) TL=0.
      TU    = TT-FLOAT(N-1)*DLT
      IF (TU .LT. 0.) TU=0.
      K1    = INT(TL/DT)+2
      K2    = INT(TU/DT)+1
C
      SUM   = SUM + RI(K1-1,TL,FLOAT(K1-1)*DT)
      SUM   = SUM + RI(K2,FLOAT(K2-1)*DT,TU)
C
      K2M   = K2-1
      IF(K2M .LT. K1)GO TO 60
      DO 50 I= K1,K2M
       SUM   = SUM + RI(I,DT*FLOAT(I-1),DT*FLOAT(I))
 50   CONTINUE
C
 60   R     = R + AL(N)*SUM
C
 90   CONTINUE
C
     RETURN
     END
C*********************************************************************
C
     FUNCTION RI(I,T1,T2)
C
C  CALCULATES INTEGRAL OF RESPONSE
```

```
C
      COMMON /BLOCK1/ RM(2050),B(2050),DT,DLT,AL(50),NP
C
      RI    = (T2-T1)*(B(I)+ RM(I)*(T2+T1)/2.)
C
      RETURN
      END
C*********************************************************************
C
      FUNCTION RINT (T1,T2)
C
C  CALCULATES INTEGRAL FROM T1 TO T2
C
      COMMON /BLOCK2/ CON(2050),TCON(2050),DTC
C
      ISTART = INT(T1/DTC) + 2
      IEND   = INT(T2/DTC) + 1
C
      SUM    = 0.
      IF (IEND .GT. ISTART) THEN
       DO 10 I=ISTART,IEND-1
         SUM    = SUM + 0.5*DTC*(CON(I)+CON(I+1))
10     CONTINUE
      ENDIF
C
      HA     = CON(ISTART-1)
      HB     = CON(ISTART)
      TA     = TCON(ISTART-1)
      TB     = TCON(ISTART)
      H1     = HA + (T1-TA)*(HB-HA)/(TB-TA)
      SUM    = SUM + 0.5*(TB-T1)*(H1+HB)
C
      HA     = CON(IEND)
      HB     = CON(IEND+1)
      TA     = TCON(IEND)
      TB     = TCON(IEND+1)
      H1     = HA + (T2-TA)*(HB-HA)/(TB-TA)
      SUM    = SUM + 0.5*(T2-TA)*(H1+HA)
C
      RINT   = SUM
C
      RETURN
      END
C*********************************************************************
C
FUNCTION GAUSRV (SEED)
```

```
C
C CALCULATES A GAUSSIAN RANDOM VARIABLE OF MEAN 0 AND
STANDARD DEVIATION 1
C
      PI          =4.*ATAN(1.)
      SEED  = 997.*SEED-AINT(997.*SEED)
      R1          = SEED
      SEED  = 997.*SEED-AINT(997.*SEED)
      R2          = SEED
      GAUSRV      = SQRT(-2.*LOG(R1))*COS(2.*PI*R2)
C
      RETURN
      END
C*********************************************************************
C
   SUBROUTINE insert (array1, array2, el1, el2, pos, size, file)
C
C  adds an element to the interior of an array
C
   character*32 file
      real array1(32), array2(32), el1, el2
      real temp1(32), TEMP2(32)
      integer pos, size, quit, tempsize

      write(*,*) 'insert'

      quit = size-pos+1

      do 100 I=1, quit
       temp1(I)=array1(pos+I-1)
       temp2(I)=array2(pos+I-1)
100   continue

      tempsize = I-1
      array1(pos)=el1
      array2(pos)=el2

      do 150 I=1, tempsize
       array1(pos+I) = temp1(I)
       array2(pos+I) = temp2(I)
150   continue

203   format(f10.2, a3, F15.10)

      OPEN (10, FILE=file, STATUS='UNKNOWN')
```

```
        do 250 I=1, size+1
         WRITE(10,203) array1(I), ',', array2(I)
250     continue
        CLOSE(10)
C
C
    RETURN
    END
C*********************************************************************

C*********************************************************************
C
    SUBROUTINE append (array1, array2, el1, el2, pos, size, file)
C
C  adds an element to the end of an array
C
        character*32 file
        real array1(32), array2(32), el1, el2
        integer pos, size

        write(*,*) 'append'

        array1(pos)=el1
        array2(pos)=el2

203     format(f10.2, a3, F15.10)

        OPEN (10, FILE=file, STATUS='UNKNOWN')

        do 250 I=1, size+1
         WRITE(10,203) array1(I), ',', array2(I)
250     continue

        CLOSE(10)
C
    RETURN
    END
C*********************************************************************
C
C*********************************************************************
C
    SUBROUTINE replace (array1, array2, el1, el2, pos, size, file)
C
C  replaces an element in an array
C
        character*32 file
```

```
      real array1(32), array2(32), el1, el2
      integer pos, size

      write(*,*) 'replace'

      array1(pos)=el1
      array2(pos)=el2

203   format(f10.2, a3, F15.10)
      OPEN (10, FILE=file, STATUS='UNKNOWN')
      do 250 I=1, size
       WRITE(10,203) array1(I), ',', array2(I)
250   continue
      CLOSE(10)
C
C
   RETURN
   END
C*********************************************************************
```

D. Overview – MLPREF.for

This program generates the scattered response from a layered material. The user defines the properties of the layered material including the number of layers, layer backing, and the properties of the layers. The user also defines the type of incident waveform and its properties including polarization and angle of incidence. In addition, the user defines the frequency range of the incident waveform. The output is a frequency domain representation of the scattered response to the defined layered material.

D.1 Source Code - MLPREF.for

```
  program mlpref
c
c   **********
c  This program reads appropriate input data for studying the reflection
c  of a plane wave pulse obliquely incident upon a grounded multi-layered
```

```
c material composite. It subsequently quantifies that reflection over a
c specified band of frequencies by calling appropriate sub-programs for
c the spectrum of an incident pulse and the spectral reflection coeffic-
c ient of the grounded composite.
c    **********
c
      implicit integer*4 (i-n)
      implicit real*8 (a-h,o-z)
      complex*16 j,epsr(0:10),mur(0:10),k(0:10),kz(0:10),z(0:10),p(0:10)
      complex*16 r(0:10),ei,ips,rc,rcm,rw
      dimension h(0:10)
      common/b1/pi,c,j
      common/b2/tau,iw
      common/b3/tha,nl,ib,ip
      common/b4/h,epsr,mur,k,kz,z,p,r
      open(8,file='mlpref.out',status='unknown')
      open(9,file='ips.dat',status='unknown')
      open(10,file='mlpref.dat',status='unknown')
c **********
c Data Entry Segment
c **********
      write(*,*) 'Enter waveform type iw (impulse=1, gaussian=2) >'
      read(*,*) iw
      if(iw.eq.2) then
       write(*,*) 'Enter gaussian pulse duration gpd in ps >'
       read(*,*) gpd
      endif
      write(*,*) 'Enter polarization index ip (perp=1, par=2) >'
      read(*,*) ip
      write(*,*) 'Enter incidence angle tha in degrees >'
      read(*,*) tha
      write(*,*) 'Enter number nl of material layers >'
      read(*,*) nl
      write(*,*) 'Enter backing index ib (1=space, 2=conductor) >'
      read(*,*) ib
      do n=1,nl,1
       write(*,*) 'Enter h (in mm), epsr and mur for layer number n =',
     + n,' >'
       read(*,*) h(n),epsr(n),mur(n)
      enddo
      write(*,*) 'Enter start,end frequencies fs,fe in GHz >'
      read(*,*) fs,fe
      write(*,*) 'Enter number nf of frequency points >'
      read(*,*) nf
c **********
c Data Output Segment
```

```
c **********
      write(*,10)
      write(8,10)
10    format(/,2x,'ESSENTIAL INPUT DATA',//)
      if(iw.eq.1) then
        write(*,14)
        write(8,14)
      elseif(iw.eq.2) then
        write(*,15) gpd
        write(8,15) gpd
      endif
14    format(/,5x,'impulse incident waveform')
15    format(/,5x,'gaussian incident waveform,',5x,'2T = ',f5.0,' ps')
      if(ip.eq.1) then
        write(*,20) tha
        write(8,20) tha
      elseif(ip.eq.2) then
        write(*,21) tha
        write(8,21) tha
      endif
20    format(5x,'perpendicular polarization,',5x,'tha = ',f4.1,
     +' degrees')
21    format(5x,'parallel polarization',5x,'tha = ',f4.1,' degrees')
      if(ib.eq.1) then
        write(*,25)
        write(8,25)
      elseif (ib.eq.2) then
        write(*,26)
        write(8,26)
      endif
25    format(5x,'free-space backing',//)
26    format(5x,'perfect-conductor backing',//)
      write(*,30)
      write(8,30)
30    format(2x,'n',4x,'h(n) in mm',10x,'epsr(n)',23x,'mur(n)',/)
      do n=1,nl,1
      write(*,31) n,h(n),epsr(n),mur(n)
      write(8,31) n,h(n),epsr(n),mur(n)
      enddo
31    format(2x,i2,4x,f5.2,5x,'(',e11.4,',',e11.4,')',5x,'(',e11.4,','
     +,e11.4,')')
      write(*,35) fs,fe,nf
      write(8,35) fs,fe,nf
35    format(//,5x,'fs = ',e12.5,' GHz',/,5x,'fe = ',e12.5,' GHz',/,5x,
     +'nf = ',i4,' pts.',//)
      write(8,40)
```

```
40   format(/,8x,'f',13x,'RWr',11x,'RWi',11x,'RWa',11x,'RWp',/)
c **********
c Initial Parameter Computation Segment
c **********
     epsr(0)=dcmplx(1.d0,0.d0)
     mur(0)=dcmplx(1.d0,0.d0)
     tau=1.d-12*gpd/2.
     do n=1,nl,1
      h(n)=h(n)*1.d-3
     enddo
     fs=fs*1.d9
     fe=fe*1.d9
     df=(fe-fs)/nf
     pi=4.*atan(1.d0)
     dpr=180./pi
     c=3.d8
     j=dcmplx(0.d0,1.d0)
         tha=tha*pi/180.d0
c **********
c Data Computation Segment
c **********
     do i=1,nf+1,1
      f=fs+(i-1)*df
      ei=ips(f)
      rc=rcm(f)
      rw=ei*rc
      eim=abs(ei)
      eip=dpr*atan2(imag(ei),dble(ei))
      rwm=abs(rw)
      rwp=dpr*atan2(imag(rw),dble(rw))
      write(8,50) f*1.d-9,rw,rwm,rwp
      write(9,51) f*1.d-9,eim,eip
      write(10,51) f*1.d-9,rwm,rwp
50   format(5(2x,e12.5))
51   format(3(2x,e12.5))
     enddo
     endfile 8
     endfile 9
     endfile 10
     end
c **********
c **********
     complex*16 function ips(f)
c
c    **********
c This subroutine sub-program computes the spectrum of the incident
```

```
c  pulse waveform.
C    **********
c
     implicit integer*4 (i-n)
     implicit real*8 (a-h,o-z)
     complex*16 j
     common/b1/pi,c,j
     common/b2/tau,iw
     omeg=2.*pi*f
     if(iw.eq.1) then
      ips=dcmplx(1.d0,0.d0)
     elseif(iw.eq.2) then
      ps=sqrt(pi)*tau*exp(-(omeg*tau)**2/4.)
      ips=dcmplx(ps,0.d0)*exp(-j*5.*omeg*tau)
     endif
     end
c **********
c **********
     subroutine param(f)
c
c  This subroutine calculates the required wave parameters for each of
c  the material layers based upon their thickness and constitutive par-
c  ameters.  It finally calculates the interfacial reflection coeffic-
c  ient Rn at the interface between the n-1'st and n'th layers.
c
     implicit integer*4 (i-n)
     implicit real*8 (a-h,o-z)
     real*8 l0,k0,kx
     complex*16 j,epsr(0:10),mur(0:10),k(0:10),kz(0:10),z(0:10),p(0:10)
     complex*16 r(0:10)
     dimension h(0:10)
     common/b1/pi,c,j
     common/b3/tha,nl,ib,ip
     common/b4/h,epsr,mur,k,kz,z,p,r
     if(f.lt.1.d0) then
      f1=1.d0
     else
      f1=f
     endif
     l0=c/f1
     zi0=120.*pi
     k0=2.*pi/l0
     kx=k0*sin(tha)
     do n=0,nl,1
      k(n)=sqrt(epsr(n)*mur(n))*k0
      kz(n)=sqrt(k(n)*k(n)-kx*kx)
```

```
      if(ip.eq.1) then
        z(n)=k0*zi0*mur(n)/kz(n)
      elseif(ip.eq.2) then
        z(n)=zi0*kz(n)/(k0*epsr(n))
      endif
      if(n.eq.0) then
        r(n)=dcmplx(0.d0,0.d0)
        p(n)=dcmplx(0.d0,0.d0)
      else
        r(n)=(z(n)-z(n-1))/(z(n)+z(n-1))
        p(n)=exp(-j*kz(n)*h(n))
      endif
    enddo
    end
c **********
c **********
    complex*16 function rcm(f)
c
c This function sub-program calculates recursively the overall reflec-
c tion coefficient at interface n=1 between free space and the first
c material layer.
c
    implicit integer*4 (i-n)
    implicit real*8 (a-h,o-z)
    complex*16 epsr(0:10),mur(0:10),k(0:10),kz(0:10),z(0:10),p(0:10)
    complex*16 r(0:10),gam(0:11)
    dimension h(0:10)
    common/b3/tha,nl,ib,ip
    common/b4/h,epsr,mur,k,kz,z,p,r
    call param(f)
    if(ib.eq.1) then
      gam(nl+1)=(z(0)-z(nl))/(z(0)+z(nl))
    elseif (ib.eq.2) then
      gam(nl+1)=dcmplx(-1.d0,0.d0)
    endif
    do n=nl,1,-1
      call rgam(n,gam)
    enddo
      rcm=gam(1)
    end
c **********
c **********
    subroutine rgam(n,gam)
c
c    **********
c This subroutine computes the spectral reflection coefficient at the
```

```
c  n'th interface of a multi-layered grounded dielectric composite in
c  terms of that at the n+1'st interface for a plane wave of either per-
c  pendicular or parallel polarization at oblique incidence.
c    **********
c
      implicit integer*4 (i-n)
      implicit real*8 (a-h,o-z)
      complex*16 epsr(0:10),mur(0:10),k(0:10),kz(0:10),z(0:10),p(0:10)
      complex*16 r(0:10),gam(0:11),p2
      dimension h(0:10)
      common/b4/h,epsr,mur,k,kz,z,p,r
      p2=p(n)*p(n)
      gam(n)=(r(n)+gam(n+1)*p2)/(1.+r(n)*gam(n+1)*p2)
      end
```

E. Overview – NFSIG.for

This program determines the natural frequencies for materials which have none zero conductivity. The inputs are the material properties including the thickness, relative permittivity, permeability, conductivity, angle of incidence, and polarization. The program allows the user to define the number of natural frequencies to calculate.

E.1 Source Code – NFSIG.for

```
Program NFSIG
c
c  This program computes the natural frequencies of a grounded dielectric slab.
c    The slab has real, constant constitutive parameters eps, mu0, sigma
c
c  This version uses values for lossless slab as guesses for lossy slab
c
c version of 8 June 2001
c
      complex guess1,guess2,funperp,funpar,ans,g1,g2
      character*20 filnam(10)
      external funperp,funpar
c
      common /b1/ epsr,sigma,delta,eps0,clite,stheta,ctheta
c
      pi = 4.*atan(1.)
      eps0 = 8.854e-12
```

```
      rmu0 = 4.*pi*1.e-7
      clite = 1./sqrt(rmu0*eps0)
      eta0 = sqrt(rmu0/eps0)
c
      filnam(1)='freq0.dat'
      filnam(2)='freq1.dat'
      filnam(3)='freq2.dat'
      filnam(4)='freq3.dat'
      filnam(5)='freq4.dat'
c
      write (*,*) 'Enter relative permittivity'
      read  (*,*) epsr
      write (*,*) 'Enter conductivity (S/m)'
      read  (*,*) sig
      write (*,*) 'Enter layer thickness (m)'
      read  (*,*) delta
      write (*,*) 'Enter incidence angle (deg)'
      read  (*,*) thetai
      thetai = pi*thetai/180.
      stheta = sin(thetai)
      sth2 = stheta*stheta
      ctheta = cos(thetai)
      write (*,*) 'Enter:  1=perpendicular polarization'
      write (*,*) '        2=parallel polarization'
      read  (*,*) ipol
      write (*,*) 'Enter number of frequencies to find'
      read  (*,*) nf
c
      if (ipol .eq. 1) then
       z1 = eta0/sqrt(epsr-sth2)
       z0 = eta0/sqrt(1.-sth2)
      end if
      if (ipol .eq. 2) then
       z1 = eta0*sqrt(epsr-sth2)/epsr
       z0 = eta0*sqrt(1.-sth2)
      end if
      gamma = (z1-z0)/(z1+z0)
      tau = 2.*delta*sqrt(epsr-sth2)/clite
      sr = log(abs(gamma))/tau
c
      iters = 100
      if (sig .gt. .5) then
       iters = int(sig/.005)
      end if
      dsig = sig/iters
c
```

```
      open(20,file='natural.in',status='unknown')
      do n=0,nf-1
       open (10,file=filnam(n+1),status='unknown')
       do i=1,iters
        sigma = i*dsig
        if (i .eq. 1) then
              guess1 = cmplx(sr,(2*n+1)*pi/tau)
         guess2 = 1.1*guess1
         g1 = guess1
         g2 = guess2
        else
         g2 = g1
         g1 = ans
         guess1 = g1
         guess2 = g2
        endif
            if (aimag(guess1) .lt. 0.d0) guess1=conjg(guess1)
        if (aimag(guess2) .lt. 0.d0) guess2=conjg(guess2)
        if (ipol .eq. 1) then
              call zsecnt (funperp,guess1,guess2,6,100,ans,its)
        end if
        if (ipol .eq. 2) then
         call zsecnt (funpar,guess1,guess2,6,100,ans,its)
        end if
        ar = real(ans)*1.e-9
        ai = aimag(ans)*1.e-9/(2*n+1)
        write (10,*) sigma,ar,ai
       enddo
       close (10)
       write (*,*) 'n=',n
       write (*,*) 'sigma=',sigma
       write (*,*) 'freq=',ans
       are = real(ans)*1e-9
       aim = imag(ans)*1e-9
       write (20,*) are,',',aim
      end do
      close(20)
c
      end
c
      complex function funperp (s)
c
      complex s,f
      common /b1/ epsr,sigma,delta,eps0,clite,stheta,ctheta
c
      f = sqrt(epsr+sigma/(s*eps0)-stheta*stheta)
```

```
      funperp = ctheta+f-(ctheta-f)*exp(-2.*delta*s*f/clite)
c
      return
      end
c
      complex function funpar (s)
c
      complex s,f,g
      common /b1/ epsr,sigma,delta,eps0,clite,stheta,ctheta
c
      g = epsr+sigma/(s*eps0)
      f = sqrt(g-stheta*stheta)
      funpar = f+g*ctheta-(f-g*ctheta)*exp(-2.*delta*s*f/clite)
c
      return
      end
c
      SUBROUTINE ZSECNT (FUNC,Z1,Z2,NSIG,ITMAX,ANS,ITS)
C
C  SOLVES FOR THE COMPLEX ZERO OF THE COMPLEX FUNCTION FUNC
C   BY USING THE SECANT METHOD
C
C  Z1,Z2 = INITIAL GUESS
C  NSIG  = NO. SIGNIFICANT DIGITS DESIRED IN ROOT
C  ITMAX = MAXIMUM ALLOWED NO. ITERATIONS
C  ANS   = ROOT
C  ITS   = NO. ITERATIONS REQUIRED
C
      COMPLEX FUNC,ANS,Z1,Z2,F1,F2,ZNEW,DER
C
      ABSIG  = 1./10.**NSIG
C
      ITS    = 0
      F2     = FUNC(Z2)
c     WRITE (*,*) 'Z = ',Z2
c     WRITE (*,*) 'F = ',F2
C
10    F1     = FUNC(Z1)
      DER    = (F2-F1)/(Z2-Z1)
      ITS    = ITS + 1
c     WRITE (*,*) '******************** ITS = ',ITS
c     WRITE (*,*) 'Z = ',Z1
c     WRITE (*,*) 'F = ',F1
c     WRITE (*,*) 'DERIVATIVE = ',DER
c     WRITE (*,*) '****************************************'
C
```

```
      ZNEW  = Z1 - F1/DER
C
      TEST1 = CABS(ZNEW-Z1)
      TEST2 = CABS(ZNEW-Z2)
      IF (TEST1 .LT. TEST2) THEN
       TEST  = TEST1/CABS(ZNEW)
       IF (TEST .LT. ABSIG) THEN
        ANS = ZNEW
        RETURN
       ENDIF
       F2   = F1
       Z2   = Z1
       Z1   = ZNEW
      ELSE
       TEST  = TEST2/CABS(ZNEW)
       IF (TEST .LT. ABSIG) THEN
        ANS = ZNEW
        RETURN
       ENDIF
       Z1   = ZNEW
      ENDIF
      IF (ITS .GE. ITMAX) THEN
       WRITE (*,*) 'MAXIMUM ITERATIONS EXCEEDED'
       ANS  = ZNEW
       RETURN
      ENDIF
C
      GO TO 10
C
      END
```

BIBLIOGRAPHY

[1] E.J. Rothwell, "Radar Target Discrimination Using the Extinction-Pulse Technique," Ph.D. dissertation, Michigan State University, 1985.

[2] E.J. Rothwell, K.M. Chen, D.P. Nyquist, W. Sun, "Frequency Domain E-Pulse Synthesis and Target Discrimination," *IEEE Transactions on Antennas and Propagation*, vol. 35, pp. 426-434, April 1987.

[3] E.J. Rothwell, D.P. Nyquist, K.M. Chen, and B. Drachman, "Radar Target Discrimination Using the Extinction Pulse Technique," *IEEE Transactions on Antennas and Propagation*, vol. 33, pp. 929-937, September 1985.

[4] C.E. Baum, E.J. Rothwell, K.M. Chen, D.P. Nyquist, "The Singularity Expansion Method and Its Application to Target Identification," *Proceedings of the IEEE*, vol. 79, pp. 1481-1492, October 1991.

[5] E.J. Rothwell, M.J. Cloud, Electromagnetics, CRC Press, Boca Raton, FL, 2001.

[6] A. Papoulis, The Fourier Integral and It's Application, McGraw Hill, New York, NY, 1962.

[7] P. Ilavarasan, "Automated Radar Target Discrimination Using E-Pulse and S-Pulse Techniques," Ph.D. dissertation, Michigan State University, 1992.

[8] A. Leon-Garcia, Probability and Random Processes for Electrical Engineering, 2nd Edition, Addison-Wesley, Reading, MA, 1994.

[9] K.M. Chen, D.P. Nyquist, E.J. Rothwell, L.L. Webb, and B. Drachman, "Radar Target Discrimination by Convolution of Radar Return with Extinction-Pulses and Single-Mode Extraction Signals," *IEEE Transactions on Antennas and Propagation*, vol. 34, pp. 896-904, July 1986.

[10] E.J. Rothwell, K.M. Chen, D.P. Nyquist, "Extraction of the Natural Frequencies of a Radar Target from a Measured Response Using E-Pulse Techniques," *IEEE Transactions on Antennas and Propagation*, vol. 35, pp. 715-720, June 1987.

[11] J.E. Ross, "Application of Transient Electromagnetic Fields to Radar Target Discrimination," Ph.D. dissertation, Michigan State University, 1992.

[12] E.F. Knott, J.F. Schaeffer, M.T. Tuley, Radar Cross Section, 2nd Edition, Artech House, Boston, MA, 1993.

[13] B.P Lathi, Signal Processing and Linear Systems, Berkley-Cambridge Press, Carmichael, CA, 1998.

[14] K.J. Vinoy, R.M. Jha, Radar Absorbing Materials: From Theory to Design and Characterization, Kluwer Academic Publishers, Boston, MA, 1996.